Spinal opioid-adrenergic analgesic interactions: Mechanistic insights on the role of the delta opioid and the alpha2A adrenergic receptors.

Anne-Julie Chabot-Doré

Integrated Program in Neuroscience
Department of Neurology and Neurosurgery
McGill University, Montreal

August 2013

A thesis submitted to McGill University in partial fulfillment of the requirements for the degree of Doctor of Philosophy.

This thesis is dedicated to my family who always believed in me and encouraged me through this ambitious project.

ABSTRACT

Opioid and α_2-adrenergic receptor (α_2AR) ligands are both analgesic when administered spinally and show a clinically beneficial synergistic interaction in the treatment of pain when co-administered. The μ- and δ-opioid receptors (MOR and DOR respectively) and the α_{2A}ARs have been shown to be capable of mediating opioid-adrenergic synergistic interactions. The development of new therapeutic approaches that exploit the combination of opioids and α_2AR agonists is currently hindered by limited mechanistic knowledge on how these drugs interact at the spinal level.

It is generally accepted that MOR mediates morphine antinociception. However, since morphine-related interactions between MOR and DOR have been reported at the spinal level, the role of DOR in spinal morphine antinociception requires further evaluation. Therefore, the First Aim of this thesis was to investigate the role of DOR in the antinociceptive effect of morphine and other opioids at the spinal level. Using the hot water tail flick assay, we observed that morphine was equally potent, but less effective in DOR-knockout (KO) mice compared to wild type (WT) mice. On the other hand, the efficacy of the DOR-selective agonists DeltII and SNC80 was maintained in DOR-KO mice. This study therefore suggests that 1) DOR is necessary to obtain full spinal morphine antinociceptive efficacy and 2) that DOR agonists are not selective in the tail flick assay.

These observations from Aim 1 raised two important questions: 1) Is DOR necessary to produce a morphine synergistic interaction with an α_2AR agonist? 2) Is DOR activation by DOR agonists sufficient to obtain a synergistic interaction with an α_2AR agonist? Thus, the Second Aim of this thesis was to determine whether DOR activation is sufficient and necessary to mediate opioid-adrenergic synergistic interactions in the spinal cord. The absence of DeltII antinociception in DOR-KO mice confirmed its selectivity in the substance P behavioral assay, therefore validating the choice of this assay. Opioid-adrenergic drug interactions were evaluated following spinal co-administration of the α_2AR agonist clonidine

with DeltII, morphine or DAMGO in WT and DOR-KO mice. Our results showed that DeltII+clonidine synergy is DOR-dependent, morphine+clonidine synergy is not DOR-dependent and DAMGO+clonidine do not interact synergistically. These findings confirm that DOR activation is sufficient but not necessary for synergy with α_2AR agonists.

The Third Aim of this thesis was to investigate the role of α_{2A}AR in spinal opioid-adrenergic synergy and opioid antinociception. We first confirmed that the α_{2A}AR mediates the synergistic interaction between clonidine and either morphine or DeltII. We also observed a potentiation of spinal morphine and spinal DeltII-mediated antinociception in α_{2A}AR-KO mice compared to WT mice; this potentiation could not be attributed to changes in the expression of opioid receptors, to alterations in opioid ligand binding properties or to enhanced noradrenergic tone in the spinal cord. Together, these findings led us to propose a model whereby the α_{2A}AR allosterically modulates spinal opioid receptors in an activation state-dependent manner.

These studies improve our understanding of the interaction between α_2-adrenergic and opioid drugs at the spinal level, which could lead to new the development of better pharmacological treatments for pain management.

RÉSUMÉ

Les ligands des récepteurs opiacés et α_2 adrénergiques (α_2AR) ont tous deux une action analgésique lorsque administrés par la voie spinale et peuvent démontrer une interaction synergétique cliniquement bénéfique lorsqu'ils sont co-administrés. Il a été démontré que les récepteurs opiacés μ et δ (MOR et DOR, respectivement) et le récepteur α_{2A}AR sont capables de générer des intéractions opiacés-adrénergiques synergétiques. Le développement de nouvelles approches thérapeutiques exploitant ces combinaisons est ralenti par une connaissance limitée des mécanismes régissant les interactions entre ces médicaments.

Il est généralement bien accepté que MOR effectue l'antinociception causée par la morphine. Cependant, puisque des interactions entre MOR et DOR médiées par la morphine ont été rapportées dans la moelle épinière, le rôle de DOR dans l'antinociception produite par la morphine requiert une évaluation plus approfondie. Donc, le premier objectif de cette thèse était d'investiguer le rôle que joue DOR dans l'effet antinociceptif de la morphine et d'autres opiacés au niveau spinal. Avec le test d'immersion de la queue en eau chaude, nous avons observé que la morphine était aussi puissante, mais moins efficace chez les souris DOR-knockout (KO) que chez les souris de type sauvage (TS). D'autre part, l'efficacité des agonistes sélectifs au DOR SNC80 et DeltII était maintenue chez les souris DOR-KO. Cette étude suggère donc que 1) DOR est nécessaire pour obtenir la pleine efficacité antinociceptive de la morphine et 2) que les agonistes du DOR ne sont pas sélectifs dans le test d'immersion de la queue en eau chaude.

Les observations faites à l'objectif 1 soulèvent deux questions importantes : 1) DOR est-il nécessaire pour produire une interaction synergétique entre la morphine et un agoniste α_2AR? 2) L'activation de DOR par des agonistes sélectifs à celui-ci est-elle suffisante pour obtenir une interaction synergétique avec un agoniste α_2AR? Le deuxième objectif de cette thèse était donc de déterminer si l'activation de DOR est suffisante et nécessaire pour entraîner la synergie entre les opiacés et les α_2AR au niveau spinal. L'absence d'effet

antinociceptif de DeltII chez la souris DOR-KO a confirmé la sélectivité de cet agoniste avec le test comportemental à la substance P et a donc validé le choix de cet essai. Les interactions opiacés-adrénergiques ont été évaluées suivant la co-administration par voie spiale de la clonidine, un agoniste α_2AR, avec la DeltII, la morphine ou le DAMGO chez les souris TS et DOR-KO. Nos résultats démontrent que la synergie entre DeltII+clonidine dépend du DOR, que la synergie entre morphine+clonidine n'est pas dépendante du DOR et que DAMGO+clonidine n'interagissent pas de façon synergétique. Ces découvertes confirment que l'activation du DOR est suffisante, mais pas nécessaire à la synergie avec les agonistes α_2AR.

Le troisième objectif de cette thèse était d'investiguer le rôle du récepteur α_{2A}AR dans la synergie opiacée-adrénergique spinale et l'effet antinociceptif des opiacés. Nous avons premièrement confirmé que le α_{2A}AR médie l'interaction synergétique entre la clonidine et la morphine ou la DeltII. Nous avons observé une potentiation de l'antinociception produite par la morphine ou la DeltII administrée par voie spinale chez la souris α_{2A}AR-KO comparativement à la souris TS; cette potentiation n'a pas pu être attribuée à des changements du niveau d'expression des récepteurs opiacés, à l'altération des propriétés de liaison des ligands ou à l'augmentation du tonus adrénergique spinal. Ensemble, ces découvertes ont mené à la proposition d'un modèle dans lequel le α_{2A}AR module de façon allostérique les récepteurs opiacés selon leur état d'activation.

Ces études améliorent notre compréhension de l'interaction entre les médicaments α_2 adrénergiques et les opiacés au niveau spinal, ce qui pourrait mener au développement de meilleurs traitements pharmacologiques pour la gestion de la douleur.

TABLE OF CONTENTS

LIST OF ABBREVIATIONS

α_{2A}AR	α_{2A}-adrenergic receptor
cAMP	Cyclic AMP
CGRP	Calcitonin gene-related peptide
CPM	Counts per minute
DA	Dopamine
DADLE	[D-Ala^2, D-Leu^5]-enkephalin
DAMGO	[D-Ala^2, NMe-Phe^4, Gly-ol^5]-enkephalin
Dbh	Dopamine β-hydroxylase
DeltII	[D-Ala^2]-deltorphin II
DOR	δ opioid receptor
DOR-KO	δ opioid receptor knockout
DPM	Disintegrations per minutes
DRG	Dorsal root ganglia
ERK	Extracellular signal-regulated kinase
GABA	γ-aminobutyric acid
GDP	Guanisine diphosphate
GIRK	G protein-coupled inwardly rectifying K^+ channel
GPCR	G protein-coupled receptor

GTP	Guanisine triphosphate
i.p.	Intraperitoneal
ir	Immunoreactivity
i.t.	Intrathecal
KO	Knockout
KOR	κ opioid receptor
L-DOPA	L3,4 dihydroxy phenylalanine
MAPK	Mitogen activated protein kinase
MPE	Maximum potential effect
MOR	μ opioid receptor
NE	Norepinephrine, Noradrenaline
NET	Norepinephrine transporter
NK-1	Neurokinin-1
PCR	Polymerase chain reaction
PKA	Protein kinase A
PKC	Protein kinase C
PLC	Phospholipase C
PPTA	Pre-pro-tachykinine
PTX	Pertussis toxin

SC	Spinal cord
SEM	Standard error of the mean
SNC80	(±)-4-[(α-R)-α-{2S,5R]-4-allyl-2,5-dimethyl-I-piperazinyl]-3-methoxybenzyl]- N,N-diethyl-benzamide
SP	Substance P
ST-91	2-(2,6-diethylphenylamino)-2-imidazoline HCl
TH	Tyrosine hydroxylase
TRPV1	Transient receptor potential vanilloid 1
VGCC	Voltage-gated Ca^{2+} channel
WT	Wild type
[^{3}H]-DeltII	DeltorphinII(D-Ala^2), [Tyrosyl-3,5-^{3}H]
6-OHDA	6-hydroxydopamine

ACKNOWLEDGMENTS

I would qualify my interactions with certain people throughout this thesis project as synergistic, as they have facilitated my best work.

I am most grateful to my supervisor, **Dr Laura Stone**, who gave me the opportunity to work on a fascinating research project and to participate in setting up a new lab. As a caring mentor, she selflessly shared advice and guided me through this project. I appreciate the patience and support she displayed while I pursued extracurricular activities, which made my graduate experiences more complete.

I would like to thank the members of my advisory committee, **Drs Ji Zhang** and **Terence Hébert**. Their critical examination of my work and their feedback inspired and enabled some of the better ideas in this thesis. I especially want to thank Dr Hébert for being so accommodating and for letting me perform radioligand binding experiments in his laboratory.

Over the years, numerous colleagues made my time at the lab more enjoyable. I would especially like to thank Dr Magali Millecamps for the many stimulating discussions, and Mrs Lina Naso for her technical support. I would also express thanks to my labmates for their genuine team spirit: Dr Maral Tajerian, Dr Stefania Echeverry, Alex Danco, Dr Catherine Ferland-Legault, Dareen Mohamed, Zarah Tabatabaei and Tony Lim. Thanks are due to Cynthia Lue-Yat and Grace Krawec for kindly providing administrative support. I am grateful for having had the opportunity to train and supervise some fantastic undergraduate students – Serge, Tharsika, Sarah and Jennifer– who made me realize how much I enjoy teaching and mentoring. I owe many thanks to the staff of the animal facility, and to Jeannine and Rosalie in particular, for looking after the most precious reagent I used during my thesis: our mice. I must thank Phan Trieu and Dr Dominic Devost for helping me with radioligand binding experiments, and everyone from Terry's lab for making me feel welcome.

This work would not have been feasible without the financial support of the Canadian Institute of Health Research, the Canadian Pain Society, the Integrated Program in Neuroscience, and the Louise and Alan Edwards Foundation.

J'aimerais aussi remercier ma famille pour m'avoir toujours encouragée dans mes efforts. Je suis particulièrement reconnaissante envers ma mère, **Lorraine Chabot**, qui, par son support inconditionnel et ses précieux conseils, m'a aidée à trouver ma voie. Mes remerciements vont aussi à mes amis dont la sincérité m'a été salutaire dans les moments difficiles et qui ont surtout mis beaucoup de joie dans mes temps libres. Je dois remercier tout particulièrement **Eric Adler**, dont le soutien dans mes mille et un projets ces dernières années m'a permis de me dépasser et d'accomplir de grandes choses.

CONTRIBUTION OF AUTHORS

The studies constituting the body of this thesis are presented in Chapters 3, 4 and 5 and discussed in Chapter 6. Manuscripts presenting the studies described in Chapter 3 and 5 are in preparation. Data shown in Chapter 4 along with parts of Chapters 2 and 6 have been published (Appendix C, **Chabot-Doré, A-J** et al., (2013) The delta-opioid receptor is sufficient, but not necessary, for spinal opioid-adrenergic synergy. *JPET* December 2013 vol. 347, no 3 773-780).

Chapter 3: The delta opioid receptor is necessary to produce full morphine antinociception at the spinal level

Design of the study: A.-J. Chabot-Doré, L.S. Stone, T.E. Hébert (ligand binding)

Execution of experiment: A.-J. Chabot-Doré, M. Millecamps (mouse breeding, tactile threshold), L. Naso (time course data), S. Amrani (radiant heat assay), L.S. Stone (i.t. injections)

Analysis of data: A.-J. Chabot-Doré

Writing of the manuscript: A.-J. Chabot-Doré, L.S. Stone

Supervision: L.S. Stone

Chapter 4: The delta opioid receptor is sufficient, but not necessary for spinal opioid-adrenergic analgesic synergy

Design of the study: A.-J. Chabot-Doré, L.S. Stone

Execution of experiment: A.-J. Chabot-Doré, M. Millecamps (mouse breeding), L.S. Stone (i.t. injections)

Analysis of data: A.-J. Chabot-Doré

Writing of the manuscript: A.-J. Chabot-Doré, L.S. Stone

Supervision: L.S. Stone

Chapter 5: Spinal opioid antinociception is allosterically modulated by the α_{2A}-adrenergic receptor.

Design of the study: A.-J. Chabot-Doré, L.S. Stone, T.E. Hébert (ligand binding)

Execution of experiment: A.-J. Chabot-Doré, Millecamps (mouse breeding), L. Naso (time course data), S. Amrani (radiant heat assay, tactile threshold), L.S. Stone (i.t. injections)

Analysis of data: A.-J. Chabot-Doré, L.S. Stone

Writing of the manuscript: A.-J. Chabot-Doré, L.S. Stone

Supervision: L.S. Stone

Chapter 1:
Introduction

STATEMENT OF THE PROBLEM

Opioids are widely used to manage all types of pain including acute pain, cancer pain, chronic neuropathic and inflammatory pain. Despite the development of new analgesic drugs, morphine remains the "gold standard" for pain management. Unfortunately, opioid-related adverse effects such as respiratory depression, tolerance, physical dependence and addiction have lead to an underutilization of these potent compounds for adequate pain relief. One way to circumvent these adverse effects is to combine morphine with other analgesic drugs. Clonidine, an α_2-adrenergic receptor (α_2AR) agonist with potent spinal and systemic analgesic action, is occasionally co-administered as an adjuvant to opioids for both acute and chronic pain management (Smith et al., 2008). Currently, the clinical application of opioid-adrenergic combination therapy is not extensive despite its potential benefits. The development of therapeutic approaches that exploit the combination of opioids and α_2-adrenergic agonists is currently limited by a lack of mechanistic knowledge on how these drugs interact at the spinal level.

In rodents, co-administration of morphine and clonidine produces a greater-than-additive (i.e. synergistic) analgesic effect that is mediated primarily at the spinal level (Ossipov et al., 1990a). This adrenergic-opioid synergy can potentially improve efficacy and/or reduce side effects, thus improving the therapeutic index (i.e. potency ratio of undesired to desired effects). Previous studies have identified δ opioid receptors (DOR) and α_{2A}ARs as a receptor pair with synergistic properties (Stone et al., 1997; Guo et al., 2003). In recent years, DOR has been the focus of intense research that revealed its ability to interact with the μ opioid receptor (MOR) in a manner that affects the morphine response in the spinal cord (Costantino et al., 2012). In order to understand how these interactions take place, we investigated the role of DOR and α_{2A}AR in spinal opioid antinociception and opioid-adrenergic synergy.

The studies described in this thesis will:

1. Examine the role of DOR in spinal morphine antinociception.

2. Determine if DOR is necessary and sufficient to mediate opioid-adrenergic synergy.

3. Investigate the role of α_{2A}AR in spinal opioid-adrenergic synergy and opioid antinociception.

The findings reported in these studies have resulted in an improved understanding of the interaction between adrenergic and opioid drugs at the spinal level, which led us to propose a unifying model to explain these receptor interactions at the molecular level.

BACKGROUND

Defining pain

The burden of pain

Pain is the leading reason for seeking health care. It is a debilitating condition that impairs one's quality of life and the ability to carry out a productive life. Patients living with persistent chronic pain often develop co-morbidities (e.g. sleep disturbances, cognitive impairment, depression, suicidal ideation, loss of mobility) that exacerbate their disability and impair their productivity. The cost of health care and lost productivity is estimated at $560-630 billion per year in the United States (Medicine, 2011), and $56-60 billion per year in Canada according to the Canadian Pain Society. Current treatments for acute and chronic pain often fail to provide adequate pain relief due to a lack of drug efficacy or intolerable side effects. There is therefore an unmet need for better analgesic therapies in order to improve treatment outcomes for patients.

Pain vs. nociception

The International Association for the Study of Pain (IASP) has defined the complex sensation we call pain as: "An unpleasant sensory and emotional experience associated with actual or potential tissue damage, or described in terms of such damage" (IASP Taxonomy Working Group, 2011). This broad definition encompasses a multitude of painful states, ranging from the pain experienced following an injury causing tissue damage, to idiopathic pain syndromes and even psychogenic pain. The term nociception is used to describe "the neuronal process of encoding noxious stimuli" (IASP Taxonomy Working Group, 2011). It is used to distinguish between the subjective experience of pain and the process by which the nervous system encodes a nociceptive stimulus, i.e. "an actually or potentially tissue-damaging event transduced and encoded by nociceptors" (IASP Taxonomy Working Group, 2011). Just as pain is not necessarily the result of nociception, nociception does not necessarily result in pain. Nociceptive pain is defined as the "pain that arises from actual or threatened damage to non-neuronal tissues and is

due to the activation of nociceptors" (IASP Taxonomy Working Group, 2011). Its primary purpose is to make the organism aware of the threat and orchestrate appropriate protective actions such as guarding an injured limb, escaping from the stimulus, and avoiding the stimulus in the future. These behaviors can be measured in animals as a proxy of the nature and intensity of the nociceptive stimulus. For example, the time it takes for a mouse to withdraw its hind paw from a source of heat indicates how sensitive the mouse is to this stimulus, and if manipulating other factors (e.g. administering analgesic drugs) influences this sensitivity. The study of nociception in animals has greatly contributed to our understanding of pain.

The neurobiology of pain

The nociceptive circuit

The neural circuit involved in the detection of a nociceptive stimulus coordinates all the steps involved in the sensation and reaction to a nociceptive stimulus (Figure 1). For example, when we step on a sharp object, this noxious stimulus activates cutaneous nociceptors that transduce the mechanical stimulus into an electric signal along its axon. The information is then relayed at the spinal cord where it is integrated. There, the nociceptive signal is transmitted to a projection neuron that takes ascending pathways to reaching the thalamus and the brainstem. The best-characterized pathways are the spinothalamic tract and the spinoreticular tract. From the thalamus, the information is then relayed to four main cortical regions: the somatosensory cortex (SI) and the secondary somatosensory cortex (SII), which are responsible for the localization of the pain stimulus, and the anterior cingulate cortex (ACC) and the insula, which are responsible for the affective component of pain. Spinal nociceptive information relayed to the reticular formation reaches the periaqueductal grey (PAG), which is an early relay of one of the main descending inhibitory pathways that sends projections back to the dorsal horn of the spinal cord to modulate pain signal.

Additionally, at the spinal cord, the incoming nociceptive signal is relayed directly or indirectly to spinal motor neurons to coordinate a withdrawal reflex that will move the threatened body part away from the stimuli.

The environment, genetic background, psychological dispositions and many other biological factors can all influence the perception of pain. Moreover, the ability to modulate nociceptive signals at each level of the nociceptive circuit renders the pain experience highly malleable. The next sections of this introduction will focus on nociceptive processing at the level of primary nociceptors and the spinal cord since these are most relevant to the work presented in this thesis.

The primary nociceptors

Sensory neurons convey touch, proprioception, itch, pain and temperature information from organs in the periphery to the central nervous system. The soma of these bipolar neurons are located in dorsal root ganglia (DRG) from which one axonal projection reaches out to the periphery while the other projects to the spinal cord. DRG neurons are heterogeneous in nature and those capable of transducing and encoding a nociceptive stimulus are termed nociceptors. Depending on the method of study, nociceptors can be classified according to different criteria: morphology, adequate stimulus modality, neurochemical markers or electrophysiological properties, reflecting their functional diversity. Sensory neurons can be classified in three subtypes based on their conduction velocity:

Aβ fibers are large myelinated fibers that rapidly conduct action potentials. They primarily carry light touch and proprioceptive information.

Aδ fibers are medium in size and lightly myelinated thereby conducting action potentials at a slower rate. These fibers are excited by different modalities: mechanonociceptors respond to noxious mechanical stimulation and polymodal nociceptors respond to a combination of mechanical, thermal or chemical nociceptive stimuli.

C fibers are the smallest of the fibers, are not myelinated and have the slowest action potential conduction velocity. The vast majority of these fibers respond to nociceptive stimuli, although a small proportion transduce itch or pleasant touch. Each fiber can respond to one or more pain modalities (mechanical, heat, cold, chemical, etc.).

For all three DRG neuron subtypes, somal size is proportional to fiber size. The difference in conduction velocity between nociceptors is experienced as a first, rapid, sharp and localized pain mediated by Aδ fibers, and a second delayed, diffuse and burning pain mediated by C fibers.

C fiber nociceptors are further classified into two subclasses according to their neurochemical characteristics. DRG neurons expressing the neuropeptides substance P (SP) or calcitonin gene-related peptide (CGRP) belong to the peptidergic class of nociceptors and typically express the transient receptor potential vanilloid 1 (TRPV1) protein. On the other hand, non-peptidergic nociceptors are labeled by positive binding of the plant protein isolectin IB4. In mice, these two subpopulations are distinct: there is almost no overlap between SP/CGRP and IB4 labeling (Molliver et al., 1997). However, in rats, these markers overlap significantly making the two subpopulations less distinguishable (Price and Flores, 2007).

Integration and relay of nociceptive input in the spinal cord

General organization

The grey matter of the spinal cord was divided in ten parallel cell layers, termed laminae, by Rexed (1952) based on the difference in shape, size and density of their neurons (Figure 2A). This division is still used to describe the spinal cord because these morphological subdivisions closely correspond to a functional subdivision. Taking into account the innervation pattern of lamina II by primary afferent neurons, this layer was further subdivided into lamina II inner (IIi) and lamina II outer (IIo). Nociceptive information is mostly processed in laminae I-II

in the dorsal horn of the spinal cord, although some pain processing also occurs in lamina III-VI.

The different elements of the neuronal circuit in the spinal cord form a complex network of synaptic connections between the nociceptors, interneurons, projection neurons and descending axons. How these neurons are interconnected and how they integrate the nociceptive signal is a subject of intense study. This section is meant to provide a general overview.

Primary afferent inputs

DRG neurons send their afferent projections to the dorsal horn of the spinal cord (Figure 2B). Most Aδ and C nociceptors innervate lamina I and II, while other sensory neurons travel deeper to reach laminae IIi-V. The two subpopulations of C fibers have different innervation patterns in the spinal cord: while the non-peptidergic nociceptors innervate lamina IIi, the peptidergic nociceptors preferentially innervate lamina I-IIo and occasionally send projections in deeper laminae. Nociceptors make excitatory glutamatergic synaptic connections onto projection neurons and interneurons in the spinal cord. The peptidergic subpopulation also releases SP and CGRP on their target neurons, but other DRG neurons can also release different neuropeptides (e.g. neuropeptide Y, somatostatin, etc.).

Projection neurons

Projection neurons in the pain pathway originate from lamina I and throughout laminae III-VI. They receive inputs from primary afferent neurons, interneurons and descending inhibitory neurons. Their axons cross the midline and travel rostrally in the spinal cord white matter to reach the brainstem and thalamic nuclei.

Interneurons

Two main categories of interneuron coexist in the superficial laminae (I-III) of the spinal cord. The excitatory interneurons use the neurotransmitter glutamate to

relay their signals, while the inhibitory interneurons release γ-aminobutyric acid (GABA) and/or glycine to inhibit their targets. Some excitatory interneurons also express the neurokinin (NK)-1 receptor for SP (Littlewood et al., 1995). Together, these two categories of interneuron participate in the integration of sensory nociceptive information: they serve as an intermediate relay between primary afferent neurons and projection neurons where they can amplify or reduce the nociceptive signal.

Descending inhibitory neurons

The medullary raphe nuclei and the locus coerulus are sending descending serotonergic and noradrenergic neurons, respectively, to the spinal cord. These nerve terminals are present at high density in laminae I and II, and at lower density in deeper laminae of the dorsal horn. Serotonin and noradrenaline are released perisynaptically rather than directly at synaptic sites, and thus play a modulatory role on neuronal excitability. The release of these monoamine neurotransmitters from their nerve terminals has an inhibitory effect on spinal cord neurons and primary afferent nerve terminals (Figure 3).

Analgesic pharmacology

When pain is unbearable, it needs to be stopped. Multidisciplinary approaches combining pharmacology, surgery, psychotherapy, physiotherapy, etc. are optimal for the management of pain. Clinicians can count on a large assortment of drugs to ameliorate pain through different mechanisms. The major analgesic drug classes are nonsteroidal anti-inflammatory drugs (NSAIDs), opioids and adjuvants (neurolytics, antidepressants, etc.). However, each drug is associated with side effects that raise concerns for safety and tolerability. The ratio between the dose causing side effects or toxicity and the dose causing a therapeutic effect is termed the therapeutic index. When this index is low, it is difficult to administer enough analgesic drugs to attain a therapeutic effect without causing adverse effects. Unfortunately, this is often the reason why patients do not receive adequate pain relief. The work presented in this thesis centers on two strategies to improve analgesic pharmacology: combination therapy and spinal drug delivery.

Spinal analgesic drug delivery

The spinal cord is a strategic site of action for analgesic drugs since it is an important relay for nociceptive signals (Figure 3). Epidural or intrathecal drug delivery via permanent subcutaneous pumps has emerged as a treatment avenue for persistent pain relief in patients refractory to conventional pain treatments or when other routes of administration can produce adequate analgesia only at doses associated with intolerable side effects. Drugs mediating analgesia at the spinal level are thus delivered at lower doses directly at the site of action and their concentration decreases as the drug diffuses away from the site of action, thereby reducing side effects. Combination therapy presents the advantage of producing analgesia by targeting different mechanisms. The potential benefits of co-administering analgesics spinally include an improved analgesic efficacy, reduced side effects and less dose escalation, especially with opioids (Walker et al., 2002).

Morphine is the most common analgesic used for intrathecal drug delivery, and its safety and efficacy have been validated for the treatment of severe nonmalignant pain over a 24 month period (Anderson and Burchiel, 1999). When administered intrathecally, morphine tolerance can develop, which results in dose escalation over time until analgesia is lost and/or side effects become intolerable. Common side effects arising from spinal morphine delivery include pruritus, nausea and vomiting, urinary retention, constipation, edema, sedation, respiratory depression and hyperalgesia (Ruan, 2007).

Clonidine, an α_2AR receptor agonist, is used spinally for perioperative pain relief and intractable cancer pain with a neuropathic component (Eisenach et al., 1995). Spinal clonidine side effects include nausea, dizziness, hypotension, sedation and dry mouth. A study showed that the duration of clonidine analgesia in continuous intrathecal clonidine administration for the prolonged treatment of pain is in the range of a few weeks, which limits its long-term use (Ackerman et al., 2003). In patients with chronic pain, the combination of clonidine with an opioid produces superior analgesia compared to either drug alone treatments and reduces the need for supplemental opioid administration (Walker et al., 2002). Therefore, spinal

clonidine is recommended as a second-line analgesic for the treatment of chronic pain when combined with an opioid.

The clinical benefits of opioid-adrenergic combinations remain largely underexploited because the development of new therapies is hindered in part by a lack of understanding of the underlying mechanism.

Opioid Receptors

The opioid receptor family

Opium, the extract from poppy plants with both analgesic and euphoric properties, had already been used for millennia across Europe and Asia before a German chemist, Sertürner, isolated its active component in 1806, naming it morphine after the god of dreams, Morpheus (Brownstein, 1993). Since then, the search for better opioid analgesics has led to the discovery of the opioid receptor family, the endogenous opioid system and the design of new opioid compounds.

Three distinct receptor subtypes have been identified pharmacologically and correspond to the three cloned opioid receptors: μ-, δ- and κ- opioid receptors, abbreviated MOR, DOR and KOR, respectively. All three receptors have the potential to mediate analgesia. MOR is the most studied opioid receptor since its activation by morphine or other MOR-selective agonists results in a robust analgesic effect. Unfortunately, it also mediates unwanted side effects such as respiratory depression, constipation, dependence, tolerance, etc. (Matthes et al., 1996; Williams et al., 2013). Currently, clinically available opioid analgesics are MOR agonists. In recent years, DOR has emerged as a promising analgesic target for the treatment of chronic pain (Pradhan et al., 2011).

MOR and DOR can mediate synergistic interactions with α_2AR agonists (Ossipov et al., 1990b; Roerig et al., 1992). Since this thesis explores the spinal mechanisms underlying opioid-adrenergic analgesic interactions, the review on opioid receptors will focus on MOR and DOR in DRG and the spinal cord. A list of MOR and DOR ligands cited in this dissertation is provided in Table 1.

Distribution of MOR and DOR in DRGs and spinal cord and their antinociceptive action

MOR and DOR are expressed throughout the nervous system as well as in non-neuronal cells. The background provided in this section focuses on the anatomical distribution of MOR and DOR in DRGs and the spinal cord, and the implication for antinociception.

MOR

The pattern of MOR-selective radioligand binding is consistent across several autoradiographic studies: MOR binding sites concentrate in the superficial dorsal horn (laminae I-II) of the spinal cord although lower binding density is also detected throughout the rest of the spinal grey matter (Goodman et al., 1980) (Zajac et al., 1989; Besse et al., 1990; Gouardères et al., 1991; Stevens and Seybold, 1995). In the dorsal horn, the labeling is found mostly in LI and LIIo on both neuronal soma and within the surrounding neuropil (Gouardères et al., 1991). Between 60-76% of binding intensity is lost following a dorsal root rhizotomy – which consists in cutting the dorsal root of the spinal nerve – indicating that the majority of MOR binding sites are from afferent DRG nerve terminals (Zajac et al., 1989; Besse et al., 1990; Gouardères et al., 1991; Stevens and Seybold, 1995).

In situ hybridization studies have localized MOR mRNA in DRG neurons and in laminae II, V, VII neurons, but not in lamina I (Mansour et al., 1994a; Mansour et al., 1994b). In DRG, 41% of MOR expressing neurons also express mRNA coding for the SP precursor protein, preprotachykinin A (PPTA) (Minami et al., 1995), suggesting that an important subpopulation of DRG neurons responding to MOR agonists are peptidergic fibers.

The immunohistochemical MOR staining pattern matches closely the distribution of MOR binding sites reported in autoradiographic studies. Dense MOR-immunoreactivity (ir) has been described in laminae I-II of the spinal cord with a significant decrease in staining intensity in LI and LIIo following dorsal root rhizotomy or neonatal capsaicin treatment (Arvidsson et al., 1995b; Ding et al.,

1996; Abbadie et al., 2002). In DRGs, MOR-ir is localized in small- and medium-sized neurons and a subset of these neurons colocalize with SP-ir and TRPV1-ir (Arvidsson et al., 1995b; Scherrer et al., 2009).

DOR

Autoradiographic studies show that DOR binding sites are detected throughout the spinal cord grey matter, but concentrated in laminae I-II of the spinal cord (Goodman et al., 1980; Zajac et al., 1989; Besse et al., 1990; Gouardères et al., 1993; Stevens and Seybold, 1995; Mennicken et al., 2003). Consistent with a contribution of DOR from primary afferent DRG neurons, a large proportion of DOR binding sites are lost in the dorsal horn of the spinal cord following dorsal root rhizotomy (Goodman et al., 1980; Zajac et al., 1989; Besse et al., 1990; Stevens and Seybold, 1995).

In situ hybridization studies in the spinal cord show that DOR mRNA is located in neuronal soma across the grey matter, from the dorsal to the ventral horn (Cahill et al., 2001a; Mennicken et al., 2003). In DRGs, small, medium and large neurons can express DOR, but the exact neuronal subtype distribution varies between studies (Mansour et al., 1994a; Minami et al., 1995; Mennicken et al., 2003; Wang et al., 2010).

There is a similar lack of consensus among immunohistochemical studies. Arvidsson et al. (1995a) reported intense DOR-ir labeling in the superficial laminae of the dorsal horn, as well as an intermediate DOR-ir staining in the ventral horn and around the central canal. The staining was exclusively in fiber-like structures and colocalized extensively with SP in the dorsal horn (Zhang et al., 1998; Riedl et al., 2009). Similarly, DOR-ir staining was found in small, medium and large DRG neurons, of which an important subset also expressed SP (Zhang et al., 1998). This immunohistochemical staining parallels the pattern observed with the autoradiographic methods mentioned above. Others have reported DOR-ir staining in spinal cord soma throughout the grey matter and

concentrated in the neuropil of laminae I-II, a pattern that parallels DOR mRNA distribution in the spinal cord (Cahill et al., 2001a; Mennicken et al., 2003).

The lack of consensus around the location of DOR was attributed to the specificity of the antibodies used in these studies and the possibility that DOR epitopes may be expressed differently in different cells (Cahill et al., 2001a). To circumvent the specificity issues of antibody approaches, Scherrer et al. (2006) designed a transgenic mouse line expressing a green fluorescent protein (GFP) tag attached to DOR C-terminal end (GFP-DOR). In these mice, DOR was distributed in small non-peptidergic or large DRG neurons, but not in SP-ir or MOR-ir neurons (Scherrer et al., 2009). Because these results challenged some fundamental assumptions about DOR, their validity in WT mice was addressed by Wang et al. (Wang et al., 2010). Using a combination of in situ hybridization, immunohistochemical staining and single cell PCR, they reported that subsets of peptidergic and non-peptidergic neurons express DOR. The exact cellular distribution of DOR is still debated and there is still more to learn about this receptor before consensus is reached.

Antinociceptive action of MOR and DOR

Given their location in DRG and the spinal cord, MOR and DOR are strategically located to block the transmission of nociceptive signals (Figure 3). In rodents, spinal delivery of MOR and DOR agonists has antinociceptive effects in a multitude of behavioral assays (Hylden and Wilcox, 1982; Pick et al., 1991). Activation of these receptors can block the release of neurotransmitters from the pre-synaptic nerve terminal (Sullivan et al., 1987; Li and Eisenach, 2001; Beaudry et al., 2011). Recently, both receptors have been shown to inhibit heat and mechanical nociception via their direct inhibition of SP release in the spinal cord (Normandin et al., 2013). Direct actions of MOR and DOR agonists on post-synaptic projection neurons can also block nociceptive transmission.

Reports of interactions between the effect of MOR and DOR ligands are numerous (reviewed in (Costantino et al., 2012). The extensive co-expression of

MOR and DOR in the spinal cord, especially in SP-containing nerve terminals (Wang et al., 2010), suggests that these interactions occur at the cellular level, possibly through actions at a MOR-DOR heteromer (Costantino et al., 2012).

Adrenergic Receptors

Biosynthesis of norepinephrine

Norepinephrine (NE, also known as noradrenaline) is a catecholamine neurotransmitter used by descending noradrenergic neurons to relay their inhibitory signal in the spinal cord by activating adrenergic receptors. The stepwise process leading to the biosynthesis of NE takes place in the nerve terminal where the enzymes necessary for its biosynthesis are present. First, the amino acid tyrosine is converted to L-3,4 dihydroxy phenylalanine (L-DOPA) by tyrosine hydroxylase (TH) and then to dopamine (DA) by DOPA decarboxylase. Next, dopamine β-hydroxylase (Dbh) converts DA to NE. The presence of Dbh therefore differentiates dopaminergic from noradrenergic neurons. The catecholamine analogue 6-hydroxydopamine (6-OHDA) is a potent neurotoxin that is used to selectively eliminate catecholaminergic neurons to study the function of these neurons (Kostrsewa, 1974; Bové, 2005).

The adrenergic receptor family

Receptors mediating the physiological effects of NE and epinephrine subdivide into the α and β adrenergic receptor (AR) subtypes (Alquist, 1948). The α family is further divided into α_1 and α_2 AR and there are three α_2AR subtypes: α_{2A}AR, α_{2B}AR and α_{2C}AR. The poor subtype selectivity of α_2AR ligands makes it difficult to determine the function of each receptor subtype and legitimize the use of genetically modified mice to this end. A list of α_2AR ligands cited in this dissertation is provided in Table 2.

In order to understand the mechanism underlying opioid-adrenergic synergy, we decided to study the α_{2A}AR subtype as it was identified as a receptor capable of mediating synergy with opioid agonists (Stone et al., 1997; Guo et al., 2003). The

following section will briefly review the anatomical distribution and antinociceptive role of this receptor in the spinal cord.

Distribution and antinociceptive action of α_{2A}AR in DRGs and the spinal cord

Autoradiographic studies revealed that α_2AR binding sites are concentrated in the superficial laminae of the dorsal horn (Unnerstall, 1984; Seybold, 1984). The α_{2A}AR is the predominant mediator of the antinociceptive effect of α_2AR agonists at the spinal cord, although α_{2C}AR is also involved for some agonists (Kable, 2000). Elsewhere in the central nervous system, the α_{2A}AR mediates the analgesic as well as antihypertensive and sedative effects of the α_2AR agonists clonidine and dexmedetomidine, which limit their use as analgesic agents (MacMillan et al., 1996; Lakhlani et al., 1997). Therefore, spinal administration of α_2AR agonists is a preferred strategy to avoid unwanted side effects while benefiting from their analgesic effects.

There is substantial evidence showing that the activation of α_2AR on nociceptors inhibits the transmission of nociceptive signals and that this is one of the mechanisms by which α_2AR mediates antinociception at the spinal cord (reviewed in Fairbanks et al., 2009). In DRGs, α_{2A}AR mRNA is found in approximately 20% of neurons and almost half of these neurons also express CGRP mRNA (Shi et al., 2000). The detection of α_{2A}AR immunoreactivity (ir) in 54% of DRG neurons, which were smaller than non-labeled neurons, further supports their presence in nociceptors (Gold et al., 1997). Stone et al. (1998) found a significant reduction of α_{2A}AR-ir and SP-ir in the dorsal horn after performing dorsal rhizotomy or neonatal capsaicin treatment. Together, these studies suggest that α_{2A}ARs are present in DRG neurons, including peptidergic nociceptors (Figure 3).

In situ hybridization studies showed that neurons expressing α_{2A}AR were found in all layers of the spinal cord, but they were most abundant in laminae I, II, V, VIII and IX (Nicholas et al., 1993; Shi et al., 1999). However, depending on the

antibody used, α_{2A}AR-ir neurons were identified in neurons around the central canal (lamina X), and in laminae I-IV of the spinal cord (Rosin et al., 1993) or exclusively on SP-ir primary afferents in the superficial dorsal horn (Stone et al., 1998; Riedl et al., 2009). The recognition of distinct epitopes on the α_{2A}AR could explain the staining discrepancies observed in these studies. Functional data support the expression of α_{2A}AR in both spinal and DRG neurons, but the poor subtype selectivity of the pharmacological agents available for the study of α_2AR limits the interpretation of these results (Fairbanks et al., 2009).

α_{2A}AR located on noradrenergic nerve terminals are presumably autoreceptors responsible for the detection of released NE and the inhibition of vesicle release. However, the presence of α_{2A}AR on descending noradrenergic nerve terminals has not reached consensus. Lesioning of descending noradrenergic fibers did not result in a decrease in α_2AR binding sites in the spinal cord (Howe and Yaksh, 1982; Roudet et al., 1994). This is further supported by the lack of colocalization between α_{2A}AR-ir and TH-ir or Dbh-ir (Stone et al., 1998). These studies would thus argue against the presence of α_{2A}AR on noradrenergic nerve terminals. However, functional evidence demonstrated that clonidine can inhibit NE release from spinal cord synaptosome preparations, but knocking down spinal α_{2A}AR decreased the effect of clonidine (Li et al., 2000). Furthermore, Gilsbach et al. (2009) generated mice that selectively express α_{2A}AR in adrenergic cells, but not in non-adrenergic cells, and showed that inhibition of NE release was normal compared to total α_{2A}AR-KO mice. Therefore, α_{2A}AR are probably expressed in descending noradrenergic neurons, albeit at levels too low to be detected with the above anatomical methods, and act as autoreceptors to inhibit NE release (Figure 3).

Opioid and α_2 adrenergic receptor coupling and signaling

Opioid receptors and α_2AR belong to the G protein-coupled receptor (GPCR) superfamily of transmembrane receptors. Members of this family share a common general structure: they have an extracellular N-terminal segment, seven

membrane-spanning domains and an intracellular C-terminal segment (Ji et al., 1998). The notion that GPCRs can form homo- and hetero- oligomeric receptor complexes is now widely accepted. These interactions contribute to the functional diversity of GPCRs and have implications for intracellular coupling, downstream signaling and regulatory processes (Terrillon and Bouvier, 2004).

GPCRs are coupled to heterotrimeric GTP-binding proteins (G proteins), which consist of three subunits: α, β and γ. Upon GPCR activation, G proteins will activate a cascade of signaling events that will mediate the cell response. The steps involved in G protein activation and inactivation are as follows: 1) ligand-induced conformational changes in the GPCR promote the exchange of GDP to GTP on the Gα subunit; 2) the GTP-bound Gα subunit dissociates from the G$\beta\gamma$ subunit; 3) both moieties can engage in separate signaling cascades; 4) the intrinsic GTPase activity of the Gα subunit eventually hydrolyses GTP to GDP, which causes the GDP-bound Gα subunit to re-assemble with the G$\beta\gamma$ subunit and deactivate the heterotrimeric G protein complex.

There are numerous Gα subtypes grouped into four main categories: $G\alpha_s$, $G\alpha_{q/11}$, $G\alpha_{12}$ and $G\alpha_{i/o}$. Different signaling cascades can be activated by the G protein complex depending on the Gα subunit subtype associated to it. Opioid receptors and α_2AR are preferentially coupled to pertussis toxin (PTX)-sensitive $G\alpha_{i/o}$ subunits. $G\alpha_{i/o}$ inhibits the production of cAMP by adenylyl cyclase, which counteracts the activation of the cAMP-dependent protein kinase A (PKA). The free G$\beta\gamma$ subunit can also act as a signaling molecule and activate downstream signaling pathways, like phospholipase C (PLC), or modulate ion channels by activating G protein-coupled inwardly-rectifying K^+ channels (GIRKs) or inhibiting voltage-gated Ca^{2+} channels (VGCCs).

The GPCR coupling dogma has been questioned and challenged over the past 20 years as studies demonstrated that GPCR signaling can be more complex than a simple on-off switch coupled to only one type of downstream signaling. Instead, each GPCR can couple to different G proteins depending on the extracellular and

intracellular contexts. Moreover, GPCRs can also elicit G protein-independent intracellular effects (Dupré and Hébert, 2006). This is a field of intense and exciting research.

Opioid-Adrenergic interactions

Synergy

In rodents, spinal co-administration of opioid and α_2AR agonists produces analgesia and they interact in a greater-than-additive manner, i.e. synergistically, when co-administered. Because the interaction is more important when the drugs are administered intrathecally compared to intravenously, it has been proposed to be mediated largely at the level of the spinal cord (Ossipov et al., 1990a). In order to gain mechanistic insight, it is necessary to know the receptor subtypes required for synergy.

DOR-mediated synergistic interactions

[D-Ala^2]-deltorphin II (DeltII), a DOR-selective peptide agonist, can synergize with the α_2AR agonists clonidine (Overland et al., 2009), ST-91 (Stone et al., 2007), moxonidine (Fairbanks et al., 2000b; Fairbanks et al., 2002), and UK 14,304 (Stone et al., 1997) when co-administered at the spinal cord in rodents. Similarly, another DOR-selective agonist, [D-Pen^2, D-Pen^5]enkephalin (DPDPE), has been shown to synergize with clonidine (Ossipov et al., 1990b; Roerig et al., 1992), norepinephrine (Roerig et al., 1992), and UK 14,304 (Guo et al., 2003), and this latter synergistic interaction persisted in MOR-KO mice (Guo et al., 2003). These studies were previously interpreted as opioid-adrenergic interactions resulting in analgesic synergy made possible by DOR activation since they could also occur in the absence of MOR. However, reports that DeltII and DPDPE retain their antinociceptive action in DOR-KO mice and that MOR mediates this effect questions the selectivity of DOR agonists (Scherrer et al., 2004; van Rijn et al., 2012). This could mean that the opioid-adrenergic synergistic interactions studied with DOR agonists are mediated by MOR and therefore justify further evaluation of the role of DOR in these interactions.

MOR-mediated synergistic interactions

Morphine has also been shown to interact synergistically with the α_2AR agonists clonidine (Ossipov et al., 1990a; Roerig et al., 1992; Fairbanks and Wilcox, 1999b), moxonidine (Fairbanks et al., 2000b), norepinephrine (Roerig et al., 1992) and ST-91 (Monasky et al., 1990). The antinociceptive effect of morphine is considered to be mediated through the MOR (Matthes et al., 1996), a finding that is consistent with its relatively selective affinity for MOR in expression systems (Raynor et al., 1994). Taken together, these studies would suggest that MOR mediates morphine's synergistic interactions with α_2AR agonists. Nevertheless, MOR agonists do not necessarily interact synergistically with α_2AR agonists. Interaction of the MOR-selective peptide agonist [D-Ala^2, *N*-Me-Phe^4, Gly-ol^5]-enkephalin (DAMGO) is sub-additive with moxonidine or NE (Roerig et al., 1992; Fairbanks et al., 2000b), additive or synergistic with clonidine (Roerig et al., 1992; Roerig, 1995), and synergistic with UK 14,304 (Stone et al., 1997). These differences could be explained by the way different MOR agonists activate the receptor.

Interactions between MOR and DOR have been shown to modulate morphine, but not DAMGO, responses *in vivo* and *in vitro* (Costantino et al., 2012). For example, the cellular response following morphine treatment is more potent in cells co-expressing MOR and DOR rather than MOR alone (Yekkirala et al., 2010). Furthermore, DOR-selective ligands can potentiate morphine analgesia *in vivo* (Gomes et al., 2004), and DOR is involved in the development of analgesic tolerance to morphine (Zhu et al., 1999). Morphine also upregulates the expression of surface DOR through its action at the MOR (Cahill et al., 2001b; Morinville et al., 2003; Gendron et al., 2006). It is currently unknown whether DOR participates in morphine's synergistic interaction with α_2AR agonists.

α_2AR receptor subtypes mediating synergistic interaction with opioids

Due to the lack of selectivity of α_2AR agonists and antagonists, the identification of α_2AR mediating opioid-adrenergic synergistic interaction was not possible before the advent of gene targeting in mice. Three opioid-adrenergic combinations were tested in a mouse line with a dysfunctional α_{2A}AR due to a targeted point mutation, the D79N-α_{2A}AR mice (MacMillan et al., 1998). Using these mice, it was shown that the synergistic interaction between UK 14,304 and DeltII or DAMGO was mediated by the α_{2A}AR (Stone et al., 1997). In contrast, the α_{2A}AR is not necessary for the synergistic interaction between moxonidine and DeltII, which is instead mediated by the α_{2C}AR (Fairbanks et al., 2002). Another α_2AR agonist, ST91, interacts synergistically with DeltII in D79N-α_{2A}AR mice and α_{2C}AR-KO mice (Stone et al., 2007). This suggests that either ST91 is versatile and can produce synergy via both α_{2A}AR and α_{2C}AR, or that α_{2B}AR is mediating this interaction. Thus, depending on the agonist used, the α_{2A}AR and the α_{2C}AR can mediate synergistic interactions. However, the α_2AR subtype(s) involved in the synergistic interaction between clonidine, the most clinically relevant α_2AR agonist, and morphine or DeltII has not been uncovered yet.

Opioid-adrenergic synergy requires the activation of PKC

Little is known about the downstream signaling mechanism(s) involved in the synergistic interaction between opioid and adrenergic agonists. To date, a few studies attempted to identify a signaling pathway specific to the synergistic interaction. Inhibition of $G_{i/o}$ with PTX is not sufficient to turn the synergistic interaction into an additive one (Roerig and Howse, 1996; Wei et al., 1996). Furthermore, increasing cAMP levels or inhibiting PKA did not affect the synergistic interaction between morphine-clonidine or DeltII and clonidine, which rules out PKA, the main downstream target of $G_{i/o}\alpha$, from playing a role in synergy (Wei and Roerig, 1998; Overland et al., 2009). The inhibition of L- or N-type VGCC did not affect synergy, but the simultaneous inactivation of $G_{i/o}\alpha$ and N-type VGCC rendered morphine-clonidine interaction additive (Wei et al.,

1996). Moreover, blocking P-type VGCC changed the interaction from synergistic to additive (Roerig and Howse, 1996). These results suggest that N- and P- type VGCCs are involved in synergy, but their exact role is unknown.

Protein kinase C (PKC) activation has been specifically implicated in opioid-adrenergic synergistic interactions. Inhibitors of PKC administered i.t. have been shown to block the synergistic interaction between morphine-clonidine (Wei and Roerig, 1998) and DeltII-clonidine (Overland et al., 2009), but not the antinociceptive effect of each drug alone. Using an assay measuring K^+-induced CGRP release from spinal cord slices, Overland et al. (Overland et al., 2009) were able to reproduce DeltII-clonidine synergy and its blockade by PKC inhibitors. Since Gβγ can activate PLC, which then generates second messengers capable of activating PKCs, the authors tested if this pathway was involved. The effect of DeltII, clonidine and their combination was lost when inhibiting PLC. This suggests that PLC mediates the antinociceptive effect of DeltII and clonidine and that it is upstream of PKC in mediating opioid-adrenergic synergy. However, the simultaneous presence of both agonists is necessary to activate PKC and further studies are necessary to identify other key elements of this signaling cascade.

RATIONALE OF THE THESIS

The primary objective of this thesis was to explore the roles of DOR and α_{2A}AR in spinal opioid-adrenergic interactions. Since the pharmacological agents available to study these receptors have limited selectivity profiles, we used DOR- and α_{2A}AR- knockout (KO) mouse strains to distinguish between receptor-specific and non-specific drug effects.

FIGURES AND TABLES

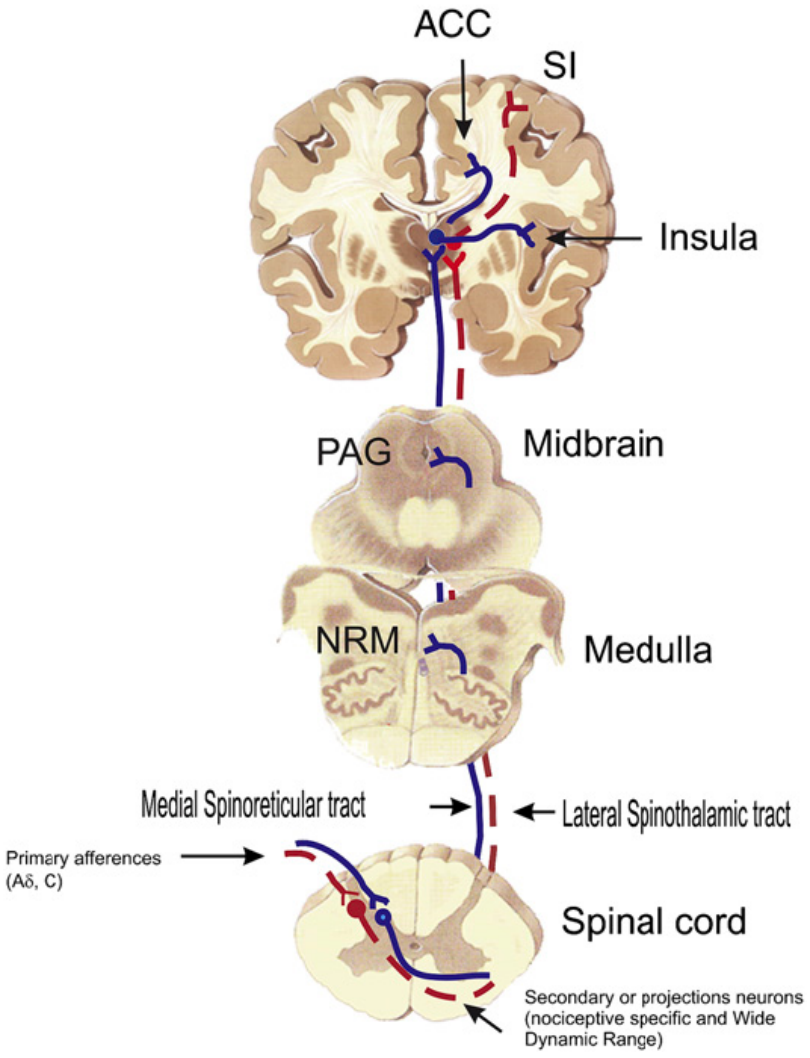

Figure 1: The ascending nociceptive pathway

Nociceptive information is carried from the periphery by primary afferent neurons to the spinal cord where they relay the information to projection neurons, which in turn send the information to the brainstem and thalamus. Neurons from these structures then send the information to sub-cortical and cortical areas involved in the interpretation of the painful signal. Modified from Marchand (2008).

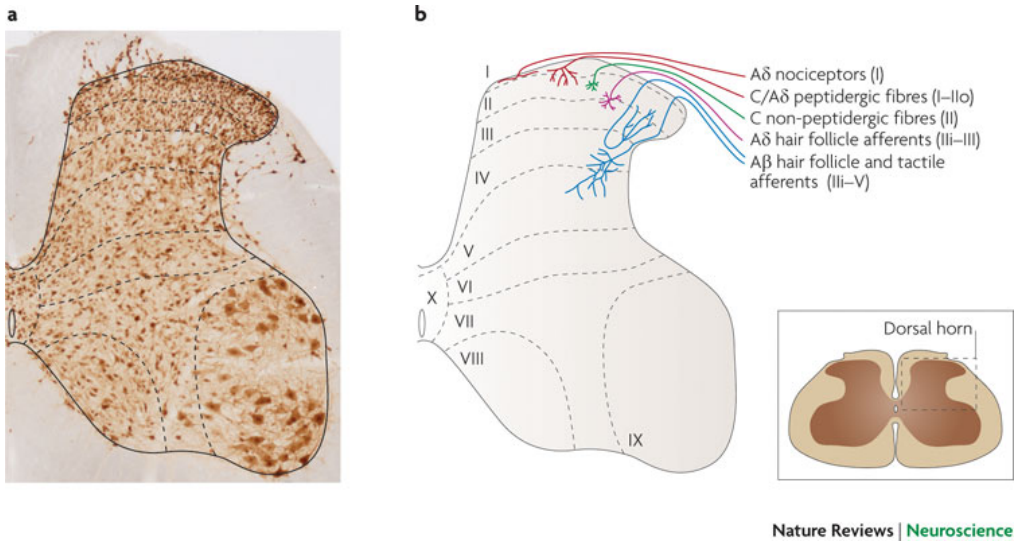

Figure 2: Anatomical organization of the spinal cord

A) A cross-section of a rat lumbar spinal cord immunostained for NeuN, a neuronal marker, showing the distribution of neurons in the grey matter. Dashed lines mark the division between the ten laminae, starting with lamina I in the superficial dorsal horn of the spinal cord (uppermost part on image) and progressing towards the ventral horn (lower part) and then centrally (left). B) Each subtype of primary afferent sensory neuron innervates the dorsal laminae of the dorsal horn following a characteristic pattern. Source: Todd (2010).

A

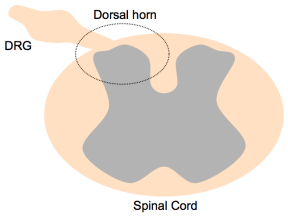
Dorsal horn
DRG
Spinal Cord

B

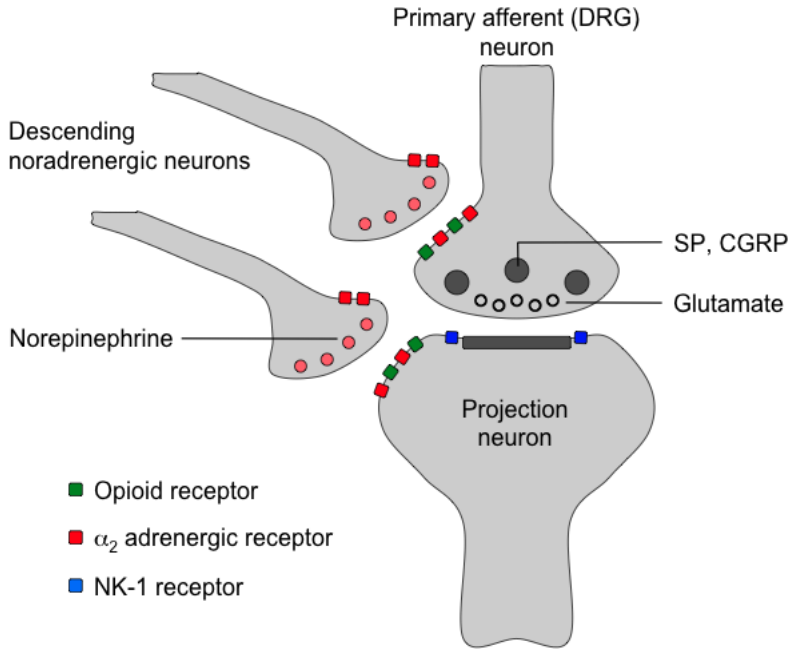
Primary afferent (DRG) neuron
Descending noradrenergic neurons
SP, CGRP
Glutamate
Norepinephrine
Projection neuron
Opioid receptor
α_2 adrenergic receptor
NK-1 receptor

Figure 3: Spinal site of action of opioid and α_2-adrenergic agonists

A) Diagram depicting the connection between the dorsal root ganglion (DRG) and the dorsal horn of the spinal cord. B) Schematic representation of the synaptic connection between a peptidergic primary afferent neuron and a projection neuron in the dorsal horn of the spinal cord. DRG neurons relay sensory information by releasing glutamate and neuropeptides such as SP and CGRP. Glutamate can activate ionotropic receptors that will depolarize second order neurons and trigger an action potential, resulting in the relay of nociceptive information, while neuropeptides have a modulatory action on the excitability of the projection neuron. Agonists activating opioid or α_2-adrenergic receptors located on primary afferent neurons and projection neurons can inhibit the transmission of nociceptive information. α_2-adrenergic receptors located on descending noradrenergic nerve terminals act as autoreceptors and inhibit norepinephrine release via a negative feedback loop.

Table 1: Commonly used MOR and DOR receptor ligands and the main effects of their agonists in rodents.

Receptor	Agonist	Antagonist	Agonist effects
MOR	Morphine DAMGO Fentanyl Hydromorphone	Naloxone Naltrexone CTAP	Analgesia, Respiratory depression, Miosis, Reduced gastrointestinal motility, Addiction, Dependence, Tolerance, Sedation
DOR	Deltorphin II DPDPE SNC80 DADLE	Naloxone Naltrindole TIPP	Analgesia, Seizure, Anxiolytic, Antidepressant

Table 2: Commonly used α_2AR receptor ligands and the main effects of α_2AR agonists in rodents.

Receptor	Agonist	Antagonist	Agonist effects
α_2AR	Norepinephrine Clonidine Moxonidine Dexmedetomidine ST-91	Idazoxan Yohimbine	Analgesia, Hypotension, Sedation, Bradycardia, Anesthetic sparing

Chapter 2:
Materials and Methods

All experiments were carried out using appropriate safety measures as per Canada's Worplace Hazardous Materials Information System (WHIMS) and McGill Environmental Health and Safety guidelines. Hazardous materials were disposed properly to minimize environmental contamination.

Animals

All procedures were approved by the Animal Care Committee at McGill University, and conformed to ethical guidelines of the Canadian Council on Animal Care (see Animal Use Protocol #5487 certificate and animal use training certificate in Appendix A).

C57BL/6, DOR-KO and α_{2A}AR-KO mice

WT: We used commercially available C57BL/6 mice (Charles River, Quebec, Canada) as wild-type (WT) controls.

DOR-KO: Mice with a targeted gene deletion in exon 1 of the delta opioid receptor gene (*Oprd1*) were developed on a mixed C57BL/6 x FVB/129 background (Filliol et al., 2000). Congenic mice backcrossed to a standard C57BL/6 background were obtained from Jackson Laboratory (Bar Harbor, Maine, B6.129S2-*Oprd1*^{tm1}*Kff*/J, stock #007557).

α_{2A}AR-KO: Mice with a targeted gene deletion introducing a premature stop codon in the third transmembrane domain of the α_{2A}AR gene (*Adra2a*) were developed on a mixed C57BL/6 x FVB/129 background (Altman et al., 1999). Congenic mice backcrossed to a standard C57BL/6 background were obtained from Jackson Laboratory (Bar Harbor, Maine, stock #004367).

For the sake of clarity, results from some experiments are presented separately to compare WT mice with DOR-KO or α_{2A}AR-KO mice in Chapters 3, 4 and 5, although these experiments were conducted simultaneously with all three mouse strains.

Colony maintenance

All three strains were bred in house and genotyping controls were performed on parent breeders to monitor the stability of the colony. Male and female mice homozygous for the gene of interest were used to form breeding couples and generate homozygous litters. Mice were maintained on a regular 12 hour light/dark cycle and given access to food and water *ad libitum*.

Genotyping

Genotyping quality controls were performed to confirm the *Adra2A* gene deletion in α_{2A}AR-KO (Peterhoff et al., 2003) and DOR-KO (Jax protocol) mice respectively. WT mice were also assessed to make sure no cross contamination happened during regular colony maintenance procedures. Parent breeders were lightly anesthetized with isofluorane before a 4 mm^2 ear sample was collected with a pair of sharp scissors cleaned with ethanol. Genomic DNA was extracted by heating ear biopsies 15 minutes at 95˚C in a 50 mM NaOH lysis solution. The reaction is then stopped by adding a 1 M TrisHCl, pH 8, 10 mM EDTA neutralizing solution. A polymerase chain reaction (PCR) was performed on the tissue extracts to amplify the genomic DNA segment of interest with a FastStart Taq DNA polymerase (Roche) with pairs of forward and reverse oligonucleotides specific to the WT or transgenic alleles of *Adra2a* and *Oprd1* (see Table 1 for primer sequence). The PCR product is then loaded onto a 1.5% agarose gel in TAE buffer and run through electrophoresis. After soaking for 5 min in a TAE solution with 1% EtBr, the gel was imaged under UV light with a digital imaging system equipped with a cooled CCD camera (ChemiGenius, Syngene). The mouse genotype is confirmed by the presence of an amplified band at the expected molecular weight according to the allele recognized by the primer pair (Table 1).

Drug preparation

Morphine sulphate was purchased from Medisca Pharmaceutica (St-Laurent, QC, Canada). Clonidine HCl and [D-Ala^2, NMe-Phe^4, Gly-ol^5]-enkephalin (DAMGO)

were purchased from R&D Systems (MN, USA) and were dissolved in saline. [D-Ala^2]-deltorphin II (DeltII; R&D Systems) was dissolved in acidified saline (0.9% NaCl, 0.05 M acetic acid). For cumulative dose-response curve experiments evaluating DAMGO and DeltII, due to the short delay between repeated i.t. injections of DAMGO and Delt II were dissolved in artificial cerebrospinal fluid (ACSF, Harvard Apparatus, MA, USA) with 0.05 M acetic acid. In other experiments, morphine, clonidine, DAMGO and DeltII drug stocks were diluted in saline to working concentrations and doses were expressed as total nmol or pmol administered in 5µl. Drug combination doses are graphed as total drug dose (i.e. the sum of each drug) or as the dose of one of the drug present in the combination. (+)-4-[(α*R*)-α-((2*S*,5*R*)-4-Allyl-2,5-di-methyl-1-piperazinyl)-3-methoxybenzyl]-*N*,*N*-diethyl-benzamide (SNC 80; R&D Systems) stock and working solutions were dissolved in saline with 0.3% tartaric acid. Substance P (SP) was purchased from AnaSpec (CA, USA) and concentrated stocks were dissolved in acidified saline. Working SP solutions were dissolved in saline at a total dose of 15 ng alone or mixed with drugs in a 5 µl volume. Naloxone (Tocris) was dissolved in saline and administered i.t. at 1 µg/5 µl. 6-hydroxydopamine (6-OHDA, Sigma) was dissolved in saline with 0.2 mg/ml ascorbic acid and administered i.t. at 20 µg/5 µl. Chelerythrine chloride (Sigma, MO, USA) was dissolved in water and administered i.t. at 1 µg/5 µl. Vehicle solutions consisted of the diluents used for the respective drug tested.

Drug administration

Intrathecal (i.t.) drug administration was done by direct lumbar puncture in a volume of 5 µl according to the method of Hylden and Wilcox (1980) in conscious mice. Briefly, a 50 µl Luer lip syringe (Hamilton, Reno, NV) was loaded with the drug and a 30 gauge 1/2 inch needle was inserted on the tip (Becton Dickinson). Mice were immobilized in a cotton cloth and held by the pelvic girdle while the needle is inserted in the intervertebral space at the L5-L6 level and directed forward inside the vertebral column where 5 µl of drug is delivered.

Intraperitoneal (i.p.) drug administrations were performed with a syringe mounted with an insulin U-100 29½ gauge needle (Becton Dickinson) and drug doses were adjusted so that the final volume administered was 5µl/g of mouse weight.

Behavioral assays

Hot water tail immersion assay

Mice were acclimatized in their home cage to the testing room for at least 45 minutes before testing. Mice were then immobilized in a cotton cloth and the bottom 2/3 of the tail was immersed in a water bath maintained at 46, 49, 52 or 55˚C. The latency for the mouse to withdraw its tail away from the water was recorded with a hand held stopwatch and cutoff time was set to 12 seconds to avoid tissue damage on the tail. To obtain reliable and stable measures, mice were given at least two training sessions on separate days during which baseline measurements were taken three times.

Measurements were taken before (baseline latency) and after drug administration (experimental latency) and results were expressed as the percent of the maximal possible effect (MPE):

$$\% \text{ MPE} = \frac{[\text{Experimental Latency} - \text{Baseline Latency} \times 100]}{12 \text{ sec} - \text{Baseline Latency}}$$

Radiant heat assay

Mice were acclimatized in their home cage to the testing room for at least 45 minutes and then for 60 minutes in individual Plexiglass compartments on the glass surface of the apparatus. Thermal heat threshold was assessed by focusing a heat radiating light beam (IITC Life Science Inc, Woodland Hills, CA) onto the center of the plantar surface of the hind paw and measuring the latency to withdraw the hind paw (Hargreaves et al., 1988). Withdrawal latencies were measured 3 times at 60 minute intervals and the average was calculated. A cutoff of 17 seconds was set to prevent tissue damage.

Mechanical sensitivity

Mice were acclimatized in their home cage to the testing room for at least 45 minutes and then for 60 min in individual compartments on a mesh surface where they were tested. Calibrated von Frey filaments (Stoelting Co., IL, USA) were applied on the plantar surface of the hind paw for 4 seconds or until withdrawal, and the 50% threshold to withdraw (grams) was calculated according to the up-down method (Chaplan et al., 1994). The stimulus intensity ranged from 0.6 to 4.0 g, corresponding to filament numbers 3.84, 4.08, 4.17, 4.31 and 4.56. For each animal, the actual filaments used within the aforementioned series were determined based on the lowest filament required to evoke a positive response followed by 5 consecutive stimulations.

Substance P behavioral assay

Mice were acclimatized in their home cage to the testing room for at least 45 minutes before testing. The antinociceptive action of single drugs and their combination was tested in the substance P (SP) behavioral assay developed by Hylden and Wilcox (1981). Briefly, 15 ng of SP was administered i.t. alone (control) or co-administered with a single drug or a drug combination (experimental) in a volume of 5µl. The number of caudally directed biting, licking and scratching behaviors were counted for 1 min and results are expressed as the percent inhibition of SP-induced behaviors:

$$\% \text{ Inhibition} = \frac{\text{Control} - \text{Experimental}}{\text{Control}} \times 100$$

The control value for each strain represents the average number of SP-induced behaviors elicited by 15 ng of SP in a group of 16-24 mice.

Locomotion assay

Locomotor capacity was measured with an accelerating rotarod (IITC Life Science Inc., CA, USA) equipped with a 3.2 cm diameter rod mouse adapter. Mice were subjected to an acceleration from 0 to 30 rotations per minute over a

90 seconds period, followed by an additional 210 seconds of constant maximal speed. The latency of the mouse to fall or to hold on to the rod for 3 consecutive rotations was recorded. Mice were trained on three occasions before the experimental day. Locomotor impairment was measured as % inhibition of baseline performance:

$$\% \text{ Inhibition} = \frac{\text{Control} - \text{Experimental}}{\text{Control}} \times 100$$

In vivo pharmacology

Aged-matched 3-6 month old males were used in all studies and experimenters were blind to the genotype and treatment.

Morphine time course and dose-response curve

WT, DOR-KO and α_{2A}AR-KO mice were tested in the hot water tail flick assay for these experiments. Water bath temperature was set at 49˚C for experiments with i.p. morphine administration and at 52˚C for experiments with i.t. morphine administration. Baseline tail flick latencies were measured before drug administration. Mice were treated with different doses of morphine or saline and measurements were repeated at 15, 30, 45, 60, 90, 120, 150, 180, 210, and 240 minutes to evaluate the time course of action of morphine at different doses in each strain. The full dose-response curves were obtained from data collected at each time point. Each dose represents a group of 4-6 animals and a group of saline-treated mice was included in each experiment. Animals were reused up to 3 times by allowing a drug washout period of 4-7 days between experiments.

Morphine antinociception and locomotor effects

WT (n = 16) and DOR-KO (n = 19) mice were tested consecutively in the 49˚C hot water tail flick assay and the rotarod assay. Baseline measurements for both assays were taken before administering morphine i.t. Mice were injected with a starting dose of 0.3 nmol morphine i.t. and subsequent doses (1. 3 and 10 nmol) were injected at 2 hour intervals. Following each i.t. morphine injection, tail flick

latency was measured at 30 minutes post-injection and locomotion capacity was measured at 45 minutes post-injection.

Cumulative DAMGO and Delt II dose-response curves

Full dose-response curves were obtained using a cumulative drug administration protocol. The same group of WT (n = 12), DOR-KO (n = 9) and α_{2A}AR-KO (n = 12) mice was used to test both DAMGO and DeltII by allowing a washout period of one week between experiments. Vehicle-treated mice were included to confirm that the repeated injections did not change the tail flick latencies (data not shown). Baseline tail flick measurements were taken prior to the administration of the first drug dose with a water bath adjusted to 49˚C. Our preliminary data indicate that these peptide agonists rapidly lose their efficacy following i.t. injection with a return to baseline at 30 minutes. Mice were therefore tested 3 min after i.t. injection and re-injected 2 minutes later, allowing for a total of 5 minutes between each injection. A total of four consecutive injections were performed with increasing doses of the drug tested. For DAMGO, we injected 0.003, 0.07, 0.3 and 1 nmol i.t. and for DeltII, we injected 1, 3, 10 and 20 nmol i.t.

SNC 80 antinociception

WT (n = 7), DOR-KO (n = 8) and α_{2A}AR-KO (n = 7) mice were tested in the 49˚C hot water tail flick assay. Baseline measurements were taken before injecting 100 nmol of SNC 80 or vehicle (i.t.). We measured the effect of SNC 80 in the tail flick assay at 3 minutes post-injection since our preliminary data determined that SNC 80 effect in the tail flick assay is maximal at 3 minutes and returns to baseline values at 10 minutes (data not shown).

Spinal inhibition of systemic morphine response

Baseline tail flick latencies were measured before and 5 min after i.t. injection of 1 µg naloxone (WT: n = 6, α_{2A}AR-KO: n = 6) or saline (WT: n = 5, α_{2A}AR-KO: n = 5) in the 49˚C hot water tail flick assay. Naloxone did not affect baseline tail flick latencies in either of the strains (data not shown). Morphine was

administered i.p. at 10 mg/kg 15 minutes after the i.t. injection of naloxone and tail flick latencies were measured 30 minutes after morphine administration.

Morphine antinociception in 6-OHDA-lesioned mice

Pre-lesion baseline tail flick latencies were measured at 52˚C in groups of 7-10 WT or α_{2A}AR-KO mice before injecting them i.t. with 20 μg of 6-OHDA or vehicle solution. 3 days post-6-OHDA administration, baseline tail flick latencies were measured and full morphine dose-response curves were obtained using a cumulative drug administration protocol with a maximum of five consecutive injections of increasing morphine doses. Morphine doses were injected at 5 minutes intervals and tail flick latencies were measured at 4 minutes post injection. Because of the potency difference between WT and α_{2A}AR-KO mice, we used a different range of morphine doses to construct the cumulative dose-response curve in each strain: in WT mice, we used 1, 3, 6, 10 and 30 nmol i.t. and in α_{2A}AR-KO mice, we used 0.1, 0.3, 1, 3 and 6 nmol i.t.

Morphine and clonidine interaction in the tail flick assay

Dose-response curves for clonidine, morphine and their combination to a 1:1 ratio were constructed in WT and α_{2A}AR-KO mice with the 49˚C hot water tail flick assay. Drugs were administered i.t., and tail flick latencies measured 10 minutes later. Each dose represents a group of 4-12 mice.

Drug interactions in the SP assay

Dose-response curves for clonidine, morphine, DeltII and DAMGO were constructed in WT, DOR-KO and α_{2A}AR-KO mice with the SP behavioral assay. Drug combination ratios were chosen so that the ratio corresponds to equieffective doses of each drug. Hence, dose-response curves were constructed for combinations of clonidine with morphine, DeltII or DAMGO. Each dose represents a group of 4-12 mice.

Effect of PKC inhibition on morphine antinociception

Morphine antinociception was measured in the 49˚C hot water tail flick assay in WT (n = 19) and α_{2A}AR-KO (n = 18) mice. Mice were injected i.t. with either 1 nmol of chelerythrine or vehicle followed 30 minutes later by 1 nmol of morphine i.t. Baseline tail flick latencies were taken before chelerythrine treatment and again 5 minutes before morphine treatment to test whether chelerythrine affected baseline tail flick latencies. Tail flick latencies were measured at 15, 30, 45 and 60 minutes after morphine administration.

Receptor expression analysis

Quantitative gene expression analysis of opioid receptors

Total RNA from spinal cords and DRGs was extracted (RNeasy Lipid Tissue Mini Kit, Quiagen) and DNase digested. Conversion to cDNA and quantification of DOR and MOR RNA by real time PCR using the SYBR-Green method was performed at the Genome Québec RNomic Center (Sherbrooke). Pairs of forward (F) and reverse (R) primers were custom designed to amplify cDNA from opioid receptor genes (*Oprm1*, *Oprd1*) and house keeping genes (*Gapdh*, *Hptr1*, *Ubc*). We designed two pairs of primers for *Oprd1*: one amplifying exon1-2 region (F1-R1) and one amplifying exon2-3 (F2-R2). Primer sequences are given in Table 2. Four mice of each strain (WT, DOR-KO and α_{2A}AR-KO) were used and amplification reactions were performed in triplicate for each tissue sample. Relative expression and quality control evaluation was computed using the QBase method (Hellemans et al., 2007) and results were normalized to the WT condition, giving it an arbitrary relative expression value of 1.

Western blot analysis

Spinal cords were collected from three WT, DOR-KO and α_{2A}AR-KO age-matched mice (n = 3 per strain) and homogenized with an automated tissue homogenizer (Precellys 24, Bertin Technologies) with 1.4 mm ceramic beads (Mo Bio Laboratories) in homogenizing buffer (25 mM Tris HCl pH 7.4, 1 mM EDTA, 2 mM $MgCl_2$) supplemented with proteinase inhibitor cocktail (Roche).

The homogenate was centrifuged 4 min at 1000g and the supernatant containing the total protein fraction was quantified with the *DC*™ protein assay (Bio-Rad). Proteins were denatured by boiling in sample buffer (TrisHCl 50 mM, 2% sodium dodecyl sulfate (SDS), 10% glycerol, 2.5% β-mercaptoethanol, bromophenol blue, pH 6.8). 40 µg of each sample was run in a 10% acrylamide SDS-PAGE and proteins were transferred onto a nitrocellulose membrane. Immunoblotting of the membranes was performed with 5% non-fat dry milk in TBST (0.1M Tris-HCl, 0.9% NaCl, 0.1% Tween 20, pH 7.4) as a blocking and antibody diluent solution. MOR immunoreactive bands were detected with a rabbit polyclonal antisera raised against amino acids 384-398 of the predicted MOR1 sequence (NHQLENLEAETAPLP; (Arvidsson et al., 1995b)) diluted 1:2500 and revealed with an HRP-coupled mouse-anti-rabbit IgG (1:10 000; Jackson ImmunoResearch). Membranes were stripped with Restore Western Blot stripping buffer (Thermo Scientific) and reprobed to detect glyceraldehyde-3-phosphate dehydrogenase (GAPDH) immunoreactive band with a mouse monoclonal antisera (1:10 000; MAB374, Millipore) and an HRP-coupled goat-anti-mouse IgG (1:10 000; Jackson ImmunoResearch) as a loading control. Immunoreactivity was revealed by enhanced chemiluminescence Western blotting substrate (Thermo Scientific) and visualized by exposing membranes to a light sensitive film that was then processed in a film developer. Films were digitized and densitometry was performed using ImageJ64 analysis software (NIH) where the 67 kDa MOR band from each mouse sample was normalized to the sample's 37 kDa GAPDH band.

[^{3}H]-DeltII binding assays

Spinal cord membrane preparation

Fresh or flash frozen WT, DOR-KO and α_{2A}AR-KO mouse spinal cords were homogenized with a handheld rotor stator homogenizer (TissueRuptor, Quiagen) in cold homogenization buffer (50 mM TrisHCl, 2.5 mM EDTA, pH 7.0) supplemented with protease inhibitors (Roche). The homogenate was centrifuged 10 minutes at 1000 g at 4˚C and the supernatant was collected in an

ultracentrifuge tube. The pellet was re-homogenized, centrifuged and the supernatant was transferred to the ultracentrifuge tube. Pooled homogenates were centrifuged at 48 000 g for 20 minutes at 4˚C. The pellet was resuspended in binding buffer (50 mM TrisHCl, 3 mM $MgCl_2$, pH 7.4 with protease inhibitor) and incubated at 37˚C for 15 min to dissociate receptor-bound endogenous opioid peptides and degrade monoamines. The membranes were centrifuged at 48 000 g for 20 minutes at 4˚C and pellets were resuspended in binding buffer. Protein content was determined with the *DC*™ protein assay (BioRad) and volume was adjusted to obtain the desired protein concentration.

[^{3}H]-DeltII saturation and competition binding assay

Binding experiments were performed with the DOR-selective radioligand deltorphinII(D-Ala^2), [Tyrosyl-3,5-^{3}H] ([^{3}H]-DeltII, PerkinElmer, MA, USA) in a binding buffer solution consisting of 50 mM TrisHCl, 3 mM $MgCl_2$ (pH 7.4). In saturation binding experiments, 200 µg of spinal cord membrane protein from WT, DOR-KO or α_{2A}AR-KO mice was combined with five concentrations of [^{3}H]-DeltII (0.3-10 nM) in a final sample volume of 300 µl. Nonspecific binding was determined by the addition of the nonselective opioid receptor antagonist naloxone (10 µM, R&D systems). In competition binding experiments, 200 µg of spinal cord membrane protein was combined with 1 nM of ^{3}H-DeltII and the DOR-selective antagonist naltrindole (R&D Systems) at concentrations ranging from 1 µM to 100 fM. Samples were prepared in triplicate and incubated for 60 min in a 37˚C water bath. Spinal cord membranes were collected by filtration on a grade GF/C glass microfiber filter (Whatman) that was previously soaked overnight in binding buffer with 0.5% polyethyleneimine (PEI) and washed three times with ice-cold washing buffer (25 mM TrisHCl, pH 7.4). Filters were transferred into 5 ml polypropylene tube and filled with 3 ml of Ecolume liquid scintillation cocktail (MP Biomedicals, OH, USA). Since the energy transferred by β particles emitted by 3H upon radioactive decay to the scintillation cocktail is released as photons, bound radioactivity was quantified using a liquid scintillation

counter (LS 6500, Beckman Coulter) and converted to disintegrations per minute (DPM) units.

Data analysis

Outliers

Data points were considered outliers and excluded from the analysis based on the following experimental and statistical criteria: 1) while still blind to the strain and treatment, the experimenter judged that the i.t. injection was not successful and no side effects were observed; 2) a known experimental error was reported for that sample (e.g. equipment failure, execution error); 3) a data point was a significant outlier according to the Grubbs' test (GraphPad Software, Inc., alpha = 0.05).

Nociceptive phenotypes

Comparison of raw baseline values (means ± SEM) obtained in behavioral assays between WT and DOR-KO or α_{2A}AR-KO were compared using GraphPad Prism 6.0 (GraphPad Software, Inc.) with a two-sided unpaired parametric Student's T-test with a 95% confidence level. Baseline tail flick latencies measured at different temperatures in WT and DOR-KO or α_{2A}AR-KO mice were compared with a 2-way ANOVA followed by a Bonferroni test for multiple comparisons.

Time course analysis

Morphine antinociceptive effect was plotted as mean %MPE ± SEM and repeated measures were graphed as time points. Comparison between WT and DOR-KO or α_{2A}AR-KO morphine antinociceptive time course for selected doses were performed in GraphPad Prism 6.0 with repeated measures 2 way analysis of variance (ANOVA) followed by a Bonferroni test for multiple comparison.

Dose-response analysis

Dose-response curve graphs were generated with GraphPad Prism 6.0. A minimum of 4 animals were used per dose and each dose point is expressed as the mean % MPE or % inhibition ± S.E.M. For drug combinations, doses reflecting

total drug concentration were used for analysis, but a curve corresponding to the concentration of only one of the drugs in the combination was sometimes also graphed. Drugs had to reach at least 50% MPE or 50% inhibition to be considered effective. ED_{50} values and 95% confidence interval (CI) were calculated using a minimum of three doses in the linear portion of each dose-response curve following the method of Tallarida and Murray (1987)with the FlashCalc 4.5.3 pharmacological statistics software package generously supplied by Dr. Michael Ossipov. Statistical comparisons of potencies are based on the confidence limits of the ED_{50} values.

Isobolographic analysis

Isobolographic analysis is the method of choice for evaluating drug interactions (Tallarida, 2006). Drug combination ratios were chosen according to the relative potency of each drug by determining an approximately equally effective potency ratio between the agonists based on their respective ED_{50} values. When two drugs were equally potent, they were mixed in a 1:1 (i.e. equieffective and equimolar) ratio. If a drug was 10 times more potent than the other, drugs were mixed in a 1:10 (i.e. equieffective) ratio. Since the relative drug potency of the drug pairs used in this study differed between the mouse strains tested, different drug ratios were tested in each strains and the experimental ED_{50} value for the drug combination was determined. To test for interactions between agonists, the ED_{50} values and S.E.M. of all dose-response curves were arithmetically arranged around the ED_{50} value using equation $(\ln(10) \times ED_{50}) \times (\text{S.E. of log } ED_{50})$ (Tallarida, 1992). This manipulation was required to perform an isobolographic analysis to evaluate if an interaction is synergistic, additive or sub-additive (Tallarida, 1992). When testing an interaction between two drugs, a theoretical additive ED_{50} value is calculated for the combination based on the dose-response curve of each drug administered separately. This theoretical value is then compared by Student's T test with the observed experimental ED_{50} value of the combination. An interaction is considered synergistic if the experimental ED_{50} is significantly less ($P < 0.05$) than the calculated theoretical additive ED_{50}.

Visualization of drug interactions can be facilitated by the use of an isobologram, i.e. a graphical representation of isobolographic analysis. The isobologram depicts the ED_{50} value of each drug as the *x*- *y*-intercept. The line connecting these two points depicts the dose combination expected to yield 50% efficacy if the interaction is purely additive and is called the theoretical additive line. The theoretical additive ED_{50} is determined mathematically and plotted on this line with its CI spanning perpendicularly from the line. The experimental ED_{50} for the combination is plotted at the corresponding *x*,*y* co-ordinates along with its 95% confidence interval for comparison with the theoretical additive ED_{50} value.

All dose-response and isobolographic analyses were performed with the FlashCalc 4.5.3 pharmacological statistics software package generously supplied by Dr. Michael Ossipov.

Drug treatments

Experiments where the effect of a drug treatment (drug vs vehicle) was compared between two mouse strains were analyzed with a 2-way ANOVA followed by a Bonferroni multiple comparison T test with GraphPad Prism 6.0.

Gene expression and western blot analysis

Comparisons of relative gene or protein expression between WT and DOR-KO or α_{2A}AR-KO mice were done in GraphPad Prism 6.0 with a two-sided unpaired Mann-Whitney U test.

[^{3}H]-Delt binding analysis

All ligand binding analyses were done in GraphPad Prism 6.0. For saturation binding, total [^{3}H]-DeltII binding and non-specific binding data were fitted using a global nonlinear regression model and non-specific binding was subtracted from total binding to obtain a specific binding curve. B_{max} and K_d with 95% CI values were obtained by nonlinear regression of specific binding. Competition binding data were fitted to a one-site non-linear regression model to determine naltrindole

K_i and IC_{50} values with 95% CI. Strain differences were evaluated with an extra sum-of-squares F test to compare the best fit values of B_{max}, K_d and K_i.

TABLES

Table 1: Sequence of oligonucleotide pairs used for genotyping and the predicted molecular weight of the amplified PCR product.

Gene	Allele	Oligonucleotide sequences	MW (bp)
Adra2a	WT	5' - GGTGACACTGACGCTGGTTT - 3' 5' - AAGGAGATGACAGCCGAGAT - 3'	400
	KO	5' - GGTGACACTGACGCTGGTTT - 3' 5' - CGAGATCCACTAGTTCTAGC - 3'	260
Oprd1	WT	5'- AGAACACGCAGCACAAAGACTGG - 3' 5'- CGCACGCAGTTTGTGATTGG - 3'	338
	KO	5'- AGAACACGCAGCACAAAGACTGG - 3' 5'- ACCGCTTCCTCGTGCTTTACGGTA - 3'	591

Table 2: Sequence of forward (F) and reverse (R) primers used for quantitative PCR analysis of gene expression in WT, DOR-KO and α_{2A}AR-KO mouse SC and DRG.

Gene	Primer	Sequences (5' → 3')
Oprm1	F	TGGTCACAGCCATCACCATCATG
	R	CATCAGGTAGTTAACACTCTGAAAGGGCA
Oprd1	F1	GTCCCTCGCCCTAGCCATCG
	R1	GCCAGATTGAAGATGTAGATGTTGGTGG
	F2	CTGCCATCCTGTCAAAGCCCT'
	R2	GCAAAGAGGAACACGCAGATCTTG
Gapdh	F	TGACGTGCCGCCTGGAGAAA
	R	AGTGTAGCCCAAGATGCCCTTCAG
Hptr1	F	GCTTGCTGGTGAAAAGGACCTCTCGAAG
	R	CCCTGAAGTACTCATTATAGTCAAGGGCAT
Ubc	F	CGTCGAGCCCAGTGTTACCACCAAGAAGG
	R	CCCCCATCACACCCAAGAACAAGCACAAG

Chapter 3:
The delta opioid receptor is necessary to produce full morphine antinociception at the spinal level

RATIONALE OF THE STUDY

Morphine is considered primarily as a MOR agonist because of its high binding affinity for MOR compared to other opioid receptors and MOR-KO mice do not respond to the antinociceptive and side effects of morphine (Matthes et al., 1996).

Under normal conditions, systemic morphine antinociception is not affected in DOR-KO mice (Filliol et al., 2000). However, studies show that DOR regulates some aspects of morphine efficacy. For example, the addition of a subanalgesic dose of DOR agonists can potentiate morphine antinociception (Barrett and Vaught, 1982), and blocking DOR with an antagonist can attenuate the development of morphine tolerance (Abdelhamid et al., 1991). At the spinal level, chronic morphine treatment induces a MOR-dependent upregulation of surface DOR and increases the efficacy of DOR agonists (Cahill et al., 2001b; Morinville et al., 2003). The role of DOR in spinal morphine antinociception is therefore not clear.

The aim of this chapter was to assess the role of DOR in antinociception produced by morphine and other opioid agonists. In order to compare opioid antinociception between WT and DOR-KO mice, we used the hot water tail flick assay and constructed full dose-response curves for morphine, DeltII and DAMGO. In order to relate the *in vivo* pharmacological results to opioid receptor expression, we examined expression levels by quantitative PCR analysis, western blot and radioligand binding.

RESULTS

Evaluation of nociceptive thresholds in WT and DOR-KO mice

We tested the possibility that the mechanical and thermal nociceptive threshold of DOR-KO mice were different from WT mice. Thermal nociception was measured in the hot water tail flick assay and the radiant heat assay. We tested four different temperatures in the hot water tail flick assay (Figure 1A). As the temperature rose, tail flick latency values became faster in both strains. DOR-KO mice were more sensitive to the thermal stimuli compared to WT mice (2-way ANOVA; strain: $F_{(1, 190)} = 6.151$, $p = 0.014$, temperature: $F_{(3, 190)} = 212.7$, $p < .0001$, interaction: $F_{(3, 190)} = 3.54$, $p = 0.014$), especially at 46˚C (WT = 6.9 +/- 0.5 sec.; DOR-KO = 5.7 +/- 0.4 sec, $P < 0.001$) and 49˚C (WT = 2.9 +/- 0.2 sec.; DOR-KO = 2.4 +/- 0.2 sec) where tail flick latencies were significantly lower in DOR-KO mice compared to WT mice. Using the radiant paw withdrawal assay to assess heat nociception, we did not observe a significant strain difference in nociceptive threshold (Figure 1B, WT = 6.7 +/- 0.3 sec.; DOR-KO = 6.9 +/- 0.5 sec). DOR-KO mice were not more sensitive to mechanical stimuli elicited by von Frey filaments compared to WT mice (Figure 1C, WT = 0.28 +/- 0.03 g; DOR-KO = 0.29 +/- 0.029 g). Thus, DOR-KO mice display a slightly, but significantly altered heat nociception phenotype compared to WT mice. However, this strain difference is not large enough to introduce a confounding factor in the next set of experiments.

Impaired spinal morphine antinociceptive efficacy in DOR-KO mice

To assess the role of DOR in morphine antinociception, we used the tail flick assay to compare spinal morphine potency and efficacy between DOR-KO and WT mice at different time points. Intrathecal saline injection did not change the tail flick latency in WT or DOR-KO mice (Figure 2A, B). In WT mice, the antinociception time course analysis showed that the morphine effect peaked between 45 or 60 minutes, depending on the dose, or started to decline at 90 minutes (Figure 2A). While the effect of the lowest doses tested had returned to

baseline (0.3, 1 and 3 nmol), the highest doses were still effective after 240 minutes (6 and 10 nmol). The highest effect was obtained with 6 nmol of morphine and the next higher dose tested was less effective (see 10 nmol). In DOR-KO mice, the peak morphine antinociceptive effect was also at 45 or 60 min for most doses and declined following a similar course as in WT mice (Figure 2B). The 3 nmol morphine dose produced the highest antinociceptive effect.

Comparing the effect of 6 nmol of morphine between WT, which produced the highest effect in this strain, and DOR-KO mice shows that morphine is less efficacious in DOR-KO mice (Figure 2C, 2 way ANOVA, strain effect: $F_{(1, 110)}$ = 22.22, $P < 0.0001$, time: $F = _{(10, 110)} = P < 0.0001$, interaction: $F_{(1, 110)} = 0.53$, $P =$ 0.86).

Morphine potency was evaluated in each mouse strain at 15, 30, 45 and 60 minutes by constructing dose-response curves and evaluating the ED_{50} value (Table 1). Morphine was ineffective in DOR-KO mice at 15 minutes (Figure 2D), but produced a dose-dependent effect similar to WT mice at subsequent time points (Table 1). For example, at 60 minutes, when morphine effect has peaked in both strains, the dose-response curve has an inverted U-shape (Figure 2E). The ascending portion of both dose-response curves overlap, indicating that morphine potency is similar in WT and DOR-KO. However, the descending part of the curve starts at a lower dose in DOR-KO mice, which reflects morphine's lower efficacy in this strain.

Therefore, morphine potency is unchanged in DOR-KO mice compared to WT, but maximal efficacy is compromised. The onset of action of morphine is also compromised since morphine antinociceptive action was absent at 10 and 15 minutes. Together, our data suggest that DOR is necessary for the antinociceptive action of morphine at the spinal level at an early time point.

Systemic morphine antinociception is not affected in DOR-KO mice

To out knowledge, this is the first report of a lack of morphine antinociceptive efficacy in DOR-KO mice, although morphine has been tested in these mice

before. Previous studies on morphine action in DOR-KO mice used a systemic route of administration and reported no antinociceptive difference with WT mice (Zhu et al., 1999). It is thus possible that the lack of efficacy reported here is specific to the spinal route of administration of morphine in our experiments. To compare with our observations from spinal morphine, we resolved the time course of action of four doses of morphine administered i.p. in WT and DOR-KO mice to compare their potency and efficacy in the tail flick assay.

Morphine antinociceptive effect followed a similar time course in WT and DOR-KO mice, where % MPE values peaked between 15 and 60 minutes depending on the dose and started to decline afterwards (Figure 3A, B). Saline administered i.p. did not produce an antinociceptive response in WT mice. At 210 minutes, all doses tested in both strains returned to baseline, except for the highest dose in DOR-KO mice (30 mg/kg). The time course of action of morphine 20 mg/kg was similar in WT and DOR-KO mice (Figure 3C; 2 way ANOVA; strain: $F_{(1, 100)} = 0.7115$, $P = .4010$, time: $F_{(9, 100)} = 12.10$, $P < .0001$, interaction: $F_{(9, 100)} = 0.3200$, $P = 0.9667$). ED_{50} values reveal no significant strain difference in morphine potency at any time point (Table 2). For example, contrary to the results obtained with spinal administration, the dose-response curve for systemic morphine was equally effective in WT and DOR-KO mice at 15 minutes (Figure 3D) and 60 minutes (Figure 3E).

Thus, morphine's time course, efficacy and potency are unchanged in DOR-KO mice when administered systemically.

Spinal morphine locomotor impairments are not affected in DOR-KO mice

In rodents, spinal morphine induces motor impairment in the lower hind limbs and there is a possibility that the increase in tail flick latency observed in the tail flick assay is a consequence of this impairment. We therefore tested the possibility that DOR-KO mice responded faster in the tail flick assay due to insensitivity to the locomotor impairments induced by morphine.

Mice were tested consecutively in the tail flick assay and the rotarod assay with increasing doses of morphine administered i.t. to generate cumulative dose-response curves for both assays. With the tail flick assay, the cumulative dosing protocol generated an inverted U-shape dose-response curve as seen in Figure 2E, F and confirmed the lower morphine antinociceptive efficacy in DOR-KO mice compared to WT mice (Figure 4A). WT and DOR-KO mice had no significant difference in their baseline latencies to fall in the rotarod assay (WT: 249 ± 22 sec., DOR-KO: 262 ± 18 sec.). Morphine locomotor impairment observed in the rotarod assay followed a dose-dependent relationship with similar potency and efficacy in WT and DOR-KO mice (Figure 4B). These data suggest that the reduced effect in DOR-KO mice is not due to a lack of locomotor impairment.

Antinociceptive effect of MOR- and DOR- selective peptide agonists in WT and DOR-KO mice

Since morphine is considered to mediate its antinociceptive effects through MOR, we tested whether the decreased antinociceptive effect in DOR-KO is also observed with the MOR-selective peptide agonist DAMGO. The tail flick assay was performed in WT and DOR-KO mice at 3 minutes following drug injection because the antinociceptive effect of DAMGO is short lasting as well as to reflect the time point where the largest strain difference was observed. The ED_{50} values calculated from the dose-response curves were not significantly different (WT: 0.17 (0.1-0.3) nmol, DOR-KO: 0.06 (0.03-0.1) nmol; Figure 5A).

We then tested the antinociceptive action of DOR-selective agonists DeltII and SNC80 in the tail flick assay. Studies have shown that these agonists have antinociceptive actions in the tail flick assay (Hylden and Wilcox, 1982), although their selectivity for DOR is not unanimous (Scherrer et al., 2004; van Rijn et al., 2012). If these agonists were selective for DOR, we expected to have no antinociceptive effect in DOR-KO mice. Surprisingly, the peptide agonist DeltII was more potent and more efficacious in DOR-KO mice than in WT mice (WT ED_{50}: 6.4 (4.0-10.4) nmol, DOR-KO ED_{50}: 1.8 (1.1-3.1) nmol; Figure 5B). WT and DOR-KO mice injected i.t. with a high dose of SNC 80 (100 nmol) responded

with a mild antinociceptive response in the tail flick assay, but there was no significant strain difference (2 way ANOVA; strain: $F_{(1, 40)} = 0.1101$, $P = 0.7417$, dose: $F_{(1, 40)} = 10.72$, $P = 0.0022$, interaction: $F_{(1, 40)} = 0.0037$, $P = 0.9517$; Figure 5C).

These data reveal that, in contrast to morphine, DAMGO-mediated antinociception is not compromised in DOR-KO mice. On the other hand, the DOR-selective agonists DeltII and SNC80 are still effective in the tail flick assay in DOR-KO mice.

MOR expression level is unchanged in DOR-KO mice

We hypothesized that the altered opioid response we observed in DOR-KO mice was due to changes in MOR mRNA or protein expression levels. Quantitative PCR analysis of the cDNA corresponding to MOR mRNA was analyzed from DRGs and SC extracts from WT and DOR-KO mice. No significant difference in MOR expression level between WT and DOR-KO mice was observed in either DRG (WT = 1 ± 0.09, DOR-KO = 1.2 ± 0.06, $P = 0.58$; Figure 6A) or SC (WT = 1 ± 0.05, DOR-KO = 1.1 ± 0.05, $P = 0.07$; Figure 6B). We further analyzed the amount of MOR receptors present in the SC by western blot analysis of purified membrane extracts from WT and DOR-KO spinal cords. We measured the density of a 67 kDa immunoreactive band corresponding to MOR and adjusted the relative density with the density of the 35 kDa GAPDH-immunoreactive band obtained after stripping and re-probing the membrane (Figure 6C). The relative MOR densitometry was not different between WT and DOR-KO mice (Mann-Whitney U test, $P = 0.9$; Figure 6D).

We conclude that neither MOR mRNA nor protein were up or downregulated in DOR-KO.

DOR-KO mice express a partial DOR mRNA tanscript

Since DOR-selective ligands retained their antinociceptive effect in DOR-KO mice in the tail flick assay, we investigated the possibility that the genetic deletion

did not completely prevent expression of DOR receptors. Three exons constitute the *Oprd1* gene encoding for DOR in mice and DOR-KO mice have been generated by deleting the first exon containing the start codon for mRNA transcription (Figure 7A). We designed two pairs of oligonucleotides to quantify DOR mRNA: one that spans the exon1-2 region to confirm exon1 deletion (F1-R1), and one that spans the exon 2-3 region to detect expression of residual *Oprd1* transcripts (F2-R2). No transcript was detected in DOR-KO mice with the F1-R1 oligonucleotides, confirming exon1 deletion (Figure 7B, C). However, the F2-R2 oligonucleotides amplified a transcript in both mouse strains, which was significantly upregulated in DOR-KO mice DRG (WT = 1 ± 0.04, DOR-KO = 1.3 ± 0.09, $P = 0.002$; Figure 7B) and SC (WT = 1 ± 0.03, DOR-KO = 2.6 ± 0.15, $P = 0.001$; Figure 7C) compared to WT mice.

Upregulation of the partial DOR transcript in DOR-KO mice could result in an increase in DeltII binding sites. To test this, we used [^{3}H]-DeltII to detect DeltII binding sites in DOR-KO mice. Binding of increasing concentrations of [^{3}H]-DeltII to spinal cord membrane extracts in the presence of naloxone, a non-selective opioid receptor competitive antagonist, was subtracted from [^{3}H]-DeltII total binding to obtain a specific binding curve. In WT mice, the saturation binding curve shows that [^{3}H]-DeltII binds to spinal cord membranes with an affinity constant (K_D) of 0.9 (0.4-1.4) nM and a B_{max} of 373 (319-426) nM. Specific [^{3}H]-DeltII binding was absent in DOR-KO mice (Figure 7E).

Thus, a partial DOR transcript is upregulated in DOR-KO mice, but there is no residual ^{3}H-DeltII binding affinity or sites.

CONCLUSION

The experiments presented in this chapter illustrate the complex role played by DOR in opioid-mediated antinociception. First, we showed that in DOR-KO mice, spinal morphine efficacy was lower and that the onset of action of morphine was delayed. This effect was specific to the spinal route of administration of morphine since the antinociceptive effect of systemic morphine was similar in both WT and DOR-KO mice. Second, we showed that morphine-induced locomotor impairments were not attenuated in DOR-KO mice, nor was antinociception. We then showed that the potency of DAMGO, a MOR-selective agonist, was unchanged in DOR-KO mice, but that two DOR-selective agonists, DeltII and SNC80, were still effective in DOR-KO mice. Our analysis of MOR expression did not reveal any up or down regulation of MOR mRNA or proteins in the SC and DRGs of DOR-KO mice. Analysis of the expression of DOR mRNA confirmed the deletion of exon 1 in the Oprd1 gene and reveled that a partial DOR mRNA transcript was upregulated in DOR-KO mice. Finally, saturation binding experiments did not reveal any residual 3H-DeltII binding sites in DOR-KO mice.

FIGURES AND TABLES

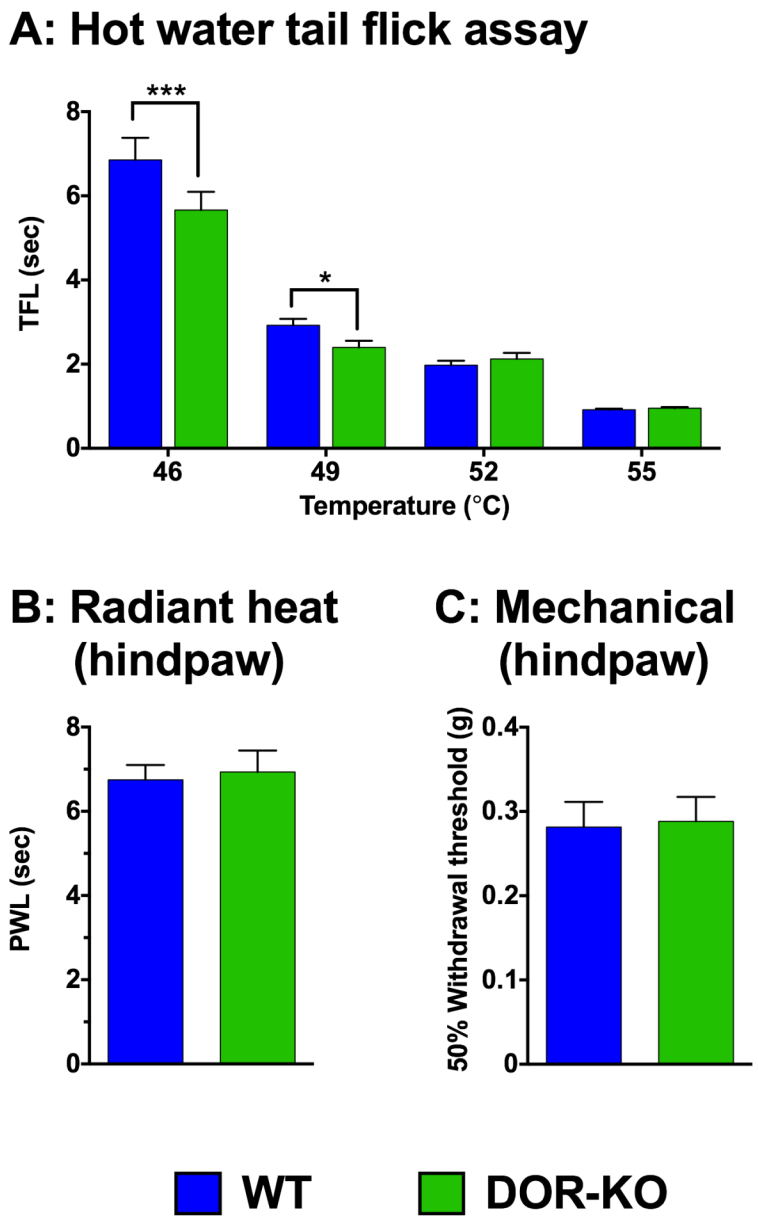

Figure 1: Comparison of thermal and mechanical nociceptive thresholds between WT and DOR-KO mice.

A) Tail flick latencies (TFL) measured at temperatures ranging from 46˚C to 52˚C in the warm water tail flick assay. DOR-KO mice (n = 14-37) were more sensitive to moderate heat (i.e. 46˚C and 49˚C) than WT mice (n = 15-33). B) Paw withdrawal latencies (PWL) measured with the radiant heat assay were similar in WT (n = 15) and DOR-KO (n = 18) mice. C) 50% mechanical threshold (g) measured with vonFrey filaments were similar on the paw of WT (n = 15) and DOR-KO (n = 18) mice. *$P < 0.05$ *** $P < 0.001$

A: WT mice

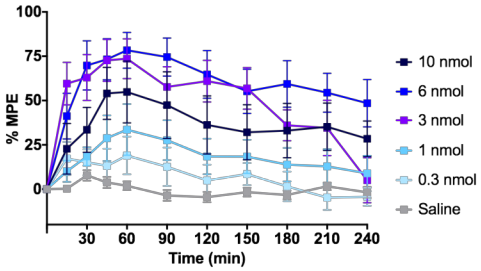

B: DOR-KO mice

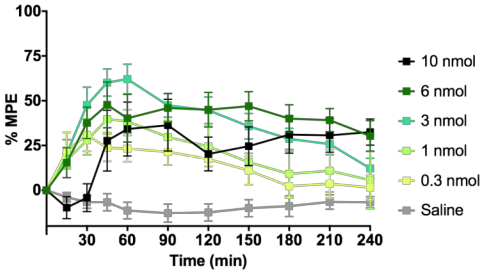

C: Morphine 6 nmol (i.t.)

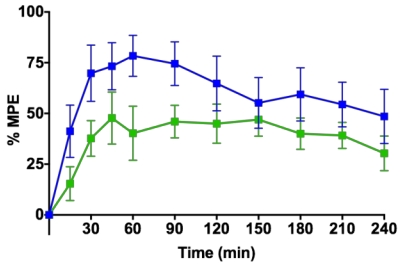

D: 15 min

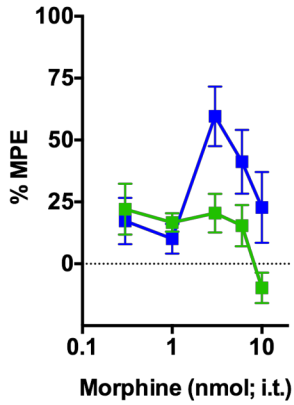

E: 60 min

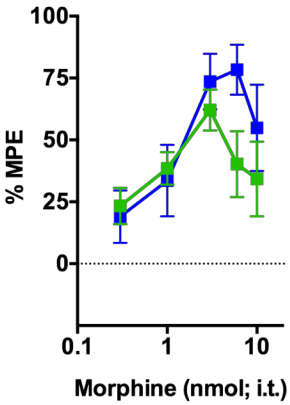

WT DOR-KO

Figure 2: Spinal morphine antinociception in WT and DOR-KO mice.

A) Time course of the antinociceptive effect of different doses of morphine administered spinally in WT mice in the hot water tail flick assay. Morphine dose-dependently increased tail flick latencies and the maximum effect was observed with the 6 nmol (i.t.) dose. B) Time course of the antinociceptive effect of different doses of morphine administered spinally in DOR-KO mice in the hot water tail flick assay. The effect is dose-dependent and reached a maximum with 3 nmol morphine (i.t.). C) Comparison of the antinociceptive response mediated by 6 nmol of morphine (i.t.) over 240 minutes between WT and DOR-KO mice shows that morphine efficacy was reduced in DOR-KO mice. D) At 15 min, high doses of morphine were efficacious in WT mice, but not in DOR-KO mice. F) Morphine dose-response curve at 60 min shows that morphine is equally potent in WT and DOR-KO mice since the ascending part of the dose-response curves overlap. However, at higher doses, morphine is less efficacious than in WT mice. ED_{50} values are reported in Table 1.

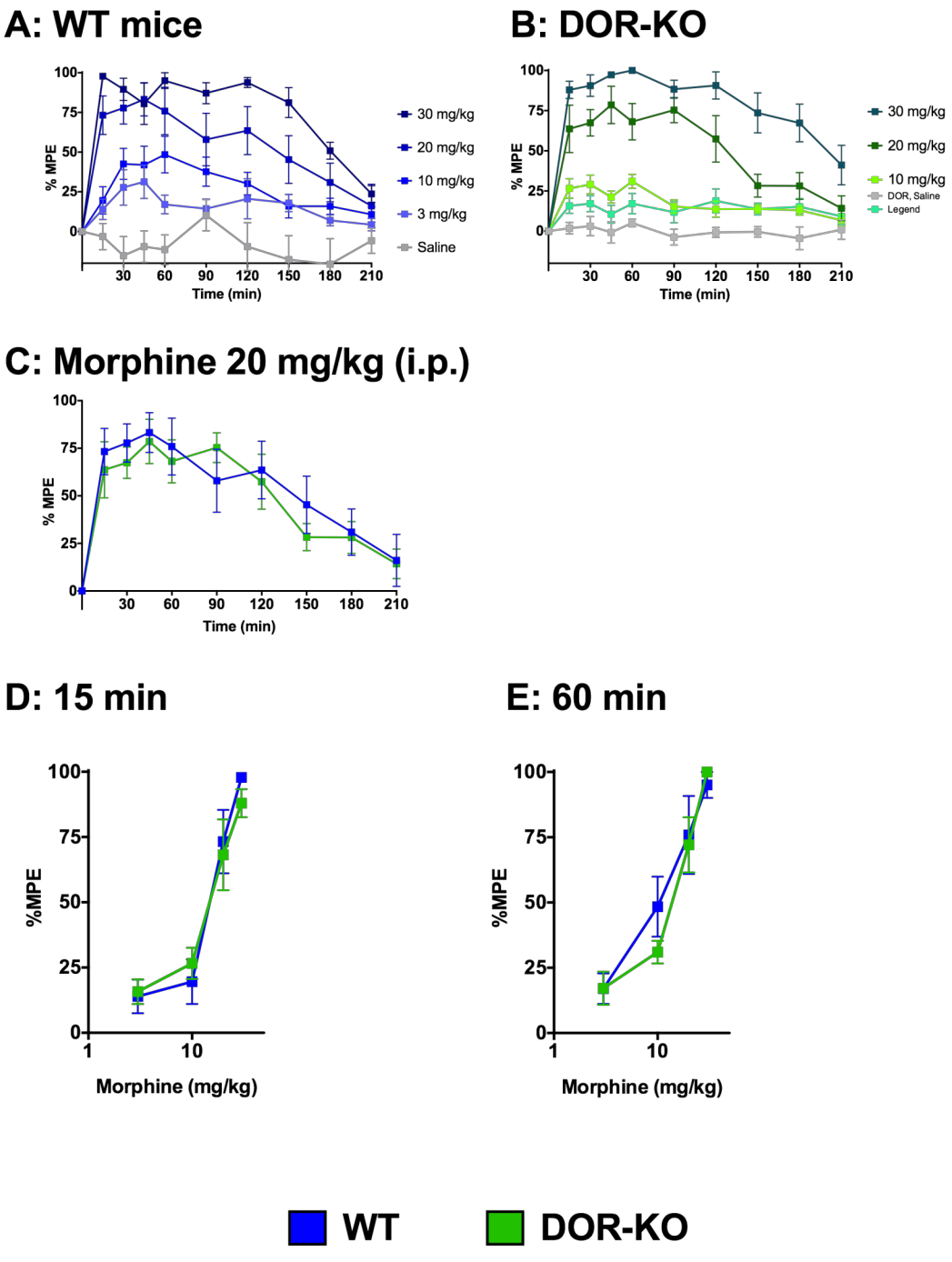
A: WT mice
B: DOR-KO
C: Morphine 20 mg/kg (i.p.)
D: 15 min
E: 60 min
% MPE
%MPE
Time (min)
Morphine (mg/kg)
30 mg/kg
20 mg/kg
10 mg/kg
3 mg/kg
Saline
DOR, Saline
Legend
WT
DOR-KO

Figure 3: Systemic morphine antinociception in WT and DOR-KO mice.

A) Time course of the antinociceptive effect of different doses of morphine administered i.p in WT mice in the hot water tail flick assay. B) Time course of the antinociceptive effect of different doses of morphine administered i.p. in DOR-KO mice in the hot water tail flick assay. Morphine dose-dependently increased tail flick latencies, producing maximal efficacy at 30 mg/kg in both strains. C) The antinociceptive effect of 20 mg/kg morphine (i.p.) over 210 minutes in WT mice was not different from that of DOR-KO mice. (D, E) Morphine dose-response curves were constructed from the time course analysis data. At 15 and 60 minutes, morphine dose-effect curves from WT or DOR-KO mice were not significantly different. ED_{50} values are reported in Table 2.

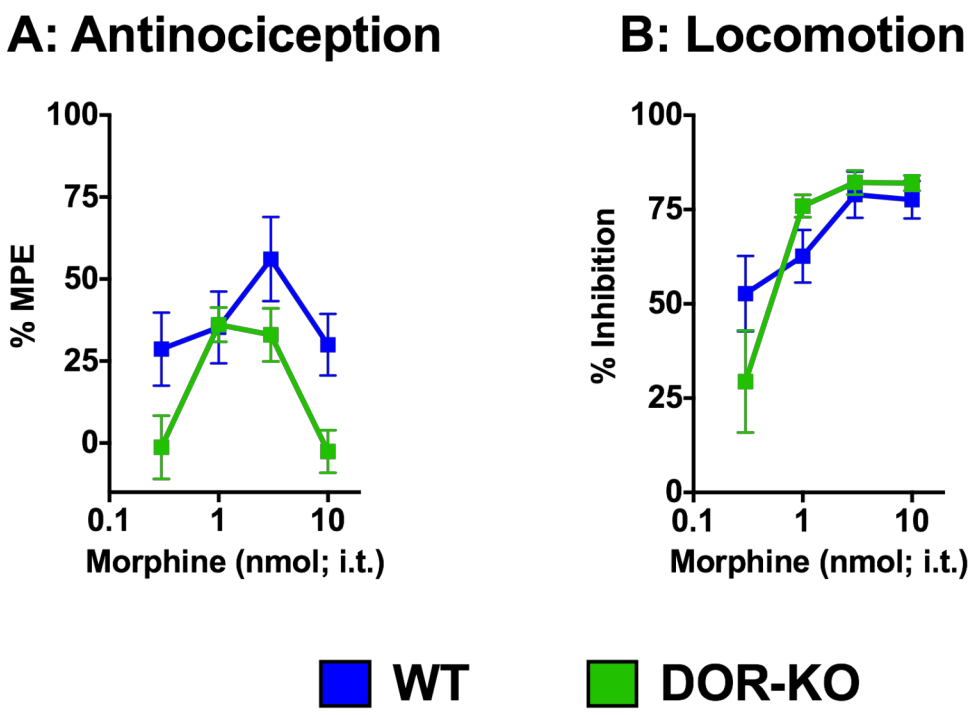

Figure 4: Comparison between morphine antinociceptive and locomotor effects in WT mice and DOR-KO mice.

A) Morphine antinociception was measured with the hot water tail flick assay with a cumulative dosage protocol. The resulting dose-response curve has an inverted U-shape in both strains and morphine was less effective in DOR-KO mice. B) Morphine locomotor impairment was measured with the rotarod assay in the same animals immediately after the tail flick assay to directly compare the antinociceptive effect with locomotor effects. We did not observe a strain difference of morphine dose-dependent inhibitory effect on locomotion between WT and DOR-KO mice.

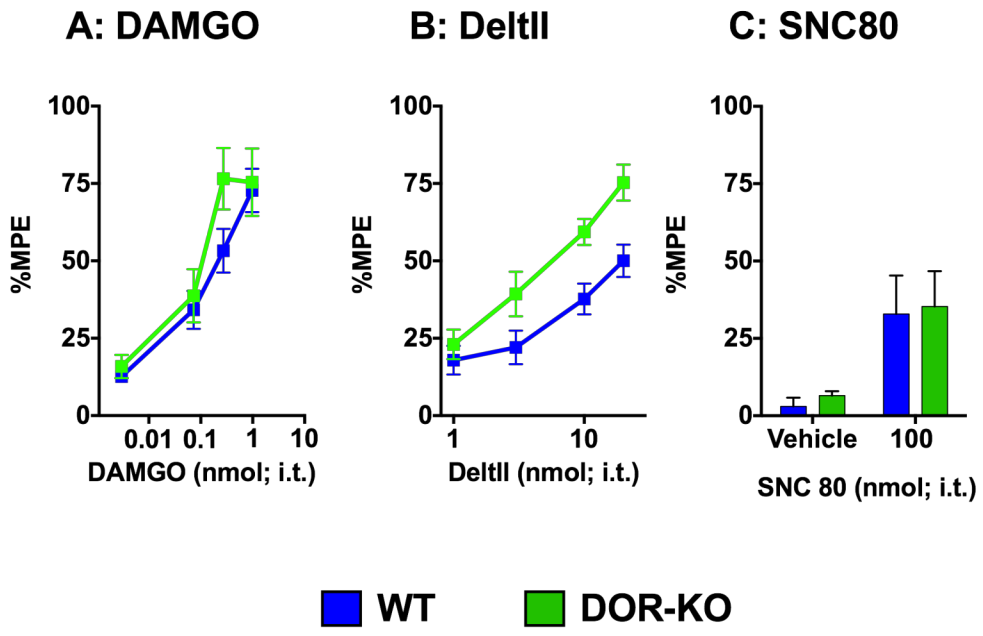

Figure 5: Antinociceptive action of MOR and DOR receptor subtype-selective agonists.

A) Dose-response analysis of the antinociceptive effect of DAMGO (i.t.) using a cumulative dosage protocol in WT and DOR-KO mice in the hot water tail flick assay. DAMGO ED_{50} values for each strain were derived and showed no significant strain differences. B) Dose-response analysis of the antinociceptive effect of DeltII (i.t.) using a cumulative dosage protocol in WT and DOR-KO mice in the hot water tail flick assay. DeltII effect is potentiated in DOR-KO mice compared to the effect in WT mice and the calculated ED_{50} values are significantly different between the two strains. C) In the hot water tail flick assay, a 100 nmol i.t. dose of SNC 80 produced a mild antinociceptive effect in WT mice compared to saline treated mice, and the effect was still present in DOR-KO mice.

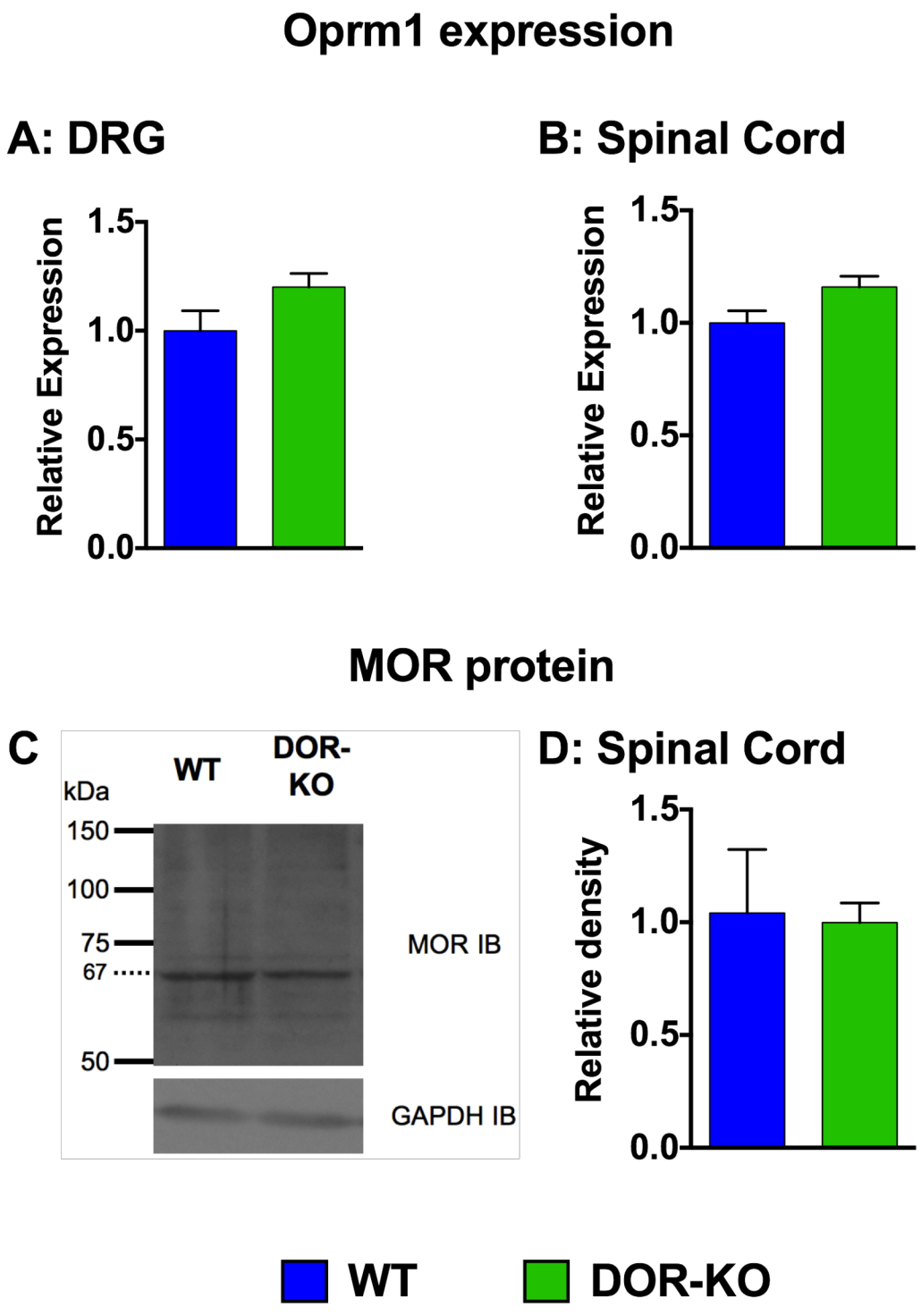
Oprm1 expression
A: DRG
Relative Expression
1.5
1.0
0.5
0.0
B: Spinal Cord
Relative Expression
1.5
1.0
0.5
0.0
MOR protein
C
WT
DOR-KO
kDa
150
100
75
67
50
MOR IB
GAPDH IB
D: Spinal Cord
Relative density
1.5
1.0
0.5
0.0
WT
DOR-KO

Figure 6: Analysis of MOR mRNA and protein expressed in dorsal root ganglia (DRG) and spinal cords (SC) of WT and DOR-KO mice.

A) Quantitative PCR analysis of the *Oprm1* gene transcript from WT and DOR-KO DRG mRNA extracts showed no strain difference in MOR expression. B) Quantitative PCR analysis of the *Oprm1* gene transcript from WT and DOR-KO spinal cord mRNA extracts showed no strain difference in MOR expression. C) Representative western blot showing the 67 kDa MOR-immunoreactive bands that were used to quantify MOR levels in the spinal cord of WT and DOR-KO mice. The GAPDH-immunoreactive band was used as a loading control to normalize the MOR-immunoreactive band. C) Densitometry analysis of western blot MOR-immunoreactive band showed no strain difference.

A: *Oprd1* gene

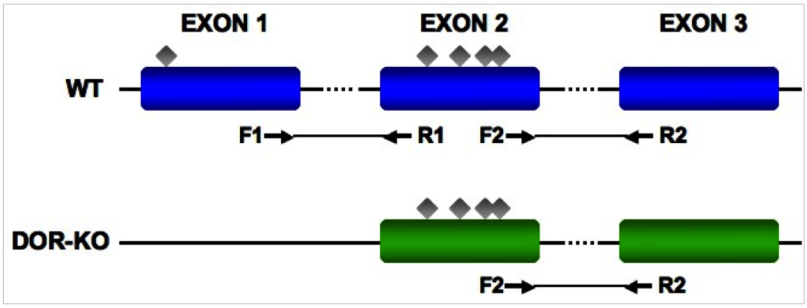

B: DRG

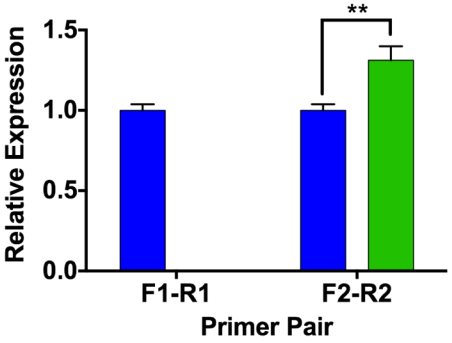

C: Spinal Cord

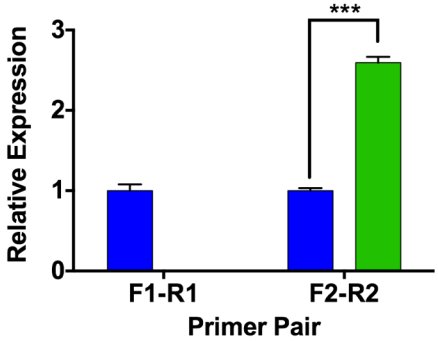

E: Saturation [^{3}H]-DeltII binding

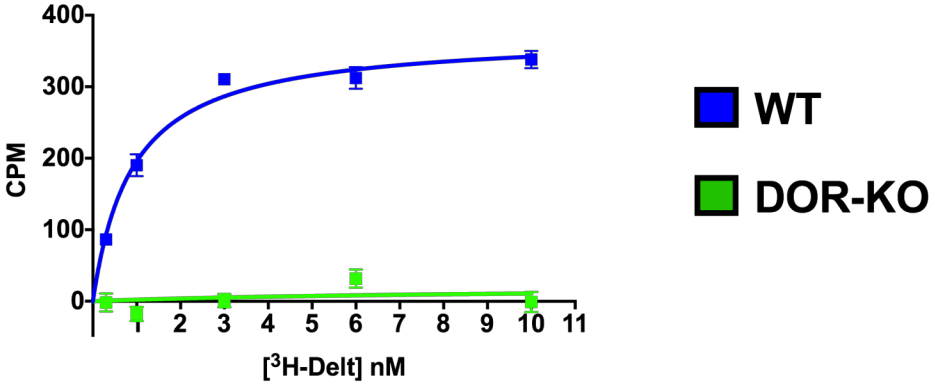

Figure 7: Analysis of DOR mRNA expression and [^{3}H]-DeltII binding sites in WT and DOR-KO mice.

A) Diagram representing the *Oprd1* gene encoding for DOR. In WT mice, the gene consists of 3 exons (blue solid boxes) and the start codon coding for the first methionine is located on the first exon (diamond), although other methionine codons are located in the second exon. The first exon of the Oprd1 gene is deleted in DOR-KO mice where the main start codon is located (green solid boxes). Two pairs of PCR primers/oligonucleotides (F1-R1; F2-R2) probing different parts of the gene transcript were designed. B) A PCR product was detected using the F1-R1 oligonucleotide pair in extracts from DRG and SC from WT mice, but not from DOR-KO mice. C) The PCR product amplified by the F2-R2 oligonucleotide pair was detected in WT mice and was upregulated in SC and DRG from DOR-KO mice. D) Saturation ligand binding assay performed on membrane protein extracts from WT and DOR-KO mouse spinal cords showing specific binding obtained by subtracting non-specific from total [^{3}H]-DeltII binding. While we observed a concentration-dependent binding in WT mice, there was a complete absence of [^{3}H]-DeltII binding in DOR-KO mice.

Table 1: Comparison of spinal morphine ED_{50} values (nmol (95% CI)) between WT and DOR-KO mice at different time points as measured with the tail flick assay.

Strain	15 min	30 min	45 min	60 min
WT	2.9 (1.8-4.6)	3.2 (1.8-5.8)	1.8 (0.9-3.6)	1.5 (0.9-2.7)
DOR-KO	No efficacy	3.4 (1.3-9.0)	1.6 (0.9-3.1)	1.5 (0.8-2.9)

Table 2: Comparison of systemic morphine ED_{50} values (mg/kg (95% CI)) between WT and DOR-KO mice at different time points as measured with the tail flick assay.

Strain	15 min	30 min	45 min	60 min
WT	13.3 (9.8-18.2)	9.1 (6.1-13.7)	9.0 (5.1-15.8)	9.3 (6.4-13.6)
DOR-KO	11.7 (8.4-16.3)	11.7 (8.4-16.4)	10.7 (8.4-13.6)	10.1 (7.6-13.0)

Chapter 4:
The delta opioid receptor is sufficient, but not necessary for spinal opioid-adrenergic analgesic synergy

RATIONALE OF THE STUDY

In order to gain mechanistic insight into opioid-adrenergic interactions, it is necessary to identify the receptor subtypes required for synergy.

Our observations from Chapter 3 called into question some assumptions about the role of DOR in opioid antinociception that could influence opioid-adrenergic synergy. First, studies using DOR agonists (e.g. DeltII, DPDPE) have demonstrated that these agonists can interact synergistically with α_2AR agonists, which was originally attributed to the activation of DOR (Roerig et al., 1992; Stone et al., 1997; Guo et al., 2003). However, we and others have shown that, in the tail flick assay, DOR agonist-mediated antinociception persists in DOR-KO mice (Scherrer et al., 2004; van Rijn et al., 2012), suggesting that other receptor targets mediate the antinociceptive effect of these agonists. Since the synergistic interactions between DOR and α_2AR agonists have never been tested in DOR-KO mice, it is therefore not clear if DOR or MOR mediates the synergy. Second, since DOR is required to produce full morphine antinociceptive efficacy, it may also be necessary to produce synergy between morphine and α_2AR agonists.

The aim of this chapter was to determine if DOR is necessary and sufficient to mediate spinal opioid-adrenergic synergy. In this study, opioid-adrenergic drug interactions were evaluated following spinal co-administration of clonidine with DeltII, morphine or DAMGO in WT and DOR-KO mice. Isobolographic analyses of dose-response curves determined whether interactions were synergistic or additive. Since DeltII-mediated antinociception was DOR-dependent in the SP behavioral assay (Fig 1B), we used this assay instead of the hot water tail flick assay to measure antinociception.

RESULTS

Comparable SP-evoked nocifensive behaviors are measured in WT and DOR-KO mice

We used the substance P (SP) behavioral assay to measure the antinociceptive effect of opioid agonists and clonidine at the spinal level. Intrathecal (i.t.) administration of SP induces a characteristic set of behaviors (biting, licking and scratching) directed at the abdomen and hind portion of the mouse receiving the exogenous SP (Hylden and Wilcox, 1981). Analgesic drugs acting at the spinal cord inhibit these nocifensive behaviors in a dose-dependent manner. There was no significant difference in SP-induced behaviors between WT (37 ± 4, n = 13) and DOR-KO (34 ± 3, n = 22) mice (two-tailed unpaired Student's t-test, $P >$ 0.05) upon intrathecal injection of 15 ng SP. Thus, there is no strain difference in sensitivity to SP nociception.

Antinociceptive action of spinally administered DeltII, DAMGO, morphine and clonidine in WT and DOR-KO mice

DeltII, morphine, DAMGO and clonidine were administered spinally (i.t.) in the SP behavioral assay in both WT and DOR-KO mice. All drugs inhibited SP-induced nocifensive behaviors in a dose-dependent manner (Figure 1, Table 1), except for DeltII, which was effective in WT but not DOR-KO mice (Figure 1B). Clonidine inhibition of SP-induced behaviors was 3-fold more potent in DOR-KO mice compared to WT mice (Figure 1A, Table 1). The inhibitory action of morphine was similar in both WT and DOR-KO mice at lower doses. As morphine dose increases, its efficacy was reduced in DOR-KO mice compared to WT mice (Figure 1C). Nevertheless, there is no significant potency difference between WT and DOR-KO mice (Table 1). No strain difference was observed with the MOR agonist DAMGO (Figure 1D). Together, these data indicate that DOR mediates DeltII antinociception in the SP assay, and that morphine and clonidine antinociception are slightly altered in DOR-KO mice.

Deltorphin II-clonidine spinal antinociceptive synergy requires DOR

We tested the DOR-selective agonist, DeltII, and clonidine alone or in combination in the SP behavioral assay in WT and DOR-KO mice. In WT mice, DeltII and clonidine inhibited SP-induced nocifensive behaviors in a dose-dependent manner and with similar potency (Figure 2A). Thus, we tested DeltII in combination with clonidine at an equieffective ratio that also corresponds to an equimolar drug ratio (1:1). The inhibition of SP-induced behaviors by the drug combination shifted the dose-response curve leftward. Isobolographic analysis revealed that the experimental ED_{50} value of the drug combination was significantly lower than the theoretical additive ED_{50} value; the drug interaction is therefore synergistic (Figure 2B, Table 2).

In DOR-KO mice, DeltII was ineffective in the SP assay at all doses tested. We therefore used the same equimolar (1:1) drug ratio to compare the DeltII+clonidine interaction in DOR-KO mice that was used in the WT mice. Because DeltII was not efficacious, isobolographic analysis was not performed. However, the inhibition of SP-induced behaviors by the DeltII+clonidine combination was equivalent to clonidine alone, i.e. DeltII did not shift the clonidine dose-response curve in DOR-KO mice, suggesting that there is no interaction between DeltII and clonidine in DOR-KO mice (Figure 2C).

Morphine-clonidine spinal antinociceptive synergy persists in the absence of DOR

Since DOR activation is sufficient to produce synergy using a DOR-selective agonist, we assessed its necessity for the synergistic interaction between morphine and clonidine.

In WT mice, spinally administered morphine and clonidine inhibited SP-induced behaviors in a dose-dependent manner. Calculated ED_{50} values obtained for each drug were within one order of magnitude, hence we combined morphine+clonidine at an equieffective and equimolar (1:1) ratio. The drug combination also inhibited SP behaviors in a dose-dependent manner and the

dose-response curve was shifted to the left compared to the single doses (Figure 3A). The isobolographic analysis demonstrated that the morphine+clonidine interaction in WT mice was synergistic (Figure 3B, Table 2).

We then assessed the interaction between morphine and clonidine in DOR-KO mice. Because the difference in ED_{50} values between morphine and clonidine in DOR-KO mice was more than one order of magnitude (Table 1), we tested an equieffective drug ratio of 1 part clonidine + 10 parts morphine (1:10). The drug combination dose-dependently inhibited SP behaviors in DOR-KO mice and the dose-response curve was shifted to the left compared to each drug alone (Figure 3C). Isobolographic analysis showed that the experimental ED_{50} value is significantly lower than the theoretical additive ED_{50} value (Figure 3D), indicating that the interaction is synergistic (Table 2).

Taken together, these results show that equieffective doses of morphine and clonidine interact synergistically in both WT and DOR-KO mice.

DAMGO-clonidine interaction is additive in both WT and DOR-KO mice

The retention of morphine+clonidine synergy in DOR-KO mice suggests that opioid-adrenergic synergy can be mediated by MOR in the absence of DOR. To understand the requirements for MOR-mediated synergy with clonidine, we tested the combination of clonidine with the MOR-selective peptide agonist, DAMGO, in WT and DOR-KO mice. In WT mice, DAMGO inhibited SP-induced behaviors with an ED_{50} value 120-fold more potent than clonidine (Table 1). We therefore tested a combination of clonidine and DAMGO at a 100:1 ratio, which also inhibited SP-induced behaviors in a dose-dependent manner (Figure 4A). The isobolographic analysis revealed that this interaction was additive (Figure 4B, Table 2).

The potency difference between DAMGO and clonidine in DOR-KO mice required the use of a 1:10 drug ratio corresponding to equieffective doses in this strain. The resulting drug interaction was also additive (Figure 4C, D, Table 2).

CONCLUSION

This study addressed the role of DOR in spinal opioid-adrenergic synergistic interactions. We first compared the antinociceptive response of clonidine, DeltII, morphine and DAMGO between WT and DOR-KO mice in the SP behavioral assay. The observed lack of DeltII efficacy in DOR-KO mice confirms its DOR selectivity in the SP behavioral assay. The addition of clonidine to DeltII resulted in a synergistic interaction in WT but not in DOR-KO mice. In contrast, a synergistic interaction between clonidine and morphine was observed in both strains and the interaction between clonidine and the MOR-selective agonist DAMGO was additive in both strains. These data support the notion that the activation of DOR is sufficient, but not necessary, to produce analgesic synergy when α_2AR are also activated. Therefore, the synergistic interaction between different opioid-α_2-adrenergic agonists is mediated via different opioid receptor pathways; one of these pathways uses DOR and another pathway is likely using MOR.

FIGURES AND TABLES

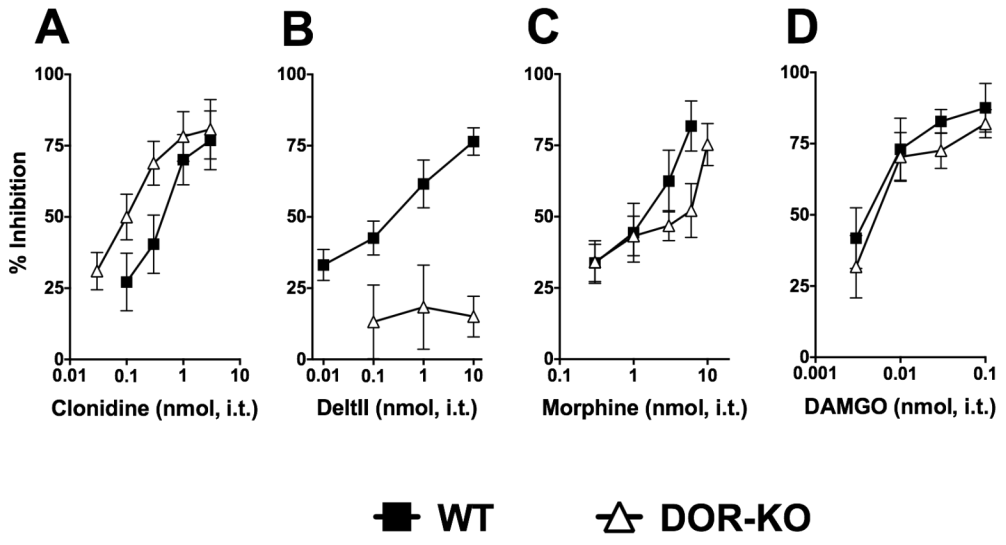

Figure 1: Effect of genetic deletion of DOR on dose-response curves in the SP behavioral assay

Dose-response curves showing the effects of clonidine, DeltII, DAMGO, and morphine in WT (■) and DOR-KO (△) mice where drugs were co-administered intrathecally (i.t.) with 15 ng of SP. (A) Clonidine was more potent in DOR-KO mice compared to WT mice. (B) DeltII inhibited SP behaviors in WT mice, but lacked efficacy in DOR-KO mice. (C) Morphine potency was not significantly different from WT mice. (D) DAMGO inhibition of SP behaviors was unchanged in DOR-KO mice compared to WT mice. Each data point represents the mean % inhibition ± SEM, n = 5 – 15 mice. The calculated ED_{50} value for each curve and the potency ratio between WT and DOR-KO are reported in Table 1.

A: WT mice

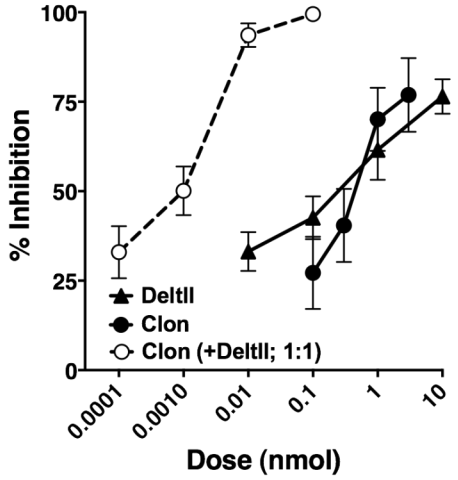

B: WT mice

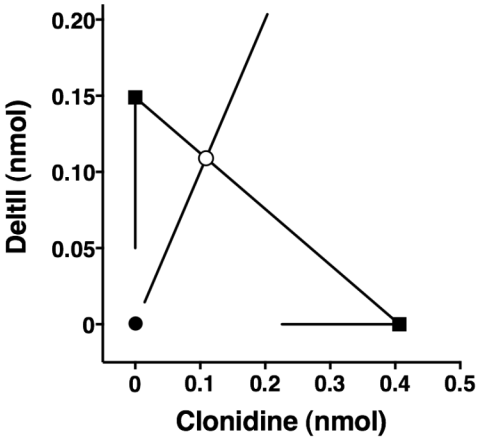

C: DOR-KO mice

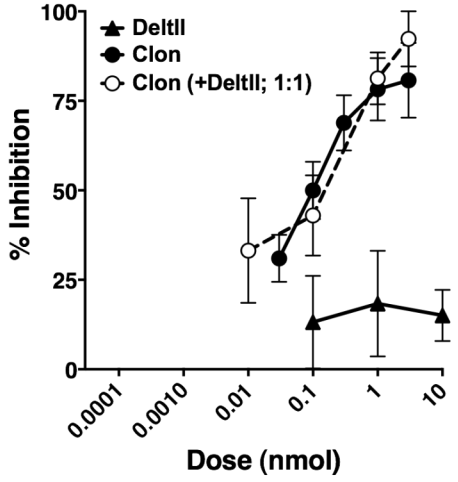

Figure 2: The interaction between DeltII and clonidine is synergistic in WT mice, but not in DOR-KO mice in the SP behavioral assay

(A) Dose-response curves of the spinal antinociceptive effect of deltorphin II (DeltII, ▲), clonidine (Clon, ●), and their combination at an equieffective 1:1 ratio graphed as the dose of clonidine present in the mixture (Clon (+DeltII; 1:1), ○). (B) Isobolographic analysis of the interaction between DeltII and clonidine in WT mice depicts the DeltII ED_{50} value with lower CI along the *y* axis, and the clonidine ED_{50} value with lower CI along the *x* axis. The measured experimental ED_{50} value for the drug combination (●) is lower than the calculated theoretical additive ED_{50} value (○), indicating that DeltII and clonidine interact in a synergistic manner. (C) In DOR-KO mice, spinal administration of DeltII (▲) was inefficacious at inhibiting SP-elicited behaviors. The dose-response curves of clonidine (Clon, ●) and of clonidine in the presence of DeltII (Clon (+DeltII; 1:1), ○) overlapped, showing that adding DeltII to clonidine did not change its potency. Isobolographic analysis of this data set was not possible since the ED_{50} value for DeltII was incalculable. The calculated ED_{50} value for the experimental and theoretical DeltII+clonidine combinations are reported in Table 2.

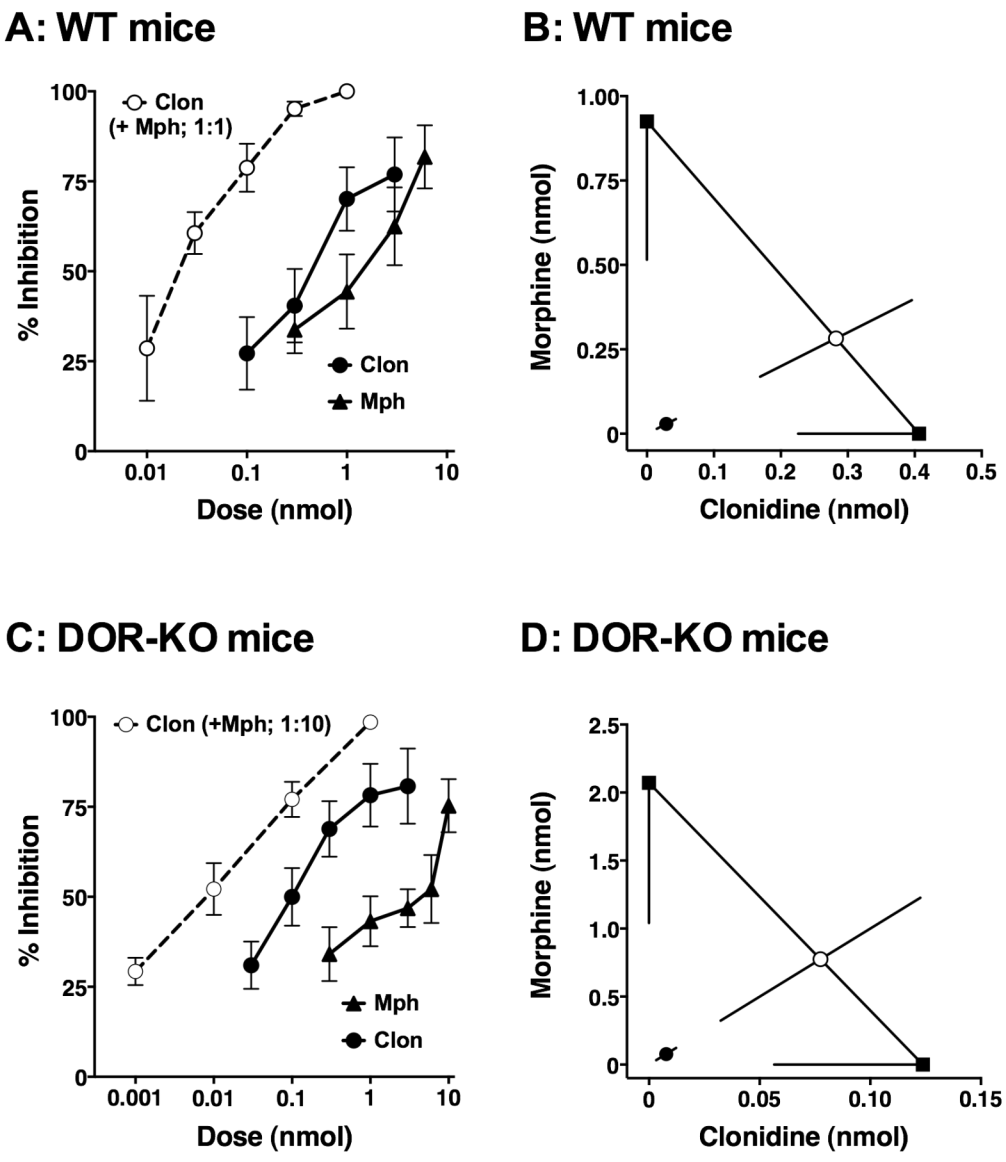
A: WT mice
B: WT mice
C: DOR-KO mice
D: DOR-KO mice
Clon
(+ Mph; 1:1)
Clon
Mph
% Inhibition
Dose (nmol)
Morphine (nmol)
Clonidine (nmol)
Clon (+Mph; 1:10)
Mph
Clon

Figure 3: Morphine and clonidine synergy persists in DOR-KO mice in the SP behavioral assay

(A) Dose-response curves of spinal morphine (Mph, ▲) and clonidine (Clon, ●) in WT mice. The dose-response curve of their equieffective 1:1 ratio combination was graphed as the dose of clonidine present in the mixture (Clon (+Mph; 1:1), ○). (B) Isobolographic analysis of the interaction between morphine and clonidine in WT mice depicts the morphine ED_{50} value with lower CI along the *y* axis, and the clonidine ED_{50} value with lower CI along the *x* axis. The measured experimental ED_{50} value (●) for the drug combination was lower than the theoretical additive ED_{50} value (○), indicating that morphine and clonidine interact in a synergistic manner. (C) Dose-response curves of spinal clonidine (Clon, ●) and morphine (Mph, ▲) in DOR-KO mice. The dose-response curve of their 10:1 ratio combination was graphed as the dose of clonidine present in the mixture (Clon (+Mph; 1:10), ○) to show the relative leftward shift in potency caused by the addition of morphine. (D) Isobolographic analysis of the interaction between morphine and clonidine in DOR-KO mice depicts the morphine ED_{50} values with lower CI along the *y* axis, and the clonidine ED_{50} value with lower CI along the *x* axis. The measured experimental ED_{50} value (●) for the combination of morphine and clonidine (10:1 ratio) and the theoretical additive ED_{50} value (○) are graphed with their upper and lower CI. The measured experimental ED_{50} value for the drug combination is below the calculated theoretical additive ED_{50} value, indicating that morphine and clonidine interact in a synergistic manner. The calculated ED_{50} value for the experimental and theoretical morphine+clonidine combinations are reported in Table 2.

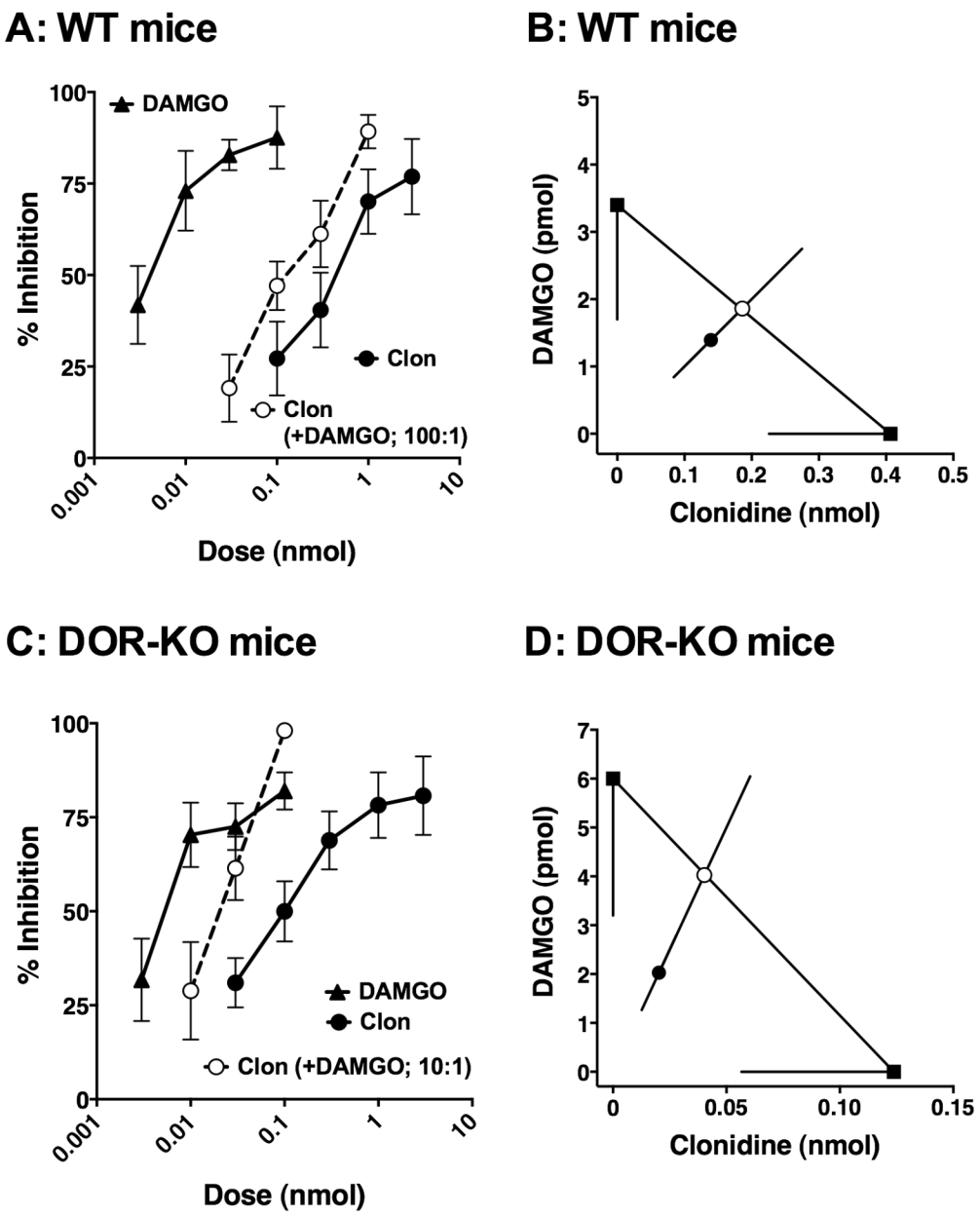
A: WT mice
B: WT mice
C: DOR-KO mice
D: DOR-KO mice
% Inhibition
Dose (nmol)
DAMGO
Clon
Clon
(+DAMGO; 100:1)
Clon (+DAMGO; 10:1)
DAMGO (pmol)
Clonidine (nmol)

Figure 4: DAMGO and clonidine are additive in WT and DOR-KO mice

(A, C) Dose-response curves of spinal DAMGO (▲) and clonidine (Clon ●) in WT and DOR-KO mice. (A) In WT mice, DAMGO+clonidine were combined at an equieffective dose ratio of 1:100 and the dose-response curve was graphed as the dose of clonidine present in the mixture (Clon (+DAMGO; 100:1), ○). (C) In DOR-KO mice, DAMGO+clonidine were combined at an equieffective 1:10 ratio (Clon (+DAMGO; 10:1), ○). (B, D) Isobolographic analysis of the interaction between DAMGO and clonidine in WT and DOR-KO mice depicts the DAMGO ED_{50} value with lower CI along the *y* axis, and the clonidine ED_{50} value with lower CI along the *x* axis. The measured experimental ED_{50} value for the drug combination (●) and the theoretical additive ED_{50} value (○) are graphed with their upper and lower CI. In both strains, the measured experimental ED_{50} value overlaps the calculated theoretical ED_{50} value, indicating that the interactions are additive. The calculated ED_{50} value for the experimental and theoretical DAMGO+clonidine combinations are reported in Table 2.

Table 1: Comparison of calculated ED_{50} (95% CI) values for single drugs administered intrathecally in the SP assay in WT and DOR-KO mice.

Single Drug	WT	DOR-KO
Clonidine (nmol)	0.4 (0.2-0.7)	0.12 (0.06-0.27)*
DeltII (nmol)	0.15 (0.05-0.44)	No efficacy
Morphine (nmol)	0.9 (0.5-1.7)	2.1 (1.0-4.1)
DAMGO (pmol)	3.4 (1.7-7)	6.0 (3.2-11)

* ED_{50} significantly different, WT vs. DOR-KO, Student's *t*-test ($P < 0.05$)

Table 2: Calculated ED_{50} values (nmol (± 95% SEM)) for drug combinations administered intrathecally in SP assay in WT and DOR-KO mice.

Drugs	WT			DOR-KO		
	Experimental	Theoretical	Interaction	Experimental	Theoretical	Interaction
DeltII + Clonidine	0.0010 (±0.0005)	0.22 (±0.19)	Synergistic*	0.20 (±0.23)	0.25 (±0.20)	No interaction [a]
Morphine + Clonidine	0.058 (±0.029)	0.56 (±0.27)	Synergistic*	0.085 (±0.050)	0.85 (±0.49)	Synergistic*
DAMGO + Clonidine	0.14 (±0.056)	0.19 (±0.09)	Additive	0.022 (±0.0084)	0.044 (±0.022)	Additive

*Indicates that the experimental ED_{50} value < theoretical ED_{50} value (Student's T test $P < 0.05$)

[a] Since DeltII was ineffective in DOR-KO mice, we compared the ED_{50} value for DeltII+clonidine combination to the ED_{50} value of clonidine alone (Student's T test, $P > 0.05$) instead of running an isobolographic analysis.

Chapter 5:

Spinal opioid antinociception is allosterically modulated by the α_{2A}-adrenergic receptor.

RATIONALE

The noradrenergic system is a key modulator of nociception. Norepinephrine (NE) and α_2-adrenergic agonists generate antinociceptive effects via activation of spinal α_{2A}AR and α_{2C}AR. Both receptors have been shown to mediate opioid-adrenergic synergy depending on the opioid-α_2AR agonist combination used (Fairbanks et al., 2002; Stone et al., 2007). However, the α_2AR subtype involved in morphine+clonidine synergy - the most studied combination in rodents and most commonly used in humans - has not been identified. Morphine also interacts synergistically with spinally administered NE (Roerig et al., 1992), suggesting that the endogenous adrenergic system can regulate opioid-mediated antinociception, but the α_2AR subtype involved is also unknown. Interestingly, opioid-adrenergic synergistic interactions seem to share a common effector signaling pathway since both morphine+clonidine and DeltII+clonidine synergy are PKC-dependent (Wei et al., 1996; Overland et al., 2009). Altogether, these studies raise the question as to whether the α_{2A}AR regulates spinal opioid antinociception and morphine+clonidine synergy.

The aims of this chapter were two-fold: 1) to investigate the role of the α_{2A}AR in opioid-adrenergic interactions, and 2) to investigate the role of the α_{2A}AR in opioid antinociception. In this study, we compared the pharmacological response of WT and α_{2A}AR-KO mice to different treatments. The tail flick assay and the SP behavioral assay were both used to evaluate opioid-adrenergic drug interactions following spinal co-administration of clonidine with DeltII, morphine or DAMGO. Isobolographic analyses of dose-response curves determined whether interactions were synergistic or additive. The single drug dose-response curves for morphine and DeltII revealed a significant potentiation of opioid antinociception in α_{2A}AR-KO compared to WT mice, which led to further investigation of the possible mechanism mediating this effect using the tail flick assay. We also examined opioid receptor expression levels by quantitative PCR analysis, western blot and radioligand binding. To assess

whether endogenous norepinephrine (NE) modulates morphine antinociception through the α_{2A}AR, we depleted spinal NE and evaluated morphine potency. Finally, we tested the possibility that the increased morphine effect observed in α_{2A}AR-KO mice is due to disinhibition of PKC activation by evaluating morphine antinociception in the presence of a PKC inhibitor.

RESULTS

Evaluation of nociceptive thresholds in WT and α_{2A}AR-KO mice

We evaluated the baseline nociceptive threshold of α_{2A}AR-KO mice compared to WT mice in order to assess the role of the α_{2A}AR in normal thermal and mechanical nociception. Thermal heat nociception was measured with the hot water tail flick assay at four different temperatures and in the radiant heat paw withdrawal assay. Compared to WT mice, α_{2A}AR-KO mice were more sensitive to the heat stimulus in the hot water tail flick assay (Figure 1A; 2-way ANOVA; strain: $F_{(1, 173)} = 17.17$, $P < 0.0001$, temperature: $F_{(3, 173)} = 175.8$, $P < 0.0001$, interaction: $F_{(3, 190)} = 2{,}681$, $P = 0.048$). The strain difference was largest when the water bath was set at 49˚C where a significant difference was observed between WT and α_{2A}AR-KO mice (WT: 2.92 ± 0.15 sec.; α_{2A}AR-KO: 1.40 ± 0.13 sec.; $P < 0.0001$). Similarly, α_{2A}AR-KO mice were also more sensitive than WT mice to heat from a radiant light beam focused on the hind paw (Figure 1B; WT: 6.75 ± 0.35 sec.; α_{2A}AR-KO: 5.60 ± 0.23 sec.; $P = 0.007$). When measuring mechanical sensitivity, we did not observe a difference between WT and α_{2A}AR-KO mouse mechanical withdrawal thresholds (Figure 1C; WT: 1.75 ± 0.157 g; α_{2A}AR-KO: 1.70 ± 0.131 g). We did not observe a significant difference in the number of nocifensive behaviors induced by SP administered intrathecally between WT and α_{2A}AR-KO (Figure 1D; WT: 37.08 ± 4.16 counts; α_{2A}AR-KO: 29.94 ± 2.52). Together, this shows that α_{2A}AR-KO mice are more sensitive to heat nociceptive stimuli than WT mice, but that mechanical and SP-induced nociception are not affected.

Spinal clonidine, morphine, DeltII, DAMGO and SNC80 antinociception change in α_{2A}AR-KO mice

We assessed the role of α_{2A}AR in spinal antinociception mediated by clonidine, morphine, DeltII and DAMGO with the hot water tail flick assay (Figure 2, upper panels) and in the SP behavioral assay (Figure 2, lower panels) by comparing each drug's ED_{50} values in WT and α_{2A}AR-KO mice (Table 1). All drugs dose-

dependently increased tail flick latencies and reduced SP-induced behaviors in WT and α_{2A}AR-KO mice (Figure 2). Interestingly, clonidine, DeltII and DAMGO were more potent in the SP assay than in the tail flick assay for both strains. Clonidine was not effective in the hot water tail flick assay, and its efficacy and potency was reduced in the SP behavioral assay in α_{2A}AR-KO mice compared to WT mice (Figure 2A). Surprisingly, morphine was as efficacious, but more potent in α_{2A}AR-KO mice than in WT mice in both assays (Figure 2B). The potency of the DOR-selective peptide agonist DeltII was also shifted to the left in α_{2A}AR-KO mice compared to WT mice (Figure 2C). The limited solubility of DeltII in a physiological vehicle and side effects observed at high doses prevented us from testing higher doses in WT to determine if DeltII maximal efficacy changed in α_{2A}AR-KO mice. The antinociceptive response of the MOR-selective peptide agonist DAMGO was slightly more potent in α_{2A}AR-KO mice than in WT mice in the tail flick assay, but no potency difference was observed in the SP assay (Figure 2D). These experiments indicate that in the absence of the α_{2A}AR, clonidine spinal antinociception is impaired and opioid spinal antinociception is potentiated.

Since the DeltII antinociceptive response was enhanced in α_{2A}AR-KO mice, we tested whether the antinociceptive response of another non-peptide DOR-selective ligand, SNC80, was also augmented in these mice (Figure 3). A high dose of SNC80 administered i.t. (100 nmol) elicited an antinociceptive response in both mouse strains compared to the saline treatment, but the response in α_{2A}AR-KO mice was significantly greater than WT mice (2 way ANOVA; strain: $F_{(1, 37)} = 4.48$, $P = 0.0409$, dose: $F_{(1, 37)} = 13.62$, $P = 0.0007$, interaction: $F_{(1, 37)} = 0.7828$, $P = 0.3828$; Figure 3). These data confirms that the enhanced antinociception in α_{2A}AR-KO mice can be observed with different DOR-selective agonists.

Deltorphin II-clonidine spinal antinociceptive synergy requires α_{2A}AR

We previously identified DOR activation as necessary for DeltII synergistic interaction with clonidine (Chapter 4, Figure 2). To evaluate the role of the α_{2A}AR in this interaction, we tested this drug combination in α_{2A}AR-KO mice and compared it to WT mice. As we have shown before, DeltII effect is selective for DOR with the SP assay (Chapter 4, Figure 1), but not the tail flick assay (Chapter 3, Figure 2). Therefore, we tested the synergistic interaction between DeltII and clonidine in WT and α_{2A}AR-KO mice with the SP assay.

In WT mice, DeltII and clonidine inhibited SP-induced behaviors with similar potency. We therefore mixed these agonists at a 1:1 ratio reflecting their equieffective ratio. The dose-response curve for the drug combination shifted to the left compared to the single doses (Figure 4A). Isobolographic analysis revealed that the experimental ED_{50} value of the drug combination was significantly lower than the theoretical additive ED_{50} value; the drug interaction is therefore synergistic (Figure 4B, Table 2).

In α_{2A}AR-KO mice, clonidine did not inhibit more than 50% of SP-induced behaviors, even at high doses, and was thus considered ineffective. Using the same 1:1 ratio to combine DeltII and clonidine as in WT mice, we tested if the addition of clonidine to DeltII shifted the dose response curve leftwards in α_{2A}AR-KO mice. Clonidine did not shift the dose-response curve, suggesting that there is no interaction between DeltII and clonidine in α_{2A}AR-KO mice (Figure 4C).

Morphine-clonidine spinal antinociceptive synergy requires α_{2A}AR

We next tested if the synergistic interaction between morphine and clonidine necessitate the α_{2A}AR by testing this combination in WT and α_{2A}AR-KO mice. We used the SP-behavioral assay and the tail flick assay to measure antinociception.

In WT mice, since the spinal morphine and clonidine antinociceptive effects had dose-response curves and calculated ED_{50} values within one order of magnitude in both assays, we combined them at a 1:1 ratio to test their interaction. The dose-response curve for the drug combination was shifted to the left compared to the single drugs in the SP-behavioral assay (Figure 5A) and the tail flick assay (Figure 6A). The isobolographic analysis demonstrated that morphine combined with clonidine interacted synergistically in the SP-behavioral assay (Figure 5B, Table 2) and the hot water tail flick assay (Figure 6B, Table 2).

We then assessed the interaction between morphine and clonidine in α_{2A}AR-KO mice. As we have previously noted, clonidine inhibited less than 50% of SP-induced behaviors and reached less than 50% MPE in the tail flick assay, which is not suitable for isobolographic analysis. The assessment of morphine+clonidine interaction in α_{2A}AR-KO mice was done using the same equimolar drug ratio (1:1) as we used in WT mice to test whether the addition of clonidine would shift the dose-response curve to the left. The dose-response curve for the drug combinations were not significantly different from morphine alone in both assays (Figures 5C, 6C, Table 2), suggesting that without the α_{2A}AR, there is no synergistic interaction between morphine and clonidine.

Spinal morphine antinociception is potentiated in α_{2A}AR-KO mice

It has been previously shown that a low dose of an α_2AR antagonist can increase morphine potency and prolong its antinociceptive effect (Milne et al., 2008). We therefore further characterized the difference in morphine potency between WT and α_{2A}AR-KO mice to see if the time course of the antinociceptive effect was also changed. We administered different morphine doses i.t. to cover the full range of efficacy and for each strain, and since it allowed us to take repeated measures over 240 minutes, we used the tail flick assay to measure antinociception.

Time course analysis of antinociception in WT mice showed that morphine effect peaked at 45 or 60 minutes, depending on the dose, and began to decline at 90

minutes (Figure 7A). While the effect of the lowest doses tested had returned to baseline (0.3, 1 and 3 nmol), the highest doses were still effective after 240 minutes (6 and 10 nmol). The time course of effect was similar in α_{2A}AR-KO, but the doses used to obtain the same effect are much lower (Figure 7B). Morphine effect peaked between 30 and 60 minutes depending on the dose and started to decline at 60 minutes for lower doses (0.03, 0.1 and 0.3 nmol) and at 120 minutes for higher doses (1 and 3 nmol). However, all doses but the highest one (3 nmol) had returned to baseline values at 240 minutes. The highest effect was obtained with 1 and 3 nmol of morphine which seem to plateau at around the same values and had no significant differences in terms of the magnitude of their effect (2 way ANOVA; dose: $F_{(1, 7)} = 0.8764$, $P = 0.3804$, time: $F_{(10, 70)} = 16.26$, $P < 0.0001$, interaction: $F_{(10, 70)} = 0.4218$, $P = 0.9315$).

When comparing the effect of 1 nmol morphine i.t. between WT and α_{2A}AR-KO mice, we observed a striking strain difference where morphine is significantly more efficacious in α_{2A}AR-KO mice (2 way ANOVA; strain: $F_{(1, 7)} = 10.84$, $P = 0.0133$, time: $F_{(10, 70)} = 12.27$, $P < 0.0001$, interaction: $F_{(10, 70)} = 3.547$, $P = 0.0008$; Figure 7C). Dose-response curves were constructed from the time course analysis to evaluate the potency difference between WT and α_{2A}AR-KO mice at different time point (Table 3). For example, at 30 minutes, the leftward shift of the dose-response curve in α_{2A}AR-KO mice compared to WT mice reflects a 30 fold potency shift (Figure 7D, Table 3). Interestingly, the maximal effect is the same in both strains.

Together, these data indicate that spinal morphine is more potent, but not more efficacious, in the absence of the α_{2A}AR.

Systemic morphine antinociception is potentiated in α_{2A}AR-KO mice

α_{2A}ARs are not only expressed in the spinal cord; they are found in supraspinal areas, in the peripheral nervous system and in non-neuronal cells. Since morphine sites of action are also widespread, it is possible that the potentiation that we observed in the spinal cord of α_{2A}AR-KO mice may be observed at peripheral or

supraspinal sites of action. We tested this possibility by administering different doses of morphine systemically (i.p.) in WT (Figure 8A) and α_{2A}AR-KO (Figure 8B) mice and measured the antinociceptive effect over 210 minutes in the hot water tail flick assay. In both strains, morphine reached a peak effect by 60 minutes and was declining at 90 minutes. By 210 minutes, all doses tested returned to baseline values, except for the 30 mg/kg dose in α_{2A}AR-KO mice, which was still effective. Morphine at 10 mg/kg generated a parallel time course in both mouse strains, but the amplitude of the antinociceptive effect was greater in α_{2A}AR-KO mice (2 way ANOVA; strain: $F_{(1, 19)} = 6.384$, $P = 0.206$, time: $F_{(9, 171)} = 17.40$, $P < 0.0001$, interaction: $F_{(9, 171)} = 2.677$, $P = 0.0062$; Figure 8C). However, this difference contributes to only a minor increase in morphine potency in α_{2A}AR-KO mice compared to WT mice since it is not observed at other doses (Table 4). For example, systemic morphine dose-dependent inhibition of tail flick latencies was approximately 2 fold more potent in α_{2A}AR-KO compared to WT mice (Figure 8D), while the potency shift was approximately 30 fold when morphine was administered spinally (Figure 7D).

We hypothesized that the small potency shift observed when morphine is administered i.p. is due to the contribution of morphine's effect at the spinal level to the overall effect. To test this, we pre-treated WT and α_{2A}AR-KO mice with a non-specific opioid receptor antagonist, naloxone (i.t.), and tested morphine 10 mg/kg (i.p.) antinociceptive response in the hot water immersion tail flick assay. Thirty minutes after administering morphine, naloxone-treated mice had a significantly lower morphine effect compared to saline-treated mice in both strains. Morphine was significantly more effective in saline-treated α_{2A}AR-KO mice, but not in naloxone-treated mice (2 way ANOVA; strain: $F_{(1, 18)} = 6.911$, $P = 0.017$, naloxone treatment: $F_{(1, 18)} = 48.97$, $P < 0.0001$, interaction: $F_{(1, 18)} = 2.594$, $P = 0.125$), indicating that once spinal morphine is counteracted, WT and α_{2A}AR-KO mice respond similarly to morphine (Figure 8E).

These data indicate that spinal morphine effect contributes greatly to the systemic effect and that this contribution is responsible for the increased morphine effect in α_{2A}AR-KO mice.

MOR expression level is unchanged in α_{2A}AR-KO mice

MOR is the main receptor target mediating morphine antinociceptive effect and an increase in its expression level could render morphine more potent.

Quantative PCR analysis of the cDNA corresponding to MOR mRNA was analyzed from DRG and spinal cord extracts from WT and α_{2A}AR-KO mice. No significant differences in MOR expression level between WT and α_{2A}AR-KO mice were observed in either DRG (WT = 1.00 ± 0.10, α_{2A}AR-KO = 1.22 ± 0.10, P = 0.153; Figure 9A) or spinal cord (1.00 ± 0.05, α_{2A}AR-KO = 1.05 ± 0.04, P = 0.472; Figure 9B). We further analyzed the amount of MOR receptors by western blot analysis of purified membrane extracts from WT and α_{2A}AR-KO spinal cords. We measured the density of a 67 kDa immunoreactive band corresponding to MOR and adjusted the relative density with the density of the 35 kDa GAPDH-immunoreactive band obtained after stripping and re-probing the membrane (Figure 9C). The relative MOR densitometry was not different between WT and a2AAR-KO mice (nonparametric T test, P = 0.7; Figure 9D).

We conclude that neither MOR mRNA nor receptor expression were up or downregulated in α_{2A}AR-KO. These data rule out the possibility that MOR expression is upregulated in α_{2A}AR-KO mice compared to WT mice.

DOR expression level is unchanged in α_{2A}AR-KO mice

Since the antinociceptive response of DeltII and SNC80 was enhanced in α_{2A}AR-KO mice, we tested the hypothesis that DOR expression levels are upregulated in these mice. We analyzed DOR spinal cord and DRG cDNA from WT and α_{2A}AR-KO mice by quantative PCR. We found no difference in the relative expression of DOR receptors in DRGs between WT (1.00 ± 0.04) and α_{2A}AR-KO mice (0.79 ± 0.09; P = 0,073; Figure 10A). Similarly, DOR relative expression in spinal cord

tissues from WT mice (1.00 ± 0.08) was not different from that of α_{2A}AR-KO mice (1.10 ± 0.05; $P = 0.334$; Figure 10B).

Endogenous norepinephrine is not necessary for the potentiation of morphine antinociceptive effect in α_{2A}AR-KO mice

D79N-α_{2A}AR mice have been reported to have a higher hippocampal norepinephrine (NE) turnover (Lakhlani et al., 1997) suggesting that a disruption in α_{2A}AR function could result in elevated levels of NE in CNS tissues. Since the co-administration of morphine with norepinephrine at the spinal cord results in analgesic synergy (Roerig et al., 1992), we hypothesize that elevated NE levels could increase spinal morphine effect in α_{2A}AR-KO mice. We tested this hypothesis by injecting the toxin 6-OHDA i.t. to eliminate spinal catecholaminergic fibers that release NE in the spinal cord of WT and α_{2A}AR-KO mice. In the spinal cord, 6-OHDA selectively enters noradrenergic fibers where its degradation products effectively destroy the nerve terminals (Fasmer et al., 1986).

In WT mice, morphine efficacy was greatly reduced in mice treated with 6-OHDA compared to mice treated with vehicle, confirming the role of endogenous NE in the antinociceptive effect of morphine (Figure 11A). The increased morphine potency was observed again in α_{2A}AR-KO mice, but the 6-OHDA treatment had no effect on morphine response in α_{2A}AR-KO mice since the dose-response curves for vehicle-treated mice overlapped with that of 6-OHDA-treated mice (Figure 11A). As a result, the calculated morphine ED_{50} values for 6-OHDA-treated mice were not different from the values obtained in vehicle-treated α_{2A}AR-KO mice (Table 5). Thus, increased morphine potency was maintained in α_{2A}AR-KO mice despite the selective lesion of noradrenergic fibers. These results refute our hypothesis, but raise new hypotheses on how the α_{2A}AR regulates opioid antinociception, perhaps through allosteric interactions with opioid receptors.

Descending noradrenergic inhibition of noxious heat responses is mediated through the α_{2A}AR

Descending noradrenergic fibers modulate endogenous inhibition of nociceptive stimuli at the spinal cord level by activating α_2AR (Gilsbach et al., 2009). We hypothesized that the lower heat nociceptive threshold observed in α_{2A}AR-KO mice (Figure 1) is due to a loss of spinal NE effect in these mice. To test this, we compared the baseline tail flick latencies from WT and α_{2A}AR-KO mice in which descending NE fibers were eliminated (Figure 11B). 6-OHDA-treated WT mice had lower tail flick latencies compared to vehicle-treated mice (WT vehicle = 1.86 ± 0.24 sec., WT 6-OHDA = 1.10 ± 0.12 sec., P = 0.01), confirming the effectiveness of the treatment and the role of descending noradrenergic fibers in heat nociception. In α_{2A}AR-KO mice, no such difference was observed in tail flick latencies between 6-OHDA- and vehicle- treated mice (α_{2A}AR-KO vehicle = 1.48 ± 0.16, α_{2A}AR-KO 6-OHDA = 1.15 ± 0.13, P = 0.14), suggesting that the α_{2A}AR subtype mediates the antinociceptive response to endogenous NE modulation of heat nociception.

DeltII binding affinity is unaffected in α_{2A}AR-KO mice

We demonstrated that DeltII antinociceptive response was enhanced in α_{2A}AR-KO mice, but that expression levels were not upregulated in either DRG or spinal cord. Changes in DeltII binding properties in the absence of the α_{2A}AR could result in increased potency independent of mRNA expression. Saturation radioligand binding assays were conducted to measure the number of binding sites and the affinity of [^{3}H]-DeltII in SC membrane preparations from WT and α_{2A}AR-KO mice. [^{3}H]-DeltII bound to membrane preparation in a concentration-dependent manner in both strains (Figure 12A) and the number of binding sites was similar in both strains (WT: B_{max} = 373 (319-426) CPM, α_{2A}AR-KO: B_{max} = 309 (201-417) CPM; nonlinear regression, P = 0.1422) and apparent dissociation constant (WT: K_D = 0.9 (0.4-1.4) nM, α_{2A}AR-KO: K_D = 1.1 (-0.4-2.6) nM; nonlinear regression, P = 0.6795) were not significantly different.

We further evaluated [^{3}H]-DeltII affinity for its binding site with a competition binding assay. The affinity of naltrindole, a DOR-selective antagonist, determined by competition with [^{3}H]-DeltII in WT and α_{2A}AR-KO was similar in both strains (P = 0.2857; Figure 12B). Naltrindole competitively inhibited [^{3}H]-DeltII binding with a K_I value of 0.17 (0.12-0.25) nM in WT membrane preparations and a K_I value of 0.14 (0.11-0.18) nM in α_{2A}AR-KO membrane preparations.

Thus, the absence of the α_{2A}AR did not change DeltII affinity or its binding sites in a way that would result in an increased antinociceptive potency or efficacy.

Role of PKC in morphine antinociception

We hypothesized that the activation of PKC by opioid receptors upon activation by morphine is controlled by the α_{2A}AR and that the increased morphine effect observed in α_{2A}AR-KO mice is due to a disinhibition of PKC activation. To test this hypothesis, we administered a broad spectrum PKC inhibitor i.t., chelerythrine, prior to testing the antinociceptive effect of spinal morphine in the tail flick assay in WT and α_{2A}AR-KO. In WT mice, there was no difference between the vehicle- and the chelerythrine- treated groups (Figure 13A). In α_{2A}AR-KO mice, chelerythrine-treated mice had a lower morphine antinociceptive response compared to vehicle-treated mice, but the effect was not significant (2 way ANOVA; interaction: $F_{(4, 132)}$ = 1.239, P = 0.297, time: $F_{(4, 132)}$ = 47.24, P < 0.0001, treatment: $F_{(1, 33)}$ = 2.702, P = 0.1097; Figure 13B). The interpretation of these results is limited by the small strain difference observed between the vehicle-treated groups. These results show that the effect of morphine in α_{2A}AR-KO mice tends to decrease when PKC is inhibited. Further experiments will be necessary in order to confirm this trend.

CONCLUSION

The consistently lower noxious heat thresholds observed in α_{2A}AR-KO mice using two different assays suggest that heat nociception, but not mechanical nociception, is modulated through the α_{2A}AR in naive conditions. Our data also shows consistency across the stimulation sites; α_{2A}AR-KO mice had lower heat thresholds whether the stimulus was applied on the tail or the plantar surface of the hind paw.

In α_{2A}AR-KO mice, spinal DeltII or morphine did not synergize with clonidine as in WT mice, suggesting that the α_{2A}AR is necessary to mediate synergistic interaction with both DOR and MOR agonists.

Our study demonstrates that under normal physiological conditions, the potency of both systemic and spinal morphine is augmented in mice lacking the α_{2A}AR. The observation that the shift in morphine potency is greater at the spinal level than at the systemic level suggests that a spinal mechanism underlies this effect. By blocking the spinal component of the systemic morphine response, we showed that morphine action at peripheral and supraspinal sites was similar between WT and α_{2A}AR-KO mice in the tail flick assay. We conclude that the enhanced morphine potency observed in α_{2A}AR-KO mice is confined to the spinal cord.

When testing opioid receptor subtype-selective agonists, we found that DeltII was more potent in α_{2A}AR-KO mice than in WT mice, while DAMGO potency did not change as much. The antinociceptive effect of SNC80 was also greater in α_{2A}AR-KO mice compared to WT mice. Therefore, the antinociceptive responses of other opioid agonists administered spinally are also amplified in α_{2A}AR-KO mice.

These changes in opioid response could not be attributed to changes in MOR or DOR expression level, increased amount of MOR in the spinal cord or altered [^{3}H]-DeltII binding properties in α_{2A}AR-KO mice.

Eliminating catecholaminergic fibers in the spinal cord did not change the shift in potency observed in α_{2A}AR-KO mice, but it completely abolished morphine efficacy in WT mice. The interpretation of these results are twofold: 1) the observation that morphine potency was lost in WT mice following the spinal ablation of catecholaminergic fibers, while it did not change in α_{2A}AR-KO mice, suggests that endogenous NE acts via the α_{2A}AR to modulate morphine antinociceptive response; 2) since the potentiation of morphine response in α_{2A}AR-KO mice is maintained in 6-OHDA-treated α_{2A}AR-KO mice, it is not due to an increased in NE tone in the spinal cord as we hypothesized.

Finally, we tested the hypothesis that α_{2A}ARs exert an inhibitory control on PKC activation by opioid agonists, and that a lack of PKC inhibition in α_{2A}AR-KO mice potentiates opioid agonists. Although the effect was not significant, blocking spinal PKC activation attenuated the effect of morphine in α_{2A}AR-KO mice, but not in WT mice. These results trend towards confirming our hypothesis and will have to be replicated.

FIGURES AND TABLES

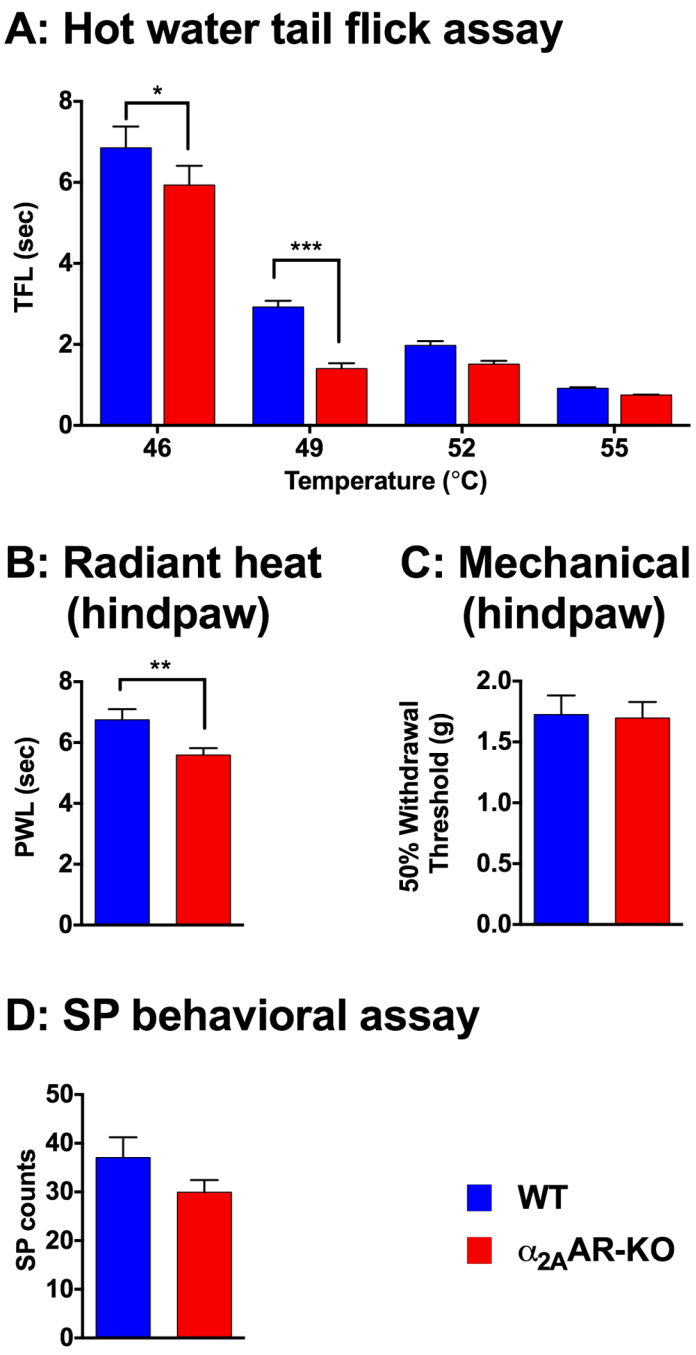

Figure 1: Comparison of thermal, mechanical and SP-induced nociceptive thresholds between WT and α_{2A}AR-KO mice.

A) Tail flick latencies (TFL) measured at temperatures ranging from 46˚C to 52˚C in the warm water tail flick assay showed that α_{2A}AR-KO mice (n = 16-26) were more sensitive than WT mice (n = 15-33) at 46˚C and 49˚C. B) Paw withdrawal latencies (PWL) measured with the radiant heat assay in α_{2A}AR-KO mice (n = 22) were faster than paw withdrawal latencies measured in WT mice (n = 15). C) 50% mechanical threshold measured with von Frey filaments were similar on the paw of WT (n = 17) and α_{2A}AR-KO (n = 16) mice. D) The number of nocifensive behaviors induced by the administration of 15 ng of SP i.t. were not significantly different between WT (n = 13) and α_{2A}AR-KO (n = 16) mice. * $P < 0.05$ *** $P < 0.001$

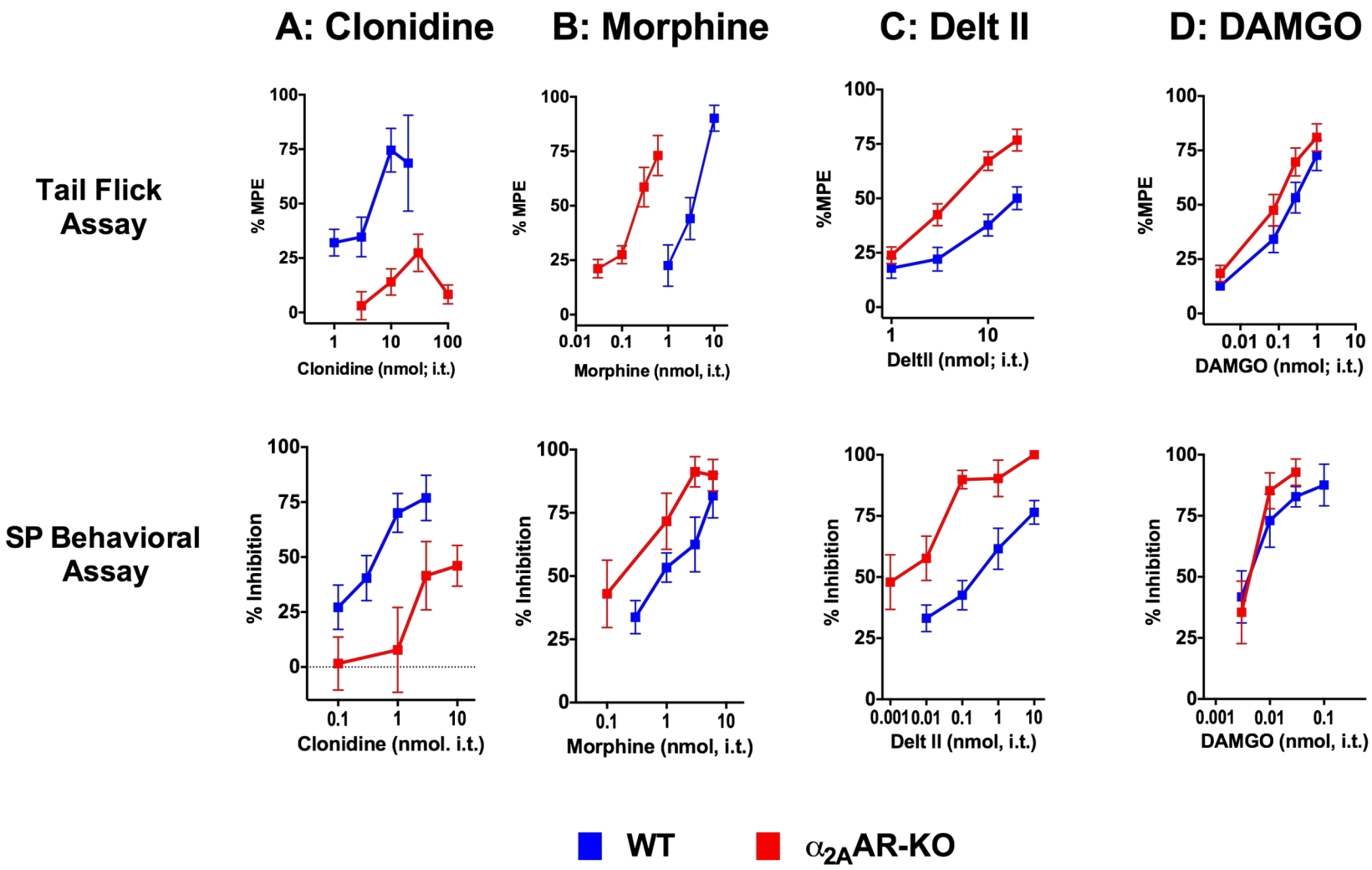
A: Clonidine
B: Morphine
C: Delt II
D: DAMGO
Tail Flick Assay
SP Behavioral Assay
% MPE
%MPE
% Inhibition
Clonidine (nmol; i.t.)
Morphine (nmol, i.t.)
DeltII (nmol; i.t.)
DAMGO (nmol; i.t.)
Clonidine (nmol. i.t.)
Morphine (nmol, i.t.)
Delt II (nmol, i.t.)
DAMGO (nmol, i.t.)
WT
α2AAR-KO

Figure 2: Dose-response analysis of spinal clonidine-, morphine-, DeltII- and DAMGO- mediated antinociception in WT and α_{2A}AR-KO mice

Dose-response curves were constructed for each drug administered i.t. in the hot water tail flick assay (upper panel) and the SP behavioral assay (lower panel). ED_{50} values are reported in Table 1. A) Tail flick latencies were measured 10 minutes after i.t. clonidine injection. The efficacy of clonidine in the tail flick assay and the SP-behavioral assay was below 50% in α_{2A}AR-KO mice compared to WT mice. B) Tail flick latencies were measured 10 minutes after i.t. morphine injection. Morphine was more potent in α_{2A}AR-KO mice than in WT mice in both assays. DeltII (C) and DAMGO (D) antinociception were measured with a cumulative dosing protocol with the hot water tail flick assay. C) In both assays, DeltII was more potent in α_{2A}AR-KO mice than in WT mice. D) In the tail flick assay, the dose response curve for DAMGO was slightly shifted to the left in α_{2A}AR-KO mice, but this shift was not observed in the SP behavioral assay.

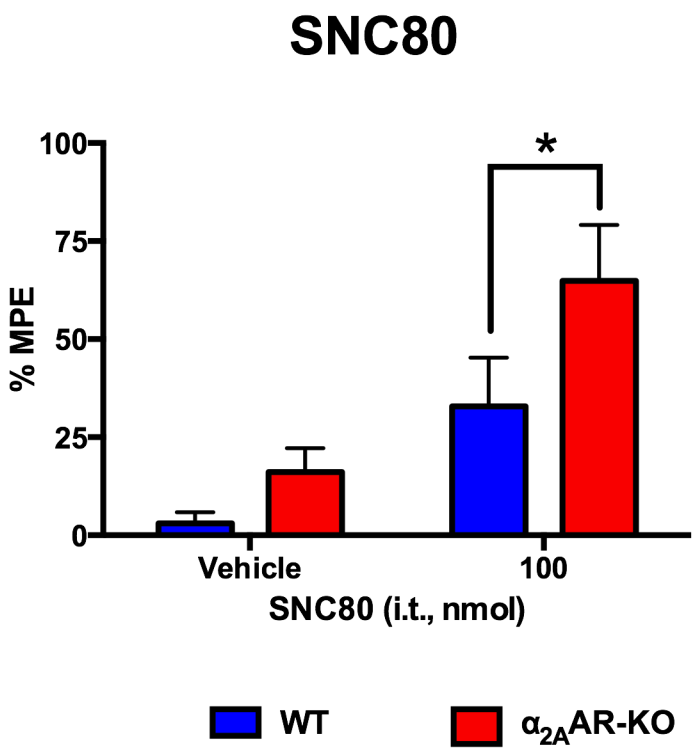

Figure 3: Antinociceptive effect of spinal SNC80 in the tail flick assay.

WT (n = 10-11) and α_{2A}AR-KO (n = 11-12) mice were treated with 100 nmol of SNC80 i.t. or vehicle and tested 3 minutes later with the hot water tail flick assay. SNC80 was more effective in α_{2A}AR-KO mice. * $P < 0.05$

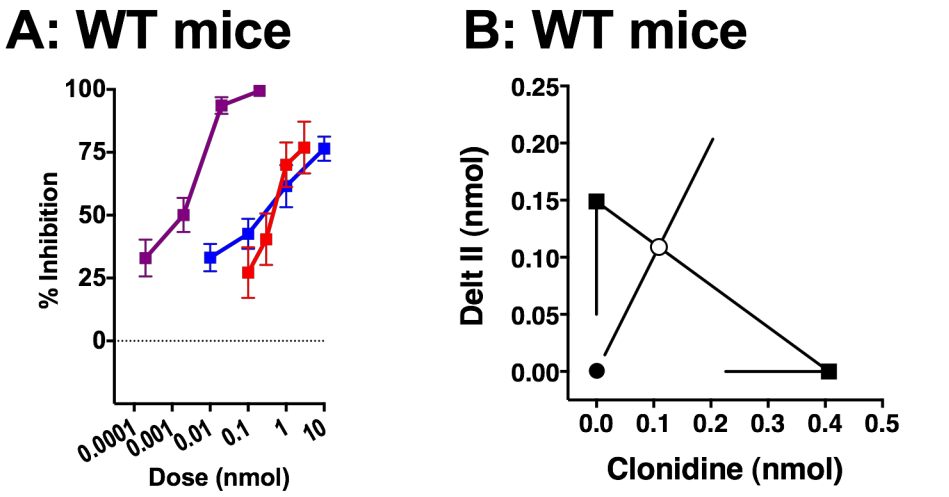
A: WT mice
100
75
50
25
0
% Inhibition
0.0001
0.001
0.01
0.1
1
10
Dose (nmol)
B: WT mice
0.25
0.20
0.15
0.10
0.05
0.00
Delt II (nmol)
0.0
0.1
0.2
0.3
0.4
0.5
Clonidine (nmol)
C: α2AAR-KO mice
100
75
50
25
0
% Inhibition
0.0001
0.001
0.01
0.1
1
10
Dose (nmol)
Clonidine
Delt II
Clonidine + Delt II (1:1)

Figure 4: The interaction between DeltII and clonidine is synergistic in WT mice, but not in α_{2A}AR-KO mice in the SP behavioral assay.

(A) Dose-response curves of the spinal antinociceptive effect of DeltII, clonidine, and their combination at an equieffective 1:1 ratio graphed as total drug dose present in the mixture. (B) Isobolographic analysis of DeltII and clonidine interaction in WT mice depicts the DeltII ED_{50} value with lower CI along the *y* axis, and the clonidine ED_{50} value with lower CI along the *x* axis. The measured experimental ED_{50} value for the drug combination (●) is lower than the calculated theoretical additive ED_{50} value (○), indicating that DeltII and clonidine interact in a synergistic manner ($P < 0.05$). (C) In α_{2A}AR-KO mice, spinal administration of clonidine was ineffective at inhibiting SP-induced behaviors. The dose-response curves of DeltII and of clonidine+DeltII overlapped, showing that adding clonidine to DeltII did not change its potency. Isobolographic analysis of this data set was not possible since the efficacy of clonidine was inferior to 50% inhibition. The calculated ED_{50} value for the experimental and theoretical DeltII+clonidine combinations are reported in Table 2.

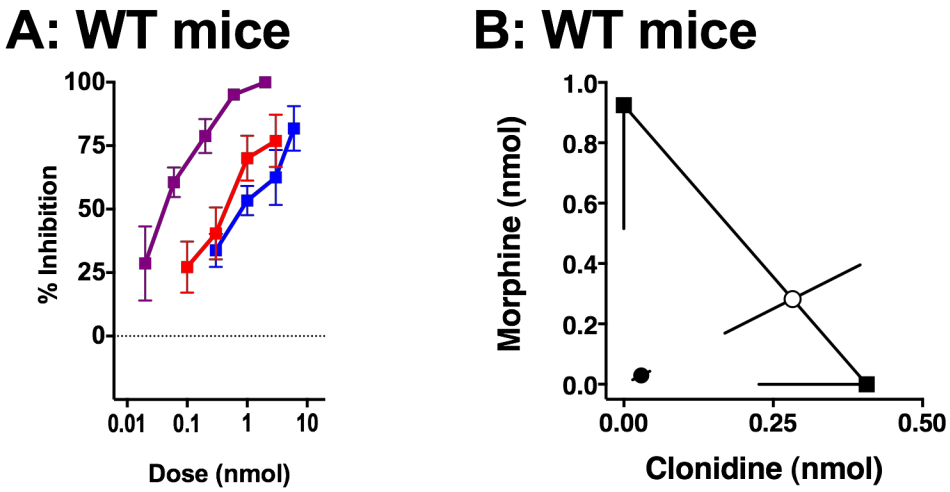
A: WT mice
100
75
50
25
0
% Inhibition
0.01
0.1
1
10
Dose (nmol)
B: WT mice
1.0
0.8
0.6
0.4
0.2
0.0
Morphine (nmol)
0.00
0.25
0.50
Clonidine (nmol)

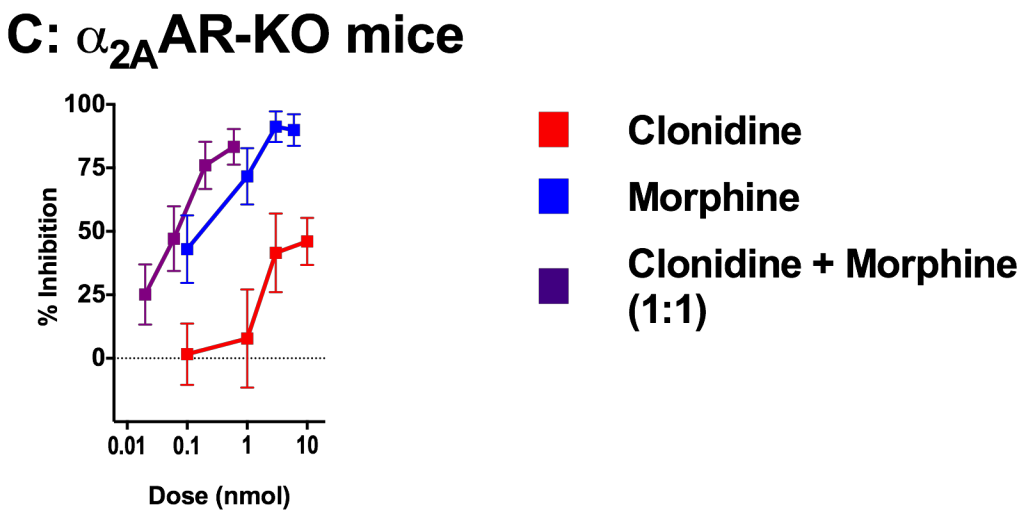
C: α2AAR-KO mice
100
75
50
25
0
% Inhibition
0.01
0.1
1
10
Dose (nmol)
Clonidine
Morphine
Clonidine + Morphine (1:1)

Figure 5: The interaction between morphine and clonidine is synergistic in WT mice, but not in α_{2A}AR-KO mice in the SP behavioral assay.

(A) Dose-response curves of spinal morphine and clonidine in WT mice. The dose-response curve of their equieffective 1:1 ratio combination was graphed as the total drug dose present in the mixture. (B) Isobolographic analysis of morphine and clonidine interaction in WT mice plotting morphine ED_{50} value with lower CI along the *y* axis, and clonidine ED_{50} value with lower CI along the *x* axis. The measured experimental ED_{50} value (●) for the drug combination was lower than the theoretical additive ED_{50} value (○), indicating that morphine and clonidine interact in a synergistic manner ($P < 0.05$). (C) In α_{2A}AR-KO mice, spinal administration of clonidine was ineffective at inhibiting SP-induced behaviors. The dose-response curves of morphine and of clonidine+morphine were similar, showing that adding clonidine to morphine did not change its potency. Isobolographic analysis of this data set was not possible since the efficacy of clonidine was inferior to 50% inhibition. The calculated ED_{50} values for the experimental and theoretical DeltII+clonidine combinations are reported in Table 2.

A: WT mice

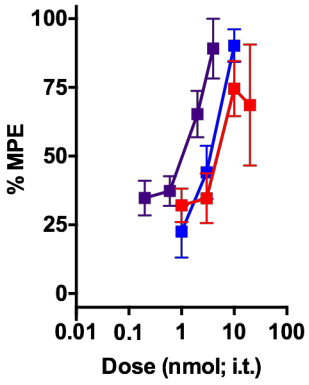

B: WT mice

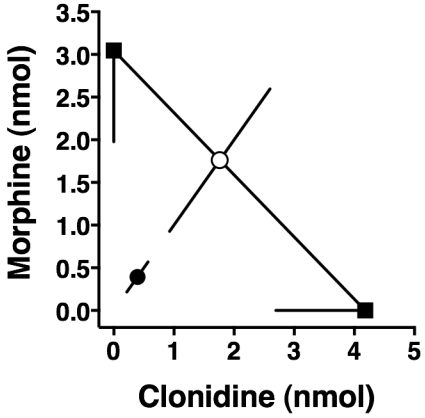

C: α_{2A}AR-KO mice

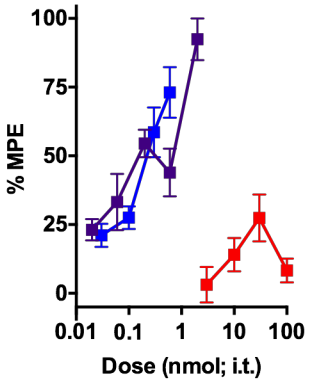

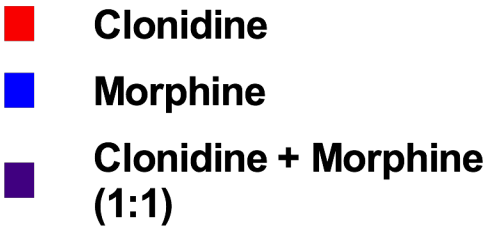

Figure 6: The interaction between morphine and clonidine is synergistic in WT mice, but not in α_{2A}AR-KO mice in the hot water tail flick assay.

(A) Dose-response curves of spinal morphine and clonidine in WT mice. The dose-response curve of their equieffective 1:1 ratio combination was graphed as the total drug dose present in the mixture. (B) Isobolographic analysis of morphine and clonidine interaction in WT mice plotting morphine ED_{50} value with lower CI along the *y* axis, and clonidine ED_{50} value with lower CI along the *x* axis. The measured experimental ED_{50} value (●) for the drug combination was lower than the theoretical additive ED_{50} value (○), indicating that morphine and clonidine interact in a synergistic manner ($P < 0.05$). (C) In α_{2A}AR-KO mice, spinal administration of clonidine was ineffective in the tail flick assay. The dose-response curves of morphine and of clonidine+morphine overlapped, showing that adding clonidine to morphine did not change its potency. Isobolographic analysis of this data set was not possible since the efficacy of clonidine was inferior to 50% MPE. The calculated ED_{50} value for the experimental and theoretical DeltII+clonidine combinations are reported in Table 2.

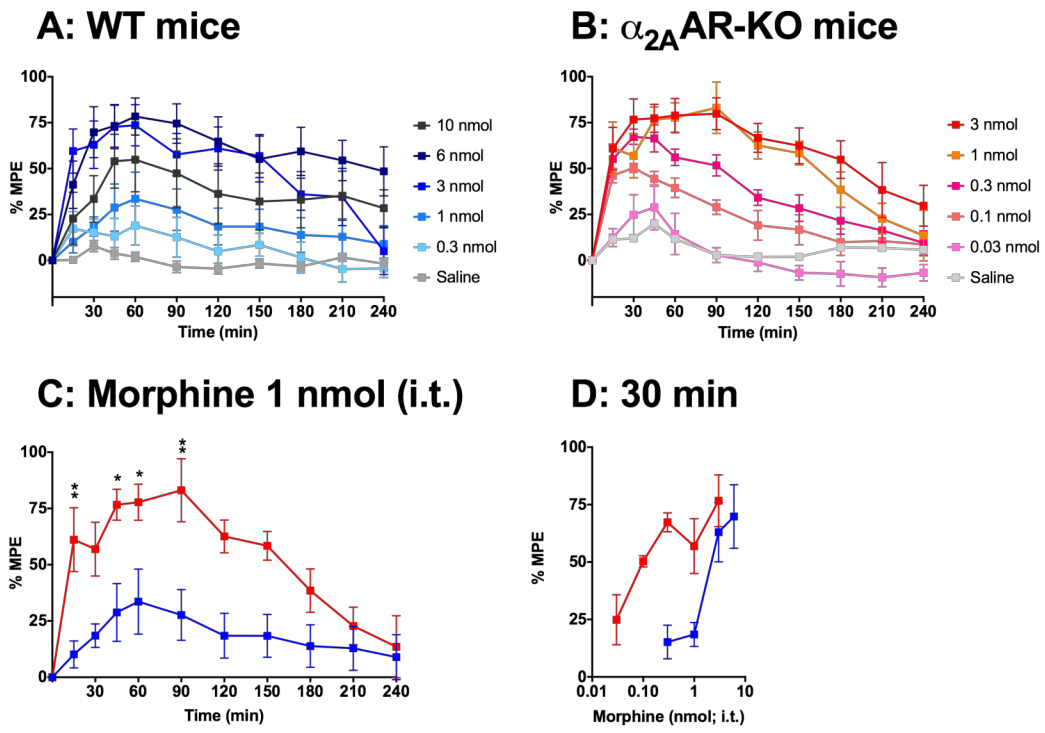
A: WT mice
B: α2AAR-KO mice
C: Morphine 1 nmol (i.t.)
D: 30 min
% MPE
Time (min)
Morphine (nmol; i.t.)
10 nmol
6 nmol
3 nmol
1 nmol
0.3 nmol
Saline
0.1 nmol
0.03 nmol
WT
α2AAR-KO

Figure 7: Spinal morphine antinociception in WT and α_{2A}AR-KO mice.

Time course of the antinociceptive effect of different doses of morphine administered spinally in WT (A) and α_{2A}AR-KO (B) mice in the hot water tail flick assay. A) In WT mice, morphine dose-dependently increased tail flick latencies and the maximum effect was observed with the 6 nmol (i.t.) dose. B) In α_{2A}AR-KO mice, the effect is dose-dependent and reached a maximum with 3 nmol morphine (i.t.). C) Comparison of the antinociceptive response mediated by 1 nmol of morphine (i.t.) over 240 minutes between WT and α_{2A}AR-KO mice shows that morphine was more efficacious in α_{2A}AR-KO mice. D) Morphine dose-response curve at 30 min shows that morphine is more potent but equally effective in α_{2A}AR-KO mice compared to WT mice. ED_{50} values are reported in Table 3.

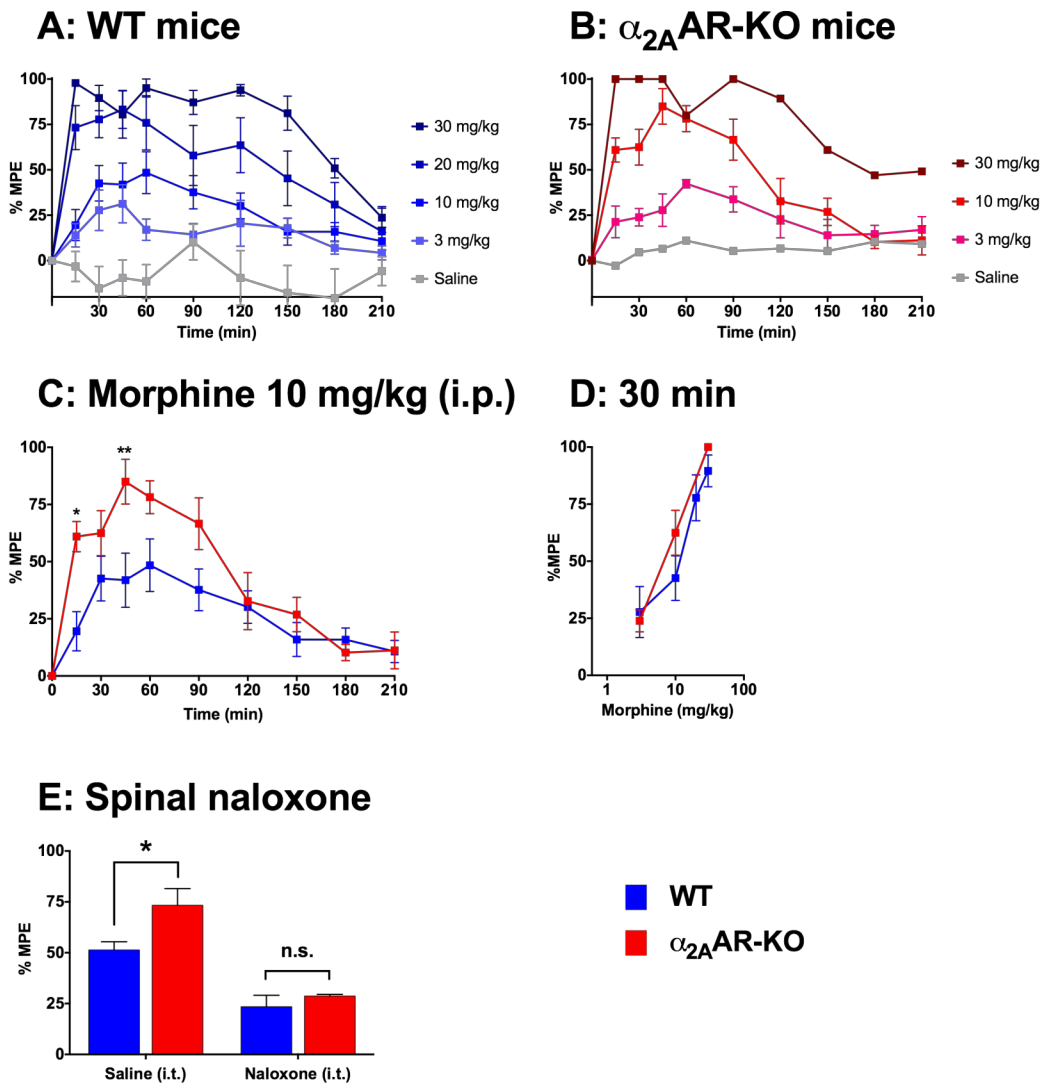
A: WT mice
% MPE
Time (min)
30 mg/kg
20 mg/kg
10 mg/kg
3 mg/kg
Saline
B: α2AAR-KO mice
% MPE
Time (min)
30 mg/kg
10 mg/kg
3 mg/kg
Saline
C: Morphine 10 mg/kg (i.p.)
% MPE
Time (min)
D: 30 min
%MPE
Morphine (mg/kg)
E: Spinal naloxone
% MPE
n.s.
Saline (i.t.)
Naloxone (i.t.)
WT
α2AAR-KO

Figure 8: Systemic morphine antinociception in WT and α_{2A}AR-KO mice.

Time course of the antinociceptive effect of different doses of morphine administered i.p in WT (A) and α_{2A}AR-KO (B) mice in the hot water tail flick assay. Morphine dose-dependently increased tail flick latencies, reaching maximal efficacy at 30 mg/kg in both strains. C) The antinociceptive effect of 10 mg/kg morphine (i.p.) over 210 minutes in WT mice was significantly lower than that of α_{2A}AR-KO mice. D) The dose-response curve for morphine at 30 minutes was constructed from the time course analysis data. A small but significant leftward shift in morphine potency was observed in α_{2A}AR-KO mice compared to WT mice. ED_{50} values are reported in Table 4. E) Morphine (10 mg/kg, i.p.) antinociceptive effect measured at 30 minutes in WT and α_{2A}AR-KO mice pre-treated with naloxone (i.t.) or saline (i.t.) showing that the strain difference is reversed by blocking spinal opioid response. * $P < 0.05$ ** $P < 0.01$

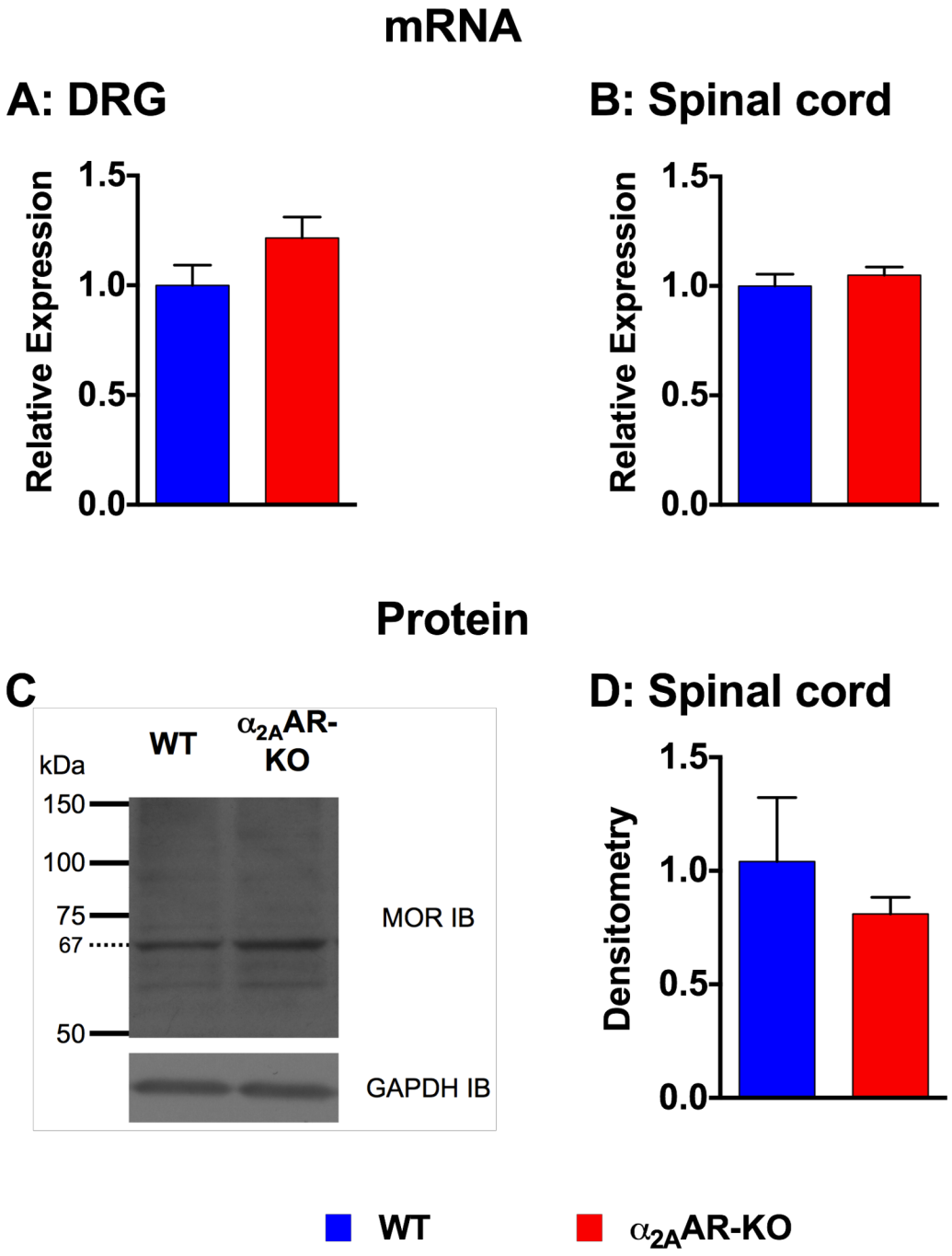
mRNA
A: DRG
Relative Expression
1.5
1.0
0.5
0.0
B: Spinal cord
Relative Expression
1.5
1.0
0.5
0.0
Protein
C
WT
α2AAR-KO
kDa
150
100
75
67
50
MOR IB
GAPDH IB
D: Spinal cord
Densitometry
1.5
1.0
0.5
0.0
WT
α2AAR-KO

Figure 9: Analysis of MOR mRNA and protein expressed in dorsal root ganglia (DRG) and spinal cords (SC) of WT and α_{2A}AR-KO mice.

Quantitative PCR analysis of the *Oprm1* gene transcript from WT and α_{2A}AR-KO DRG (A) and SC (B) mRNA extracts showed no strain difference in MOR expression. Gene expression data were normalized to the WT condition. C) Representative western blot showing the 67 kDa MOR-immunoreactive bands that were used to quantify MOR levels in the spinal cord of WT and α_{2A}AR-KO mice. The GAPDH-immunoreactive band was used as a loading control to normalize the MOR-immunoreactive band. C) Densitometry analysis of western blot MOR-immunoreactive band normalized to the WT condition showed no strain difference.

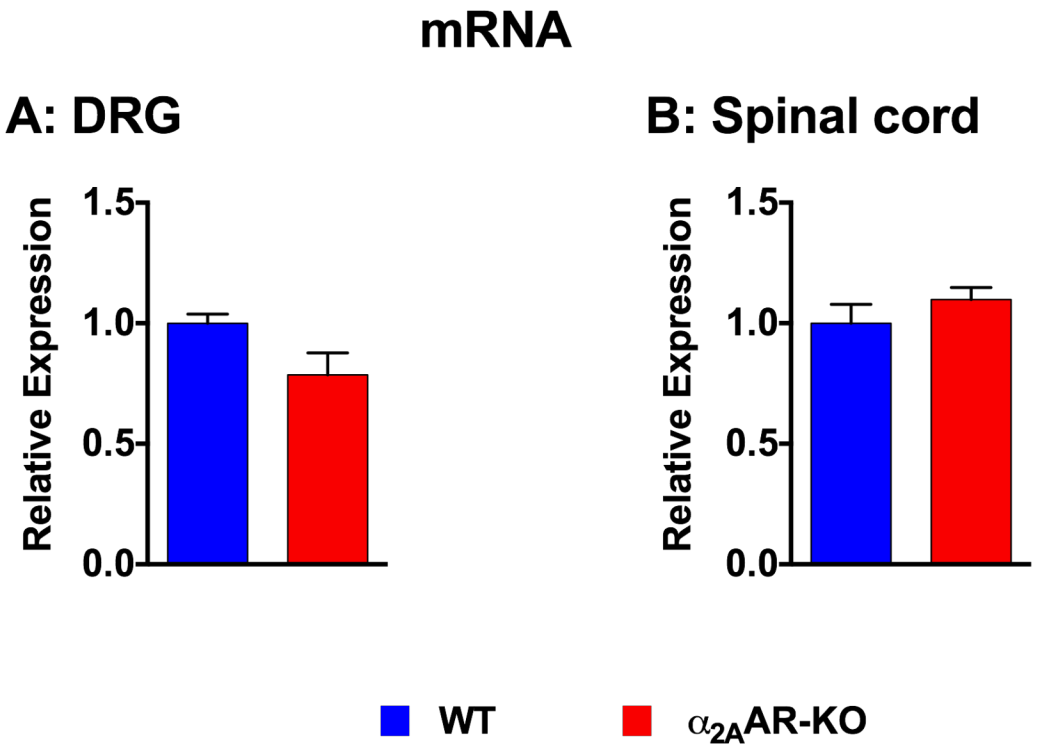

Figure 10: Analysis of DOR mRNA expression in dorsal root ganglia (DRG) and spinal cords (SC) of WT and α_{2A}AR-KO mice.

Quantitative PCR analysis of the *Oprd1* gene transcript from WT and α_{2A}AR-KO DRG (A) and SC (B) mRNA extracts showed no strain difference in DOR mRNA expression.

A: Morphine

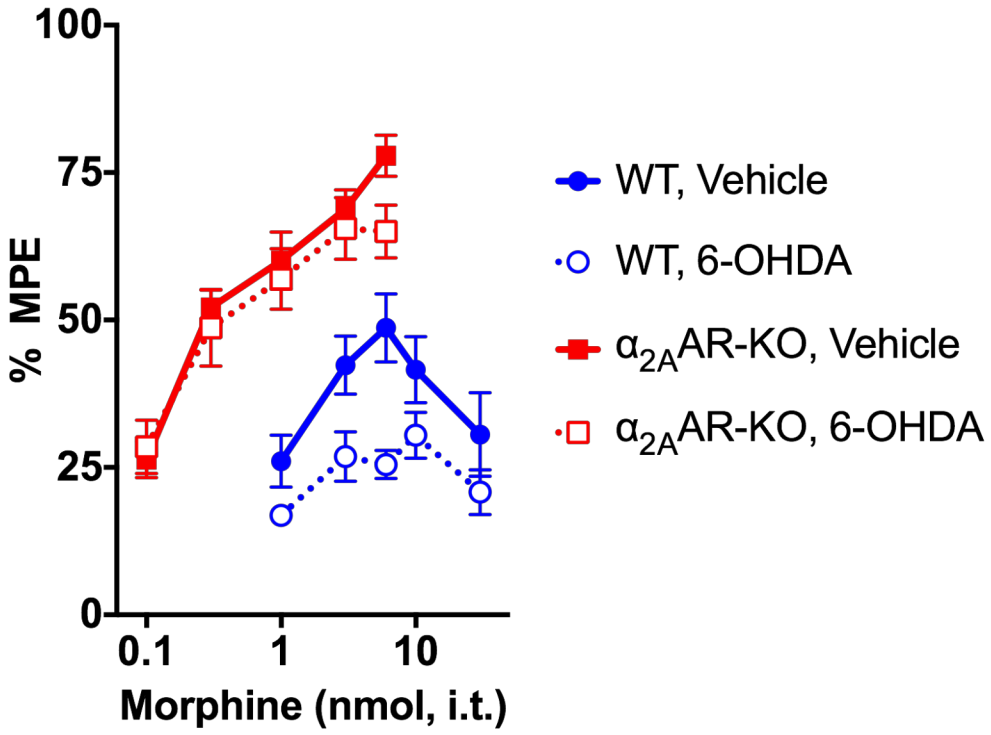

B: Baselines

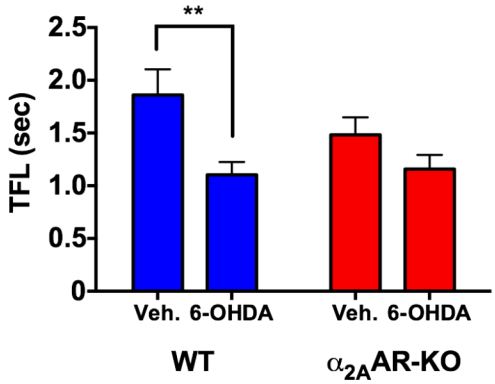

Figure 11: Effect of selective elimination of spinal catecholaminergic nerve terminals on morphine antinociception and heat nociception.

WT and α_{2A}AR-KO mice were injected i.t. with either 6-OHDA or vehicle solution to eliminate catecholaminergic nerve fibers containing NE. A) Morphine dose-response curves were constructed using a cumulative dosage protocol. 6-OHDA reduced morphine response in WT mice, but not in α_{2A}AR-KO mice. ED_{50} values are reported in Table 4. B) Baseline tail flick latency (TFL) values were lower in 6-OHDA-treated WT mice compared to vehicle-treated mice. The 6-OHDA treatment had no effect on baseline tail flick latencies of α_{2A}AR-KO mice.

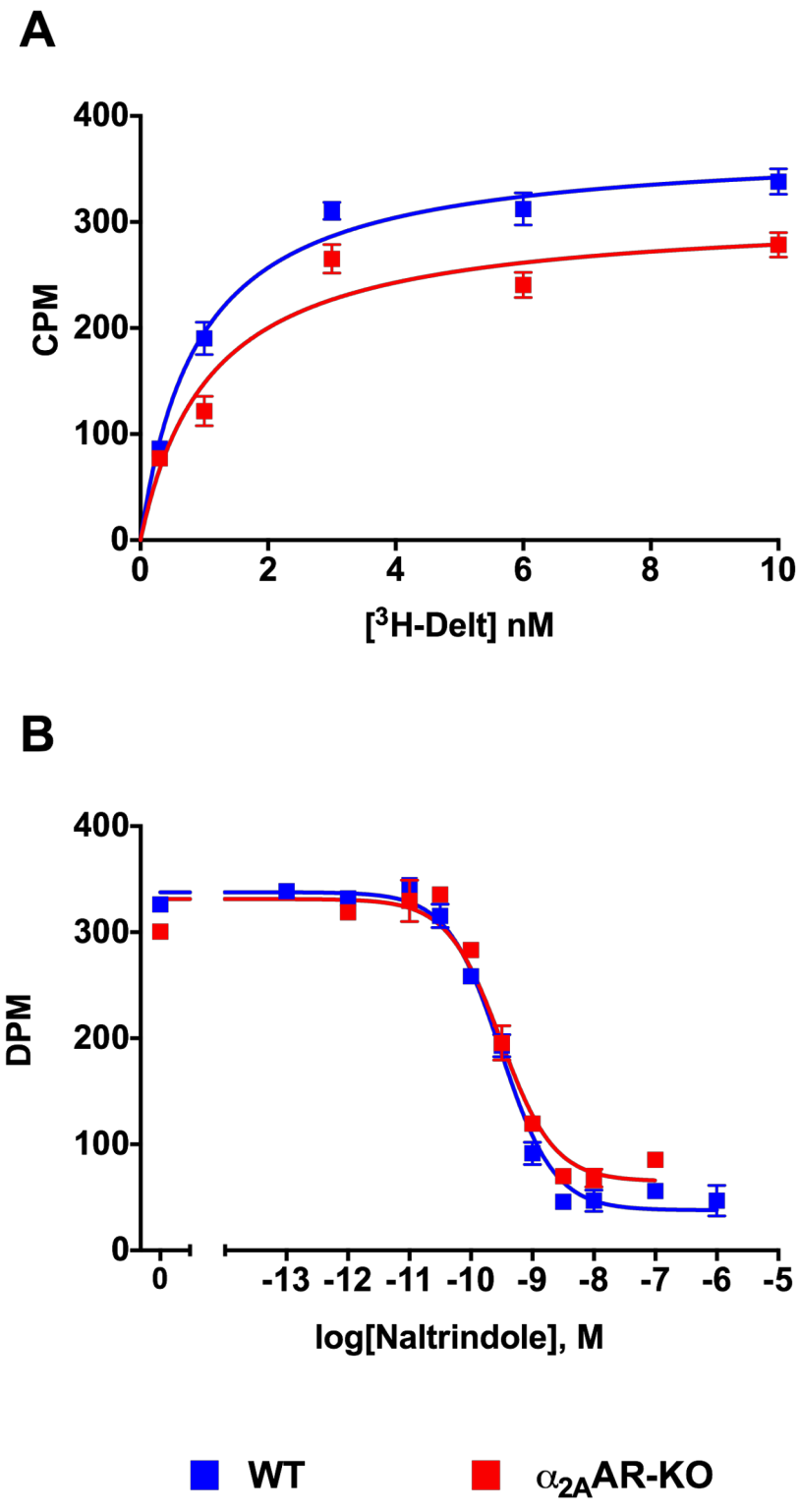
A
400
300
200
100
0
CPM
0
2
4
6
8
10
[3H-Delt] nM
B
400
300
200
100
0
DPM
0
-13
-12
-11
-10
-9
-8
-7
-6
-5
log[Naltrindole], M
WT
α2AAR-KO

Figure 12: [^{3}H]-DeltII binding analysis of WT and α_{2A}AR-KO mice spinal cord extracts.

A) Saturation ligand binding assay performed on membrane protein extracts from WT and α_{2A}AR-KO mouse spinal cords showing specific binding obtained by subtracting non-specific from total [^{3}H]-DeltII binding. The binding was concentration-dependent and no significant strain difference was measured. B) Competition of 1 nM [^{3}H]-DeltII binding to membranes from spinal cords by naltrindole was similar in WT and α_{2A}AR-KO mice. CPM = counts per minute. DPM = disintegrations per minute.

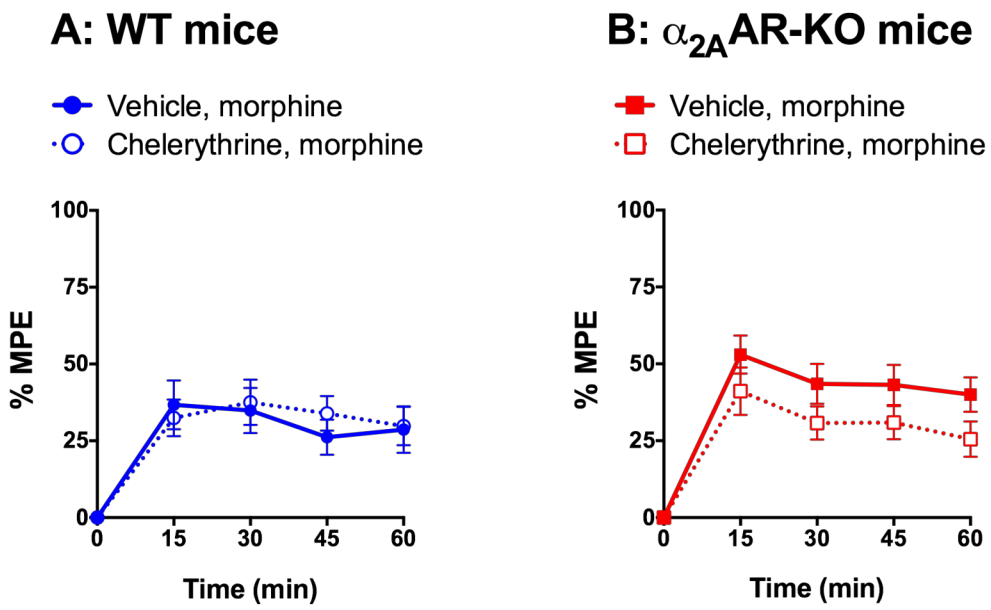

Figure 13: Effect of the PKC inhibitor chelerythrine treatment on morphine response in WT and α_{2A}AR-KO mice.

WT and α_{2A}AR-KO mice were injected i.t. with either chelerythrine or vehicle solution prior to receiving 1 nmol morphine i.t. Mice were tested in the hot water tail flick assay every 15 minutes for 60 minutes. A) In WT mice, chelerythrine did not affect morphine response. B) In α_{2A}AR-KO mice, morphine response tended to be consistently lower in chelerythrine-treated mice.

Table 1: Comparison of spinal clonidine, morphine, DeltII and DAMGO ED_{50} values (nmol (95% CI)) between WT and α_{2A}AR-KO mice in the hot water tail flick assay and the SP behavioral assay.

Assay	Strain	Clonidine	Morphine	DeltII	DAMGO
Hot water tail flick	WT	4.18 (1.98-4.69)	3.05 (2.0-4.7)	21.2 (11.4-39.2)	0.17 (0.09-0.32)
	α_{2A}AR-KO	No efficacy	0.26 (0.18-0.38)	4.29 (3.37-5.48)	0.06 (0.03-0.10)
	Potency ratio	N/A	11.8* (6.7-20.8)	4.9 * (3.1-7.9)	2.9* (1.3-6.4)
SP behavioral assay	WT	0.41 (0.23-0.73)	0.93 (0.52-1.66)	0.15 (0.05-0.44)	0.0034 (0.0017-0.007)
	α_{2A}AR-KO	8.40 (2.64-26.7)	0.12 (0.03-0.46)	0.0021 (0.0006-0.008)	0.0041 (0.0026-0.0065)
	Potency ratio	0.05* (0.01-0.18)	0.12 * (0.03-0.46)	70* (12-394)	0.8 (0.4 to 2.0)

* ED_{50} significantly different, WT vs. DOR-KO, Student's *t*-test ($P < 0.05$)

Table 2: Calculated ED_{50} values (nmol (± 95% SEM)) for drug combinations administered intrathecally in the SP-behavioral assay and the hot water tail flick assay in WT and α_{2A}AR-KO mice.

Drug	Assay	WT			α_{2A}AR-KO		
		Experimental	Theoretical	Interaction	Experimental	Theoretical	Interaction
DeltII + Clonidine	SP	0.0010 (±0.0005)	0.22 (±0.19)	Synergistic*	0.009 (±0.015)	0.004 (±0.006)	No interaction[a]
Morphine + Clonidine	SP	0.058 (±0.029)	0.56 (±0.27)	Synergistic*	0.0714 (±0.044)	0.243 (±0.313)	No interaction[a]
	TF	0.785 (±0.354)	3.52 (±1.67)	Synergistic*	0.285 (±0.127)	0.014 (±0.161)	No interaction[a]

* Indicates that the experimental ED_{50} value < theoretical ED_{50} value (Student's T test $P < 0.05$)

[a] Since clonidine was ineffective in α_{2A}AR-KO mice, we compared the ED_{50} value for the drug combination to the ED_{50} value of DeltII or morphine alone (Student's T test, $P > 0.05$) instead of running an isobolographic analysis.

Table 3: Comparison of spinal morphine ED_{50} values (nmol (95% CI)) between WT and α_{2A}AR-KO mice at different time points as measured with the tail flick assay.

Strain	15 min	30 min	45 min	60 min
WT	6.6 (2.3-19)	3.15 (1.5-6.6)	1.9 (1.0-3.4)	1.5 (0.9-2.7)
α_{2A}AR-KO	0.26* (0.12-0.58)	0.10* (0.07-0.16)	0.13* (0.08-0.20)	0.20* (0.14-0.29)

* ED_{50} significantly different, WT vs. α_{2A}AR-KO, Student's T test ($P < 0.05$)

Table 4: Comparison of systemic morphine ED_{50} values (mg/kg (95% CI)) between WT and α_{2A}AR-KO mice at different time points as measured with the tail flick assay.

Strain	15 min	30 min	45 min	60 min
WT	13.3 (9.8-18.2)	9.1 (6.1-13.7)	10.0 (4.9-20.5)	9.3 (6.4-13.5)
α_{2A}AR-KO	7.1* (5.6-9.0)	4.4* (2.9-6.6)	2.5* (1.1-5.6)	3.3* (2.5-4.4)

* ED_{50} significantly different, WT vs. α_{2A}AR-KO, Student's *t*-test ($P < 0.05$)

Table 5: Morphine calculated ED50 values in WT and α_{2A}AR-KO mice treated with 6-OHDA (i.t.).

Strain	Treatment	ED_{50} (95% CI)
WT	Vehicle	6.17 nmol (3.86 – 9.86)
	6-OHDA	No efficacy
α_{2A}AR-KO	Vehicle	0.48 nmol (0.36 – 0.64)
	6-OHDA	0.55 nmol (0.33 – 0.91)

Chapter 6:
Discussion

DISCUSSION

The goal of this thesis was to improve our understanding of the role of DOR and α_{2A}AR in opioid-adrenergic interactions in the spinal cord. The results acquired in three separate projects exploring the neuropharmacology of nociception revealed interesting findings that warrant further interpretation in order to understand their implication for the modulation of nociceptive transmission.

Role of DOR and α_{2A}AR in nociception

The roles of DOR and α_{2A}AR are to mediate the modulatory actions of endogenous opioids and norepinephrine (NE), respectively. Given their widespread distribution in the nervous system, especially at several levels of the nociceptive circuit, the deletion of DOR and α_{2A}AR reveals the importance of these receptors in nociceptive processing.

DOR-KO mice are more sensitive to heat stimulus

Small diameter C-fiber nociceptors are preferentially activated by a slow increase in temperature stimuli while Aδ-fibers respond to rapid temperature increase (Yeomans and Proudfit, 1996). We observed a small but significant hypersensitivity to heat in DOR-KO mice in the tail flick assay at 46 and 49˚C, but not at 52 and 55˚C. Lower water bath temperatures could induce a slower heating of the tail skin, thereby preferentially activating C-fibers. Thus, the strain difference in responsiveness to heat at lower temperatures suggests that DOR regulates heat nociception in small diameter DRG neurons. When generating these transgenic mice, Filliol et al. (2000) characterized their nociceptive phenotype and found no effect of the genetic deletion using the 52˚C tail flick assay, the hot plate assay and the tail pressure test. Another mouse line generated by the same group with a selective deletion of DOR in DRG neurons expressing Nav1.8 (DOR-Nav1.8-KO mice) also had a normal heat and mechanical nociceptive profile (Gavériaux-Ruff et al., 2011). These results are consistent with ours, because they did not explore lower temperatures. In contrast, our results clearly indicate a role for DOR in thermal antinociception.

The α_{2A}AR modulates heat nociception

The hypersensitivity to heat we observed in α_{2A}AR-KO mice compared to WT mice using the tail flick and radiant heat assays suggests that heat nociception is endogenously modulated through the α_{2A}AR in non-injured conditions. Our data also show consistency across stimulation sites since α_{2A}AR-KO mice had lower heat thresholds whether the stimulus was applied on the tail or the plantar surface of the hind paw. Changes in thermal thresholds were not observed in previous studies using α_{2A}AR-D79N mice in which a point mutation rendered the α_{2A}AR non-functional and decreased its expression (Lakhlani et al., 1997; Malmberg et al., 2001). The endogenous inhibition of noxious heat could require the physical presence of α_{2A}AR, but not its intact coupling. However, differences in heat nociception were not previously reported using α_{2A}AR-KO mice in the radiant heat assay (Lähdesmäki et al., 2003). As shown with the water immersion tail flick assay in our study, increasing the stimulus intensity from 49˚C to 52˚C decreased the strain difference in response latencies. It is possible that, in some experimental settings, the intensity of the heat stimulus does not reveal the hyperalgesic phenotype in α_{2A}AR-KO mice. This could also reflect the different heat sensitivities of C and Aδ fibers (Yeomans and Proudfit, 1996). As reported previously (Malmberg et al., 2001; Lähdesmäki et al., 2003), we have not observed a strain difference in tactile threshold. Our results demonstrate a modality-specific role for the α_{2A}AR in the endogenous modulation of nociception.

Noradrenergic descending pathways contribute to the endogenous inhibition of pain through activation of α_2ARs (Sagen and Proudfit, 1984). α_2AR antagonists were shown to decrease tail flick and hot plate latencies in rats (Sagen and Proudfit, 1984), suggesting that adrenergic receptors can set the threshold for thermal nociception. A decrease in noxious heat threshold, but not tactile threshold, was reported in rats and mice following the lesioning of cathecolaminergic fibers with 6-OHDA (Kuraishi et al., 1983; Fasmer et al., 1986). Furthermore, Jasmin et al. (2002) observed a similar thermal, but not

mechanical, hypersensitivity in Dbh-/- mice, which lack an enzyme that converts dopamine to NE. Similarly, an elevated thermal nociceptive threshold was noted in mice with elevated extracellular NE levels resulting from a genetic deletion of the NE transporter (Bohn et al., 2000). These studies suggest that endogenous NE modulates heat nociception. In our study, we confirm a significant decrease in heat threshold following an i.t. 6-OHDA injection in WT mice that is not matched in α_{2A}AR-KO mice when compared to vehicle-treated mice. Thus, we show evidence that the α_{2A}AR is involved in the inhibition of noxious heat by descending noradrenergic fibers in the spinal cord in naïve animals.

Opioid agonist pharmacology in DOR-KO mice

Role of DOR in morphine antinociception: early phase and efficacy

In MOR-KO mice, morphine antinociceptive effect is absent whether it is injected systemically (Matthes et al., 1996), intracerebroventricularly or intrathecally (Hosohata et al., 2000), confirming that MOR is the opioid receptor mediating morphine antinociception. Moreover, the efficacy of systemically administered morphine is unaffected in DOR-KO mice as reported previously by Zhu et al. (1999), which we have confirmed. Thus, the lower i.t. morphine efficacy we observed in DOR-KO mice indicates that DOR plays a role in morphine antinociception that is restricted to the spinal cord.

DOR has been implicated in other spinal morphine effects. For example, chronic administration of morphine results in an increase in the surface expression of DOR and efficacy of DOR agonists (Cahill et al., 2001b; Gendron et al., 2006). The role of DOR in acute morphine antinociceptive effects is largely unexplored and our study provides evidence that DOR, although not sufficient alone, is necessary to obtain full morphine efficacy. A similar observation has been reported where morphine inhibition of VGCC is impaired in DRG neurons from DOR-KO mice (Walwyn et al., 2009). Since the closing of presynaptic VGCC by morphine blocks nociceptive signal transmission, the parallel between this study

and our behavioral observations suggests that DOR could participate in morphine antinociception in DRG neurons.

The interaction between MOR and DOR arising from their extensive colocalization in DRGs (Wang et al., 2010), and their interaction as a heteromeric receptor complex (Costantino et al., 2012) could explain this relationship. There are many possible mechanisms that could underlie this interaction.

For example, DOR could change morphine ligand recognition specificity and receptor activation. In systems expressing a homogenous opioid receptor population, morphine has a high affinity for MOR, medium affinity for KOR and virtually no affinity for DOR (Raynor et al., 1994). However, data from Yu and Sadée et al. (1986) show that DADLE can be displaced with morphine in a cell line expressing DOR and MOR endogenously. Similarly, Emmerson et al. (1994) shows that morphine affinity is only 50-fold higher for MOR than for DOR in a membrane preparation from monkey brain. This suggests that morphine binding properties are altered by DOR in specific contexts, such as in native tissues where the receptor population is heterogeneous. This hypothesis was tested in cell lines expressing only one or a combination of opioid receptors (Yekkirala et al., 2010). In this study, morphine more potently and efficiently activated intracellular Ca2+ release from cells expressing MOR+DOR than cells expressing MOR alone. It is thus possible that missing DOR in DRG neurons reduces the signaling output of morphine at the MOR due to the absence of MOR+DOR heteromers. One of the future directions of this project should therefore include the investigation of the signaling output by morphine in WT and DOR-KO mice, for example with a GTPγS binding assay.

Hormesis dose-response curve

In the tail flick assay, morphine dose-response curves follow an inverted U-shaped curve with an ascending phase at lower doses and a descending phase at higher doses. This phenomena called hormesis can be observed in a wide array of biological phenomenon such as radiation toxicity, stress response, etc. (Calabrese

and Baldwin, 2003). It is defined as a biphasic dose-response relationship with a stimulatory effect at low doses and an inhibitory effect at high dose caused by a compensatory mechanism or the triggering of a side effect opposing the stimulatory effect. In our study, it is not clear what causes morphine efficacy to decrease at higher doses. It is possible that morphine antinociception (i.e. the stimulatory effect) is counteracted by side effects at higher doses. For example, morphine can cause hyperalgesia by activating spinal microglial cells via the toll-like receptor 4 (Watkins et al., 2009).

DOR-selective agonists are still effective in the tail flick assay, but not in the SP behavioral assay

In DOR-KO mice, we showed that DeltII was still efficacious in the tail flick assay while it is not in the SP behavioral assay. Other studies have also reported the maintenance of DOR agonist efficacy in DOR-KO mice using the tail flick assay (Scherrer et al., 2004; van Rijn et al., 2012). A dose dependent DeltII or SNC80 stimulated GTPγS binding was detected in membrane extracts from WT and MOR-KO mice, but not from DOR-KO mice (Scherrer et al., 2004). However, in behavioral assays, DeltII and SNC80 were effective in DOR-KO mice, but not in MOR-KO mice (Scherrer et al., 2004; van Rijn et al., 2012). Moreover, a MOR-selective antagonist, but not a DOR-selective antagonist could reverse the antinociceptive effect of DeltII. Thus, despite a lack of detectable GPCR activation and ligand binding, DeltII can produce MOR-dependent antinociceptive effects in WT and DOR-KO mice.

Other studies have proposed that DOR-agonists are ineffective in naive mice and that functional DOR only emerge following a nerve injury, chronic morphine treatment, inflammation or even chronic ethanol exposure (Cahill et al., 2001b; Lucido et al., 2005; Gendron et al., 2006; van Rijn et al., 2012). In these studies, the antinociceptive effect of DOR agonists could be reversed by DOR antagonists or was not observed in DOR-KO mice. In our studies, the efficacy of DeltII and SNC80 in WT mice in the tail flick assay was rather limited, reaching a maximum of 50% MPE. However, in the SP assay, DeltII efficacy was comparable to

morphine and DAMGO in WT mice and the antinociceptive effect was DOR-dependent. This suggests that the SP assay is sensitive to the activation of a population of functional DOR, while the tail flick assay is not.

Is a truncated version of DOR mediating DeltII antinociception in DOR-KO mice?

DOR-KO mice were generated by deleting the first exon of the Oprd1 gene, which codes for the C-terminal and the first transmembrane domains of DOR. Our expression analysis confirms the upregulation of a partial DOR mRNA transcript in DOR-KO mice spinal cord and DRG neurons. Wang et al. (2010) also detected this partial transcript in DOR-KO mice and confirmed that it was from the Oprd1 gene by sequencing the PCR amplification product. Since this partial mRNA transcript contains four putative start codons, its translation could result in a truncated DOR with six transmembrane domains in DOR-KO mice. Functional truncated GPCRs have been reported. For example, there are several splice variants of the MOR (Majumdar et al., 2011). The MOR-1G splice variant lacks the first transmembrane domain, leaving it with six transmembrane domains (Majumdar et al., 2011). This truncated GPCR can mediate pharmacological effects *in vivo*, but is inactive when expressed on its own in cultured cells. However, co-expression of MOR-1G with another GPCR reestablishes MOR-1G function *in vitro*. Therefore, the possibility that a truncated DOR mediates DeltII effect in DOR-KO mice needs to be considered when regarding DOR agonist-mediated antinociception in these mice.

Opioid-Adrenergic synergy: Mechanistic insights from DOR-KO and α_{2A}AR-KO mice

In Chapters 4 and 5, we tested the outcome of the interaction between different opioid-adrenergic combinations with two behavioral assays in three different mouse strains. Taken together, the results revealed important roles for α_{2A}AR, DOR and MOR in analgesic synergy.

Pharmacokinetic mechanisms

Opioid-adrenergic synergy could arise from pharmacokinetic interactions. In addition to their antinociceptive effects, α_2AR agonists like clonidine have a local vasoconstrictive effect (Asada and Lee, 1992; Iida et al., 1999) that can reduce drug clearance from the site of injection. Clonidine could therefore enhance the effect of another drug by maintaining it at a high local drug concentration. Following this logic, clonidine should interact synergistically with other drug classes. For example, in a post-operative pain model, clonidine interacts synergistically following intrathecal injection with gabapentin and with an allosteric adenosine receptor modulator (Cheng et al., 2000; Obata et al., 2004). However, since we and others have reported synergistic interactions with some, but not all, opioid agonists, altered drug clearance remains an unlikely mechanism. Furthermore, ST-91, an α_2AR agonist with hypertensive effects (Yasuoka and Yaksh, 1983; Nagasaka and Yaksh, 1990), interacts synergistically with morphine but does not affect morphine clearance from the spinal cord (Monasky et al., 1990). Thus, the pharmacokinetic actions of α_2AR agonists are unlikely to mediate spinal opioid-adrenergic synergy.

Pharmacodynamic mechanisms

Pharmacodynamic interactions between opioids and α_2AR agonists that result in analgesic synergy could involve intercellular or intracellular mechanisms. Drugs delivered into the intrathecal space at the lumbar level act on the spinal cord and DRGs. These structures are important in nociceptive signal processing and have opioid and adrenergic receptors capable of inhibiting the transmission of afferent nociceptive signals. Since spinal MOR, DOR and α_2ARs are distributed on both primary afferent and spinal neurons (Stone et al., 1998; Wall et al., 2006), it is possible that the cumulative inhibition of neurons in the nociceptive circuit is supra-additive. Synergistic interactions could also result from the co-expression of both opioid and adrenergic receptors in the same cells where their simultaneous activation results in synergistic output as proposed by Overland et al. (2009).

DOR is sufficient to produce opioid-adrenergic synergistic interactions

Previous studies have shown that spinal co-administration of the DOR-selective peptide agonists DPDPE and DeltII with clonidine results in a synergistic interaction in both the tail flick and SP behavioral assays (Ossipov et al., 1990b; Roerig et al., 1992; Roerig, 1995; Overland et al., 2009). These interactions persist in MOR-KO mice, suggesting that MOR is not required (Guo et al., 2003).

Using the SP behavioral assay, we showed that DeltII antinociception was absent in DOR-KO mice, which validated the use of the SP behavioral assay to examine the role of DOR in synergistic interactions. As a result, the absence of DeltII-clonidine synergy in DOR-KO mice confirms that DOR activation is sufficient to interact synergistically with α_2AR agonists. This finding may not generalize to other assays where the agonist is not selective for DOR.

We did not test the synergistic interaction between DeltII and clonidine in the tail flick assay since we have shown that DeltII antinociception is still present in DOR-KO mice. Others have made similar observations and attributed the analgesic effects of DeltII in the tail flick assay to MOR (Scherrer et al., 2004; van Rijn et al., 2012), raising the possibility that these synergistic interactions with α_2AR agonists are MOR-mediated rather than DOR-mediated.

Therefore, assays should be carefully selected and validated when studying DOR-mediated synergistic interactions because DOR agonists behave differently across assays.

DOR is not necessary to mediate morphine-clonidine synergy

The synergistic interaction between morphine and clonidine is well documented in rodents using different assays (Fairbanks et al., 2009). Because the interaction is stronger when the drugs are administered intrathecally compared to systemically, it has been proposed to be mediated largely at the level of the spinal cord (Ossipov et al., 1990a). Also at the spinal cord, MOR and DOR can interact

together and form heteromeric complexes with altered signaling properties upon morphine treatment (Costantino et al., 2012), which led us to hypothesize that the morphine+clonidine synergistic interaction may involve DOR. This is also supported by our observation that morphine antinociceptive effect requires DOR to reach full efficacy (Chapter 3). Because we measured drug interactions at 10 minutes in the tail flick assay, it was not possible to test the synergistic interaction between morphine and clonidine in DOR-KO mice since morphine is not effective at this time point. Using the SP behavioral assay, we demonstrate that in DOR-KO mice, the synergistic interaction between morphine and clonidine is still present, allowing us to conclude that DOR is not the only opioid receptor able to mediate opioid-adrenergic synergistic interactions. Since morphine is not efficacious in the SP behavioral assay in MOR-KO compared to WT mice (Guo et al., 2003), the activation of MOR likely mediates the synergistic interaction between morphine and clonidine.

α_{2A}AR is necessary for clonidine's synergistic interaction with DeltII and morphine

The spinal analgesic effect of clonidine is attributed to the α_{2A}AR (Fairbanks and Wilcox, 1999a), an observation that we confirmed with α_{2A}AR-KO mice both the SP behavioral assay and the tail flick assay (Chapter 5). Other α_2AR agonists such as dexmetomidine, UK 14,304 and ST-91 also mediate their antinociceptive effect at least in part through the α_{2A}AR (Lakhlani et al., 1997; Stone et al., 1997; Stone et al., 2007). Since there is no α_{2A}AR-selective agonist available, the role of α_{2A}AR in opioid-adrenergic synergistic interaction has been evaluated before with D79N-α_{2A}AR mice, which express a mutated and dysfunctional α_{2A}AR (Surprenant et al., 1992; MacMillan et al., 1996; Lakhlani et al., 1997). While the synergistic interaction between DeltII and UK 14,304 was lost in these mice (Stone et al., 1997), it was not the case for the combination between DeltII and ST91 (Stone et al., 2007) or moxonidine (Fairbanks et al., 2002). Our data provide evidence that clonidine synergizes with DeltII via the α_{2A}AR (Chapter 5). Therefore, the α_{2A}AR is sufficient, but not necessary, for synergistic interaction

with DeltII depending on the adrenergic ligand. For other α_2AR agonists, contributions from the α_{2C}AR contribute to this interaction (Fairbanks et al., 2002).

Furthermore, we demonstrated that the α_{2A}AR is responsible for the synergistic interaction observed between morphine and clonidine. To our knowledge, this is the first report identifying the adrenergic receptor involved in this widely studied and clinically relevant drug interaction.

DOR and α_{2A}AR co-activation results in synergistic interaction

In identifying DOR and α_{2A}AR activation as a requirement for DeltII-clonidine synergy, we have confirmed that the receptor pair, DOR and α_{2A}AR, interact synergistically at the spinal level to mediate analgesia. DOR and α_{2A}AR can both exert their analgesic action by inhibiting transmitter release from primary afferent terminals (Glaum et al., 1994; Kawasaki et al., 2003). Evidence suggests that the synergistic interaction between DeltII and clonidine is maintained at the level of the primary afferent nerve terminal; for example, the drug combination inhibited KCl-induced CGRP release synergistically from spinal cord slices (Overland et al., 2009). This suggests that peptidergic primary afferent neurons are a site of action of opioid-adrenergic synergy. We have demonstrated that DOR and α_{2A}AR receptors are co-expressed in primary afferent neurons and highly co-localize in SP-immunoreactive neurons and isolated nerve terminals (Riedl et al., 2009). Although the localization of DOR in SP neurons is debated (Scherrer et al., 2009; Wang et al., 2010), the above-mentioned physiological and anatomical evidence support the presence of DOR and α_{2A}AR in peptidergic neurons where they would be positioned to inhibit neurotransmitter release in a synergistic manner.

MOR-mediated synergy is assay- and ligand-dependent

Co-activation of MOR with an α_2AR agonist produces different types of interactions depending on the experimental conditions and agonists used. While the interaction between DAMGO and clonidine was either additive (Chapter 4) or subadditive in the SP behavioral assay (Roerig et al., 1992) this drug combination

was synergistic in the tail flick assay (Roerig, 1995). Furthermore, the combination of DAMGO with different α_2AR agonists in the SP behavioral assay can produce either synergistic (Stone et al., 1997) or sub-additive (Fairbanks et al., 2000b) interactions. Thus, depending on the assay and the ligands used, MOR activation may or may not contribute to spinal opioid-adrenergic synergistic interactions.

The contrasting results obtained using two agonists that activate MOR suggest that the mechanism underlying these interactions may involve ligand-biased signaling. Morphine and DAMGO engage different downstream signaling cascades upon binding and activation of MOR. While DAMGO produces robust βarrestin-dependent MOR translocation and desensitization, morphine produces PKC-dependent desensitization (Johnson et al., 2006; Chu et al., 2008). In cultured DRG neurons, DAMGO cross-desensitizes clonidine's inhibition of Ca^{2+} currents and produces co-internalization of MOR with α_{2A}AR through the βarrestin 2 and p38 MAPK signaling pathway; morphine produces neither of these effects (Tan et al., 2009). This cross-desensitization between DAMGO and clonidine could explain why their interaction is typically not synergistic *in vivo*. On the other hand, morphine activates PKCε in HEK 293 cells expressing MOR, but not DAMGO (Chu et al., 2010). Interestingly, synergistic interactions arising from morphine-clonidine (Wei and Roerig, 1998) and DeltII-clonidine (Overland et al., 2009) combinations are PKC-dependent. This signaling event is unconventional for opioid and adrenergic receptors that are usually coupled to the pertussis toxin (PTX)-sensitive Gi/o signaling pathway. Intrathecal PTX treatment, a toxin that uncouples the $G\alpha_{i/o}$ subunit from the receptor, decreases morphine and clonidine potency, but does not block their synergistic interaction (Roerig and Howse, 1996; Wei et al., 1996). Therefore, morphine-clonidine synergy probably arises from a signaling pathway independent of the pathways activated by either drug alone, and involves PKC.

Clinical applications of opioid-adrenergic synergy

The synergistic interactions observed in rodents support the notion that combination therapy can be beneficial for pain management by reducing the doses of drugs necessary to produce analgesia, increasing efficacy or reducing side effects compared to single drug therapy. Our studies have identified two pairs of receptors capable of mediating synergistic interactions: α_{2A}AR-MOR and α_{2A}AR-DOR. Both pairs present advantages and limitations for translation into effective clinical pain treatments.

The benefit of combining morphine and clonidine has been clearly demonstrated in clinical studies (for review, see (Walker et al., 2002). In pre-clinical studies, morphine and clonidine analgesic synergy is observed in a model of neuropathic pain (Ossipov et al., 1997; Fairbanks et al., 2000a), a rodent model of low back pain (Tajerian et al., 2012) and the formalin test (Przesmycki et al., 1997). Our work suggests that MOR and α_{2A}AR mediate the synergistic interaction of this combination in naïve/healthy animals, but it is not known if this receptor pair still mediates the synergistic interaction in these chronic pain models or if other receptor subtypes are involved. In models of neuropathic pain, spinal α_2AR agonists ameliorate signs of mechanical allodynia and heat hyperalgesia by activating the α_{2A}AR (Kingery et al., 2000; Malmberg et al., 2001). In a different study, the antinociceptive effect of spinally administered clonidine switches from α_{2A}AR in non-injured to α_{2C}AR after nerve injury (Duflo et al., 2002). This observation is supported by the decreased expression of α_{2A}AR in the superficial lamina of the spinal cord in three rodent models of painful nerve injury, while the expression of α_{2C}AR is maintained (Stone et al., 1999). The therapeutic potential of the α_{2A}AR to relieve neuropathic pain may therefore be limited in certain models. Its potential remains largely unexplored in other chronic pain models, including in inflammatory pain models. Here, the analgesic potency of α_2AR agonists is enhanced, although that analgesic effect has not yet been linked to a specific receptor subtype (Pertovaara, 2006). MOR mediates the analgesic effect of morphine, as well as important side effects that limit the use of opioids for the

treatment of chronic pain (Matthes et al., 1996). Clinically, an important proportion of patients presenting with neuropathic pain have a reduced sensitivity to morphine and other opioids (Arnér and Meyerson, 1988). Lower spinal morphine potency and efficacy is also observed in rodent models of neuropathic pain and is associated with reduced MOR function and receptor levels (Ossipov et al., 1995). These changes in α_{2A}AR and MOR function following a chronic pain state could explain the diverging conclusions obtained in clinical studies examining the combination of morphine and clonidine depending on the pain condition under study (Ackerman et al., 2003).

The synergistic interaction involving DOR and α_{2A}AR has not been tested in chronic pain models, so this receptor pair has yet to be validated pre-clinically for the relief of chronic pain. There are no clinically approved DOR-agonists for the treatment of pain or other conditions, although a growing body of pre-clinical evidence suggests that DOR represents a promising drug target (Pradhan et al., 2011). The potency of spinally delivered DOR-selective agonists is enhanced in models of neuropathic pain (Mika et al., 2001; Holdridge and Cahill, 2007) and inflammatory pain (Stewart and Hammond, 1994; Cahill et al., 2003). Unlike morphine, acute and chronic DeltII treatment does not lead to analgesic tolerance (Beaudry et al., 2009). Furthermore, recently developed DOR-agonists have reduced side effects at doses that are effective to ameliorate hyperalgesia and allodynia when compared to morphine or SNC80 (Codd et al., 2009; Nozaki et al., 2012).

Therefore, DOR can be regarded as an alternative therapeutic target to MOR for chronic pain conditions due to the potentially greater therapeutic index of some DOR-selective agonists. Opioid-adrenergic drug combinations that activate DOR to produce analgesic synergy may therefore yield a better therapeutic profile than MOR-mediated synergistic interactions.

Opioid antinociception is potentiated in the absence of the α_{2A}AR

Potentiation of morphine antinociception at the spinal cord level

Morphine exerts its action at peripheral, spinal, and supraspinal sites in the nervous system. Under normal physiological conditions, the potency of both systemic and spinal morphine was augmented in mice lacking the α_{2A}AR (Chapter 5). The observation that the shift in morphine potency is greater at the spinal level than at the systemic level suggests that a spinal mechanism underlies this effect. By blocking the spinal component of the systemic morphine response, we showed that morphine action at peripheral and supraspinal sites was unaffected in the tail flick assay.

Other studies have examined the role of α_{2A}AR in the antinociceptive action of morphine using genetically modified mice. In α_{2A}AR-D79N mice, spinal morphine potency in the warm water tail flick assay was not different from WT mice, but a decreased potency in the SP assay was reported (Stone et al., 1997). Our data report the opposite: the potency of morphine is augmented in α_{2A}AR-KO mice with both the tail flick and the SP behavioral assay. In another study, no difference in systemic morphine antinociceptive effect was observed between WT and α_{2A}AR-D79N mice in the hot plate assay (Lakhlani et al., 1997). These diverging results between D79N and α_{2A}AR-KO mice raise two possibilities: 1) that morphine potentiation requires the absence of the α_{2A}AR and/or 2) that the dysfunctional D79N-α_{2A}AR still couples to signaling mechanisms that prevents morphine potentiation. Using α_{2A}AR-KO mice, Ozdogan et al. (2006) observed an enhanced response to morphine (i.p.) and other partial opioid agonists with the tail flick assay, but not for the full agonist fentanyl or with the hot plate assay. This is consistent with our observation of greater potentiation of spinal morphine efficacy compared to the small potentiation of the full MOR agonist, DAMGO (i.t.), in α_{2A}AR-KO mice. In contrast, using a single morphine test dose (i.p.), the same group previously reported no strain difference in morphine effect (Ozdogan

et al., 2004). In our study, the strain difference in systemic morphine potency was only 2-fold and it is possible that this difference may not be detectable under some experimental conditions. The use of different behavioral assays could also be a source of discrepancy between different studies. For example, Lähdesmäki et al. (2003) tested the effect of morphine on mechanical thresholds in α_{2A}AR-KO mice and reported no stain differences. Thus, the conditions required to observe the enhancement of morphine response indicate that it takes place at the spinal level when the α_{2A}AR is absent and can be detected with the tail flick or the SP behavioral assay.

Opioid-adrenergic interactions were also investigated in pharmacological studies using α_2AR antagonists. The dose of α_2AR antagonist determines whether it will cross inhibit (high dose) or potentiate (ultra-low dose) morphine efficacy.

Milne et al. (2008) reported an increase in spinal morphine antinociception in the presence of an ultra low dose of α_2AR antagonist in which the time course of action was prolonged and tolerance was prevented. The similar enhancement of morphine between this observation and ours suggested that the effect of the α_2AR antagonist is mediated by the α_{2A}AR. We therefore investigated whether the absence of the α_{2A}AR would have an incidence on the time course of action of morphine. In our study, potency, rather than the time course, was changed in the absence of the α_{2A}AR. Thus, the mechanism by which morphine antinociception is prolonged in the presence of a low dose of α_2AR antagonist is not mimicked by the absence of the α_{2A}AR, indicating that either the receptor is not involved or that its physical presence alone is required to mediate the effect.

Combining morphine with high doses of the α_2AR adrenergic antagonists yohimbine or idazoxan has been reported to decrease morphine efficacy (Browning et al., 1982; Stone et al., 1997; Morales et al., 2001). Interestingly, this interaction was paralleled in binding studies on CNS membranes whereby α_2AR ligands could displace radiolabeled μ or δ opioid ligands (Browning et al., 1982). These two classes of ligands do not bind the same receptor sites, suggesting that

an allosteric interaction rather than a direct competition affected opioid binding properties. This raises the possibility that an α_2AR antagonist, by displacing opioid binding to its receptor, might counteract the effect of opioids. In our study, [^{3}H]-DeltII binding properties did not change in α_{2A}AR-KO compared to WT mice in a manner that could explain the behavioral difference we observed.

DOR agonists are more potent and effective in α_{2A}AR-KO mice

In both the tail flick and the SP behavioral assays, DeltII antinociception was enhanced in α_{2A}AR-KO mice, which could not have been predicted from studies conducted in D79N mice. DeltII-mediated antinociception was unchanged in α_{2A}AR-D79N mice in the SP behavioral assay (Stone et al., 1997; Fairbanks et al., 2002; Stone et al., 2007). Since we have demonstrated that DeltII efficacy is mediated by DOR with this assay, we are confident that DOR also mediates DeltII antinociception in α_{2A}AR-KO mice. However, because we have also established that the antinociceptive effect of DeltII in the tail flick assay is not DOR-mediated, we cannot conclude with certainty that the enhanced DeltII efficacy in α_{2A}AR-KO mice is mediated by DOR. We confirmed this enhancement with another DOR-selective ligand, SNC80, demonstrating that the effect extends to other DOR-selective agonists. Upregulation of functional DOR has been reported following inflammation, nerve injury, morphine treatment and prolonged exposure to ethanol (Cahill et al., 2001b; Cahill et al., 2003; Lucido et al., 2005; Gendron et al., 2006; van Rijn et al., 2012). The absence of the α_{2A}AR could also trigger such an upregulation. It would therefore be interesting to reverse DeltII antinociception in α_{2A}AR-KO with naltrindole, a DOR-selective antagonist, or CTAP, a MOR-selective antagonist, to determine if the enhanced DeltII efficacy in α_{2A}AR-KO is attributable to MOR or DOR in the tail flick assay.

Endogenous norepinephrine (NE) modulates opioid antinociception

Our results from spinal 6-OHDA-lesioned mice gave us insight in the role of NE in opioid antinociception and allowed us to draw two important conclusions regarding the role of the α_{2A}AR in these actions.

In the spinal cord, a subset of α_{2A}AR act as autoreceptors regulating the release of NE from noradrenergic nerve fibers via negative feedback inhibition, thereby regulating levels of NE under normal conditions (Gilsbach et al., 2009). The absence of α_{2A}AR could disrupt this inhibition and increase spinal levels of NE, which could potentiate the morphine response. If this were the case, we would have observed no difference in morphine potency and efficacy in 6-OHDA-treated mice from both strains. Instead, the morphine response of α_{2A}AR-KO mice was unchanged by the chemical lesion. Therefore, we first conclude that the enhanced potency of morphine in α_{2A}AR-KO mice is not due to an excess of NE in α_{2A}AR-KO mice. The mechanism must therefore be independent of endogenous NE levels. Since we demonstrated that morphine efficacy decreased in 6-OHDA-treated WT mice, but not in α_{2A}AR-KO mice, we also conclude that, under normal conditions, spinal morphine efficacy requires the action of endogenous NE on the α_{2A}AR.

Studies that investigated the link between the endogenous noradrenergic system and opioid response by manipulating NE levels have arrived at contradictory conclusions. Depleting spinal levels of NE with different methods has been shown to reduce the antinociceptive effect of morphine in rodents (Berge and Ogren, 1984; Zhong et al., 1985; Jasmin et al., 2003). Others have found that these treatments had no effect on morphine antinociception (Pappas et al., 1982; Sawynok et al., 1991; Milne et al., 2008). These discrepancies may be attributed to differences in experimental design such as the choice of behavioral assay and time point. For example, NE depletion following 6-OHDA lesioning is maintained for at least 28 days, but behavioral changes are only detected during the first week (Howe and Yaksh, 1982). It is possible that the reduced morphine effect can only be observed during a specific period after eliminating descending noradrenergic fibers. Morphine efficacy is also decreased in mice lacking dopamine β-hydroxylase (Dbh), the enzyme that converts DA to NE (Jasmin et al., 2002). Interestingly, the reverse is also true: when NE levels are upregulated such as in NE transporter (NET)-KO mice, morphine efficacy is enhanced (Bohn

et al., 2000). These studies point at a role for the noradrenergic system in modulating morphine antinociception. Our study further identifies the α_{2A}AR as the receptor mediating this effect.

Summary

These paradoxical findings reveal a dual role for the α_{2A}AR, since its activation or absence both result in the potentiation of opioid responses. It is possible that at basal levels, the α_{2A}AR exerts an inhibitory influence on opioid receptors and that in α_{2A}AR-KO mice, opioid receptors are released from this influence. A low dose of α_2 antagonist would mimic this effect, but at high dose, the antagonist would cross inhibit the opioid response. Under normal conditions, stimulating the α_{2A}AR with an agonist would override its inhibitory action on opioid receptors and synergize with opioid agonists.

Unifying model: The α_{2A}AR allosterically modulates spinal opioid antinociception

The α_{2A}AR allosterically modulates DOR and MOR at the spinal level: Proposed model

In this thesis, we describe a set of seemingly contradictory observations on the regulation of opioid antinociception by the α_{2A}AR. These observations are summarized in Figure 1 using morphine as an example, although similar observations have been made with DeltII. First, we report that morphine and DeltII synergy with clonidine is mediated by the α_{2A}AR. This synergy could also be viewed as an enhancement of opioid effect when the α_{2A}AR is activated by clonidine. Second, morphine and DeltII potency was enhanced in the absence of the α_{2A}AR to ED_{50} values similar to those obtained with the opioid-clonidine combinations in WT mice. Third, morphine antinociception was diminished following the depletion of spinal NE in WT mice, but not in α_{2A}AR-KO.

The above findings have led us to propose an allosteric regulation model in order to explain the different interactions we observed in our studies (Figure 2). This

model predicts that the agonist-occupied α_{2A}AR potentiates opioid analgesia, such as when clonidine is given in combination with morphine or DeltII. The model also predicts that the non-occupied α_{2A}AR actually inhibits opioid analgesia, as we observed after depleting spinal NE. Finally, it predicts that loss of the α_{2A}AR in the KO animals would remove this constitutive inhibitory action on opioid analgesia, thereby potentiating it. This suggests that the α_{2A}AR allosterically modulates spinal opioid receptors in an activation state-dependent manner. Due to the tonic release of NE in the spinal cord, an equilibrium exists between a subset of occupied and unoccupied α_{2A}AR that give rise to an intermediate response to morphine and DeltII in WT mice under normal conditions. Removing NE will favor the constitutive inhibition while adding an excess of α_{2A}AR agonists, such as clonidine, shifts the equilibrium state towards the occupied side and favors an uninhibited opioid response.

This model offers a new perspective on a broad array of opioid-adrenergic interactions with opposite effects. For example, Overland et al. (2009) proposed that clonidine-DeltII synergy results from the *de novo* activation of PKC through the simultaneous activation of DOR and α_2AR. Instead, our model proposes that the co-activation of DOR and α_{2A}AR removes a constitutive inhibition of DOR signaling and permits its full activation. Our model can also explain the inhibitory effects sometimes observed with α_2AR antagonists on opioid responses (Browning et al., 1982; Stone et al., 1997; Morales et al., 2001), but does not explain the opposing effect, i.e. an increase in morphine antinociceptive effect, observed with and ultra-low doses of α_2AR antagonists (Milne et al., 2008). By stabilizing the α_{2A}AR in an inactive conformation and displacing endogenous NE, α_2AR antagonists promote the inhibition of opioid responses.

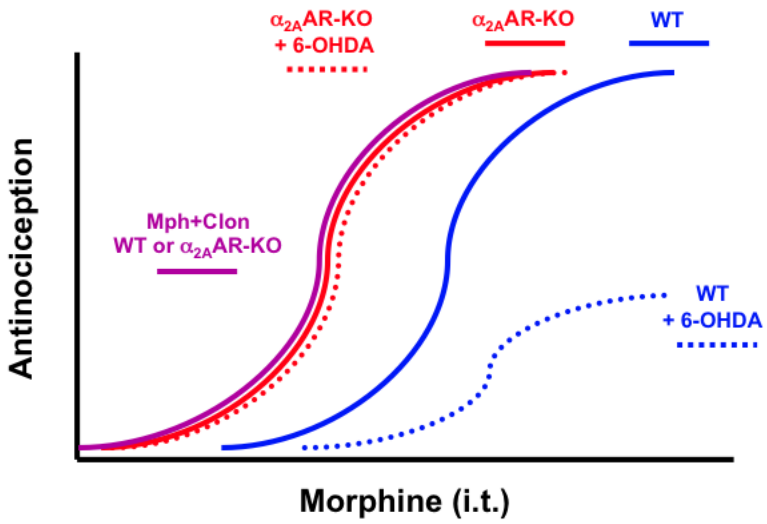

Figure 1: Schematic comparing the spinal morphine dose-response curve obtained with different experimental conditions.

In WT mice, morphine has a dose dependent antinociceptive effect (blue solid line), which is greatly reduced in mice treated with 6-OHDA (blue dashed line) and the addition of clonidine to morphine produces a leftward shift of the dose response curve (purple solid line). In α_{2A}AR-KO mice, morphine was more potent than in WT mice (red solid line), but neither the 6-OHDA treatment (red dashed line) nor the addition of clonidine (purple solid line) shifted morphine dose-response curve.

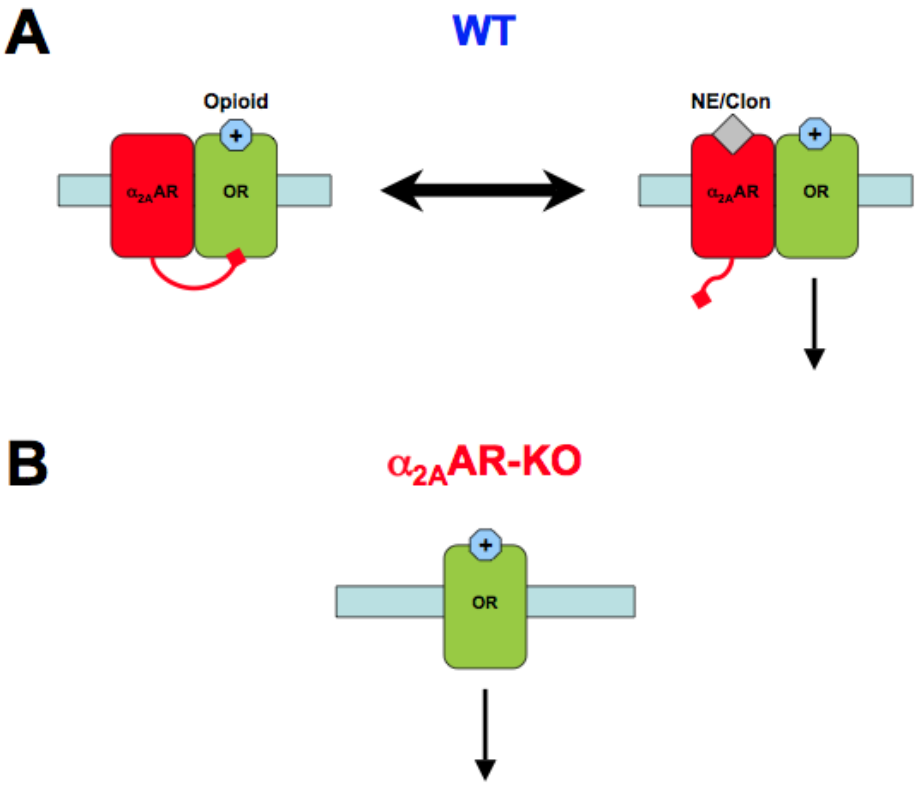

Figure 2: Proposed model of allosteric regulation of opioid receptors by the α_{2A}AR.

(A) In WT mice, opioid receptors (OR, green) are inhibited by the α_{2A}AR (red) in its inactive state, which results in a decreased opioid receptor antinociceptive output when it is activated by an agonist. When an agonist like clonidine (Clon) or norepinephrine (NE) activates the α_{2A}AR, the inhibitory action on the opioid receptor is removed, allowing the agonist-activated opioid receptor to generate a full antinociceptive response. Under normal condition, tonic NE release from descending noradrenergic fibers maintains an equilibrium state between agonist-occupied α_{2A}AR and unbound α_{2A}AR. When NE is depleted, the equilibrium is shifted towards the inactive and inhibitory α_{2A}AR state, and when exogenous clonidine is administered, the equilibrium is shifted towards an active and disinhibited α_{2A}AR state. (B) In α_{2A}AR-KO mice, whether α_2AR agonists are present or not, opioid receptors are not subjected to inhibition by the α_{2A}AR and are thus always fully activated.

Allosteric modulation as a functional consequence of GPCR oligomerization

GPCRs are no longer viewed as simple monomeric receptors. Instead, their ability to oligomerize with each other has given rise to significant re-evaluation of the mechanisms regulating GPCR function. Hetero-oligomerization can affect many aspects of GPCR function, including synthesis, surface expression, ligand binding, signal transduction and internalization, all of which may have important functional implications (Terrillon and Bouvier, 2004). One of the many ways these functional and pharmacological effects can result from GPCR interaction is through allosteric interactions. As defined by Kenakin et al. (2010) :

> "Receptor-receptor interactions: when the binding of a ligand to the orthosteric or allosteric sites of one receptor causes, via direct allosteric interactions, a change in the ligand recognition, decoding and trafficking processes of another receptor".

The state-dependent α_{2A}AR regulation of opioid effects is consistent with such an allosteric interaction. Allosteric interactions depend on direct physical contact between the interacting receptors; however, similar functional interactions could be mediated by intracellular signaling in the absence of direct physical interaction between the receptors. Moreover, when measuring the effect of drug interactions at the behavioral level, one cannot exclude the possibility that the interaction involves distinct cells in the system under study.

Co-expression of α_{2A}AR with DOR or MOR *in vitro* and *in vivo*

For allosteric interactions between the α_{2A}AR and DOR or MOR to take place, these receptors must be co-expressed and interact physically. Different lines of evidence suggest that these two receptor pairs may form hetero-oligomers *in vivo*.

DOR and α_{2A}AR

As discussed previously in this chapter, functional and anatomical studies have placed DOR and α_{2A}AR in SP expressing DRG neurons (Overland et al., 2009;

Riedl et al., 2009). In HEK 293 cells expressing epitope-tagged DOR and α_{2A}AR, the receptors were demonstrated to be within 100Å distance and part of the same protein complex as shown by co-immunoprecipitation assay (Rios et al., 2004). Thus, DOR and α_{2A}AR are co-expressed in DRG neurons, and are close enough to interact physically in expression systems. This receptor pair most likely forms hetero-oligomers that mediate opioid-adrenergic synergy *in vivo*.

MOR and α_{2A}AR

We identified MOR and α_{2A}AR as the receptor subtypes targeted by morphine and clonidine, respectively, to mediate their synergistic interaction. Given the similar distribution of these receptors in DRG and spinal cord neurons (see Chapter 1), their co-expression is very likely. For example, peptidergic nociceptors have been found to express both MOR (Wang et al., 2010) and α_{2A}AR (Stone et al., 1998; Riedl et al., 2009). However, the only direct assessment of their co-expression in the spinal cord showed that MOR- and α_{2A}AR-ir did not overlap (Riedl et al., 2009). It is possible that the antibodies used in this study each recognized only a subset of their specific receptor (e.g. splice variant). Using different primary antibodies raised against MOR and α_{2A}AR, other immunohistochemical studies showed different labeling patterns in the spinal cord (Rosin et al., 1993; Arvidsson et al., 1995b; Gold et al., 1997). However, Tan et al. (2009) showed an extensive MOR- and α_{2A}AR-ir colocalization at the cell surface and in neuronal projections of cultured DRG neurons. They also showed that MOR and α_{2A}AR co-internalization upon morphine and clonidine treatment was associated with a functional cross-desensitization of the receptors. These demonstrations, together with the observations that morphine and clonidine can both inhibit C fiber-evoked responses (Sullivan et al., 1987) and capsaicin-induced glutamate release from spinal cord synaptosomes (Li and Eisenach, 2001), make a strong case for the co-expression and functional interaction of MOR and α_{2A}AR in nociceptors.

In heterologous expression systems, MOR and α_{2A}AR have been shown to interact physically and functionally. When co-expressed, the receptors are in close enough proximity to produce bioluminescence resonance energy transfer (BRET) (Jordan et al., 2003) or fluorescence resonance energy transfer (FRET; (Vilardaga et al., 2008), and they can be co-immunoprecipitated in the same protein complex (Jordan et al., 2003; Zhang and Limbird, 2004). This direct interaction between MOR and α_{2A}AR has important functional consequences. Vilardaga et al. (2008) studied the effect of ligand-induced cross-conformational change between MOR and α_{2A}AR and how it modulates coupling to downstream signaling. They showed that morphine reduced the conformational changes in the α_{2A}AR and activation of G_i induced by NE. The inhibition of G_i signaling was strongly correlated with the inhibition of the ERK1/2 signaling pathway. This study demonstrated the ability of MOR to allosterically modulate α_{2A}AR, but did not test the reverse, i.e. the ability of α_{2A}AR to allosterically modulate MOR. If allosteric interactions are bidirectional within a receptor oligomer, then α_{2A}AR could also cross-inhibit MOR. Interestingly, their observation that G_i signaling output decreases when both receptors are occupied by an agonist is in agreement with the decrease in GTPγS binding and phosphorylation of MAPK upon morphine+clonidine treatment in cells expressing MOR and α_{2A}AR observed by Jordan et al., (2003). In the presence of a single agonist, MOR and α_{2A}AR normally activate MAPK signaling pathways. The suppression of G_i-protein coupling and downstream signaling may indicate that the MOR-α_{2A}AR heteromer switches to a different signaling pathway under these conditions. In our model, this alternate signaling pathway would be under the inhibitory control of α_{2A}AR, where its activation would relieve this constitutive inhibition, possibly via allosteric interactions in the context of a receptor heterodimer.

Is α_{2A}AR controlling the activation of PKC by MOR?

PKC activation has been identified as a downstream effector of opioid-adrenergic analgesic synergy *in vivo* (Wei et al., 1996) and *in vitro* (Overland et al., 2009). If PKC activation is a downstream effector of the co-activation of α_{2A}AR and MOR

or DOR, our model predicts that PKC activation would be inhibited by the unbound α_{2A}AR, but is fully activated in α_{2A}AR-KO mice. We tested the hypothesis that the increased morphine potency observed in α_{2A}AR-KO mice is due to the activation of PKC, and that inhibiting PKC with chelerythrine would decrease the antinociceptive effect of morphine to levels similar to WT mice. Chelerythrine did not affect morphine antinociception in WT mice, which is consistent with previous studies (Wei et al., 1996). In α_{2A}AR-KO mice, the lower morphine antinociception in chelerythrine-treated compared to vehicle-treated mice, although not significant, is consistent with our prediction. The results of this preliminary experiment warrant further investigation.

Investigating allosteric interactions between DOR and α_{2A}AR with radioligand binding

Allosteric interactions within heteromers may change ligand binding properties, leading to negative or positive cooperativity as measured in binding experiments. For example, changes in the shape and slope of saturation and competition binding curves could reflect alterations in maximal binding capacity or ligand affinity (Durroux, 2005; Albizu et al., 2006). Our behavioral results and allosteric interaction model predicts that, in the absence of the α_{2A}AR, B_{max} would increase or K_D and K_i values would decrease. Using [^{3}H]-DeltII binding to spinal cord membrane preparations from WT and α_{2A}AR-KO mice, we saw a small decrease in maximal binding sites in α_{2A}AR-KO mice, but ligand affinity was not different. However, allosteric interactions usually occur when the orthosteric binding site is occupied by an agonist or an antagonist. For example, Browning et al. (1982) reported a displacement of [^{3}H]DADLE, a DOR agonist, by α_2AR ligands in rat brain membranes, but the effect was not attributed to a specific adrenergic receptor subtype. Therefore, competition binding experiments with [^{3}H]DeltII in the presence of α_2AR ligands would provide further information on the allosteric interaction and complement our study.

Potential limitations and future directions

The interpretations of the results presented in this thesis, as with all research studies, have certain limitations. Here, we discuss some important elements to consider that are relevant to the work presented in this dissertation.

Use of genetically modified animals

Our experimental approach relies mainly on the comparison of WT mice with a mouse strain carrying a genetic deletion of DOR or α_{2A}AR. This approach has the advantage of assessing the function of the receptor of interest when the available pharmacological reagents are not selective enough. For example, clonidine is a non-selective α_2AR agonist that can bind to all three receptor subtypes (α_{2A}AR, α_{2B}AR, α_{2C}AR), but our results show that α_{2A}AR is the principal mediator of clonidine analgesia in the spinal cord. We also showed that DeltII was selective for DOR in the SP behavioral assay, but not the tail flick assay, which allowed us to conclude with confidence that DOR mediates DeltII-clonidine synergy in the SP behavioral assay.

The use of transgenic KO mice presents certain caveats that must be considered. First, the global KO suppresses the expression of DOR and α_{2A}AR not only in DRGs and the spinal cord, but also in all tissues. The deletion of these receptors could therefore lead to compensatory mechanisms or dysfunctions in the expression of other genes or in the regulation of other physiological systems, which could introduce confounding factors in the interpretation of our results. We confirmed that the expression of MOR was unchanged in DOR-KO mice (Chapter 3), and that MOR and DOR expression were unchanged in α_{2A}AR-KO mice (Chapter 5). Furthermore, it was shown that the maximum number of binding sites and binding affinity for MOR and KOR was unaffected in DOR-KO mice (Filliol et al., 2000). However, the possibility that genes that do not code for opioid receptors are dysregulated by the genetic deletions cannot be ruled out.

Both mouse strains have distinct phenotypes due to the genetic deletion. For instance, DOR-KO mice show signs of anxiety and depressive-like behaviors

(Filliol et al., 2000), which could affect pain measurements. Furthermore, the α_{2A}AR is involved in the inhibition of insulin release in response to adrenaline (Peterhoff et al., 2003). As a consequence, α_{2A}AR-KO mice could have elevated insulin levels, which could promote the storage of blood glucose into adipose tissues and cause the increased weight gain we observed compared to WT mice. The long-term effects of this metabolic imbalance on nociception have not been evaluated. New generations of transgenic mice with cell type-specific gene deletions can improve KO mouse models by restricting the gene deletion to a subset of cells of interest, e.g. peripheral sensory neurons, leaving the expression of this gene in other cells intact (Gavériaux-Ruff et al., 2011).

Exclusion of females in pre-clinical pain studies

Women represent a larger proportion than men amongst chronic pain sufferers and respond differently to pain management therapies (Unruh, 1996). Understanding why is a primary concern and a growing area of pain research. Unfortunately, the majority of pre-clinical studies are performed in male subjects, and our studies are no exception to this trend. Our primary objective was to understand the role of DOR and α_{2A}AR in the interaction between opioid and adrenergic drugs. When designing our experiments, we considered other studies that examined sex differences in opioid and adrenergic antinociceptive responses and decided not to include females in our experimental groups to avoid variability in our measurements. For example, clonidine antinociception is attenuated by estrogen in female rats, resulting in a low clonidine response during the proestrous phase of the cycle when estrogen levels are high, and a high response to clonidine during the diestrous phase when estrogen levels are low (Nag and Mokha, 2006; Thompson et al., 2008). The antinociceptive response to clonidine is also under gonadal hormone regulation in males in which testosterone is necessary to get full clonidine antinociception (Thompson et al., 2008). Since levels of testosterone are stable in males, there is less variability in clonidine antinociception (Thompson et al., 2008). Moreover, a review compiling studies examining sex differences in morphine antinociception reported that morphine

was more potent or effective in males than females (Craft, 2003). Due to the variability of opioid and adrenergic responses in females versus males, we could have observed sex differences in our studies, which would have added a level of complexity beyond the scope of our study. In future studies, it would be informative and clinically relevant to investigate sex differences in opioid-adrenergic interactions with carefully designed experiments following the recommendations proposed by Greenspan and colleagues (2007).

Confirmation of the 6-OHDA lesion in WT and α_{2A}AR-KO mice

6-OHDA has been used to chemically destroy catecholaminergic, i.e. dopaminergic and noradrenergic, structures for over 40 years (Kostrzewa and Jacobowitz, 1974). 6-OHDA is a dopamine analog with high affinity for catechomaminergic membrane transporters. The effect of 6-OHDA is determined by its route of administration. Since it poorly crosses the blood-brain barrier (BBB), it must be injected at the site of interest to produce the desired lesion. When injected intrathecally, 6-OHDA enters noradrenergic nerve terminals via NE transporters (NET) for which it has high affinity. Once inside the cell, 6-OHDA molecules oxidize and release reactive oxygen species, which have deleterious long-term effects on the nerve terminal (Przedborski and Ischiropoulos, 2005). In the spinal cord, the chemical lesion is highly localized and specific to NA nerve terminals (Fasmer et al., 1986), leaving other cells and neurons intact and produce a long-lasting depletion of NE (Bloom et al., 1969; Kostrzewa and Jacobowitz, 1974; Post et al., 1987). For example, a single 20 µg dose of 6-OHDA administered i.t. produced behavioral changes and NE depletion as early as two days post-treatment (Howe and Yaksh, 1982). We performed our experiments at 3 days post-6-OHDA treatment, but we were unable to confirm the efficacy of the lesion after the experiment. To confirm the lesion, we measured the levels of tyrosine hydroxylase (TH) in spinal cords from all four treatment groups by western blot. We did not detect a significant difference between vehicle- and 6-OHDA- treated WT mice (data not shown). This approach may have failed because 1) the lesion did not work, 2) the lesion was below the limit

of detection, 3) the spinal cord segment used contained regions that were not affected by the lesion, and 4) the antibody used had a poor signal to noise ratio.

However, the observation of a strong decrease in morphine effect in 6-OHDA-treated WT mice suggests that the noradrenergic fiber lesion was effective. The lack of effect of the treatment in α_{2A}AR-KO mice suggests two possibilities: NE modulates morphine via the α_{2A}AR or that 6-OHDA did not induce a lesion in α_{2A}AR-KO mice. The latter seems less plausible since the mechanism by which 6-OHDA destroys catecholaminergic nerve terminals is independent of the α_{2A}AR. However, it is possible that due to excess NE in the spinal cord, these transporters are desensitized or downregulated, and therefore protects NE fibers from 6-OHDA.

It will be important to confirm the 6-OHDA-induced lesion in the spinal cord of α_{2A}AR-KO mice in order to complete the study presented in Chapter 5. For example, detection of NE in spinal cord extracts by HPLC or immunohistological analysis of lumbar spinal cord segments with a catecholaminergic neuronal marker such as TH have both successfully demonstrated the lesioning of noradrenergic nerve fibers.

Acute pain studies in naive mice contribute to understanding chronic pain

The findings from our studies have limited clinical application for chronic pain since they were conducted in naïve mice. The nociceptive circuit of patients suffering from chronic pain is different from healthy individuals in many regards. Furthermore, there are important differences between the etiologies of different pain conditions. Therefore, one cannot conclude that findings in healthy mice are directly transposable to chronic pain conditions. Animal models of chronic pain are better suited to test whether opioid-adrenergic interactions, such as synergy, occur under chronic pain conditions. Few studies have addressed this issue. For example, studies in neuropathic rats and mice have confirmed that the morphine and clonidine interaction is still synergistic in this condition (Ossipov et al., 1997;

Fairbanks et al., 2000a). Moreover, Tajerian et al. (2012) demonstrated that the synergy between morphine and clonidine was also maintained in a mouse model of low back pain. These studies further validate the use of combination therapy for the treatment of chronic pain conditions.

The objective of the current work was to gain insight into the basic mechanism mediating the interaction between opioid and adrenergic drugs, a phenomenon that we are only beginning to comprehend under normal conditions. We decided to use behavioral assays that model nociceptive pain in order to compare our results with previous studies. Our findings directly contribute to the understanding of acute nociception and can be related to clinical situations whereby a patient without prior ongoing pain history presents with acute pain due to an injury or needs to undergo a painful procedure.

Interestingly, uncovering the role of the α_{2A}AR in the modulation of pain and opioid sensitivity by NE raises the possibility that some chronic pain conditions result from an imbalance in adrenergic signaling in the spinal cord. For example, the etiology of fibromyalgia syndrome (FMS) is still largely unknown. The cerebrospinal fluid (CSF) levels of SP are higher in FMS patients than in normal individuals (Russell, 1998), but the CSF levels of methoxyhydroxyphenylglycol, a metabolite of NE, are lower (Russell et al., 1992). This suggests that FMS patients have reduced noradrenergic tone, which reduces the inhibition of SP release from nociceptors and sensitize the nociceptive circuit in the spinal cord. According to our model, low levels of NE in the spinal cord could also decrease the effect of endogenous or exogenous opioids in FMS patients. Therefore, restoring NE levels would ameliorate the pain symptoms associated with FMS. Tramadol is a noradrenergic reuptake inhibitor and a weak MOR agonist that is efficacious for the treatment of FMS (Russell et al., 2000). According to our proposed model, the success of this treatment could be attributed to its dual action: 1) the reuptake inhibitor restores spinal NE levels, which favors the agonist-occupied form of the α_{2A}AR and releases the inhibition on MOR so that 2) the action of tramadol on MOR can be fully effective.

ORIGINAL CONTRIBUTIONS TO KNOWLEDGE

The studies presented in this thesis contain novel and original elements that contribute to the understanding of nociceptive processing and opioid-adrenergic interactions at the spinal cord. These elements are listed below.

Chapter 3: The delta opioid receptor is necessary to produce full morphine antinociception at the spinal level

Documentation of DOR-dependent endogenous inhibition of thermal antinociception at mildly nociceptive temperatures.

Demonstration that DOR contributes to spinal morphine analgesia.

Chapter 4: The delta opioid receptor is sufficient, but not necessary for spinal opioid-adrenergic analgesic synergy

Validation of the DOR agonist DeltII selectivity for DOR in the SP behavioral assay.

Identification of DOR as a mediator of opioid-adrenergic synergy.

Demonstration that morphine+clonidine synergy is independent of DOR.

Chapter 5: Spinal opioid antinociception is allosterically modulated by the α_{2A}-adrenergic receptor.

Documentation of a NE-dependent endogenous inhibition of noxious heat antinociception mediated by the α_{2A}AR.

Identification of α_{2A}AR as a mediator of spinal morphine+clonidine synergy, the most clinically relevant drug combination.

Potentiation of opioid antinociception (morphine and DeltII) in the absence of α_{2A}AR.

Assessement of the role of the α_{2A}AR in DeltII binding to spinal cord membranes.

Association of the effect of NE on spinal opioid antinociception to its action on the α_{2A}AR.

Chapter 6: Discussion

Development of an integrated model proposing that α_{2A}AR allosterically modulates spinal opioid receptors.

Publications

Findings reported in Chapter 4 have been published in Chabot-Doré et al. (2013)

In addition to the work included in this thesis, I have also collaborated on related projects that resulted in two publications (see Appendix B). In these publications, I demonstrated the enrichment of DOR and α_{2A}AR in a spinal cord synaptosome preparations (Riedl et al., 2009); Figure 6) and I confirmed that DOR-ir colocalizes with SP-ir in the dorsal horn of the mouse spinal cord (Overland et al., 2009); Figure 1).

References

Abbadie C, Lombard MC, Besson JM, Trafton JA and Basbaum AI (2002) Mu and delta opioid receptor-like immunoreactivity in the cervical spinal cord of the rat after dorsal rhizotomy or neonatal capsaicin: an analysis of pre- and postsynaptic receptor distributions. *Brain research* **930**:150-162.

Abdelhamid EE, Sultana M, Portoghese PS and Takemori AE (1991) Selective blockage of delta opioid receptors prevents the development of morphine tolerance and dependence in mice. *The Journal of Pharmacology and Experimental Therapeutics* **258**:299-303.

Ackerman LL, Follett KA and Rosenquist RW (2003) Long-term outcomes during treatment of chronic pain with intrathecal clonidine or clonidine/opioid combinations. *Journal of Pain and Symptom Management* **26**:668-677.

Albizu L, Balestre MN, Breton C, Pin J-P, Manning M, Mouillac B, Barberis C and Durroux T (2006) Probing the Existence of G Protein-Coupled Receptor Dimers by Positive and Negative Ligand-Dependent Cooperative Binding. *Molecular Pharmacology* **70**:1783-1791.

Altman JD, Trendelenburg AU, MacMillan L, Bernstein D, Limbird L, Starke K, Kobilka BK and Hein L (1999) Abnormal regulation of the sympathetic nervous system in alpha2A-adrenergic receptor knockout mice. *Molecular Pharmacology* **56**:154-161.

Anderson VC and Burchiel KJ (1999) A prospective study of long-term intrathecal morphine in the management of chronic nonmalignant pain. *Neurosurgery* **44**:289-300; discussion 300-281.

Arnér S and Meyerson BA (1988) Lack of analgesic effect of opioids on neuropathic and idiopathic forms of pain. *Pain* **33**:11-23.

Arvidsson U, Dado RJ, Riedl M, Lee JH, Law PY, Loh HH, Elde R and Wessendorf MW (1995a) delta-Opioid receptor immunoreactivity: distribution in brainstem and spinal cord, and relationship to biogenic

amines and enkephalin. *The Journal of neuroscience : the official journal of the Society for Neuroscience* **15**:1215-1235.

Arvidsson U, Riedl M, Chakrabarti S, Lee JH, Nakano AH, Dado RJ, Loh HH, Law PY, Wessendorf MW and Elde R (1995b) Distribution and targeting of a mu-opioid receptor (MOR1) in brain and spinal cord. *The Journal of neuroscience : the official journal of the Society for Neuroscience* **15**:3328-3341.

Asada Y and Lee TJ (1992) Alpha 2-adrenoceptors mediate norepinephrine constriction of porcine pial veins. *The American journal of physiology* **263**:H1907-1910.

Barrett RW and Vaught JL (1982) The effects of receptor selective opioid peptides on morphine-induced analgesia. *European journal of pharmacology* **80**:427-430.

Beaudry H, Dubois D and Gendron L (2011) Activation of Spinal μ- and δ-Opioid Receptors Potently Inhibits Substance P Release Induced by Peripheral Noxious Stimuli. *The Journal of neuroscience : the official journal of the Society for Neuroscience* **31**:13068-13077.

Beaudry H, Proteau-Gagné A, Li S, Dory Y, Chavkin C and Gendron L (2009) Differential noxious and motor tolerance of chronic delta opioid receptor agonists in rodents. *Neuroscience* **161**:381-391.

Berge OG and Ogren SO (1984) Limited involvement of central noradrenergic pathways in morphine-induced antinociception. *Neuropharmacology* **23**:1179-1185.

Besse D, Lombard MC, Zajac JM, Roques BP and Besson JM (1990) Pre- and postsynaptic distribution of mu, delta and kappa opioid receptors in the superficial layers of the cervical dorsal horn of the rat spinal cord. *Brain research* **521**:15-22.

Bloom FE, Algeri S, Groppetti A, Revuelta A and Costa E (1969) Lesions of central norepinephrine terminals with 6-OH-dopamine: biochemistry and fine structure. *Science (New York, NY)* **166**:1284-1286.

Bohn LM, Xu F, Gainetdinov RR and Caron MG (2000) Potentiated opioid analgesia in norepinephrine transporter knock-out mice. *The Journal of neuroscience : the official journal of the Society for Neuroscience* **20**:9040-9045.

Browning S, Lawrence D, Livingston A and Morris B (1982) Interactions of drugs active at opiate receptors and drugs active at alpha 2-receptors on various test systems. *British Journal of Pharmacology* **77**:487-491.

Cahill CM, McClellan KA, Morinville A, Hoffert C, Hubatsch D, O'Donnell D and Beaudet A (2001a) Immunohistochemical distribution of delta opioid receptors in the rat central nervous system: evidence for somatodendritic labeling and antigen-specific cellular compartmentalization. *The Journal of comparative neurology* **440**:65-84.

Cahill CM, Morinville A, Hoffert C, O'Donnell D and Beaudet A (2003) Up-regulation and trafficking of delta opioid receptor in a model of chronic inflammation: implications for pain control. *Pain* **101**:199-208.

Cahill CM, Morinville A, Lee MC, Vincent JP, Collier B and Beaudet A (2001b) Prolonged morphine treatment targets delta opioid receptors to neuronal plasma membranes and enhances delta-mediated antinociception. *The Journal of neuroscience : the official journal of the Society for Neuroscience* **21**:7598-7607.

Calabrese EJ and Baldwin LA (2003) Hormesis: the dose-response revolution. *Annual review of pharmacology and toxicology* **43**:175-197.

Chabot-Doré A-J, Millecamps M and Stone LS (2013) The delta-opioid receptor is sufficient, but not necessary, for spinal opioid-adrenergic synergy. *Journal of Pharmacology and Experimental Therapeutics*.

Chaplan SR, Bach FW, Pogrel JW, Chung JM and Yaksh TL (1994) Quantitative assessment of tactile allodynia in the rat paw. *Journal of neuroscience methods* **53**:55-63.

Cheng JK, Pan HL and Eisenach JC (2000) Antiallodynic effect of intrathecal gabapentin and its interaction with clonidine in a rat model of postoperative pain. *Anesthesiology* **92**:1126-1131.

Chu J, Zheng H, Loh HH and Law P-Y (2008) Morphine-induced mu-opioid receptor rapid desensitization is independent of receptor phosphorylation and beta-arrestins. *Cellular Signalling* **20**:1616-1624.

Chu J, Zheng H, Zhang Y, Loh HH and Law P-Y (2010) Agonist-dependent mu-opioid receptor signaling can lead to heterologous desensitization. *Cellular Signalling* **22**:684-696.

Codd EE, Carson JR, Colburn RW, Stone DJ, Van Besien CR, Zhang S-P, Wade PR, Gallantine EL, Meert TF, Molino L, Pullan S, Razler CM, Dax SL and Flores CM (2009) JNJ-20788560 [9-(8-azabicyclo[3.2.1]oct-3-ylidene)-9H-xanthene-3-carboxylic acid diethylamide], a selective delta opioid receptor agonist, is a potent and efficacious antihyperalgesic agent that does not produce respiratory depression, pharmacologic tolerance, or physical dependence. *The Journal of Pharmacology and Experimental Therapeutics* **329**:241-251.

Costantino CM, Gomes I, Stockton SD, Lim MP and Devi LA (2012) Opioid receptor heteromers in analgesia. *Expert Reviews in Molecular Medicine* **14**.

Craft RM (2003) Sex differences in opioid analgesia: "from mouse to man". *The Clinical journal of pain* **19**:175-186.

Ding YQ, Kaneko T, Nomura S and Mizuno N (1996) Immunohistochemical localization of mu-opioid receptors in the central nervous system of the rat. *The Journal of comparative neurology* **367**:375-402.

Duflo F, Li X, Bantel C, Pancaro C, Vincler M and Eisenach JC (2002) Peripheral nerve injury alters the alpha2 adrenoceptor subtype activated by clonidine for analgesia. *Anesthesiology* **97**:636-641.

Dupré DJ and Hébert TE (2006) Biosynthesis and trafficking of seven transmembrane receptor signalling complexes. *Cellular Signalling* **18**:1549-1559.

Durroux T (2005) Principles: a model for the allosteric interactions between ligand binding sites within a dimeric GPCR. *Trends in pharmacological sciences* **26**:376-384.

Eisenach JC, DuPen S, Dubois M, Miguel R and Allin D (1995) Epidural clonidine analgesia for intractable cancer pain. The Epidural Clonidine Study Group. *Pain* **61**:391-399.

Emmerson PJ, Liu MR, Woods JH and Medzihradsky F (1994) Binding affinity and selectivity of opioids at mu, delta and kappa receptors in monkey brain membranes. *The Journal of Pharmacology and Experimental Therapeutics* **271**:1630-1637.

Fairbanks CA, Nguyen HO, Grocholski BM and Wilcox GL (2000a) Moxonidine, a selective imidazoline-alpha2 -adrenergic receptor agonist, produces spinal synergistic antihyperalgesia with morphine in nerve-injured mice. *Anesthesiology* **93**:765-773.

Fairbanks CA, Posthumus IJ, Kitto KF, Stone LS and Wilcox GL (2000b) Moxonidine, a selective imidazoline/alpha(2) adrenergic receptor agonist, synergizes with morphine and deltorphin II to inhibit substance P-induced behavior in mice. *Pain* **84**:13-20.

Fairbanks CA, Stone LS, Kitto KF, Nguyen HO, Posthumus IJ and Wilcox GL (2002) alpha(2C)-Adrenergic receptors mediate spinal analgesia and adrenergic-opioid synergy. *The Journal of Pharmacology and Experimental Therapeutics* **300**:282-290.

Fairbanks CA, Stone LS and Wilcox GL (2009) Pharmacological profiles of alpha 2 adrenergic receptor agonists identified using genetically altered mice and isobolographic analysis. *Pharmacology & therapeutics* **123**:224-238.

Fairbanks CA and Wilcox GL (1999a) Moxonidine, a selective alpha2-adrenergic and imidazoline receptor agonist, produces spinal antinociception in mice. *The Journal of Pharmacology and Experimental Therapeutics* **290**:403-412.

Fairbanks CA and Wilcox GL (1999b) Spinal antinociceptive synergism between morphine and clonidine persists in mice made acutely or chronically tolerant to morphine. *The Journal of Pharmacology and Experimental Therapeutics* **288**:1107-1116.

Fasmer OB, Berge OG, Tveiten L and Hole K (1986) Changes in nociception after 6-hydroxydopamine lesions of descending catecholaminergic pathways in mice. *Pharmacology, biochemistry, and behavior* **24**:1441-1444.

Filliol D, Ghozland S, Chluba J, Martin M, Matthes HW, Simonin F, Befort K, Gaveriaux-Ruff C, Dierich A, LeMeur M, Valverde O, Maldonado R and Kieffer BL (2000) Mice deficient for delta- and mu-opioid receptors exhibit opposing alterations of emotional responses. *Nature genetics* **25**:195-200.

Gavériaux-Ruff C, Nozaki C, Nadal X, Hever XC, Weibel R, Matifas A, Reiss D, Filliol D, Nassar MA, Wood JN, Maldonado R and Kieffer BL (2011) Genetic ablation of delta opioid receptors in nociceptive sensory neurons increases chronic pain and abolishes opioid analgesia. *Pain* **152**:1238-1248.

Gendron L, Lucido AL, Mennicken F, O'Donnell D, Vincent J-P, Stroh T and Beaudet A (2006) Morphine and pain-related stimuli enhance cell surface availability of somatic delta-opioid receptors in rat dorsal root ganglia. *The Journal of neuroscience : the official journal of the Society for Neuroscience* **26**:953-962.

Gilsbach R, Röser C, Beetz N, Brede M, Hadamek K, Haubold M, Leemhuis J, Philipp M, Schneider J, Urbanski M, Szabo B, Weinshenker D and Hein L (2009) Genetic dissection of alpha2-adrenoceptor functions in adrenergic versus nonadrenergic cells. *Molecular Pharmacology* **75**:1160-1170.

Glaum SR, Miller RJ and Hammond DL (1994) Inhibitory actions of delta 1-, delta 2-, and mu-opioid receptor agonists on excitatory transmission in lamina II neurons of adult rat spinal cord. *The Journal of neuroscience : the official journal of the Society for Neuroscience* **14**:4965-4971.

Gold MS, Dastmalchi S and Levine JD (1997) Alpha 2-adrenergic receptor subtypes in rat dorsal root and superior cervical ganglion neurons. *Pain* **69**:179-190.

Gomes I, Gupta A, Filipovska J, Szeto HH, Pintar JE and Devi LA (2004) A role for heterodimerization of mu and delta opiate receptors in enhancing morphine analgesia. *Proceedings of the National Academy of Sciences of the United States of America* **101**:5135-5139.

Goodman RR, Snyder SH, Kuhar MJ and Young WS (1980) Differentiation of delta and mu opiate receptor localizations by light microscopic autoradiography. *Proceedings of the National Academy of Sciences of the United States of America* **77**:6239-6243.

Gouardères C, Beaudet A, Zajac JM, Cros J and Quirion R (1991) High resolution radioautographic localization of [125I]FK-33-824-labelled mu opioid receptors in the spinal cord of normal and deafferented rats. *NSC* **43**:197-209.

Gouardères C, Tellez S, Tafani JA and Zajac JM (1993) Quantitative autoradiographic mapping of delta-opioid receptors in the rat central nervous system using [125I][D.Ala2]deltorphin-I. *Synapse (New York, NY)* **13**:231-240.

Greenspan JD, Craft RM, LeResche L, Arendt-Nielsen L, Berkley KJ, Fillingim RB, Gold MS, Holdcroft A, Lautenbacher S, Mayer EA, Mogil JS, Murphy AZ, Traub RJ and Consensus Working Group of the Sex G, and Pain SIG of the IASP (2007) Studying sex and gender differences in pain and analgesia: a consensus report., in *Pain* pp S26-45.

Guo X-h, Fairbanks CA, Stone LS and Loh HH (2003) DPDPE-UK14,304 synergy is retained in mu opioid receptor knockout mice. *Pain* **104**:209-217.

Hargreaves K, Dubner R, Brown F, Flores C and Joris J (1988) A new and sensitive method for measuring thermal nociception in cutaneous hyperalgesia. *Pain* **32**:77-88.

Hellemans J, Mortier G, De Paepe A, Speleman F and Vandesompele J (2007) qBase relative quantification framework and software for management and automated analysis of real-time quantitative PCR data. *Genome biology* **8**:R19.

Holdridge SV and Cahill CM (2007) Spinal administration of a delta opioid receptor agonist attenuates hyperalgesia and allodynia in a rat model of neuropathic pain. *European journal of pain (London, England)* **11**:685-693.

Hosohata Y, Vanderah TW, Burkey TH, Ossipov MH, Kovelowski CJ, Sora I, Uhl GR, Zhang X, Rice KC, Roeske WR, Hruby VJ, Yamamura HI, Lai J and Porreca F (2000) delta-Opioid receptor agonists produce antinociception and [35S]GTPgammaS binding in mu receptor knockout mice. *European journal of pharmacology* **388**:241-248.

Howe JR and Yaksh TL (1982) Changes in sensitivity to intrathecal norepinephrine and serotonin after 6-hydroxydopamine (6-OHDA), 5,6-dihydroxytryptamine (5,6-DHT) or repeated monoamine administration. *The Journal of Pharmacology and Experimental Therapeutics* **220**:311-321.

Hylden JL and Wilcox GL (1980) Intrathecal morphine in mice: a new technique. *European journal of pharmacology* **67**:313-316.

Hylden JL and Wilcox GL (1981) Intrathecal substance P elicits a caudally-directed biting and scratching behavior in mice. *Brain research* **217**:212-215.

Hylden JL and Wilcox GL (1982) Intrathecal opioids block a spinal action of substance P in mice: functional importance of both mu- and delta-receptors. *European journal of pharmacology* **86**:95-98.

Iida H, Ohata H, Iida M, Watanabe Y and Dohi S (1999) Direct effects of alpha1- and alpha2-adrenergic agonists on spinal and cerebral pial vessels in dogs. *Anesthesiology* **91**:479-485.

Jasmin L, Boudah A and Ohara PT (2003) Long-term effects of decreased noradrenergic central nervous system innervation on pain behavior and opioid antinociception. *The Journal of comparative neurology* **460**:38-55.

Jasmin L, Tien D, Weinshenker D, Palmiter RD, Green PG, Janni G and Ohara PT (2002) The NK1 receptor mediates both the hyperalgesia and the resistance to morphine in mice lacking noradrenaline. *Proceedings of the National Academy of Sciences of the United States of America* **99**:1029-1034.

Ji TH, Grossmann M and Ji I (1998) G protein-coupled receptors. I. Diversity of receptor-ligand interactions. *The Journal of biological chemistry* **273**:17299-17302.

Johnson EA, Oldfield S, Braksator E, Gonzalez-Cuello A, Couch D, Hall KJ, Mundell SJ, Bailey CP, Kelly E and Henderson G (2006) Agonist-selective mechanisms of mu-opioid receptor desensitization in human embryonic kidney 293 cells. *Molecular Pharmacology* **70**:676-685.

Jordan BA, Gomes I, Rios C, Filipovska J and Devi LA (2003) Functional interactions between mu opioid and alpha 2A-adrenergic receptors. *Molecular Pharmacology* **64**:1317-1324.

Kawasaki Y, Kumamoto E, Furue H and Yoshimura M (2003) Alpha 2 adrenoceptor-mediated presynaptic inhibition of primary afferent glutamatergic transmission in rat substantia gelatinosa neurons. *Anesthesiology* **98**:682-689.

Kenakin T, Agnati LF, Caron M, Fredholm B, Guidoli D, Kobilka B, Lefkowitz RW, Lohse M, Woods A and Fuxe K (2010) International Workshop at the Nobel Forum, Karolinska Institutet on G protein-coupled receptors: finding the words to describe monomers, oligomers, and their molecular mechanisms and defining their meaning. Can a consensus be reached? *Journal of receptor and signal transduction research* **30**:284-286.

Kingery WS, Guo TZ, Davies MF, Limbird L and Maze M (2000) The alpha(2A) adrenoceptor and the sympathetic postganglionic neuron contribute to the development of neuropathic heat hyperalgesia in mice. *Pain* **85**:345-358.

Kostrzewa RM and Jacobowitz DM (1974) Pharmacological actions of 6-hydroxydopamine. *Pharmacological Reviews* **26**:199-288.

Kuraishi Y, Harada Y, Aratani S, Satoh M and Takagi H (1983) Separate involvement of the spinal noradrenergic and serotonergic systems in morphine analgesia: the differences in mechanical and thermal algesic tests. *Brain research* **273**:245-252.

Lähdesmäki J, Scheinin M, Pertovaara A and Mansikka H (2003) The alpha2A-adrenoceptor subtype is not involved in inflammatory hyperalgesia or morphine-induced antinociception. *European journal of pharmacology* **468**:183-189.

Lakhlani PP, MacMillan LB, Guo TZ, McCool BA, Lovinger DM, Maze M and Limbird LE (1997) Substitution of a mutant alpha2a-adrenergic receptor via "hit and run" gene targeting reveals the role of this subtype in sedative, analgesic, and anesthetic-sparing responses in vivo. *Proceedings of the National Academy of Sciences of the United States of America* **94**:9950-9955.

Li X and Eisenach JC (2001) alpha2A-adrenoceptor stimulation reduces capsaicin-induced glutamate release from spinal cord synaptosomes. *The Journal of Pharmacology and Experimental Therapeutics* **299**:939-944.

Li X, Zhao Z, Pan HL, Eisenach JC and Paqueron X (2000) Norepinephrine release from spinal synaptosomes: auto-alpha2 -adrenergic receptor modulation. *Anesthesiology* **93**:164-172.

Littlewood NK, Todd AJ, Spike RC, Watt C and Shehab SA (1995) The types of neuron in spinal dorsal horn which possess neurokinin-1 receptors. *NSC* **66**:597-608.

Lucido AL, Morinville A, Gendron L, Stroh T and Beaudet A (2005) Prolonged morphine treatment selectively increases membrane recruitment of delta-opioid receptors in mouse basal ganglia. *Journal of molecular neuroscience : MN* **25**:207-214.

MacMillan LB, Hein L, Smith MS, Piascik MT and Limbird LE (1996) Central hypotensive effects of the alpha2a-adrenergic receptor subtype. *Science (New York, NY)* **273**:801-803.

MacMillan LB, Lakhlani P, Lovinger D and Limbird LE (1998) Alpha 2-adrenergic receptor subtypes: subtle mutation of the alpha 2A-adrenergic receptor in vivo by gene targeting strategies reveals the role of this subtype in multiple physiological settings. *Recent progress in hormone research* **53**:25-42.

Majumdar S, Grinnell S, Le Rouzic V, Burgman M, Polikar L, Ansonoff M, Pintar J, Pan Y-X and Pasternak GW (2011) Truncated G protein-coupled mu opioid receptor MOR-1 splice variants are targets for highly potent opioid analgesics lacking side effects. *Proceedings of the National Academy of Sciences* **108**:19778-19783.

Malmberg AB, Hedley LR, Jasper JR, Hunter JC and Basbaum AI (2001) Contribution of alpha(2) receptor subtypes to nerve injury-induced pain and its regulation by dexmedetomidine. *British Journal of Pharmacology* **132**:1827-1836.

Mansour A, Fox CA, Burke S, Meng F, Thompson RC, Akil H and Watson SJ (1994a) Mu, delta, and kappa opioid receptor mRNA expression in the rat CNS: an in situ hybridization study. *The Journal of comparative neurology* **350**:412-438.

Mansour A, Fox CA, Thompson RC, Akil H and Watson SJ (1994b) mu-Opioid receptor mRNA expression in the rat CNS: comparison to mu-receptor binding. *Brain research* **643**:245-265.

Marchand S (2008) The physiology of pain mechanisms: from the periphery to the brain. *Rheumatic diseases clinics of North America* **34**:285-309.

Matthes HW, Maldonado R, Simonin F, Valverde O, Slowe S, Kitchen I, Befort K, Dierich A, Le Meur M, Dollé P, Tzavara E, Hanoune J, Roques BP and Kieffer BL (1996) Loss of morphine-induced analgesia, reward effect and withdrawal symptoms in mice lacking the mu-opioid-receptor gene. *Nature* **383**:819-823.

Medicine Io (2011) *Relieving Pain in America: A Blueprint for Transforming Prevention, Care Education, and Research*. The National Academies Press, Washington, DC.

Mennicken F, Zhang J, Hoffert C, Ahmad S, Beaudet A and O'Donnell D (2003) Phylogenetic changes in the expression of delta opioid receptors in spinal cord and dorsal root ganglia. *The Journal of comparative neurology* **465**:349-360.

Mika J, Przewłocki R and Przewłocka B (2001) The role of delta-opioid receptor subtypes in neuropathic pain. *European journal of pharmacology* **415**:31-37.

Milne B, Sutak M, Cahill CM and Jhamandas K (2008) Low doses of alpha 2-adrenoceptor antagonists augment spinal morphine analgesia and inhibit development of acute and chronic tolerance. *British Journal of Pharmacology* **155**:1264-1278.

Minami M, Maekawa K, Yabuuchi K and Satoh M (1995) Double in situ hybridization study on coexistence of mu-, delta- and kappa-opioid receptor mRNAs with preprotachykinin A mRNA in the rat dorsal root ganglia. *Brain research Molecular brain research* **30**:203-210.

Molliver DC, Wright DE, Leitner ML, Parsadanian AS, Doster K, Wen D, Yan Q and Snider WD (1997) IB4-binding DRG neurons switch from NGF to GDNF dependence in early postnatal life. *Neuron* **19**:849-861.

Monasky MS, Zinsmeister AR, Stevens CW and Yaksh TL (1990) Interaction of intrathecal morphine and ST-91 on antinociception in the rat: dose-response analysis, antagonism and clearance. *The Journal of Pharmacology and Experimental Therapeutics* **254**:383-392.

Morales L, Perez-Garcia C and Alguacil LF (2001) Effects of yohimbine on the antinociceptive and place conditioning effects of opioid agonists in rodents. *British Journal of Pharmacology* **133**:172-178.

Morinville A, Cahill CM, Esdaile MJ, Aibak H, Collier B, Kieffer BL and Beaudet A (2003) Regulation of delta-opioid receptor trafficking via mu-opioid receptor stimulation: evidence from mu-opioid receptor knock-out mice. *The Journal of neuroscience : the official journal of the Society for Neuroscience* **23**:4888-4898.

Nag S and Mokha SS (2006) Activation of alpha2-adrenoceptors in the trigeminal region produces sex-specific modulation of nociception in the rat. *NSC* **142**:1255-1262.

Nagasaka H and Yaksh TL (1990) Pharmacology of intrathecal adrenergic agonists: cardiovascular and nociceptive reflexes in halothane-anesthetized rats. *Anesthesiology* **73**:1198-1207.

Nicholas AP, Pieribone V and Hökfelt T (1993) Distributions of mRNAs for alpha-2 adrenergic receptor subtypes in rat brain: an in situ hybridization study. *The Journal of comparative neurology* **328**:575-594.

Normandin A, Luccarini P, Molat JL, Gendron L and Dallel R (2013) Spinal μ and δ Opioids Inhibit Both Thermal and Mechanical Pain in Rats. *The Journal of neuroscience : the official journal of the Society for Neuroscience* **33**:11703-11714.

Nozaki C, Le Bourdonnec B, Reiss D, Windh RT, Little PJ, Dolle RE, Kieffer BL and Gavériaux-Ruff C (2012) δ-Opioid mechanisms for ADL5747 and ADL5859 effects in mice: analgesia, locomotion, and receptor internalization. *Journal of Pharmacology and Experimental Therapeutics* **342**:799-807.

Obata H, Li X and Eisenach JC (2004) Spinal adenosine receptor activation reduces hypersensitivity after surgery by a different mechanism than after nerve injury. *Anesthesiology* **100**:1258-1262.

Ossipov MH, Harris S, Lloyd P and Messineo E (1990a) An isobolographic analysis of the antinociceptive effect of systemically and intrathecally administered combinations of clonidine and opiates. *The Journal of Pharmacology and Experimental Therapeutics* **255**:1107-1116.

Ossipov MH, Lopez Y, Bian D, Nichols ML and Porreca F (1997) Synergistic antinociceptive interactions of morphine and clonidine in rats with nerve-ligation injury. *Anesthesiology* **86**:196-204.

Ossipov MH, Lopez Y, Nichols ML, Bian D and Porreca F (1995) Inhibition by spinal morphine of the tail-flick response is attenuated in rats with nerve ligation injury. *Neuroscience letters* **199**:83-86.

Ossipov MH, Lozito R, Messineo E, Green J, Harris S and Lloyd P (1990b) Spinal antinociceptive synergy between clonidine and morphine, U69593, and DPDPE: isobolographic analysis. *Life sciences* **47**:PL71-76.

Overland AC, Kitto KF, Chabot-Doré A-J, Rothwell PE, Fairbanks CA, Stone LS and Wilcox GL (2009) Protein kinase C mediates the synergistic interaction between agonists acting at alpha2-adrenergic and delta-opioid receptors in spinal cord. *The Journal of neuroscience : the official journal of the Society for Neuroscience* **29**:13264-13273.

Ozdogan UK, Lähdesmäki J, Hakala K and Scheinin M (2004) The involvement of alpha 2A-adrenoceptors in morphine analgesia, tolerance and withdrawal in mice. *European journal of pharmacology* **497**:161-171.

Ozdogan UK, Lähdesmäki J and Scheinin M (2006) The analgesic efficacy of partial opioid agonists is increased in mice with targeted inactivation of the alpha2A-adrenoceptor gene. *European journal of pharmacology* **529**:105-113.

Pappas B, Ings R and Roberts D (1982) Neonatal intraspinal 6-hydroxydopamine, 5,7-dihydroxytryptamine or their combination: effects on nociception and morphine analgesia. *European journal of pharmacology* **86**:157-166.

Pertovaara A (2006) Noradrenergic pain modulation. *Progress in Neurobiology* **80**:53-83.

Peterhoff M, Sieg A, Brede M, Chao C-M, Hein L and Ullrich S (2003) Inhibition of insulin secretion via distinct signaling pathways in alpha2-adrenoceptor knockout mice. *European journal of endocrinology / European Federation of Endocrine Societies* **149**:343-350.

Pick CG, Paul D and Pasternak GW (1991) Comparison of naloxonazine and beta-funaltrexamine antagonism of mu 1 and mu 2 opioid actions. *Life sciences* **48**:2005-2011.

Post C, Persson ML, Archer T, Minor BG, Danysz W and Sundström E (1987) Increased antinociception by alpha-adrenoceptor drugs after spinal cord noradrenaline depletion. *European journal of pharmacology* **137**:107-116.

Pradhan AA, Befort K, Nozaki C, Gavériaux-Ruff C and Kieffer BL (2011) The delta opioid receptor: an evolving target for the treatment of brain disorders. *Trends in pharmacological sciences* **32**:581-590.

Price TJ and Flores CM (2007) Critical Evaluation of the Colocalization Between Calcitonin Gene-Related Peptide, Substance P, Transient Receptor Potential Vanilloid Subfamily Type 1 Immunoreactivities, and Isolectin B4 Binding in Primary Afferent Neurons of the Rat and Mouse. *The Journal of Pain* **8**:263-272.

Przedborski S and Ischiropoulos H (2005) Reactive oxygen and nitrogen species: weapons of neuronal destruction in models of Parkinson's disease. *Antioxidants & redox signaling* **7**:685-693.

Przesmycki K, Dzieciuch JA, Czuczwar SJ and Kleinrok Z (1997) Isobolographic analysis of interaction between intrathecal morphine and clonidine in the formalin test in rats. *European journal of pharmacology* **337**:11-17.

Raynor K, Kong H, Chen Y, Yasuda K, Yu L, Bell GI and Reisine T (1994) Pharmacological characterization of the cloned kappa-, delta-, and mu-opioid receptors. *Molecular Pharmacology* **45**:330-334.

Rexed B (1952) The cytoarchitectonic organization of the spinal cord in the cat. *The Journal of comparative neurology* **96**:414-495.

Riedl MS, Schnell SA, Overland AC, Chabot-Doré A-J, Taylor AM, Ribeiro-da-Silva A, Elde RP, Wilcox GL and Stone LS (2009) Coexpression of alpha 2A-adrenergic and delta-opioid receptors in substance P-containing terminals in rat dorsal horn. *The Journal of comparative neurology* **513**:385-398.

Rios C, Gomes I and Devi LA (2004) Interactions between delta opioid receptors and alpha-adrenoceptors. *Clinical and experimental pharmacology & physiology* **31**:833-836.

Roerig SC (1995) Decreased spinal morphine/clonidine antinociceptive synergism in morphine-tolerant mice. *Life sciences* **56**:PL115-122.

Roerig SC and Howse KM (1996) Omega-agatoxin IVA blocks spinal morphine/clonidine antinociceptive synergism. *European journal of pharmacology* **314**:293-300.

Roerig SC, Lei S, Kitto K, Hylden JK and Wilcox GL (1992) Spinal interactions between opioid and noradrenergic agonists in mice: multiplicativity involves delta and alpha-2 receptors. *The Journal of Pharmacology and Experimental Therapeutics* **262**:365-374.

Rosin DL, Zeng D, Stornetta RL, Norton FR, Riley T, Okusa MD, Guyenet PG and Lynch KR (1993) Immunohistochemical localization of alpha 2A-adrenergic receptors in catecholaminergic and other brainstem neurons in the rat. *NSC* **56**:139-155.

Roudet C, Mouchet P, Feuerstein C and Savasta M (1994) Normal distribution of alpha 2-adrenoceptors in the rat spinal cord and its modification after noradrenergic denervation: a quantitative autoradiographic study. *Journal of neuroscience research* **39**:319-329.

Ruan X (2007) Drug-related side effects of long-term intrathecal morphine therapy. *Pain physician* **10**:357-366.

Russell IJ (1998) Advances in fibromyalgia: possible role for central neurochemicals. *The American journal of the medical sciences* **315**:377-384.

Russell IJ, Kamin M, Bennett RM, Schnitzer TJ, Green JA and Katz WA (2000) Efficacy of tramadol in treatment of pain in fibromyalgia. *Journal of*

clinical rheumatology : practical reports on rheumatic & musculoskeletal diseases **6**:250-257.

Russell IJ, Vaeroy H, Javors M and Nyberg F (1992) Cerebrospinal fluid biogenic amine metabolites in fibromyalgia/fibrositis syndrome and rheumatoid arthritis. *Arthritis and rheumatism* **35**:550-556.

Sagen J and Proudfit HK (1984) Effect of intrathecally administered noradrenergic antagonists on nociception in the rat. *Brain research* **310**:295-301.

Sawynok J, Reid A and Nance D (1991) Spinal antinociception by adenosine analogs and morphine after intrathecal administration of the neurotoxins capsaicin, 6-hydroxydopamine and 5,7-dihydroxytryptamine. *The Journal of Pharmacology and Experimental Therapeutics* **258**:370-380.

Scherrer G, Befort K, Contet C, Becker J, Matifas A and Kieffer BL (2004) The delta agonists DPDPE and deltorphin II recruit predominantly mu receptors to produce thermal analgesia: a parallel study of mu, delta and combinatorial opioid receptor knockout mice. *The European journal of neuroscience* **19**:2239-2248.

Scherrer G, Imamachi N, Cao Y-Q, Contet C, Mennicken F, O'Donnell D, Kieffer BL and Basbaum AI (2009) Dissociation of the opioid receptor mechanisms that control mechanical and heat pain. *Cell* **137**:1148-1159.

Scherrer G, Tryoen-Tóth P, Filliol D, Matifas A, Laustriat D, Cao YQ, Basbaum AI, Dierich A, Vonesh J-L, Gavériaux-Ruff C and Kieffer BL (2006) Knockin mice expressing fluorescent delta-opioid receptors uncover G protein-coupled receptor dynamics in vivo. *Proceedings of the National Academy of Sciences of the United States of America* **103**:9691-9696.

Shi TJ, Winzer-Serhan U, Leslie F and Hökfelt T (1999) Distribution of alpha2-adrenoceptor mRNAs in the rat lumbar spinal cord in normal and axotomized rats. *Neuroreport* **10**:2835-2839.

Shi TS, Winzer-Serhan U, Leslie F and Hökfelt T (2000) Distribution and regulation of alpha(2)-adrenoceptors in rat dorsal root ganglia. *Pain* **84**:319-330.

Smith HS, Deer TR, Staats PS, Singh V, Sehgal N and Cordner H (2008) Intrathecal drug delivery. *Pain physician* **11**:S89-S104.

Stevens CW and Seybold VS (1995) Changes of opioid binding density in the rat spinal cord following unilateral dorsal rhizotomy. *Brain research* **687**:53-62.

Stewart PE and Hammond DL (1994) Activation of spinal delta-1 or delta-2 opioid receptors reduces carrageenan-induced hyperalgesia in the rat. *The Journal of Pharmacology and Experimental Therapeutics* **268**:701-708.

Stone LS, Broberger C, Vulchanova L, Wilcox GL, Hökfelt T, Riedl MS and Elde R (1998) Differential distribution of alpha2A and alpha2C adrenergic receptor immunoreactivity in the rat spinal cord. *The Journal of neuroscience : the official journal of the Society for Neuroscience* **18**:5928-5937.

Stone LS, Kitto KF, Eisenach JC, Fairbanks CA and Wilcox GL (2007) ST91 [2-(2,6-diethylphenylamino)-2-imidazoline hydrochloride]-mediated spinal antinociception and synergy with opioids persists in the absence of functional alpha-2A- or alpha-2C-adrenergic receptors. *The Journal of Pharmacology and Experimental Therapeutics* **323**:899-906.

Stone LS, MacMillan LB, Kitto KF, Limbird LE and Wilcox GL (1997) The alpha2a adrenergic receptor subtype mediates spinal analgesia evoked by alpha2 agonists and is necessary for spinal adrenergic-opioid synergy. *The Journal of neuroscience : the official journal of the Society for Neuroscience* **17**:7157-7165.

Stone LS, Vulchanova L, Riedl MS, Wang J, Williams FG, Wilcox GL and Elde R (1999) Effects of peripheral nerve injury on alpha-2A and alpha-2C adrenergic receptor immunoreactivity in the rat spinal cord. *Neuroscience* **93**:1399-1407.

Sullivan AF, Dashwood MR and Dickenson AH (1987) Alpha 2-adrenoceptor modulation of nociception in rat spinal cord: location, effects and interactions with morphine. *European journal of pharmacology* **138**:169-177.

Surprenant A, Horstman DA, Akbarali H and Limbird LE (1992) A point mutation of the alpha 2-adrenoceptor that blocks coupling to potassium but not calcium currents. *Science (New York, NY)* **257**:977-980.

Tajerian M, Millecamps M and Stone LS (2012) Morphine and clonidine synergize to ameliorate low back pain in mice. *Pain research and treatment* **2012**:150842.

Tallarida RJ (1992) Statistical analysis of drug combinations for synergism. *Pain* **49**:93-97.

Tallarida RJ (2006) An overview of drug combination analysis with isobolograms. *The Journal of Pharmacology and Experimental Therapeutics* **319**:1-7.

Tallarida RJ and Murray RB (1987) Tallarida and Murray (1987) Manual of pharmacologic calculations with computer programs.

Tan M, Walwyn WM, Evans CJ and Xie C-W (2009) p38 MAPK and beta-arrestin 2 mediate functional interactions between endogenous micro-opioid and alpha2A-adrenergic receptors in neurons. *The Journal of biological chemistry* **284**:6270-6281.

Terrillon S and Bouvier M (2004) Roles of G-protein-coupled receptor dimerization. *EMBO reports* **5**:30-34.

Thompson AD, Angelotti T, Nag S and Mokha SS (2008) Sex-specific modulation of spinal nociception by alpha2-adrenoceptors: differential regulation by estrogen and testosterone. *NSC* **153**:1268-1277.

Todd AJ (2010) Neuronal circuitry for pain processing in the dorsal horn. *Nature Reviews Neuroscience* **11**:823-836.

Unruh AM (1996) Gender variations in clinical pain experience. *Pain* **65**:123-167.

van Rijn RM, Brissett DI and Whistler JL (2012) Emergence of Functional Spinal Delta Opioid Receptors After Chronic Ethanol Exposure. *BPS* **71**:232-238.

Vilardaga J-P, Nikolaev VO, Lorenz K, Ferrandon S, Zhuang Z and Lohse MJ (2008) Conformational cross-talk between alpha2A-adrenergic and mu-opioid receptors controls cell signaling. *Nature chemical biology* **4**:126-131.

Walker SM, Goudas LC, Cousins MJ and Carr DB (2002) Combination spinal analgesic chemotherapy: a systematic review. *Anesthesia & Analgesia* **95**:674-715.

Wall PD, Melzack R, McMahon SB and Koltzenburg M (2006) *Textbook of Pain*. Churchill Livingstone.

Walwyn W, John S, Maga M, Evans CJ and Hales TG (2009) Delta receptors are required for full inhibitory coupling of mu-receptors to voltage-dependent Ca(2+) channels in dorsal root ganglion neurons. *Molecular Pharmacology* **76**:134-143.

Wang H-B, Zhao B, Zhong Y-Q, Li K-C, Li Z-Y, Wang Q, Lu Y-J, Zhang Z-N, He S-Q, Zheng H-C, Wu S-X, Hökfelt TGM, Bao L and Zhang X (2010) Coexpression of delta- and mu-opioid receptors in nociceptive sensory neurons. *Proceedings of the National Academy of Sciences* **107**:13117-13122.

Watkins LR, Hutchinson MR, Rice KC and Maier SF (2009) The "toll" of opioid-induced glial activation: improving the clinical

efficacy of opioids by targeting glia. *Trends in pharmacological sciences* **30**:581-591.

Wei ZY, Karim F and Roerig SC (1996) Spinal morphine/clonidine antinociceptive synergism: involvement of G proteins and N-type voltage-dependent calcium channels. *The Journal of Pharmacology and Experimental Therapeutics* **278**:1392-1407.

Wei ZY and Roerig SC (1998) Spinal morphine/clonidine antinociceptive synergism is regulated by protein kinase C, but not protein kinase A activity. *The Journal of Pharmacology and Experimental Therapeutics* **287**:937-943.

Williams JT, Ingram SL, Henderson G, Chavkin C, von Zastrow M, Schulz S, Koch T, Evans CJ and Christie MJ (2013) Regulation of μ-Opioid Receptors: Desensitization, Phosphorylation, Internalization, and Tolerance. *Pharmacological Reviews* **65**:223-254.

Yasuoka S and Yaksh TL (1983) Effects on nociceptive threshold and blood pressure of intrathecally administered morphine and alpha-adrenergic agonists. *Neuropharmacology* **22**:309-315.

Yekkirala AS, Kalyuzhny AE and Portoghese PS (2010) Standard Opioid Agonists Activate Heteromeric Opioid Receptors: Evidence for Morphine and [d-Ala 2-MePhe 4-Glyol 5]Enkephalin as Selective μ−δ Agonists. *ACS Chemical Neuroscience* **1**:146-154.

Yeomans DC and Proudfit HK (1996) Nociceptive responses to high and low rates of noxious cutaneous heating are mediated by different nociceptors in the rat: electrophysiological evidence. *Pain* **68**:141-150.

Yu VC, Richards ML and Sadée W (1986) A human neuroblastoma cell line expresses mu and delta opioid receptor sites. *The Journal of biological chemistry* **261**:1065-1070.

Zajac JM, Lombard MC, Peschanski M, Besson JM and Roques BP (1989) Autoradiographic study of mu and delta opioid binding sites and neutral endopeptidase-24.11 in rat after dorsal root rhizotomy. *Brain research* **477**:400-403.

Zhang X, Bao L, Arvidsson U, Elde R and Hökfelt T (1998) Localization and regulation of the delta-opioid receptor in dorsal root ganglia and spinal cord of the rat and monkey: evidence for association with the membrane of large dense-core vesicles. *Neuroscience* **82**:1225-1242.

Zhang YQ and Limbird LE (2004) Hetero-oligomers of alpha2A-adrenergic and mu-opioid receptors do not lead to transactivation of G-proteins or altered endocytosis profiles. *Biochemical Society transactions* **32**:856-860.

Zhong FX, Ji XQ and Tsou K (1985) Intrathecal DSP4 selectively depletes spinal noradrenaline and attenuates morphine analgesia. *European journal of pharmacology* **116**:327-330.

Zhu Y, King MA, Schuller AG, Nitsche JF, Reidl M, Elde RP, Unterwald E, Pasternak GW and Pintar JE (1999) Retention of supraspinal delta-like analgesia and loss of morphine tolerance in delta opioid receptor knockout mice. *Neuron* **24**:243-252.

Appendix A:
Research Compliance Certificates

McGill

University Animal Care Committee
Animal Compliance Office
McGill University
1555 peel Street, 11th Floor
www.mcgill.ca/researchoffice/compliance/animal
Montreal Quebec, Canada H3A 3L8

Comité universitaire de protection des animaux
Éthique Animale
Université McGill
1555 rue Peel, 11ième étage

Montréal, Québec, Canada H3A 3L8

Tel : (514) 398-2639
Fax: (514) 398-4644

May 10th, 2010

The McGill University Animal Care Committee certifies that

Anne-Julie Chabot-Doré

has successfully completed the
Advanced Level
of the
Theory Training Course on Animal Use for Research and Teaching
on ***May 3rd, 2010.***

The training includes the following topics:

- **Basic Level:** Regulations & Procedures, Ethics, Basic Animal Care, Occupational Health & Safety
- **Advanced Level:** Anesthesia, Analgesia, Euthanasia, Categories, Influencing Factors, and Environmental Enrichment

Please note that this certificate does NOT include practical training, which is obtained by successfully completing an Animal Methodology Workshop where another certificate is issued.

Certification is valid for 5 years, starting on the date indicated above.

Jennifer Henri
Animal Care Training Coordinator, animalcare@mcgill.ca

(Confirmation of training can be obtained by request to the above email address)

Note: Trainee should keep this certificate as other institutions may request it as evidence of training

McGill University
Environmental Health and Safety

THIS IS TO CERTIFY THAT

Anne-Julie Chabot-Dore

Faculty of Dentistry

SUCCESSFULLY COMPLETED CORE TRAINING IN

Workplace Hazardous Materials Information System (W.H.M.I.S.)

ON

Wednesday, January 23, 2013

Joseph Vincelli
EHS Operations Manager

Wayne Wood
Associate Director, EHS

Valid Until Saturday, January 23, 2016

McGill University
Environmental Health and Safety

Room 426, McTavish 3610 Montreal, Quebec H3A 1Y2

THIS IS TO CERTIFY THAT

Anne-Julie Chabot-Dore

Please sign above

Faculty of Dentistry

SUCCESSFULLY COMPLETED CORE TRAINING IN

Principles of Laboratory Radiation Safety (Refresher)

including Transportation of Dangerous Goods Act Regulations (Class 7) for opening and handling Type A packages

ON

Friday, August 20, 2010

Joseph Vincelli
EHS Operations Manager

Mario Badillo
EHS Radiation Safety Officer

Wayne Wood
Associate Director, EHS

Valid Until Monday, August 19, 2013

McGill Internal Radioisotope Permit

R-00326 2013

Permit Holder	Building (Office)		Building (Main Lab)			Emergency Phone No.:	Date Issued
Dr Laura Stone	**PENFIELD 740**		**PENFIELD 740**			**Downtown Campus: 3000**	**2009-09-01**
Department	Room Number(s)	Telephone	Room Number(s)	Telephone	Permit Classification	**Macdonald Campus: 7777**	Expiry Date
Dentistry	**3200**	**514.398.7203**	**3203**	**(514)398-7203**	**Basic**		**2013-08-31**

PERSONS APPROVED TO WORK WITH RADIOISOTOPES

Name	Train	Condition(s)	Class(es)	Radioisotope(s)
Chabot-Doré, Anne-Julie, PhD.Stud.	Y	2,4	3	H-3, S-35
Danco, Alexander Teneyck, GrdS	N	6	6	
Ferland-Legault, Catherine Estelle, PDF	N	6	6	
Millecamps, Magali	N	6	6	
Naso, Lina	N	6	6	
Stone, Laura, PI	N	6	6	
Tabatabaei Shafiei, Zahra Sadat, GrdS	N	6	6	
Tajerian, Maral Minas	N	6	6	

LAB CLASSIFICATIONS

Bldg	Lab	Classification
239	3200	N/A
239	3203	Basic

Building Codes

Code	Building Name
239	PENFIELD 740

GENERAL LICENCE CONDITIONS (OPEN AND/OR SEALED SOURCES)

- The permit must be posted with CNSC safety poster in the permit holder's premises
- Radioisotope handling shall be in accordance with the McGill Radiation Safety Policy Manual.
- The permit holder must ensure that all persons mandated to work with radioisotopes be properly trained in radiation safety prior to start of work.
- Radioactive work areas must be clearly identified with radiation warning signs.
- Smoking, eating, drinking, storage of foods or drink and the application of cosmetics and contact lenses are prohibited in areas where radioisotopes are used.
- All procedures involving radioactive materials should be carried out on spill trays or on benches lined with disposable absorbent material.
- Procedures that might produce airborne radioactive contamination should be carried out in a functioning fume hood.
- When hand or clothing contamination is possible, protective gloves and clothing must be worn.
- After handling radioactive material and especially before leaving the laboratory, personnel must ensure that all parts of their clothing are not contaminated.
- Purchase and disposal of radioisotopes must be kept electronically and documented in a log book. For disposal of radioactive waste, consult the McGill Radiation Safety Policy Manual and/or contact Hazardous Waste Management (HWM) at 514-398-5066.
- Wipe tests must be performed and records kept in a log book.
- The permit must reflect the exact conditions under which radioisotope material is used. If changes must be made, contact the RSO at 398-2245.
- The device(s) containing the sealed source(s) must have a radiation symbol and an identification label bearing the name and telephone number of the permit holder.
- Leak tests must be performed on sealed sources equal to or greater than 50 MBq (1.35mCi).
- Extremity dosimeter (i.e. ring or wrist badges) must be worn if 50 MBq or more of P-32, Sr-89, Sr-90 & Y-90 are used.
- Every person using I-125 or I-131 in an open room (2 MBq), in a fume hood (200 MBq) or in a glove box (20 GBq) must participate to thyroid monitoring session within 5 days of use.

APPROVED UNSEALED RADIOISOTOPE(S) AND LOCATION(S)

Isotope	Possession Limit	Ship Limit	Building	Stored	Handled
H-3	< 41 MBq (1.1 mCi)	1 mCi	239	3203	3203
S-35	< 10 MBq (0.27 mCi)	0.25 mCi	239	3203	3203

Personnel Conditions

1 Must attend thyroid bioassays within 5 days if I-125 or I-131 are manipulated in an open area (2 MBq or 54 µCi) and/or in a fume hood (200 MBq or 5.4 mCi)
2 Must wear a whole-body film badge, if gamma, x-ray or high energy beta emitters are used.
3 Must wear an extremity TLD dosimeter, if more than 50 MBq (1.35 mCi) of P-32, Sr-89, Sr-90 or Y-90 are used.
4 Classified as Radiation User.
5 Classified as Nuclear Energy Worker (NEW).
6 Does not work with any radioisotopes but may be indirectly exposed.

Workload Classes

1 Work load < 10MBq (270 uCi) of unsealed radioisotopes in open areas.
2 Work load < 10MBq (270 uCi) of unsealed radioisotopes in a fume hood.
3 Work load > 10MBq (270 uCi) of unsealed radioisotopes in open areas.
4 Work load > 10 MBq (270 uCi) of unsealed radioisotopes in a fume hood.
5 Work with sealed sources.
6 Individual does not work with radioactive sources but normal working conditions involve presence in a room where radioactive material is used or stored.

Mario Badillo

2012-08-13

Date (Latest Amendment)

Mario Badillo, Ph.D.
EHS Radiation Safety Officer
McGill Environmental Health & Safety Tel.: 514-398-2245

For: Wayne Wood, Chair (Interim)
McGill University Laboratory Safety Committee
Associate Director (Environmental Health and Safety)

Rev 20120403

Appendix B:
Publications

1521-0103/347/3/773–780$25.00
THE JOURNAL OF PHARMACOLOGY AND EXPERIMENTAL THERAPEUTICS

http://dx.doi.org/10.1124/jpet.113.206581
J Pharmacol Exp Ther 347:773–780, December 2013

The Delta-Opioid Receptor Is Sufficient, but Not Necessary, for Spinal Opioid-Adrenergic Analgesic Synergy

Anne-Julie Chabot-Doré, Magali Millecamps, and Laura S. Stone

Alan Edwards Centre for Research on Pain (A.-J.C.-D., M.M., L.S.S.), Integrated Program in Neuroscience (A.-J.C.-D.), McGill Scoliosis & Spine Research Group (M.M., L.S.S.), Faculty of Dentistry (M.M., L.S.S.), Departments of Anesthesiology (L.S.S.), Pharmacology & Therapeutics (L.S.S.), Neurology & Neurosurgery (A.-J.C.-D., L.S.S.), Faculty of Medicine (A.-J.C.-D., L.S.S.), McGill University, Montreal, Quebec, Canada

Received June 28, 2013; accepted September 13, 2013

ABSTRACT

Spinal administration of opioid and α_2-adrenergic receptor (α_2AR) agonists produces analgesia, and agonists interact synergistically when coadministered. The molecular mechanism underlying this synergy is largely unknown. Pharmacological studies have identified both the delta and the mu-opioid receptors (DOR and MOR) as candidate receptors capable of interacting synergistically with α_2AR agonists. However, recent studies attribute the antinociceptive effect of DOR agonists to actions at the MOR, calling the role of DOR in opioid-adrenergic synergy into question. Other studies suggesting that DOR is implicated in morphine antinociception raise the possibility that DOR is nonetheless required for morphine synergy with α_2AR agonists. This study aimed to determine whether DOR activation is sufficient and necessary to mediate opioid-adrenergic synergistic interactions in the spinal cord. The antinociceptive effects of clonidine, [D-Ala^2]-deltorphin II (DeltII), morphine, and [D-Ala^2, *N*-Me-Phe^4, Gly-ol^5]-enkephalin (DAMGO) were evaluated using the substance P (SP) behavioral assay in wild type (WT) and DOR-knockout (KO) mice. Opioid-adrenergic drug interactions were evaluated after spinal coadministration of clonidine with DeltII, morphine, or DAMGO. Isobolographic analyses of dose-response curves determined whether interactions were synergistic or additive. The absence of DeltII antinociceptive efficacy in DOR-KO confirmed its selectivity in the SP assay. Although DeltII+clonidine interacted synergistically in WT mice, no interaction with clonidine was observed in DOR-KO mice. Clonidine was synergistic with morphine in both mouse strains. DAMGO did not synergize with clonidine in either strain. These findings confirm that although other opioid receptors can interact synergistically with α_2AR agonists, DOR is sufficient for spinal opioid-adrenergic interactions.

Introduction

Patients with acute or chronic pain need better analgesic therapies to provide currently unmet pain relief. Opioid and α_2-adrenergic receptor (α_2AR) agonists are potent analgesic drugs, but their use is limited by their side effects or lack of efficacy in certain clinical conditions. Compared with the analgesic effects of drugs acting independently, analgesic synergy arising from drug combinations is advantageous because it produces adequate analgesia at lower doses, which can potentially reduce side effects and tolerance (Walker et al., 2002). Pain management using opioid-α_2AR agonist combinations reduces side effects associated with both α_2AR and opioid treatments (Eisenach et al., 1994), and such combinations may also be effective in treating chronic pain conditions with reduced opioid sensitivity (Eisenach et al., 1995). In rodents, the opioid agonist morphine and the α_2AR agonist clonidine synergize when coadministered at the spinal level, suggesting that beneficial opioid-adrenergic drug interactions occur at the spinal cord (Alguacil and Morales, 2004). The clinical benefits of opioid-adrenergic combinations remain largely underexploited because the development of new therapies taking advantage of the synergistic interaction is hindered, in part, by a lack of understanding of the underlying mechanism.

To gain mechanistic insight, it is necessary to know the receptor subtypes required for synergy. Opioid agonists can mediate their analgesic action at the spinal cord by activating the delta- (DOR), mu- (MOR), and kappa-opioid receptor subtypes. [D-Ala^2]-Deltorphin II (DeltII), a DOR-selective peptide agonist, can synergize with the α_2AR agonists clonidine (Overland et al., 2009), ST-91 [2-(2,6-diethylphenylamino)-2-imidazoline hydrochloride] (Stone et al., 2007),

This work was supported by Canadian Institutes for Health Research (CIHR) [Operating Grant MOP-86691], Bourse de chercheur-boursier from Fonds de Recherche en Santé du Québec (FRSQ), and Réseau de recherche en santé buccodentainre et osseuse (RSBO) infrastructure support (to L.S.S.). A.J.C.D. received studentship support from CIHR, the McGill University Integrated Program in Neuroscience (IPN), and the Louise and Alan Edwards Foundation and travel support from the Quebec Pain Research Network and the IPN.

This work was previously presented: Chabot-Doré A-J, Millecamps M, and Stone L (2012) Lack of opioid-adrenergic spinal analgesic synergy in d-opioid receptor knock-out mice (poster 882.22/DD15); *42nd Annual Meeting of the Society for Neuroscience*; 13–17 October 2012; New Orleans, LA.

dx.doi.org/10.1124/jpet.113.206581.

ABBREVIATIONS: α_2AR, α_2-adrenergic receptor; CI, confidence interval; DAMGO, [D-Ala^2, *N*-Me-Phe^4, Gly-ol^5]-enkephalin; DeltII, [D-Ala^2]-deltorphin II; DOR, delta-opioid receptor; DPDPE, [D-Pen^2,D-Pen^5]enkephalin; KO, knockout; MOR, mu-opioid receptor; *Oprd1*, mouse opioid receptor delta gene; SP, substance P; WT, wild type.

moxonidine (Fairbanks et al., 2000, 2002), and UK 14,304 (5-Bromo-6-(2-imidazolin-2-ylamino)quinoxaline) (Stone et al., 1997) when coadministered in rodents at the spinal cord. Similarly, another DOR-selective agonist, [D-Pen^2,D-Pen^5] enkephalin (DPDPE), has been shown to synergize with clonidine (Ossipov et al., 1990b; Roerig et al., 1992), norepinephrine (Roerig et al., 1992), and UK 14,304 (Guo et al., 2003), and this latter synergistic interaction persists in MOR-KO mice (Guo et al., 2003). Thus, opioid-adrenergic interactions resulting in analgesic synergy are possible when activating DOR and can occur in the absence of MOR. However, reports that DeltII and DPDPE retain their antinociceptive action in DOR-KO mice and that MOR mediates this effect questions the selectivity of DOR agonists (Scherrer et al., 2004; van Rijn et al., 2012). This could mean that opioid-adrenergic synergistic interactions studied with DOR agonists are mediated by MOR and therefore justify further evaluation of the role of DOR in these interactions.

Morphine has been shown to interact synergistically with the α_2AR agonists clonidine (Ossipov et al., 1990a; Roerig et al., 1992; Fairbanks and Wilcox, 1999b), moxonidine (Fairbanks et al., 2000), norepinephrine (Roerig et al., 1992), and ST-91 (Monasky et al., 1990). The antinociceptive effect of morphine is considered to be MOR mediated (Matthes et al., 1996), which is consistent with its relative selective affinity for MOR in expression systems (Raynor et al., 1994). Taken together, these studies would suggest that MOR mediates morphine's synergistic interactions with α_2AR agonists. However, interactions between MOR and DOR have been shown to modulate morphine response in vivo and in vitro (Costantino et al., 2012). For example, the cellular response after morphine treatment is more potent in cells coexpressing MOR and DOR rather than MOR alone (Yekkirala et al., 2010). Furthermore, DOR-selective ligands potentiate morphine analgesia in vivo (Gomes et al., 2004), and DOR is involved in the development of analgesic tolerance to morphine (Zhu et al., 1999). Morphine also upregulates the expression of surface DOR through its action at the MOR (Cahill et al., 2001; Morinville et al., 2003; Gendron et al., 2006). It is currently unknown whether DOR participates in morphine's synergistic interaction with α_2AR agonists.

The aim of this study was to disambiguate the role of DOR in the synergistic interaction between opioid and α_2AR agonists administered spinally. Therefore, we determined whether DOR activation is sufficient to produce synergy and whether DOR modulates MOR-mediated synergistic interactions with clonidine, the only α_2AR agonist approved for epidural analgesic use. The antinociceptive interaction between clonidine and DeltII, morphine, or the MOR-specific agonist DAMGO was compared between wild-type (WT) and DOR-KO mice, which have a genetic deletion in the *Oprd1* gene (Filliol et al., 2000). We observed that the synergistic interaction between DeltII and clonidine required DOR. In contrast, the interaction between morphine and clonidine remained synergistic in DOR-KO mice, and DAMGO failed to synergize with clonidine in either strain. Our results demonstrate that DOR is sufficient, but not necessary, to mediate opioid-α_2 adrenergic analgesic synergy at the spinal cord.

Materials and Methods

Animals. Mice with a targeted gene deletion introducing a genetic deletion in exon 1 of the delta-opioid receptor gene (*Oprd1*) were developed on a mixed C57Bl/6×FVB/129 background (Filliol et al., 2000). Congenic mice backcrossed to a standard C57Bl/6 background were obtained from The Jackson Laboratory (B6.129S2-*Oprd1*^{tm1Kff}/J, stock #007557; Bar Harbor, ME). Mice with a targeted gene deletion introducing a premature stop codon in the third transmembrane domain of the α_{2A}AR gene (*Adra2a*) were developed on a mixed C57Bl/6×FVB/129 background (Altman et al., 1999). Congenic mice backcrossed to a standard C57Bl/6 background were obtained from The Jackson Laboratory (stock #004367). Commercially available C57BL/6 mice (Charles River Laboratories, Quebec, Canada) were purchased and used as wild type (WT). All strains were bred in house, and genotyping controls were performed on parent breeders to monitor the stability of the colony.

Mice were maintained on a regular 12-hour light/dark cycle and given access to food and water ad libitum. Aged-matched 3- to 6-month-old WT, DOR-KO, and α_{2A}AR-KO males were used in this study, and experimenters were blind to both genotype and treatment. All procedures were approved by the Animal Care Committee at McGill University and conformed to the ethical guidelines of the Canadian Council on Animal Care.

Drugs. Substance P (SP; Arg-Pro-Lys-Pro-Gln-Gln-Phe-Phe-Gly-Leu-Met-NH_2) was purchased from AnaSpec (Fremont, CA), and concentrated stocks were dissolved in acidified saline (0.9% NaCl, 0.05 M acetic acid). Morphine sulfate (Medisca Pharmaceuticals, Montreal, QC, Canada) was dissolved in saline. [D-Ala^2, NMe-Phe^4, Gly-ol^5]-Enkephalin (DAMGO) and clonidine HCl [*N*-(2,6-dichlorophenyl)-4,5-dihydro-1*H*-imidazol-2-amine; R&D Systems, Minneapolis, MN] were dissolved in saline. [D-Ala^2]-deltorphin II (DeltII; R&D Systems) was dissolved in acidified saline. Drug stocks were diluted in saline to working concentrations.

Pharmacological Treatment. Intrathecal drug administration was done by direct lumbar puncture in a volume of 5 μl according to the method of Hylden and Wilcox (1980) in conscious mice. DeltII, morphine, DAMGO, and clonidine doses are expressed as total nanomoles or picomoles, and drug combination doses are graphed as total drug doses (i.e., the sum of both drugs) in 5 μl and expressed in nanomoles. Drugs were administered simultaneously with 15 ng of SP in a single 5-μl volume. After randomization, each mouse was reused with a minimum of 5 days between testing session to allow for drug wash out.

SP Behavioral Assay. The antinociceptive action of single drugs and their combination was tested in the substance P (SP) behavioral assay developed by Hylden and Wilcox (1981). In brief, 15 ng of SP was administered intrathecally alone (control) or coadministered with a single drug or a drug combination in a volume of 5 μl. The number of caudally directed biting, licking, and scratching behaviors were counted for 1 minute and results are expressed as the percent inhibition of SP-induced behaviors.

$$\%\ \text{Inhibition} = \frac{\text{Control} - \text{Experimental}}{\text{Control}} \times 100$$

Dose-Response Analysis. Dose-response graphs were generated with GraphPad Prism 6.0 (GraphPad Software, Inc., La Jolla, CA). A minimum of five animals was used per dose, and each dose point is expressed as the mean percent inhibition with S.E.M. For drug combinations, the dose-response curve was graphed according to the dose of clonidine present in the mixture. Drugs had to reach at least 50% inhibition to be considered effective. ED_{50} values and 95% confidence intervals (CI) were calculated using a minimum of three doses in the linear portion of each dose-response curve following the method of Tallarida and Murray (1987). Statistical comparisons of potencies based on the confidence limits of the ED_{50} values were calculated to obtain the relative potency ratio between two drugs.

Isobolographic Analysis. Drug combination ratios were chosen according to the relative potency of each drug by determining an approximately equally effective potency ratio between the agonists based on their respective ED_{50} values. When two drugs were equally potent, they were mixed in a 1:1 (i.e., equieffective and equimolar) ratio. If a drug was 10 times more potent than the other, drugs were

mixed in a 1:10 (i.e., equieffective) ratio. Because the relative drug potency of the drug pairs used in this study differed between WT and DOR-KO mice, different drug ratios were tested in each strain, and the experimental ED_{50} value for the drug combination was determined. To test for interactions between agonists, the ED_{50} values and S.E.M. of all dose-response curves were arithmetically arranged around the ED_{50} value using equation [ln(10) × ED_{50}] × (S.E. of log ED_{50}) (Tallarida, 1992). This manipulation was required to perform an isobolographic analysis, the appropriate method to evaluate if an interaction is synergistic, additive, or subadditive (Tallarida, 1992). When testing an interaction between two drugs, a theoretical additive ED_{50} value is calculated for the combination based on the dose-response curve of each drug administered separately. This theoretical value is then compared by a Student's t test with the observed experimental ED_{50} value of the combination. An interaction is considered synergistic if the experimental ED_{50} is significantly less ($P < 0.05$) than the calculated theoretical additive ED_{50}.

Visualization of drug interactions can be facilitated by graphical representation of isobolographic analysis. This representation depicts the ED_{50} value of each drug as the x- or y-intercept. The line connecting these two points depicts the dose combination expected to yield 50% efficacy if the interaction is purely additive and is called the theoretical additive line. The theoretical additive ED_{50} is determined mathematically and plotted on this line with its CI spanning perpendicularly from the line. The experimental ED_{50} for the combination is plotted at the corresponding x,y coordinates along with its 95% confidence interval for comparison with the theoretical additive ED_{50} value.

All dose-response and isobolographic analyses were performed with the FlashCalc 4.5.3 pharmacological statistics software package generously supplied by Dr. Michael Ossipov.

Results

Comparable SP-Evoked Nocifensive Behaviors Are Measured in WT and DOR-KO Mice. We used the SP behavioral assay to measure the antinociceptive effect of opioid agonists and clonidine at the spinal level. Intrathecal administration of SP induces a characteristic set of behaviors (biting, licking, and scratching) directed at the abdomen and hind portion of the mouse receiving the exogenous SP (Hylden and Wilcox, 1981). Analgesic drugs acting at the spinal cord inhibit these nocifensive behaviors in a dose-dependent manner. There was no significant difference in SP-induced behaviors between WT (37 ± 4, n = 13), DOR-KO (34 ± 3, n = 22), and α_{2A}AR-KO (29 ± 3, n = 18) mice (unpaired one-way ANOVA, $P > 0.05$) upon intrathecal injection of 15 ng SP. Thus, there is no strain difference in sensitivity to SP nociception.

Antinociceptive Action of Spinally Administered DeltII, DAMGO, Morphine, and Clonidine in WT, DOR-KO, and α_{2A}AR-KO Mice. DeltII, morphine, DAMGO, and clonidine were administered intrathecally in both WT and DOR-KO mice. All drugs inhibited SP-induced nocifensive behaviors in a dose-dependent manner (Fig. 1; Table 1), except for DeltII, which was effective in WT but not DOR-KO mice (Fig. 1B). Clonidine inhibition of SP-induced behaviors was 3-fold more potent in DOR-KO mice compared with WT mice (Fig. 1A; Table 1). The inhibitory action of morphine was similar in both WT and DOR-KO mice at lower doses. As morphine dose increases, its efficacy was reduced in DOR-KO mice compared with WT mice (Fig. 1C). Nevertheless, there is no significant potency difference between WT and DOR-KO mice (Table 1). No strain difference was observed with the MOR agonist DAMGO (Fig. 1D). In α_{2A}AR-KO mice, clonidine efficacy was reduced to less than 50% inhibition and potency was reduced by 20-fold compared with WT mice (Fig. 1E). Together, these data indicate that DOR mediates DeltII antinociception in the SP assay, morphine and clonidine antinociception are slightly altered in DOR-KO mice, and clonidine antinociception is largely mediated by the α_{2A}AR.

Deltorphin II-Clonidine Spinal Antinociceptive Synergy Requires DOR. We tested the DOR-selective agonist DeltII and clonidine alone or in combination in the SP behavioral assay in WT and DOR-KO mice. In WT mice, DeltII and clonidine inhibited SP-induced nocifensive behaviors in a dose-dependent manner with similar potency (Fig. 2A). Thus, we tested DeltII in combination with clonidine at an equieffective ratio that also corresponds to an equimolar drug ratio (1:1). The inhibition of SP-induced behaviors by the drug combination shifted the dose-response curve leftward. Isobolographic analysis revealed that the experimental ED_{50} value of the drug combination was significantly lower than the theoretical additive ED_{50} value; the drug interaction is therefore synergistic (Fig. 2B; Table 2).

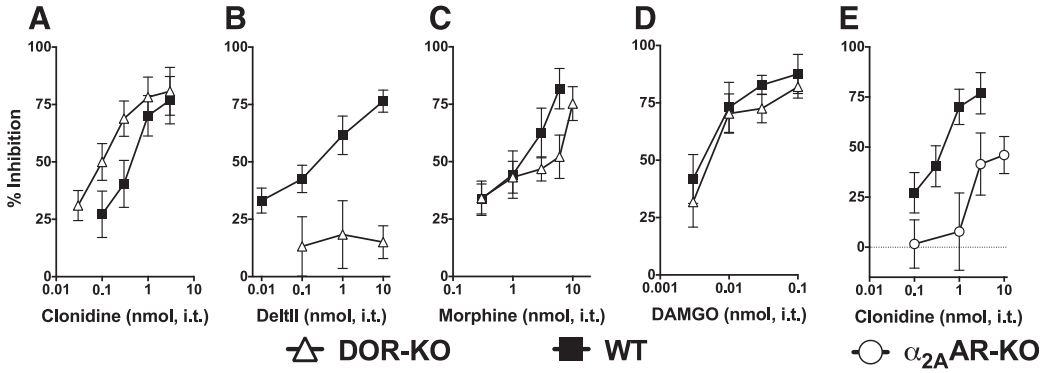

Fig. 1. Clonidine, DeltII, DAMGO, and morphine dose-response curves in the SP behavioral assay. Dose-response curves showing the effects of clonidine, DeltII, DAMGO, and morphine in WT (■), DOR-KO (△), and α_{2A}AR-KO (○) mice where drugs were coadministered intrathecally with 15 ng of SP. (A) Clonidine was more potent in DOR-KO mice compared with WT mice. (B) DeltII inhibited SP behaviors in WT mice, but lacked efficacy in DOR-KO mice. (C) Morphine potency was not significantly different from WT mice. (D) DAMGO inhibition of SP behaviors was unchanged in DOR-KO mice compared with WT mice. (E) Clonidine efficacy and potency decreased in α_{2A}AR-KO mice compared with WT mice. Each data point represents the mean % inhibition ± S.E.M., n = 5–15 mice. The calculated ED_{50} value for each curve obtained in WT and DOR-KO mice and their potency ratio are reported in Table 1.

TABLE 1
Comparison of calculated ED_{50} (95% CI) values for single drugs administered intrathecally in the SP assay in WT and DOR-KO mice

Single Drug	WT	DOR-KO
Clonidine (nmol)	0.4 (0.2–0.7)	0.12 (0.06–0.27)*
DeltII (nmol)	0.15 (0.05–0.44)	No efficacy
Morphine (nmol)	0.9 (0.5–1.7)	2.1 (1.0–4.1)
DAMGO (pmol)	3.4 (1.7–7)	6.0 (3.2–11)

*ED_{50} significantly different, WT versus DOR-KO, Student's t test ($P < 0.05$).

In DOR-KO mice, DeltII was ineffective in the SP assay at all doses tested. We therefore used the same equimolar (1:1) drug ratio to compare the DeltII+clonidine interaction in DOR-KO mice that was used in the WT mice. Because DeltII was not efficacious, isobolographic analysis was not possible. However, the inhibition of SP-induced behaviors by the DeltII+clonidine combination was equivalent to clonidine alone, i.e., DeltII did not shift the clonidine dose-response curve in DOR-KO mice, suggesting that there is no interaction between DeltII and clonidine in DOR-KO mice (Fig. 2C).

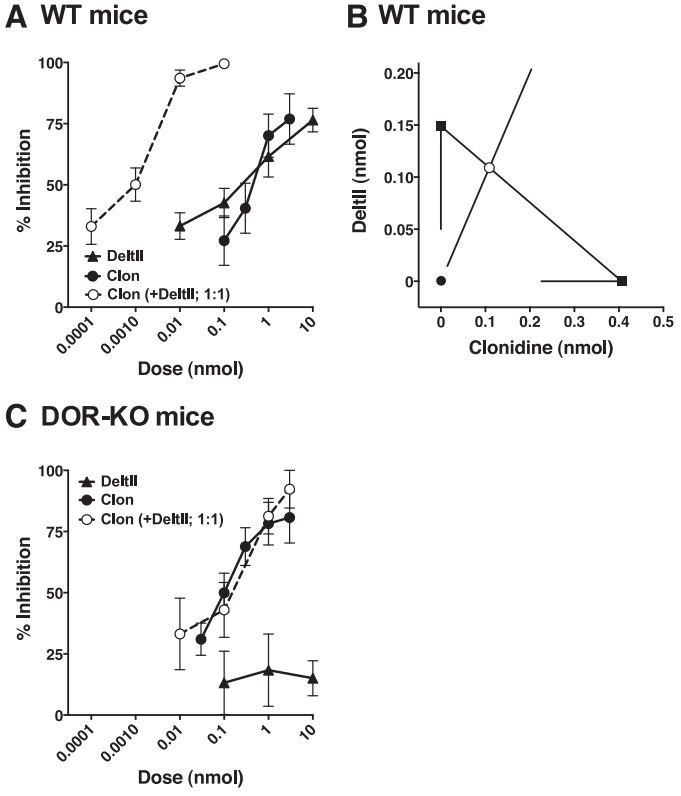

Fig. 2. The interaction between DeltII and clonidine is synergistic in WT mice but not in DOR-KO mice in the SP behavioral assay. (A) Dose-response curves of the spinal antinociceptive effect of deltorphin II (DeltII; ▲), clonidine (Clon; ●), and their combination at an equieffective 1:1 ratio graphed as the dose of clonidine present in the mixture [Clon (+DeltII; 1:1); ○]. (B) Isobolographic analysis of the interaction between DeltII and clonidine in WT mice depicts the DeltII ED_{50} value with lower CI along the y-axis and the clonidine ED_{50} value with lower CI along the x-axis. The measured experimental ED_{50} value for the drug combination (●) is lower than the calculated theoretical additive ED_{50} value (○), indicating that DeltII and clonidine interact in a synergistic manner. (C) In DOR-KO mice, spinal administration of DeltII (▲) was inefficacious at inhibiting SP-elicited behaviors. The dose-response curves of clonidine (●) and of clonidine in the presence of DeltII (○) overlapped, showing that adding DeltII to clonidine did not change its potency. Isobolographic analysis of this data set was not possible because the ED_{50} value for DeltII was incalculable. The calculated ED_{50} value for the experimental and theoretical DeltII+clonidine combinations are reported in Table 2.

Morphine-Clonidine Spinal Antinociceptive Synergy Persists in the Absence of DOR. Because DOR activation is sufficient to produce synergy using a DOR-selective agonist, we assessed its necessity for the synergistic interaction between morphine and clonidine.

In WT mice, spinally administered morphine and clonidine inhibited SP-induced behaviors in a dose-dependent manner. Calculated ED_{50} values obtained for each drug were within one order of magnitude; hence, we combined morphine + clonidine at an equieffective and equimolar (1:1) ratio. The drug combination also inhibited SP behaviors in a dose-dependent manner, and the dose-response curve was shifted to the left compared with the single doses (Fig. 3A). The isobolographic analysis demonstrated that the morphine + clonidine interaction in WT mice was synergistic (Fig. 3B; Table 2).

We then assessed the interaction between morphine and clonidine in DOR-KO mice. Because the difference in ED_{50} values between morphine and clonidine in DOR-KO mice was more than one order of magnitude (Table 1), we tested an equieffective drug ratio of 1 part clonidine + 10 parts morphine (1:10). The drug combination dose-dependently inhibited SP behaviors in DOR-KO mice and the dose-response curve was shifted to the left compared with each drug alone (Fig. 3C). Isobolographic analysis showed that the experimental ED_{50} value is significantly lower than the theoretical additive ED_{50} value (Fig. 3D), indicating that the interaction is synergistic (Table 2).

Taken together, these results show that equieffective doses of morphine and clonidine interact synergistically in both WT and DOR-KO mice.

DAMGO-Clonidine Interaction Is Additive in Both WT and DOR-KO Mice. The retention of morphine + clonidine synergy in DOR-KO mice suggests that opioid-adrenergic synergy can be mediated by MOR in the absence of DOR. To understand the requirements for MOR-mediated synergy with clonidine, we tested the combination of clonidine with the MOR-selective peptide agonist DAMGO in WT and DOR-KO mice. In WT mice, DAMGO inhibited SP-induced behaviors with an ED_{50} value 120-fold more potent than clonidine (Table 1). Therefore, we tested a combination of clonidine and DAMGO at a 100:1 ratio, which also inhibited SP-induced behaviors in a dose-dependent manner (Fig. 4A). The isobolographic analysis revealed that this interaction was additive (Fig. 4B; Table 2).

The potency difference between DAMGO and clonidine in DOR-KO mice required the use of a 1:10 drug ratio corresponding to equieffective doses in this strain. The resulting drug interaction was also additive (Fig. 4, C and D; Table 2).

Discussion

This study addressed the role of DOR in spinal opioid-adrenergic synergistic interactions. We first compared the antinociceptive response of clonidine, DeltII, morphine, and DAMGO between WT and DOR-KO mice in the SP behavioral assay. The observed lack of DeltII efficacy in DOR-KO mice confirms its DOR selectivity in the SP behavioral assay. The addition of clonidine to DeltII resulted in a synergistic

TABLE 2
Calculated ED_{50} values [nmol (± 95% S.E.M.)] for drug combinations administered intrathecally in SP assay in WT and DOR-KO mice

Drug	WT				DOR-KO			
	Ratio	Experimental	Theoretical	Interaction	Ratio	Experimental	Theoretical	Interaction
DeltII + Clonidine	1:1	0.0010 (±0.0005)	0.22 (±0.19)	Synergistic*	1:1	0.20 (±0.23)	0.25 (±0.20)	No interaction [a]
Morphine + Clonidine	1:1	0.058 (±0.029)	0.56 (±0.27)	Synergistic*	10:1	0.085 (±0.050)	0.85 (±0.49)	Synergistic*
DAMGO + Clonidine	1:100	0.14 (±0.056)	0.19 (±0.09)	Additive	1:10	0.022 (±0.0084)	0.044 (±0.022)	Additive

[a]Because DeltII was ineffective in DOR-KO mice, we compared the ED_{50} value for DeltII + clonidine combination to the ED_{50} value of clonidine alone (Student's t test, $P > 0.05$) instead of running an isobolographic analysis.
*Experimental ED_{50} value < theoretical ED_{50} value (Student's t test $P < 0.05$).

interaction in WT but not in DOR-KO mice. In contrast, a synergistic interaction between clonidine and morphine was observed in both strains, and the interaction between clonidine and the MOR-selective agonist DAMGO was additive in both strains. These data demonstrate that DOR is sufficient, but not necessary, for opioid-adrenergic synergistic interaction at the spinal cord.

Mechanisms Mediating Opioid-Adrenergic Synergy. Opioid-adrenergic synergy could arise from pharmacokinetic interactions. In addition to their antinociceptive effects, α_2AR agonists such as clonidine have a local vasoconstrictive effect (Asada and Lee, 1992; Iida et al., 1999) that can reduce drug clearance from the site of injection. Clonidine could therefore enhance the effect of another drug by maintaining it at a high local drug concentration. Following this logic, clonidine should interact synergistically with other drug classes. For example, in a postoperative pain model, clonidine interacts synergistically after intrathecal injection with gabapentin and with an allosteric adenosine receptor modulator (Cheng et al., 2000; Obata et al., 2004). However, reports of synergistic interactions with some, but not all, opioids makes altered drug clearance an unlikely mechanism. Furthermore, ST-91, an α_2AR agonist with hypertensive effects (Yasuoka and Yaksh, 1983; Nagasaka and Yaksh, 1990), interacts synergistically with morphine but does not affect morphine clearance from the spinal cord (Monasky et al., 1990). Thus, the pharmacokinetic actions of α_2AR agonists are unlikely mediators of spinal opioid-adrenergic synergy.

The diffusion of intrathecally administered drugs to supraspinal sites is negligible over a short period of time (Hylden and Wilcox, 1980). Rather, intrathecally administered compounds act locally on the spinal cord and nociceptors, which have opioid and adrenergic receptors capable of inhibiting the transmission of afferent nociceptive signals.

Pharmacodynamic interactions between opioids and α_2AR agonists resulting in analgesic synergy could involve spinal intercellular or intracellular mechanisms. Because spinal MOR, DOR, and α_2AR are distributed on both primary afferent and

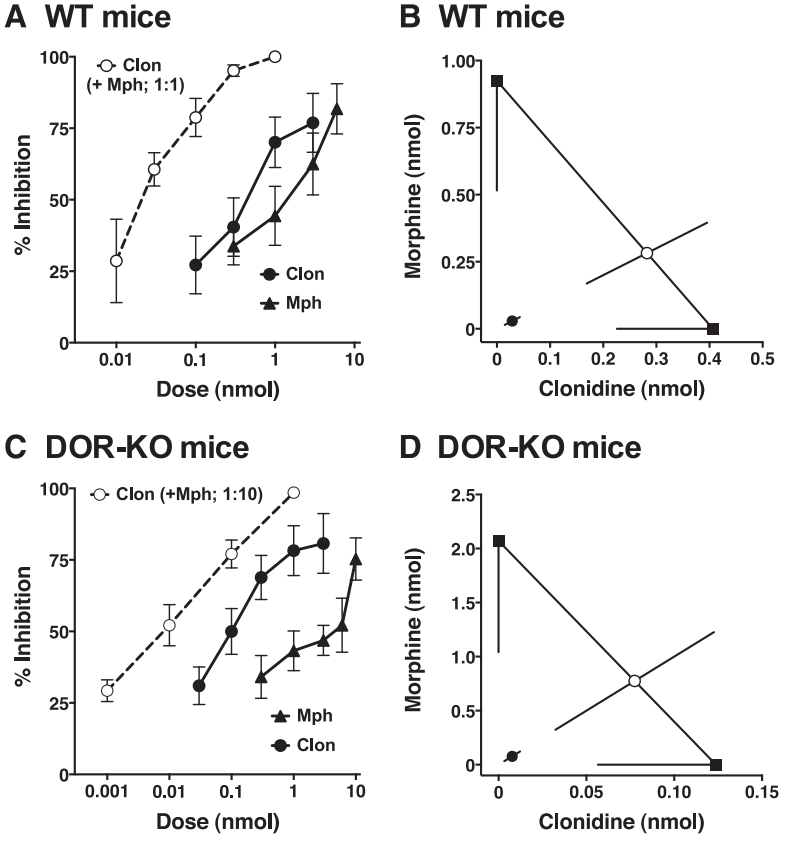

Fig. 3. Morphine and clonidine synergy persists in DOR-KO mice in the SP behavioral assay. (A) Dose-response curves of spinal morphine (Mph; ▲) and clonidine (Clon; ●) in WT mice. The dose-response curve of their equieffective 1:1 ratio combination was graphed as the dose of clonidine present in the mixture [Clon (+Mph; 1:1); ○]. (B) Isobolographic analysis of the interaction between morphine and clonidine in WT mice depicts the morphine ED_{50} value with lower CI along the y-axis and the clonidine ED_{50} value with lower CI along the x-axis. The measured experimental ED_{50} value (●) for the drug combination was lower than the theoretical additive ED_{50} value (○), indicating that morphine and clonidine interact in a synergistic manner. (C) Dose-response curves of spinal clonidine (●) and morphine (▲) in DOR-KO mice. The dose-response curve of their 10:1 ratio combination was graphed as the dose of clonidine present in the mixture (○) to show the relative leftward shift in potency caused by the addition of morphine. (D) Isobolographic analysis of the interaction between morphine and clonidine in DOR-KO mice depicts the morphine ED_{50} values with lower CI along the y-axis and the clonidine ED_{50} value with lower CI along the x-axis. The measured experimental ED_{50} value (●) for the combination of morphine and clonidine (10:1 ratio) and the theoretical additive ED_{50} value (○) are graphed with their upper and lower CI. The measured experimental ED_{50} value for the drug combination is below the calculated theoretical additive ED_{50} value, indicating that morphine and clonidine interact in a synergistic manner. The calculated ED_{50} value for the experimental and theoretical morphine+clonidine combinations are reported in Table 2.

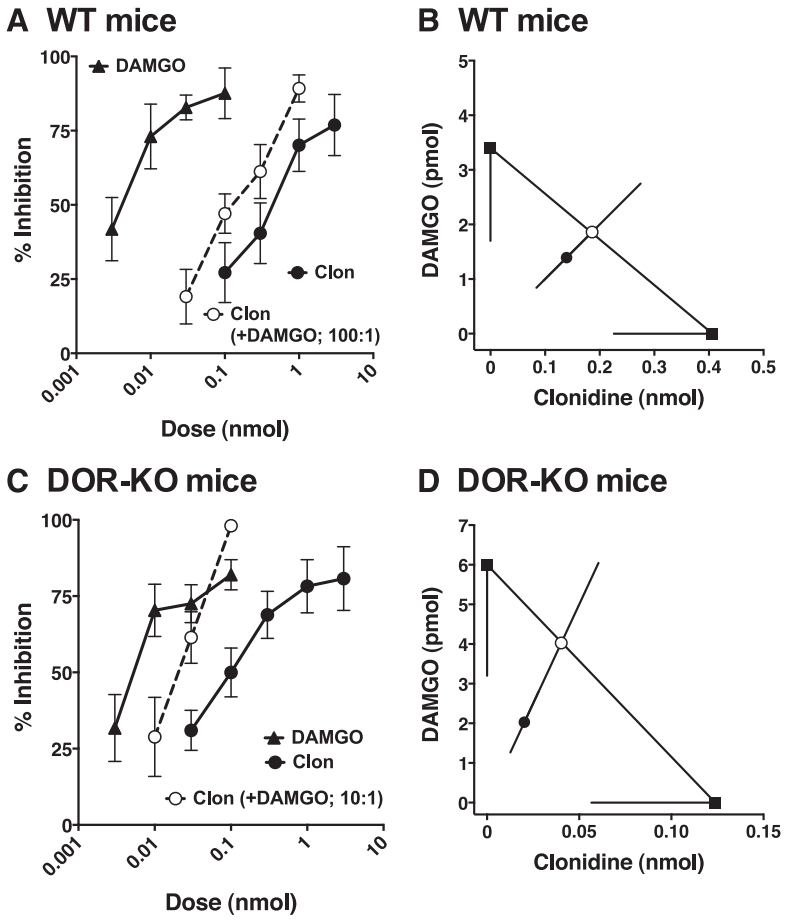

Fig. 4. DAMGO and clonidine are additive in WT and DOR-KO mice. (A, C) Dose-response curves of spinal DAMGO (▲) and clonidine (Clon; ●) in WT and DOR-KO mice. (A) In WT mice, DAMGO+clonidine were combined at an equieffective dose ratio of 1:100, and the dose-response curve was graphed as the dose of clonidine present in the mixture [Clon (+DAMGO; 100:1); ○]. (C) In DOR-KO mice, DAMGO+clonidine were combined at an equieffective 1:10 ratio [Clon (+DAMGO; 10:1); ○]. (B and D) Isobolographic analysis of the interaction between DAMGO and clonidine in WT and DOR-KO mice depicts the DAMGO ED_{50} value with lower CI along the *y*-axis and the clonidine ED_{50} value with lower CI along the *x*-axis. The measured experimental ED_{50} value for the drug combination (●) and the theoretical additive ED_{50} value (○) are graphed with their upper and lower CI. In both strains, the measured experimental ED_{50} value overlaps the calculated theoretical ED_{50} value, indicating that the interactions are additive. The calculated ED_{50} value for the experimental and theoretical DAMGO+clonidine combinations are reported in Table 2.

spinal neurons (Stone et al., 1998; Wall et al., 2006), it is possible that the cumulated neuronal inhibition in the nociceptive circuit is supra-additive. Synergistic interactions could also result from the coexpression of opioid and adrenergic receptors in the same cells where their simultaneous activation results in synergistic output as proposed by Overland et al. (2009).

DOR is Sufficient to Produce Opioid-Adrenergic Synergy. Previous studies have shown that spinal coadministration of the DOR-selective peptide agonists DPDPE and DeltII with clonidine results in a synergistic interaction in both the tail-flick and SP behavioral assays (Ossipov et al., 1990b; Roerig et al., 1992; Roerig, 1995; Overland et al., 2009). These interactions persist in MOR-KO mice, suggesting that MOR is not required (Guo et al., 2003). However, the analgesic effects of DeltII have been attributed to MOR in some behavioral assays such as the tail-flick assay (Scherrer et al., 2004; van Rijn et al., 2012), raising the possibility that these synergistic interactions with α_2AR agonists are MOR mediated rather than DOR mediated. In the current study, DeltII antinociception was absent in DOR-KO mice, validating the use of the SP behavioral assay as a tool to examine the role of DOR in synergistic interactions. As a result, the absence of DeltII-clonidine synergy in DOR-KO mice confirms that DOR activation is sufficient to interact synergistically with α_2AR agonists. Assays should be carefully validated when studying DOR-mediated synergistic interactions because the current findings may not generalize to different assays.

In the spinal cord, clonidine has been shown to interact with both α_2AR and imadazoline binding sites, but the antinociceptive effect of clonidine is mediated by α_2AR rather than imadazoline receptors (Monroe et al., 1995a,b). Our data further suggest that the α_{2A}AR is a key mediator of clonidine antinociception. This observation is consistent with previous studies showing the loss of clonidine antinociceptive efficacy observed in mice expressing a dysfunctional α_{2A}AR (Fairbanks and Wilcox, 1999a). The α_{2A}AR is also necessary for analgesic synergy between DeltII and the α_2AR agonist UK 14,304 (Stone et al., 1997). DOR and α_{2A}AR can both exert their analgesic action by inhibiting transmitter release from primary afferent terminals (Glaum et al., 1994; Kawasaki et al., 2003). Data suggest that the synergistic interaction between DeltII and clonidine is maintained at the level of the primary afferent nerve terminal; for example, this drug combination inhibited KCl-induced CGRP release synergistically from spinal cord slices (Overland et al., 2009). Thus, peptidergic primary afferent neurons are a potential site of action of opioid-adrenergic synergy. We demonstrated that DOR and α_{2A}AR receptors are coexpressed in primary afferent neurons and highly colocalize in SP-immunoreactive neurons and isolated nerve terminals (Riedl et al., 2009). Although the localization of DOR in SP neurons is debated (Scherrer et al., 2009; Wang et al., 2010), the above-mentioned physiologic and anatomic evidence support the presence of DOR and α_{2A}AR in peptidergic neurons where they would be positioned to inhibit neurotransmitter release in a synergistic manner.

DOR Is Not Necessary to Mediate Morphine-Clonidine Synergy. The synergistic interaction between morphine and clonidine is well documented in rodents using different assays (Fairbanks et al., 2009). Because the interaction is stronger when the drugs are administered intrathecally compared with intravenously, it has been proposed to be mediated largely at the level of the spinal cord (Ossipov et al., 1990a). Spinal MOR and DOR can interact together and form heteromeric complexes with altered signaling properties upon morphine treatment (Costantino et al., 2012), which led us to hypothesize that the morphine+clonidine synergistic interaction may require DOR. Our data demonstrate that in DOR-KO mice, a synergistic interaction between morphine and clonidine is still present, allowing us to conclude that DOR is not the only opioid receptor able to mediate opioid-adrenergic analgesic synergistic interactions. Because morphine is not efficacious in the SP behavioral assay in MOR-KO compared with WT mice (Guo et al., 2003), the activation of MOR likely mediates the synergistic interaction between morphine and clonidine.

Synergistic Interactions Involving MOR are Assay Dependent and Ligand Biased. Coactivation of MOR with an α_2AR agonist produces different interactions depending on the experimental conditions and agonists used. Although the interaction between DAMGO and clonidine is either additive (Fig. 4) or subadditive in the SP behavioral assay (Roerig et al., 1992), this drug combination is synergistic in the tail-flick assay (Roerig, 1995). Furthermore, the combination of DAMGO with different α_2AR agonists in the SP behavioral assay can produce either synergistic (Stone et al., 1997) or subadditive (Fairbanks et al., 2000) interactions. Thus, depending on the assay and ligands used, MOR activation may or may not contribute to spinal opioid-adrenergic synergistic interactions.

The contrasting results obtained using two agonists that activate MOR suggest the mechanism underlying these interactions may involve ligand-biased signaling. Morphine and DAMGO engage different downstream signaling cascades upon binding and activation of MOR. Although DAMGO produces robust β-arrestin-dependent MOR translocation and desensitization, morphine produces PKC-dependent desensitization (Johnson et al., 2006; Chu et al., 2008). In cultured sensory neurons, DAMGO cross-desensitizes clonidine's inhibition of Ca^{2+} currents and produces cointernalization of MOR with α_{2A}AR through the β-arrestin 2 and p38 MAPK signaling pathway; morphine produces neither of these effects (Tan et al., 2009). This cross-desensitization between DAMGO and clonidine could explain why their interaction is typically not synergistic in vivo. On the other hand, morphine activates PKCε in HEK 293 cells expressing MOR, but not DAMGO (Chu et al., 2010). It is noteworthy that synergistic interactions arising from morphine-clonidine (Wei and Roerig, 1998) and DeltII-clonidine (Overland et al., 2009) combinations are PKC dependent. This signaling event is unconventional for the opioid and adrenergic receptors that are usually coupled to the pertussis toxin-sensitive $G_{i/o}$ signaling pathway. Intrathecal pertussis toxin treatment decreases morphine and clonidine potency but does not block their synergistic interaction (Roerig and Howse, 1996; Wei et al., 1996). Therefore, morphine-clonidine synergy probably arises from a signaling pathway independent of the pathways activated by the drugs alone and involves PKC activation. The direct interaction between MOR and the α_{2A}AR demonstrated in expression systems support the hypothesis that these interactions could occur via heteromeric G protein-coupled receptor interactions (Vilardaga et al., 2008).

Conclusion

Our data support that activation of DOR is sufficient, but not necessary, to produce analgesic synergy when α_2AR are also activated. Therefore, the synergistic interaction between different opioid-α_2 adrenergic agonists is mediated via different opioid receptor pathways; one of these pathways uses DOR and another pathway is likely using MOR.

Currently clinically used opioids act through MOR, which mediates both their analgesic and side effects. Despite the benefits of mixing morphine and clonidine, side effects are still an issue for some patients. We therefore encourage the development and use of DOR-selective ligands in combination with α_2AR agonists as an alternative to currently available opioid agonists.

Acknowledgments

The authors thank Lina Naso for technical support and Dr. Ossipov for the permission to use FlashCalc 4.5.3.

Authorship Contributions

Participated in research design: Chabot-Doré, Stone, Millecamps.
Conducted experiments: Chabot-Doré, Stone, Millecamps.
Wrote or contributed to the writing of the manuscript: Chabot-Doré, Stone.

References

Alguacil L and Morales L (2004) Alpha-2 adrenoceptor ligands and opioid drugs: pharmacological interactions of therapeutic interest. *Curr Neuropharmacol* **2**: 343–352.
Altman JD, Trendelenburg AU, MacMillan L, Bernstein D, Limbird L, Starke K, Kobilka BK, and Hein L (1999) Abnormal regulation of the sympathetic nervous system in alpha2A-adrenergic receptor knockout mice. *Mol Pharmacol* **56**:154–161.
Asada Y and Lee TJ (1992) Alpha 2-adrenoceptors mediate norepinephrine constriction of porcine pial veins. *Am J Physiol* **263**:H1907–H1910.
Cahill CM, Morinville A, Lee MC, Vincent JP, Collier B, and Beaudet A (2001) Prolonged morphine treatment targets delta opioid receptors to neuronal plasma membranes and enhances delta-mediated antinociception. *J Neurosci* **21**: 7598–7607.
Cheng JK, Pan HL, and Eisenach JC (2000) Antiallodynic effect of intrathecal gabapentin and its interaction with clonidine in a rat model of postoperative pain. *Anesthesiology* **92**:1126–1131.
Chu J, Zheng H, Loh HH, and Law P-Y (2008) Morphine-induced mu-opioid receptor rapid desensitization is independent of receptor phosphorylation and beta-arrestins. *Cell Signal* **20**:1616–1624.
Chu J, Zheng H, Zhang Y, Loh HH, and Law P-Y (2010) Agonist-dependent mu-opioid receptor signaling can lead to heterologous desensitization. *Cell Signal* **22**: 684–696.
Costantino CM, Gomes I, Stockton SD, Lim MP, and Devi LA (2012) Opioid receptor heteromers in analgesia. *Expert Rev Mol Med* **14**:e9:1–15.
Eisenach JC, D'Angelo R, Taylor C, and Hood DD (1994) An isobolographic study of epidural clonidine and fentanyl after cesarean section. *Anesth Analg* **79**:285–290.
Eisenach JC, DuPen S, Dubois M, Miguel R, and Allin D; The Epidural Clonidine Study Group (1995) Epidural clonidine analgesia for intractable cancer pain. *Pain* **61**:391–399.
Fairbanks CA, Posthumus IJ, Kitto KF, Stone LS, and Wilcox GL (2000) Moxonidine, a selective imidazoline/alpha(2) adrenergic receptor agonist, synergizes with morphine and deltorphin II to inhibit substance P-induced behavior in mice. *Pain* **84**:13–20.
Fairbanks CA, Stone LS, Kitto KF, Nguyen HO, Posthumus IJ, and Wilcox GL (2002) alpha(2C)-Adrenergic receptors mediate spinal analgesia and adrenergic-opioid synergy. *J Pharmacol Exp Ther* **300**:282–290.
Fairbanks CA, Stone LS, and Wilcox GL (2009) Pharmacological profiles of alpha 2 adrenergic receptor agonists identified using genetically altered mice and isobolographic analysis. *Pharmacol Therap* **123**:224–238.
Fairbanks CA and Wilcox GL (1999a) Moxonidine, a selective alpha2-adrenergic and imidazoline receptor agonist, produces spinal antinociception in mice. *J Pharmacol Exp Ther* **290**:403–412.
Fairbanks CA and Wilcox GL (1999b) Spinal antinociceptive synergism between morphine and clonidine persists in mice made acutely or chronically tolerant to morphine. *J Pharmacol Exp Ther* **288**:1107–1116.

Filliol D, Ghozland S, Chluba J, Martin M, Matthes HW, Simonin F, Befort K, Gavériaux-Ruff C, Dierich A, and LeMeur M, et al. (2000) Mice deficient for delta- and mu-opioid receptors exhibit opposing alterations of emotional responses. *Nat Genet* **25**:195–200.

Gendron L, Lucido AL, Mennicken F, and O'Donnell DVincent J-PStroh T, and-Beaudet A (2006) Morphine and pain-related stimuli enhance cell surface availability of somatic delta-opioid receptors in rat dorsal root ganglia. *J Neurosci* **26**: 953–962.

Glaum SR, Miller RJ, and Hammond DL (1994) Inhibitory actions of delta 1-, delta 2-, and mu-opioid receptor agonists on excitatory transmission in lamina II neurons of adult rat spinal cord. *J Neurosci* **14**:4965–4971.

Gomes I, Gupta A, Filipovska J, Szeto HH, Pintar JE, and Devi LA (2004) A role for heterodimerization of mu and delta opiate receptors in enhancing morphine analgesia. *Proc Natl Acad Sci USA* **101**:5135–5139.

Guo XH, Fairbanks CA, Stone LS, and Loh HH (2003) DPDPE-UK14,304 synergy is retained in mu opioid receptor knockout mice. *Pain* **104**:209–217.

Hylden JL and Wilcox GL (1980) Intrathecal morphine in mice: a new technique. *Eur J Pharmacol* **67**:313–316.

Hylden JL and Wilcox GL (1981) Intrathecal substance P elicits a caudally-directed biting and scratching behavior in mice. *Brain Res* **217**:212–215.

Iida H, Ohata H, Iida M, Watanabe Y, and Dohi S (1999) Direct effects of alpha1- and alpha2-adrenergic agonists on spinal and cerebral pial vessels in dogs. *Anesthesiology* **91**:479–485.

Johnson EA, Oldfield S, Braksator E, Gonzalez-Cuello A, Couch D, Hall KJ, Mundell SJ, Bailey CP, Kelly E, and Henderson G (2006) Agonist-selective mechanisms of mu-opioid receptor desensitization in human embryonic kidney 293 cells. *Mol Pharmacol* **70**:676–685.

Kawasaki Y, Kumamoto E, Furue H, and Yoshimura M (2003) Alpha 2 adrenoceptor-mediated presynaptic inhibition of primary afferent glutamatergic transmission in rat substantia gelatinosa neurons. *Anesthesiology* **98**:682–689.

Matthes HW, Maldonado R, Simonin F, Valverde O, Slowe S, Kitchen I, Befort K, Dierich A, Le Meur M, and Dollé P, et al. (1996) Loss of morphine-induced analgesia, reward effect and withdrawal symptoms in mice lacking the mu-opioid-receptor gene. *Nature* **383**:819–823.

Monasky MS, Zinsmeister AR, Stevens CW, and Yaksh TL (1990) Interaction of intrathecal morphine and ST-91 on antinociception in the rat: dose-response analysis, antagonism and clearance. *J Pharmacol Exp Ther* **254**:383–392.

Monroe PJ, Smith DL, Kirk HR, and Smith DJ (1995a) Spinal nonadrenergic imidazoline receptors do not mediate the antinociceptive action of intrathecal clonidine in the rat. *J Pharmacol Exp Ther* **273**:1057–1062.

Monroe PJ, Smith DL, and Smith DJ (1995b) Spinal imidazoline receptors do not mediate the antinociceptive action of intrathecal clonidine in the rat. *Ann N Y Acad Sci* **763**:497–500.

Morinville A, Cahill CM, Esdaile MJ, Aibak H, Collier B, Kieffer BL, and Beaudet A (2003) Regulation of delta-opioid receptor trafficking via mu-opioid receptor stimulation: evidence from mu-opioid receptor knock-out mice. *J Neurosci* **23**: 4888–4898.

Nagasaka H and Yaksh TL (1990) Pharmacology of intrathecal adrenergic agonists: cardiovascular and nociceptive reflexes in halothane-anesthetized rats. *Anesthesiology* **73**:1198–1207.

Obata H, Li X, and Eisenach JC (2004) Spinal adenosine receptor activation reduces hypersensitivity after surgery by a different mechanism than after nerve injury. *Anesthesiology* **100**:1258–1262.

Ossipov MH, Harris S, Lloyd P, and Messineo E (1990a) An isobolographic analysis of the antinociceptive effect of systemically and intrathecally administered combinations of clonidine and opiates. *J Pharmacol Exp Ther* **255**:1107–1116.

Ossipov MH, Lozito R, Messineo E, Green J, Harris S, and Lloyd P (1990b) Spinal antinociceptive synergy between clonidine and morphine, U69593, and DPDPE: isobolographic analysis. *Life Sci* **47**:PL71–PL76.

Overland AC, Kitto KF, Chabot-Doré A-J, Rothwell PE, Fairbanks CA, Stone LS, and Wilcox GL (2009) Protein kinase C mediates the synergistic interaction between agonists acting at alpha2-adrenergic and delta-opioid receptors in spinal cord. *J Neurosci* **29**:13264–13273.

Raynor K, Kong H, Chen Y, Yasuda K, Yu L, Bell GI, and Reisine T (1994) Pharmacological characterization of the cloned kappa-, delta-, and mu-opioid receptors. *Mol Pharmacol* **45**:330–334.

Riedl MS, Schnell SA, Overland AC, Chabot-Doré A-J, Taylor AM, Ribeiro-da-Silva A, Elde RP, Wilcox GL, and Stone LS (2009) Coexpression of alpha 2A-adrenergic and delta-opioid receptors in substance P-containing terminals in rat dorsal horn. *J Comp Neurol* **513**:385–398.

Roerig SC (1995) Decreased spinal morphine/clonidine antinociceptive synergism in morphine-tolerant mice. *Life Sci* **56**:PL115–PL122.

Roerig SC and Howse KM (1996) Omega-agatoxin IVA blocks spinal morphine/clonidine antinociceptive synergism. *Eur J Pharmacol* **314**:293–300.

Roerig SC, Lei S, Kitto K, Hylden JK, and Wilcox GL (1992) Spinal interactions between opioid and noradrenergic agonists in mice: multiplicativity involves delta and alpha-2 receptors. *J Pharmacol Exp Ther* **262**:365–374.

Scherrer G, Befort K, Contet C, Becker J, Matifas A, and Kieffer BL (2004) The delta agonists DPDPE and deltorphin II recruit predominantly mu receptors to produce thermal analgesia: a parallel study of mu, delta and combinatorial opioid receptor knockout mice. *Eur J Neurosci* **19**:2239–2248.

Scherrer G, Imamachi N, Cao Y-Q, Contet C, Mennicken F, O'Donnell D, Kieffer BL, and Basbaum AI (2009) Dissociation of the opioid receptor mechanisms that control mechanical and heat pain. *Cell* **137**:1148–1159.

Stone LS, Broberger C, Vulchanova L, Wilcox GL, Hökfelt T, Riedl MS, and Elde R (1998) Differential distribution of alpha2A and alpha2C adrenergic receptor immunoreactivity in the rat spinal cord. *J Neurosci* **18**:5928–5937.

Stone LS, Kitto KF, Eisenach JC, Fairbanks CA, and Wilcox GL (2007) ST91 [2-(2,6-diethylphenylamino)-2-imidazoline hydrochloride]-mediated spinal antinociception and synergy with opioids persists in the absence of functional alpha-2A- or alpha-2C-adrenergic receptors. *J Pharmacol Exp Ther* **323**:899–906.

Stone LS, MacMillan LB, Kitto KF, Limbird LE, and Wilcox GL (1997) The alpha2a adrenergic receptor subtype mediates spinal analgesia evoked by alpha2 agonists and is necessary for spinal adrenergic-opioid synergy. *J Neurosci* **17**:7157–7165.

Tallarida RJ (1992) Statistical analysis of drug combinations for synergism. *Pain* **49**: 93–97.

Tallarida RJ and Murray RB (1987) *Manual of Pharmacologic Calculations with Computer Programs*. Springer Verlag, New York.

Tan M, Walwyn WM, Evans CJ, and Xie C-W (2009) p38 MAPK and beta-arrestin 2 mediate functional interactions between endogenous micro-opioid and alpha2A-adrenergic receptors in neurons. *J Biol Chem* **284**:6270–6281.

van Rijn RM, Brissett DI, and Whistler JL (2012) Emergence of functional spinal delta opioid receptors after chronic ethanol exposure. *Biol Psychiatry* **71**: 232–238.

Vilardaga J-P, Nikolaev VO, Lorenz K, Ferrandon S, Zhuang Z, and Lohse MJ (2008) Conformational cross-talk between alpha2A-adrenergic and mu-opioid receptors controls cell signaling. *Nat Chem Biol* **4**:126–131.

Walker SM, Goudas LC, Cousins MJ, and Carr DB (2002) Combination spinal analgesic chemotherapy: a systematic review. *Anesth Analg* **95**:674–715.

Wall PD, Melzack R, McMahon SB, and Koltzenburg M (2006) *Textbook of Pain*, Churchill Livingstone, Philadelphia.

Wang H-B, Zhao B, Zhong Y-Q, Li K-C, Li Z-Y, Wang Q, Lu Y-J, Zhang Z-N, He S-Q, and Zheng H-C, et al. (2010) Coexpression of delta- and mu-opioid receptors in nociceptive sensory neurons. *Proc Natl Acad Sci USA* **107**:13117–13122.

Wei ZY, Karim F, and Roerig SC (1996) Spinal morphine/clonidine antinociceptive synergism: involvement of G proteins and N-type voltage-dependent calcium channels. *J Pharmacol Exp Ther* **278**:1392–1407.

Wei ZY and Roerig SC (1998) Spinal morphine/clonidine antinociceptive synergism is regulated by protein kinase C, but not protein kinase A activity. *J Pharmacol Exp Ther* **287**:937–943.

Yasuoka S and Yaksh TL (1983) Effects on nociceptive threshold and blood pressure of intrathecally administered morphine and alpha-adrenergic agonists. *Neuropharmacology* **22**:309–315.

Yekkirala AS, Kalyuzhny AE, and Portoghese PS (2010) Standard opioid agonists activate heteromeric opioid receptors: evidence for morphine and [d-Ala(2)-MePhe (4)-Glyol(5)]enkephalin as selective μ-δ agonists. *ACS Chem Neurosci* **1**:146–154.

Zhu Y, King MA, Schuller AG, Nitsche JF, Reidl M, Elde RP, Unterwald E, Pasternak GW, and Pintar JE (1999) Retention of supraspinal delta-like analgesia and loss of morphine tolerance in delta opioid receptor knockout mice. *Neuron* **24**: 243–252.

Address correspondence to: Dr. Laura S. Stone, Alan Edwards Centre for Research on Pain, Faculty of Dentistry, McGill University, 740 Penfield Ave., Suite 3200, Montreal, Quebec H3A 0G1, Canada. E-mail: laura.s.stone@mcgill.ca

The Journal of Comparative Neurology 513:385–398 (2009)

Coexpression of α_{2A}-Adrenergic and δ-Opioid Receptors in Substance P-Containing Terminals in Rat Dorsal Horn

MAUREEN S. RIEDL,[1] STEPHEN A. SCHNELL,[1] AARON C. OVERLAND,[1] ANNE-JULIE CHABOT-DORÉ,[2] ANNA M. TAYLOR,[2,3] ALFREDO RIBEIRO-DA-SILVA,[2,3] ROBERT P. ELDE,[1,4] GEORGE L. WILCOX,[1,4,5] AND LAURA S. STONE[2,3,6]*

[1]Department of Neuroscience, University of Minnesota, Minneapolis, Minnesota 55455
[2]Alan Edwards Centre for Research on Pain, McGill University, Montreal, Quebec H3A 1A4, Canada
[3]Department of Pharmacology and Therapeutics, Faculty of Medicine, McGill University, Montreal, Quebec H3A 1A4, Canada
[4]Department of Pharmacology, University of Minnesota, Minneapolis, Minnesota 55455
[5]Department of Dermatology, University of Minnesota, Minneapolis, Minnesota 55455
[6]Faculty of Dentistry, McGill University, Montreal, Quebec H3A 1A4, Canada

ABSTRACT

Agonists acting at α_2-adrenergic and opioid receptors (α_2ARs and ORs, respectively) inhibit pain transmission in the spinal cord. When coadministered, agonists activating these receptors interact in a synergistic manner. Although the existence of α_2AR/OR synergy has been well characterized, its mechanism remains poorly understood. The formation of heterooligomers has been proposed as a molecular basis for interactions between neuronal G-protein-coupled receptors. The relevance of heterooligomer formation to spinal analgesic synergy requires demonstration of the expression of both receptors within the same neuron as well as the localization of both receptors in the same neuronal compartment. We used immunohistochemistry to investigate the spatial relationship between α_2ARs and ORs in the rat spinal cord to determine whether coexpression could be demonstrated between these receptors. We observed extensive colocalization between α_{2A}-adrenergic and δ-opioid receptors (DOP) on substance P (SP)-immunoreactive (-ir) varicosities in the superficial dorsal horn of the spinal cord and in peripheral nerve terminals in the skin. α_{2A}AR- and DOP-ir elements were colocalized in subcellular structures of 0.5 μm or less in diameter in isolated nerve terminals. Furthermore, coincubation of isolated synaptosomes with α_2AR and DOP agonists resulted in a greater-than-additive increase in the inhibition of K^+-stimulated neuropeptide release. These findings suggest that coexpression of the synergistic receptor pair α_{2A}AR-DOP on primary afferent nociceptive fibers may represent an anatomical substrate for analgesic synergy, perhaps as a result of protein–protein interactions such as heterooligomerization. J. Comp. Neurol. 513:385–398, 2009. © 2009 Wiley-Liss, Inc.

Indexing terms: immunohistochemistry; large dense-core vesicle; synaptosome; primary afferent; nociceptor; terminal

Agonists acting at spinal α_2-adrenergic and opioid receptors (α_2ARs and ORs, respectively) share common signal transduction systems mediated through inhibitory G proteins, the activation of which inhibits pain transmission. In addition, agonists acting at α_2ARs and ORs interact in a greater-than-additive (i.e., synergistic) manner when coadministered to the spinal cord (for review see Alguacil and Morales, 2004). Synergistic interactions between analgesic agents acting at ORs and α_2ARs have been observed repeatedly in several laboratories after spinal administration using both behavioral (Hylden and Wilcox, 1983; Stevens et al., 1988; Monasky et al., 1990; Ossipov et al., 1990a–c; Roerig et al., 1992) and electrophysiological (Sullivan et al., 1987; Wilcox et al., 1987; Omote et al., 1990) methods. Synergistic interactions can result in greater than 100-fold increases in analgesic potency as well as increased maximum efficacy. Synergy is important in clinical pain management, in that it makes possible production of analgesia at lower doses for each drug, thus reducing undesired side effects and improving treatment outcomes (for review see Walker et al., 2002). Despite the widespread evaluation and characterization of these interactions, the mechanisms underlying analgesic synergy are unclear.

Grant sponsor: National Institutes of Health; Grant number: R01-DA-01933 (to G.L.W.); Grant number: R01-DA-15438 (to G.L.W.); Grant number: R01-DA-06299 (to R.P.E.); Grant number: R21-DA-017075 (to L.S.S.); Grant sponsor: Canadian Institutes of Health Research; Grant number: MOP-86691 (to L.S.S.).

*Correspondence to: Laura S. Stone, McGill Centre for Research on Pain, Faculty of Dentistry, McGill University, 740 Dr. Penfield, Suite 3200, Montreal, Quebec H3A 1A4, Canada. E-mail: laura.s.stone@mcgill.ca

Received 20 January 2006; Revised 31 October 2007; Accepted 16 December 2008

DOI 10.1002/cne.21982

Published online in Wiley InterScience (www.interscience.wiley.com).

Within the α_2ARs, there are three primary subtypes, α_{2A}-, α_{2B}-, and α_{2C}AR (for reviews see Aantaa et al., 1995; MacDonald et al., 1997; Philipp et al., 2002). Similarly, there are three primary OR subtypes, δ (DOP), μ (MOP), and κ (KOP; for reviews see Kieffer, 1999; Law and Loh, 1999). Pairs of receptors for which α_2AR-OR synergistic interactions have been documented include DOP and α_{2A}AR (Stone et al., 1997), MOP and α_{2A}AR (Roerig et al., 1992; Stone et al., 1997), and DOP and α_{2C}AR (Fairbanks et al., 2002; Guo et al., 2003).

It is now recognized that G-protein-coupled receptors (GPCRs) can form oligomeric complexes in addition to the traditionally envisaged monomeric species. The demonstration of functional oligomers in transfected cells has led to significant reevaluation of the mechanisms thought to be involved in GPCR function in vivo. These associations can result in novel pharmacological properties distinct from those of either component receptor, including enhancement of ligand binding affinity, changes in functional coupling, and altered receptor trafficking (for reviews see George et al., 2002; Bulenger et al., 2005). The generation of novel properties upon heterooligomer formation may represent a molecular mechanism for synergistic interactions between neuronal GPCRs that colocalize in vivo. Physical associations suggestive of heterooligomer formation have been demonstrated between α_2ARs and ORs in transfected cells in vitro (Jordan et al., 2003; Rios et al., 2004; Zhang and Limbird, 2004; Vilardaga et al., 2008). The potential relevance of these in vitro studies to spinal synergy requires the expression of both receptors within the same neuron as well as the localization of both receptors in the same neuronal compartment.

We examined the expression of DOP, MOP, α_{2A}AR, and α_{2C}AR in the superficial dorsal horn of the spinal cord to determine the spatial relationships between these receptors. Coexpression in the spinal cord dorsal horn would provide anatomical evidence to support a role for oligomerization in the phenomena of α_2AR/OR functional synergy. To determine whether simultaneous activation of colocalized receptors results in functional synergy, we challenged depolarization-elicited CGRP release from spinal cord synaptosomes with agonists directed at DOP and α_2AR.

MATERIALS AND METHODS

Animals

Male Sprague Dawley rats (150–250 g; Harlan) were housed in pairs in a temperature- and humidity-controlled environment and maintained on a 12-hour light/dark cycle with free access to food and water. All experiments were approved by either the University of Minnesota's Institutional Animal Care and Use Committee or the McGill University Animal Care and Ethics Committees.

Antisera

The α_{2A}AR antiserum (1:1,000) was prepared in rabbit against a synthetic peptide corresponding to $\alpha_{2A}AR_{358-371}$ (KASRWRGRQNREKR). This antiserum has been previously characterized and was determined to be specific for α_{2A}AR based on the elimination of staining following preadsorption of the antisera with peptide (KASRWRGRQNREKR) and the ability of the antisera to label MDCK cells transfected with α_{2A}AR but not those transfected with α_{2B}AR or α_{2C}AR (Stone et al., 1998). This antiserum recognizes an ~50-kDa band by Western blot analysis (see Fig. 6).

The rabbit- and rat-derived DOP antisera were prepared against synthetic peptides and have been previously characterized. Rabbit anti-DOP_{3-17} (1:1,000; LVPSARAELQSSPLV) was previously shown to exhibit staining identical to that of antisera raised against other regions of the receptor, including the rabbit anti-DOP_{30-46} (1:1,000) and rat anti-DOP_{30-46} (1:300) antisera used in the current study (AGANASGSPGARSASSL; gift of Dr. Martin W. Wessendorf; Arvidsson et al., 1995a). Staining with these antisera is eliminated after preadsorption with the corresponding peptides (Dado et al., 1993; Arvidsson et al., 1995a), is reduced following knock-down of DOP with antisense oligonucleotides (Lai et al., 1996), and is virtually eliminated by deletion of the DOP gene in mice (Zhu et al., 1999). The rabbit anti-DOP_{30-46} antiserum recognizes an ~45-kDa band by Western blot analysis (see Fig. 6).

The rabbit- and guinea pig-derived MOP antisera were prepared against a synthetic peptide corresponding to $MOP_{384-398}$ (QLENLEAETAPLP) of the predicted rat MOR1 gene and have been previously characterized (Arvidsson et al., 1995b). The rabbit-derived antiserum was determined to be specific for MOP based on the elimination of staining after preadsorption of the antiserum with the cognate peptide (QLENLEAETAPLP), the ability of the antiserum to label COS-7 cells transfected with MOP but not DOP or KOP, and the recognition of an immunoreactive band by Western blot analysis of ~60 kDa in rat brain membranes (Arvidsson et al., 1995b). The guinea pig-derived antiserum was generated against the same peptide and produces a staining pattern identical to that of the previously described rabbit-derived antiserum.

The α_{2C}AR antisera were prepared in both guinea pig and rabbit against a synthetic peptide corresponding to $\alpha_{2C}AR_{446-458}$ (HILFRRRRRGFRQ). These antisera have been previously characterized and were determined to be specific for α_{2C}AR based on the elimination of staining after preadsorption of the antisera with the cognate peptide (HILFRRRRRGFRQ), the ability of the antisera to label MDCK cells transfected with α_{2C}AR but not those transfected with α_{2A}AR or α_{2B}AR (Stone et al., 1998), and a reduction in immunoreactivity after knockdown of α_{2C}AR with antisense oligonucleotides (Fairbanks et al., 2002). These antisera produce identical staining patterns and colocalize extensively.

SP antibodies raised in three different species and obtained from three different sources were used in these studies and produced similar results: rat anti-SP (1:1,000; Accurate Chemical, Westbury, NY), rabbit anti-SP (1:1,000; gift of Dr. R. Ho to R.P.E.), and guinea pig anti-SP (1:500; Neuromics Antibodies, Minneapolis, MN). The rat anti-SP recognizes the COOH terminal of SP and was originally characterized by Cuello et al. (1979). This antibody is secreted from hybrid clone line NCI/34 derived from fusion of a mouse NSI/1-Ag 4-1 spleen cell and a spleen cell from a Wistar rat immunized with SP (CRPKPQQFFGLM) conjugated to BSA. This antibody shows no cross-reactivity to leu- or met-enkephalin, somatostatin, or beta-endorphin by radioimmunoassay. Immunofluorescence is blocked by preadsorption with synthetic SP (220 μg/ml; Cuello et al., 1979). The rabbit-derived SP antiserum was obtained after immunization with a synthetic SP-thyroglobulin conjugate as originally reported by Ho and DePalatis (1980). Immunoreactivity was blocked by preincubation of this anti-

serum with synthetic SP (10 μg/ml) but not by pretreatment with met-enkephalin, neurophysin, or somatostatin (Ho and DePalatis, 1980). The polyclonal GP-derived antiserum was directed against residues 1–11 of rat SP and is blocked by preadsorption with 10 μg/ml of synthetic SP (data not shown). All three antibodies produce similar staining patterns and colocalize extensively.

The antibodies used as loading controls in Western blot analysis were both purchased from commercial sources. The rabbit polyclonal pan-cadherin antiserum (catalog No. ab16505; Abcam, Cambridge, MA) was generated against a synthetic peptide conjugated to KLH derived from within residues 850 to the C-terminus of human pan-cadherin. This antiserum recognizes a band of approximately 135 kDa in Western blot analysis that is blocked by preadsorption with the cognate peptide (catalog No. ab17098; Abcam). A monoclonal antibody to the housekeeping gene glyceraldehyde-3-phosphate dehydrogenase (GAPDH) was purchased from Millipore (Bedford, MA; catalog No. MAB374; clone 6C5). This antibody was directed against the entire GAPDH protein isolated from rabbit muscle and recognizes a single band in rat spinal cord membranes by Western blot analysis (see Fig. 6).

Tissue preparation (spinal cord)

Animals were anesthetized with an intramuscular injection of a mixture of 75 mg/kg ketamine, 5 mg/kg xylazine, and 1 mg/kg acepromazine and perfused transcardially with 180 ml of oxygenated ice-cold Tyrode's solution (116 mM NaCl, 5 mM KCl, 2 mM $MgCl_2 \cdot 6H_2O$, 406 μM $MgSO_4 \cdot 7H_2O$, 2.9 mM glucose, 26 mM $NaHCO_2$). This was followed by 500 ml of fixative [4% (w/v) paraformaldehyde, 0.2% (v/v) saturated picric acid] solution in 0.1 M phosphate-buffered saline (PBS; 150 mM KH_2PO_4, 170 mM $NaHPO_4 \cdot 7H_2O$, pH 6.9) and thereafter by 400 ml of 10% sucrose solution [10% (w/v) sucrose in PBS]. Spinal cords were dissected and stored overnight in 10% sucrose at 4°C. Tissue sections were prepared with a cryostat at a thickness of 10 or 14 μm, thaw-mounted onto gelatin-coated slides, and stored at –20°C.

Immunofluorescence histochemistry (spinal cord)

Cryostat sections were preincubated for 1 hour at room temperature (RT) in diluent containing 1% normal donkey serum, 0.3% Triton X-100, 0.01% sodium azide, and 1% BSA in PBS. Sections were incubated overnight at 4°C in a humid chamber with primary antisera, rinsed for 3 × 10 minutes with PBS, incubated with fluorescently tagged species-specific secondary antisera (Jackson Immunoresearch, West Grove, PA) for 1 hour at RT, rinsed for 3 × 10 minutes with PBS, and either coverslipped with a mixture of glycerol and PBS containing 0.1% p-phenylenediamine or dehydrated, cleared in xylene, and mounted with DPX (Fluka). Double- and triple-labeling procedures were adapted from previous studies (Wessendorf and Elde, 1985).

Adsorption controls

To control for cross-reactivity between DOP and α_{2A}AR antisera, immunohistochemistry was performed as described above, with the exception that the primary antibodies were preincubated with 10 μg/ml of either peptide $\alpha_{2A}AR_{358-371}$ (KASRWRGRQNREKR) or peptide $DOP1_{30-46}$ (AGANASGSPGARSASSL; Arvidsson et al., 1995a; Stone et al., 1998). To ensure that secondary antibodies did not cross-react, control experiments were performed in which one or the other primary antiserum was omitted, and no staining was observed in either of these cases.

Tissue preparation (skin)

Animals were anesthetized with 0.4 ml/kg Equithesin (6.5 mg chloral hydrate and 3 mg sodium pentobarbital in a volume of 0.3 ml, i.p., per 100 g body weight) and perfused transcardially with a mixture of 4% paraformaldehyde and 15% (v/v) saturated solution of picric acid in 0.1 M phosphate buffer (PB), pH 7.4, for 30 minutes. Rat lower lip skin was dissected and postfixed for 1 hour in the above-mentioned fixative. The tissue was then incubated in a 30% sucrose solution in PB for at least 12 hours before further processing.

Immunofluorescence histochemistry (skin)

Tissue sections were trimmed and embedded in an Optimum Cutting Temperature (OCT) compound (Tissue-Tek, Sakura Finetek USA, Torrance, CA). Fifty-micrometer sections were cut on a cryostat (Leica) and collected in PBS containing 0.2% Triton X-100 (PBS+T). Sections were treated with 50% ethanol for 30 minutes and then 0.3% hydrogen peroxide (H_2O_2) in PBS for 10 minutes at RT. Nonspecific staining was blocked by incubating sections in 10% normal goat serum and 10% normal donkey serum (NDS) in PBS+T for 1 hour. Sections were incubated overnight at 4°C in primary antisera, washed with PBS+T, and then incubated for 2 hours with fluorescently tagged species-specific secondary antisera. These included the highly cross-adsorbed Alexa Fluor 488-conjugated goat anti-rabbit IgG (1:400; Molecular Probes, Eugene, OR) and the rhodamine red X-conjugated donkey anti-guinea pig IgG (1:500; Jackson Immunoresearch, West Grove, PA). Sections were mounted on gelatin-coated slides and coverslipped with Aquapolymount (Polysciences, Warrington, PA).

Synaptosome preparation

This preparation is described in greater detail elsewhere (Goracke-Postle et al., 2006). Briefly, spinal cords were collected, homogenized, and centrifuged at 800*g* for 10 minutes at 4°C. The supernatant (S1) was then centrifuged at 15,000*g* for 20 minutes at 4°C. The resultant pellet (P2) was resuspended, and the synaptosomes were further purified by sucrose gradient as previously described (Fried et al., 1989). This preparation has been validated by both functional and anatomical criteria (Goracke-Postle et al., 2006, 2007).

Synaptosome immunofluorescence

The synaptosomes were aliquoted into four-well Nunc Lab-Tek II CC2 Chamber Slides and incubated at 37°C for 30 minutes. Slides were then exposed to fixative (see above) for 15 minutes and washed for 3 × 5 minutes in PBS and incubated in diluent (see above) for 15 minutes. Slides were then incubated with primary antisera for 30 minutes at RT in a humid chamber, rinsed for 3 × 5 minutes with PBS, incubated with fluorescently tagged species-specific secondary antisera (Jackson Immunoresearch) for 30 minutes at RT, and rinsed for 3 × 5 minutes with PBS. The barriers separating the individual wells were removed, and the slides were coverslipped with Vectashield mounting medium (Vector Laboratories, Burlingame, CA).

Western blot analysis

Proteins from the S1, P2, and synaptosomal fraction obtained from mouse spinal cord were denatured in SDS sample buffer, and 20 μg of protein was loaded onto a 10% SDS-PAGE gel and transferred to a PVDF membrane. Membranes were blocked with 5% nonfat dry milk in TBST (Tris-buffered saline with 0.01% Tween, pH 7.4) for 1 hour at RT, followed by incubation with either rabbit anti-DOP (1:1,000) or anti-α_{2A}AR (1:1,000) for 3 hours at RT. After washing for 3 × 10 minutes with TBST, blots were incubated with a peroxidase-conjugated mouse anti-rabbit IgG antibody (1:10,000, Jackson Immunoresearch) and washed for a further 3 × 10 minutes. Membranes were revealed with SuperSignal West Femto Chemiluminescent Substrate (Pierce, Rockford, IL) and visualized with a digital imaging system equipped with a cooled CCD camera (ChemiGenius, Syngene). Membranes were then stripped with Restore Western Blot Stripping Buffer (Pierce) and probed with either a mouse anti-GAPDH (1:20,000; Chemicon, Temecula, CA) or a rabbit anti-cadherin antibody (1:20,000; Abcam) for 60 minutes at RT. After washing for 3 × 10 minutes with TBST, blots were incubated with a peroxidase-conjugated mouse anti-rabbit IgG or goat anti-mouse secondary antibody (1:10,000; Jackson Immunoresearch). After the final 3 × 10 minute washes in TBST, membranes were revealed with enhanced chemiluminescence (Pierce) and exposed to light-sensitive film (Clonex Corporation).

Confocal microscopy

Images of spinal cords and synaptosomes were collected using a Bio-Rad MRC 1000 confocal microscope (Bio-Rad Microscience Division, Cambridge, MA). A ×60, 1.4 NA objective and zoom values ranging from 1 to 5 were used for high magnification. Illumination was supplied by a Kr/Ar-ion laser with emission lines at 488, 568, and 647 nm. The skin samples were examined with a Zeiss LSM 510 confocal scanning laser microscope with argon and helium neon lasers. Micrograghs used in plates were minimally processed (adjusted for sharpness, contrast, and brightness) and assembled in Adobe Photoshop. Semiquantitative analysis of the images in Figure 1, fourth column, was performed in Photoshop by counting yellow (colocalized) pixels and dividing by the total number of red, green, and yellow pixels. Similar results were obtained with the colocalization RGB plugin in ImageJ; data are reported for the Photoshop method.

Neuropeptide release assay

Synaptosomes were prepared as described above, oxygenated for 1 minute, and allowed to seal during an incubation period of 30 minutes at 37°C. Samples were centrifuged for 5 minutes at 21,380*g*, and supernatant was removed. After an initial wash in HEPES, a 10-minute baseline sample was collected. The synaptosomes were then exposed to either vehicle or test compound (deltorphin II, clonidine, or a combination) for 10 minutes and subsequently stimulated with 60 mM K^+ (10 minutes). Samples were centrifuged again for 5 minutes at 21,380*g*. All supernatants were collected for analysis of immunoreactive calcitonin gene-related peptide (iCGRP) content by a commercial radioimmunoassay (RIA) kit (Phoenix Pharmaceuticals, Burlingame, CA). Data are presented as mean ± SEM and expressed as the percentage inhibition of neuropeptide release according to the equation: percentage inhibition = [(high K^+ + drug) – (high K^+)]/(high K^+) × 100.

RESULTS

Relationship among α_{2A}AR-ir, α_{2C}AR-ir, DOP-ir, and MOP-ir in the dorsal horn of rat spinal cord

The anatomical relationships among α_{2A}AR-ir, α_{2C}AR-ir, DOP-ir, and MOP-ir were investigated in rat lumbar spinal cord. We observed extensive colocalization between α_{2A}AR-ir and DOP-ir. In contrast, colocalization was minimal between α_{2A}AR-ir and MOP-ir, α_{2C}AR-ir and DOP-ir, or α_{2C}AR-ir and MOP-ir (Fig. 1). Semiquantitative assessment of colocalization at high magnification ranged from 58% (Fig. 1D, α_{2A}AR-ir + DOP-ir) to 8.2% (Fig. 1H, α_{2A}AR-ir + MOP-ir), 6.1% (Fig. 1L, α_{2C}AR-ir + DOP-ir), and 6.7% (Fig. 1P, α_{2C}AR-ir + MOP-ir).

Colocalization of α_2AR-ir and DOP-ir in the dorsal horn of rat spinal cord

The anatomical relationship between α_{2A}AR-ir and DOP-ir was further investigated. In rat lumbar spinal cord, extensive colocalization (white) between α_{2A}AR-ir and DOP-ir was observed in the superficial dorsal horn (Fig. 2). This level of colocalization was apparent in confocal images of coronal (Fig. 2A–F) and horizontal (Fig. 2G–O) spinal cord sections. Sections were double labeled with rabbit-derived anti-α_{2A}AR (Fig. 2, first column) and rat-derived anti-DOP (Fig. 2, second column), and each image represents a single optical section. These pairs of unmerged images illustrate the similarity in staining patterns observed with the different antisera. The results of digital merging revealed extensive colocalization (Fig. 2, third column). High-magnification microscopy detected α_{2A}AR-ir and DOP-ir colocalization within the same neuronal processes 0.25 μm or less in diameter.

Adjacent sections of rat spinal cord were double labeled for α_{2A}AR-ir and DOP-ir in the presence or absence of each receptor's cognate peptide (Fig. 3). Each cognate peptide binds with high affinity to its corresponding antiserum, thereby inhibiting binding to the tissue and reducing the degree of immunoreactivity observed for that target while leaving the binding of other antiserum unaffected. In the presence of the α_{2A}AR cognate peptide, α_{2A}AR-ir was absent (Fig. 3B), whereas DOP-ir (Fig. 3E) was unaffected. Similarly, preincubation with the cognate peptide for the DOP antiserum blocked DOP-ir (Fig. 3F) but not α_{2A}AR-ir (Fig. 3C). In parallel experiments, tissue was exposed to one or the other primary antiserum and both secondary antibodies or one primary and both secondary antibodies. In these experiments, only immunoreactivity corresponding to the anticipated pair of primary and secondary antibodies was observed (data not shown). Taken together, these studies indicate that the antisera used in this study do not cross-react.

Colocalization of α_{2A}AR-ir, DOP-ir, and SP-ir in the dorsal horn of rat spinal cord

Previous reports have demonstrated that both α_{2A}AR and DOP are expressed in the peptidergic population of primary afferent sensory neurons (Dado et al., 1993; Arvidsson et al., 1995a; Stone et al., 1998; Zhang et al., 1998). Therefore, we double or triple labeled spinal cord sections with antibodies directed against α_{2A}AR, DOP, and the neuropeptide SP (Fig. 4). Colocalization of α_{2A}AR-ir and SP-ir was observed with the rabbit-derived α_{2A}AR and both rat- and guinea pig-derived SP antibodies obtained from independent sources (Fig. 4A–D,M). Similarly, rabbit-derived anti-DOP labeling colocalized with both

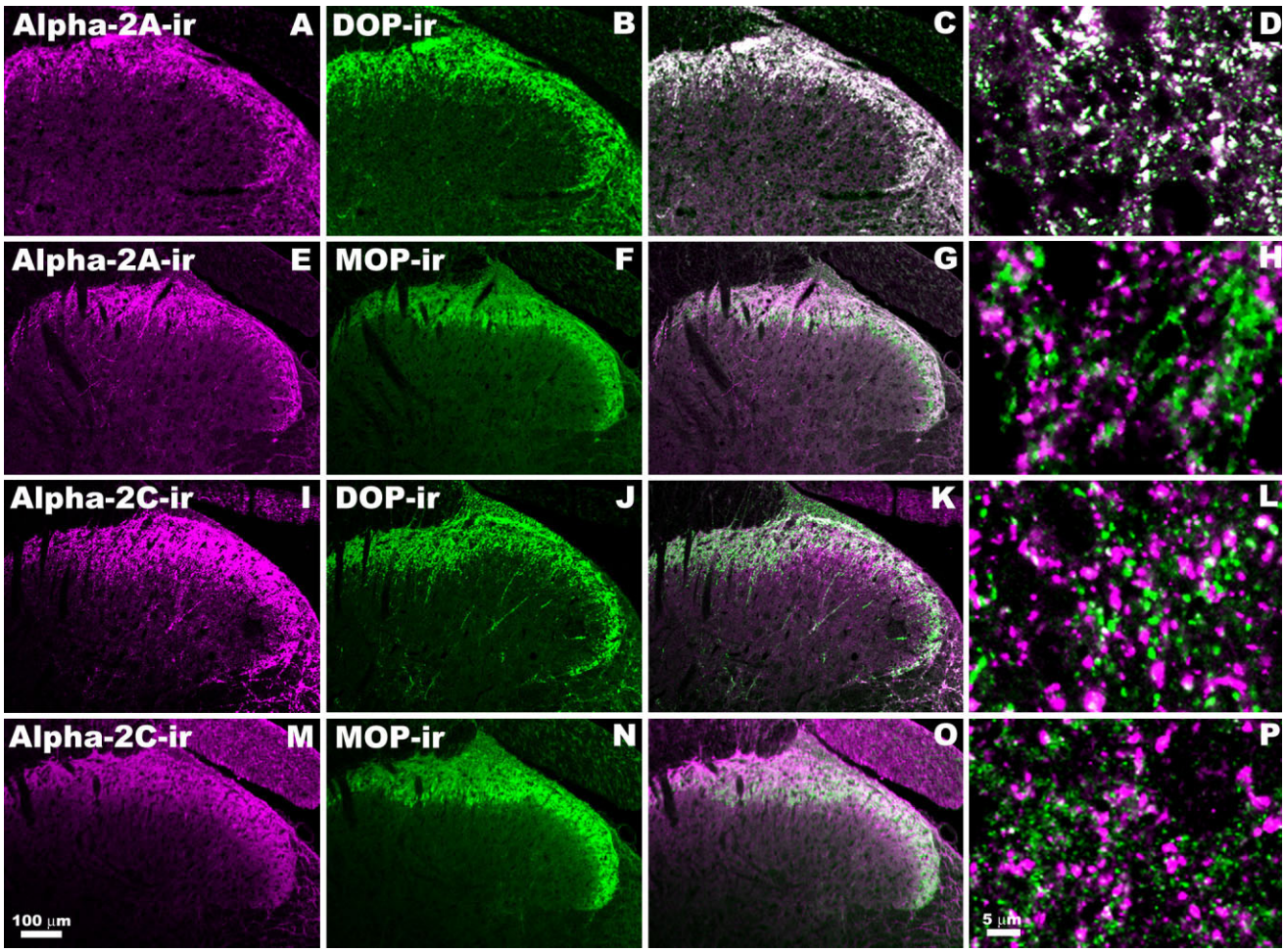

Figure 1.
Relationship among α_{2A}AR-ir, α_{2C}AR-ir, DOP-ir, and MOP-ir in rat spinal cord dorsal horn. Single confocal optical sections of lumbar rat spinal cord were double labeled with combinations of guinea pig-, rat-, or rabbit-derived antisera. The first column depicts immunoreactivity of antisera directed against α_{2A}AR (A,E) and α_{2C}AR (I,M). The second column represents the same sections double labeled with either DOP (B,J) or MOP (G,O) antisera. In the third column, the results of digitally merging images from the first two columns are shown (C,G,K,O). The fourth column contains higher magnification images of these combinations (D,H,L,P). In merged images, the appearance of white indicates probable colocalization. Antisera combinations were as follows. **A–D:** Rabbit-derived anti-α_{2A}AR (A) with rat-derived anti-DOP (B), highly colocalized (C,D). **E–H:** Rabbit-derived anti-α_{2A}AR (E) with guinea pig-derived anti-MOP (F), rarely colocalized (G,H). **I–L:** Guinea pig-derived anti-α_{2C}AR (I) with rabbit-derived anti-DOP (J), rarely colocalized (K,L). **M–P:** Rabbit-derived anti-α_{2C}AR (M) with guinea pig-derived anti-MOP (N), rarely colocalized (O,P). The lack of overlap between α_{2C}AR and MOP was further supported by identical results obtained with rabbit-derived MOP paired with guinea pig-derived α_{2C}AR (data not shown). Scale bars = 100 μm in M (applies to A–C, E–G, I–K, M–O); 5 μm in P (applies to D, H, L, P).

the rat- and the guinea pig-derived SP antibodies (Fig. 4E–H; data not shown). The independent colocalization of α_{2A}AR-ir and DOP-ir with several SP antibodies strongly suggests that the colocalization observed between α_{2A}AR-ir and DOP-ir is not artifactual. Furthermore, DOP-ir and SP-ir colocalization was observed with rabbit- and rat-derived anti-DOP antisera that target different regions of the receptor (Fig. 4E–H,N).

Triple-labeled sections of spinal cord are depicted in Figure 4I–U. Images resulting from each antiserum alone (Fig. 4I–K) and all possible digitally merged pairs (Fig. 4M–O) are shown separately to illustrate the extensive overlap between the antigens. Upon merging of the digital images of sections labeled with all three antisera, triple-labeled elements appear white (Fig. 4L,P). Apparent single fibers were identified that showed α_{2A}AR-ir, DOP-ir, and SP-ir (Fig. 4Q–T). An enlargement of one such fiber demonstrates colocalization of all three markers along the fiber (Fig. 4U).

Colocalization of α_{2A}AR-ir and DOP-ir with SP-ir in rat peripheral nerve terminals

Coincident colocalization of SP-ir was observed with α_{2A}AR-ir and DOP-ir in epidermis (Fig. 5) and dermis (data not shown) of skin obtained from the rat lip. Although direct colocalization of α_{2A}AR-ir and DOP-ir was not possible in peripheral tissues because of technical considerations (the rat-derived DOP antiserum needed for direct α_{2A}AR/DOP costaining is incompatible with peripheral rat tissues), the coincident colocalization of each of the rabbit-derived recep-

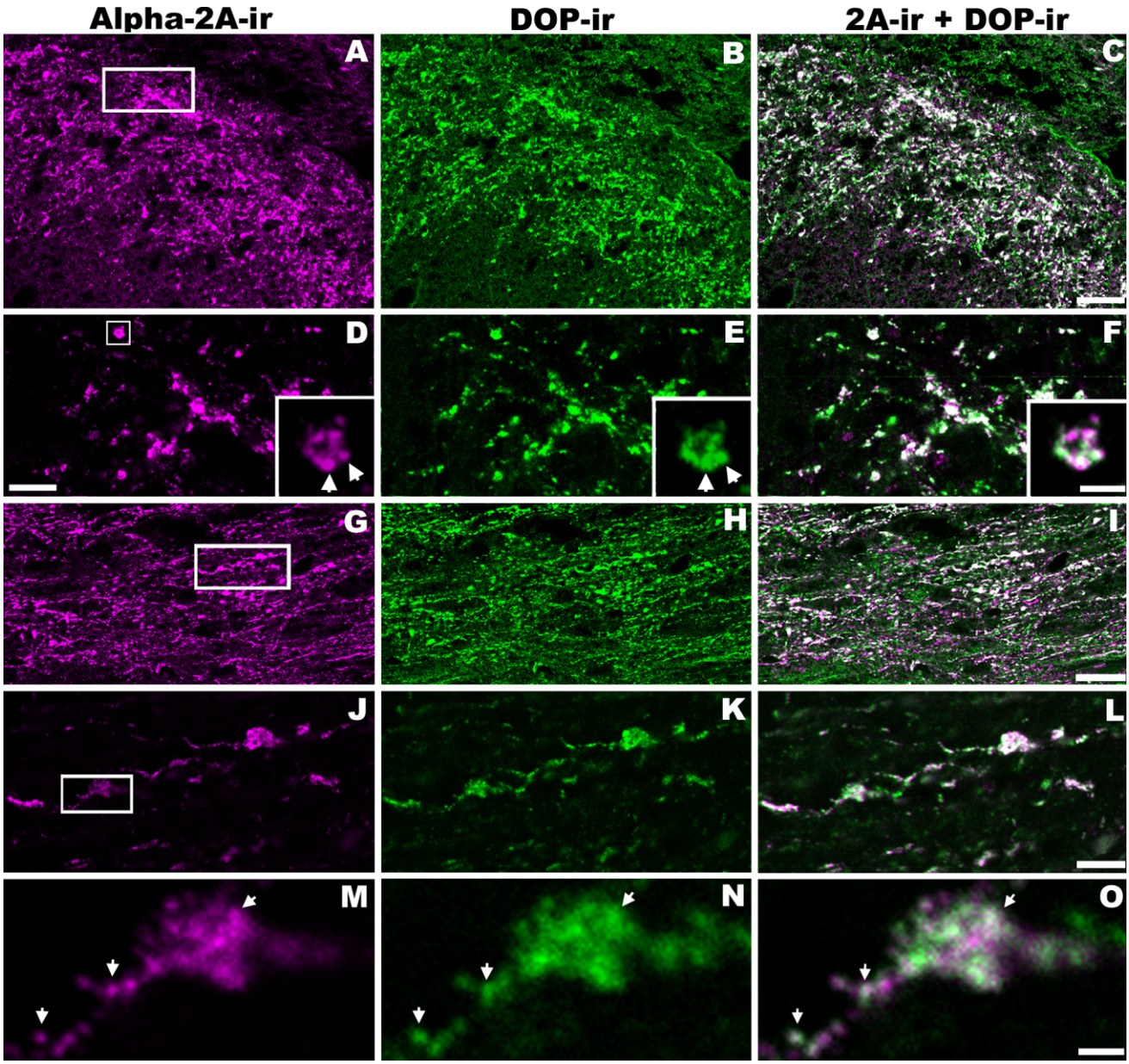

Figure 2.
Close association of DOP-ir and α_{2A}AR-ir in rat spinal cord dorsal horn. Single confocal optical sections of rat spinal cord dorsal horn double labeled with rabbit-derived α_{2A}AR and rat-derived DOP antisera. The first column depicts α_{2A}AR-ir (A,D,G,J,M), and the second column represents DOP-ir (B,E,H,K,N) in the same sections. Pairs of unmerged images illustrate the similarity in expression patterns of α_{2A}AR and DOP. When the images in the first and second columns are digitally merged (C,F,I,L,O), the large proportion of white suggests extensive colocalization. **A–F:** Coronal sections of rat dorsal horn at low (A–C) and higher (D–F) magnification. The **insets** in D–F are enlargements of the boxed area in D. **G–I:** A horizontal section at moderate magnification. **J–L:** Higher magnification images of the boxed area in G. **M–O:** Enlargements of the boxed region in J. Images in D–F (insets) and M–O demonstrate close associations of α_{2A}AR-ir and DOP-ir in the same subcellular regions 0.25 μm or less in diameter (arrows indicate possible vesicles or clusters of vesicles). Scale bars = 20 μm in C (applies to A–C); 5 μm in D (applies to D–F); 20 μm in I (applies to G–I); 5 μm in L (applies to J–L); 1 μm in O (applies to M–O); 1 μm in insets.

tor antisera with SP strongly suggests that α_{2A}AR and DOP colocalize in peripheral nerve terminals.

Localization of α_{2A}AR-ir and DOP-ir to isolated spinal cord synaptosomes

To determine whether α_{2A}AR and DOP are colocalized in nerve terminals, isolated nerve terminals (synaptosomes) obtained from whole rat spinal cords were examined. Colocalization of α_{2A}AR-ir, DOP-ir, and SP-ir was observed within synaptosomes isolated from rat spinal cord (Fig. 6A–G). At the light level, this triple labeling of structural elements within the synaptosome preparation appeared to be localized in substructures less than 0.5 μm in diameter, consistent with localization on presynaptic vesicles.

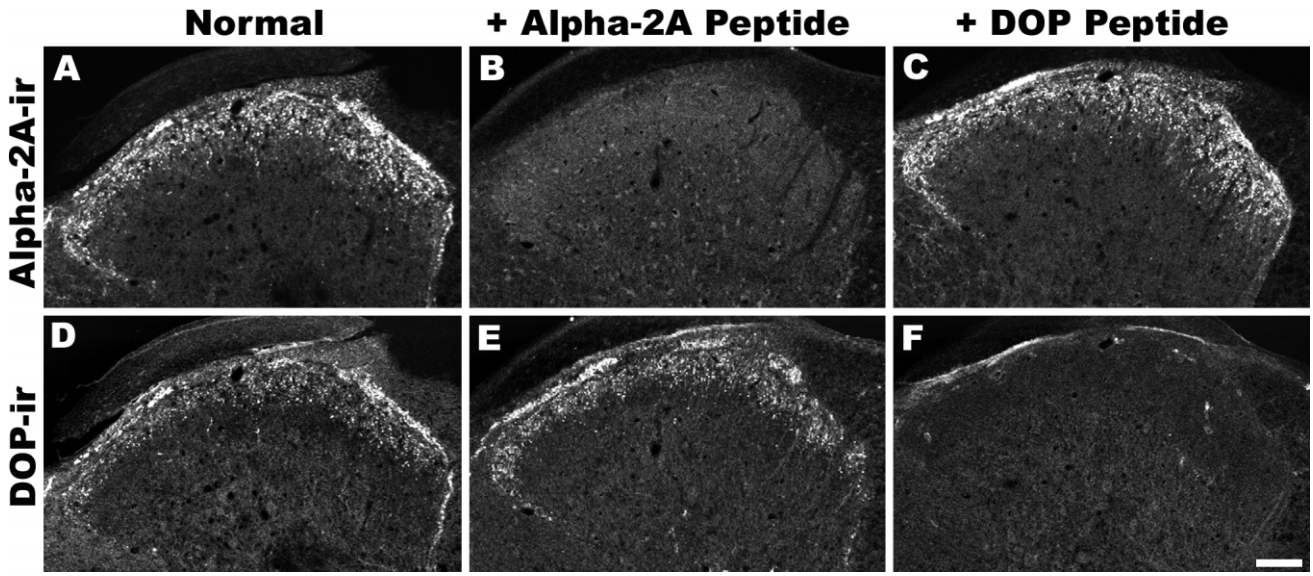

Figure 3.
Cross-reactivity controls for DOP-ir and α_{2A}AR-ir colocalization. Single confocal optical sections show the results of double labeling in the presence or absence of cognate peptide absorption controls in three adjacent sections. Under normal conditions, α_{2A}AR-ir (**A**) and DOP-ir (**D**) exhibit similar patterns of expression. In the presence of its cognate peptide, labeling for α_{2A}AR is absent (**B**), whereas DOP-ir (**E**) is unaffected. Similarly, preincubation with the cognate peptide for the DOP antisera blocks DOP-ir (**F**) but not α_{2A}AR-ir (**C**). Scale bar = 100 μm.

To confirm the localization of DOP and α_{2A}AR to presynaptic nerve terminals, we analyzed the composition of the S1, P2, and synaptosomal fractions obtained during synaptosome preparation by Western blot analysis. According to the subcellular fractionation procedure used, S1 should contain total cell extract minus large structures such as nuclei and cellular debris; P2 is a crude membrane preparation including synaptosomes, mitochondria, and other organelles; and the synaptosomal fraction is enriched in isolated nerve terminals. We observed an ~50-kDa immunoreactive band when probing with the rabbit anti-α_{2A}AR (Fig. 6H) and an ~45-kDa immunoreactive band when probing with the rabbit anti-DOP (Fig. 6I); both bands increase in intensity as the fractions become enriched in nerve terminals.

Although the same amount of protein from each fraction was loaded in each gel, we could not use a typical loading control strategy because the S1, P2, and synaptosomes fractions have different cytosolic to membrane protein ratios. We therefore used a membrane protein marker, pan-cadherin (Fig. 6J), and a cytosolic protein marker, GAPDH (Fig. 6K), to demonstrate the simultaneous enrichment in membrane proteins and depletion in cytosolic proteins as the purification progressed. Consistent with our observations with α_{2A}AR and DOP, the intensity of the immunoreactive pan-cadherin band increased as the samples became enriched in synaptosomes. On the other hand, the GAPDH immunoreactive band intensity decreased from S1 to P2, indicating that cytosolic proteins were lost at this step. The slight increase in GAPDH intensity between P2 and the synaptosome fraction is expected because membrane-bound synaptosomes containing some cytoplasm are segregated from the total membrane fraction, resulting in a relative increase in cytosolic proteins.

The synaptosome preparation used here is known to produce a fraction enriched in nerve endings packed with synaptic vesicles containing numerous neurotransmitters, including SP (Gray and Whittaker, 1962; Fried et al., 1989). Our observation that α_{2A}AR and DOP are both enriched in synaptosomes, together with the previously demonstrated enrichment of SP, further supports the hypothesis that the receptors may be localized in SP-expressing presynaptic nerve terminals in spinal cord dorsal horn.

Greater-than-additive inhibition of neuropeptide release by α_{2A}AR and DOP agonists in spinal cord synaptosomes

We tested our synaptosome preparation for evidence of functional α_{2A}AR and DOP by evaluating the ability of agonists acting at these receptors to inhibit K^+-stimulated release of the neuropeptide CGRP. Upon stimulation of spinal cord synaptosomes with 60 mM K^+, immunoreactive CGRP (iCGRP) was increased from 127 pg/ml to 161 pg/ml. This increase was inhibited in a concentration-dependent manner by the non-α_2AR subtype-selective agonist clonidine and by the DOP agonist deltorphin II (Fig. 7). To determine whether an interaction exists between the receptors in the synaptosome preparation, samples were incubated with both drugs in combination, and the resultant inhibition of K^+-stimulated release was determined. The combination treatment resulted in significant enhancement in both potency and efficacy, suggesting that a synergistic interaction exists between the receptors on isolated spinal nerve terminals.

DISCUSSION

The current study revealed extensive overlap between α_{2A}AR-ir and DOP-ir on SP-expressing primary afferent fibers in the dorsal horn of the rat spinal cord, in rat skin obtained from the lip, and in isolated nerve terminals (synaptosomes)

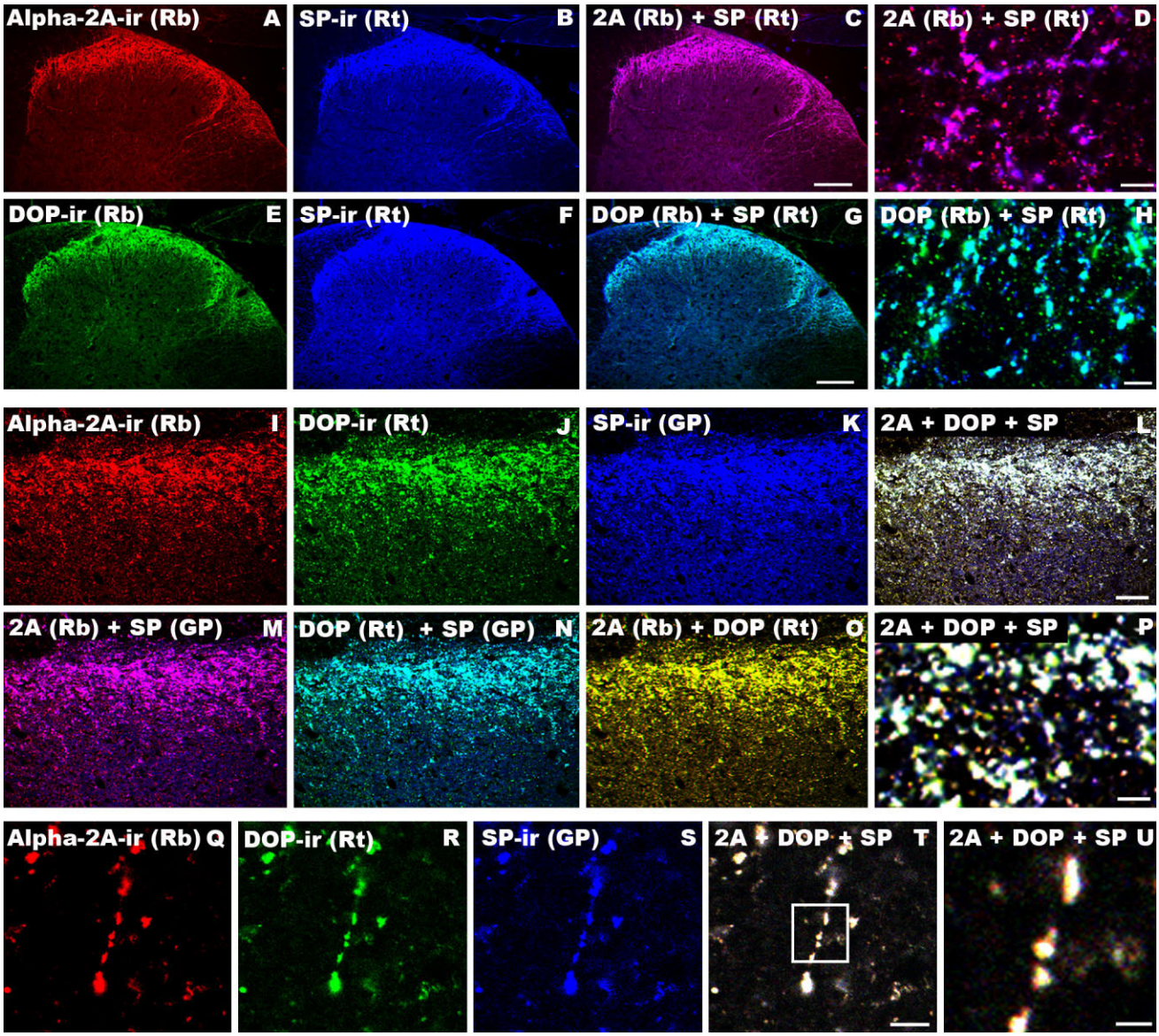

Figure 4.
Triple labeling of α_{2A}AR-ir, DOP-ir, and SP-ir in rat spinal cord dorsal horn. **A–D:** Representative section of rat spinal cord double labeled with rabbit-derived α_{2A}AR (A, red) and rat-derived SP (B, blue) antibodies. When images A and B are digitally merged (C,D), instances of colocalization appear as fuchsia. **E–H:** Representative section of rat spinal cord double labeled with rabbit-derived DOP (E, green) and rat-derived SP (F, blue) antisera. When images E and F are digitally merged (G,H), instances of colocalization appears as turquoise. **I–P:** A single confocal optical section of rat spinal cord triple labeled with rabbit-derived α_{2A}AR (I, red), rat-derived DOP (J, green), and guinea pig-derived SP (K, blue) antisera. Each of the possible digital pairings of these images is shown, where M = α_{2A}AR-ir + SP-ir (colocalization = fuchsia); N = DOP-ir + SP-ir (colocalization = turquoise), and O = α_{2A}AR-ir + DOP-ir (colocalization = yellow). L is the result of digital combination of I–K in which triple-labeled elements appear white. Enlargement of an area from L is shown in P. **Q–U:** Example of a triple-labeled single fiber for α_{2A}AR-ir (Q, red), DOP-ir (R, green), and SP-ir (S, blue). T is the result of digital combination of Q–S in which triple-labeled elements appear white. U is an enlargement the area indicated in T. The close association of all three markers along a single fiber suggests that α_{2A}AR and DOP may be associated with SP-containing presynaptic vesicles. Scale bars = 150 μm in C (applies to A–C); 5 μm in D,H; 150 μm in G (applies to E–G); 20 μm in L (applies to I–O); 5 μm in P; 4 μm in T (applies to Q–T); 1 μm in U.

prepared from whole spinal cord. In contrast, colocalization was not observed between any of the other α_2AR/OR receptor subtype pairs: α_{2A}AR/MOP, α_{2C}AR/MOP, or α_{2C}AR/DOP.

Simultaneous activation of α_{2A}AR and DOP resulted in a greater-than-additive interaction in a functional assay measuring inhibition of K^+-stimulated neuropeptide release in synaptosomes. These data indicate that the synergistic interaction observed in vivo between spinally administered α_{2A}AR and DOP agonists may be mediated at the level of colocalized receptor pairs within single nerve terminals and has significant implications regarding the mechanism(s) underlying that synergy. Although synergy is not a guaranteed consequence of

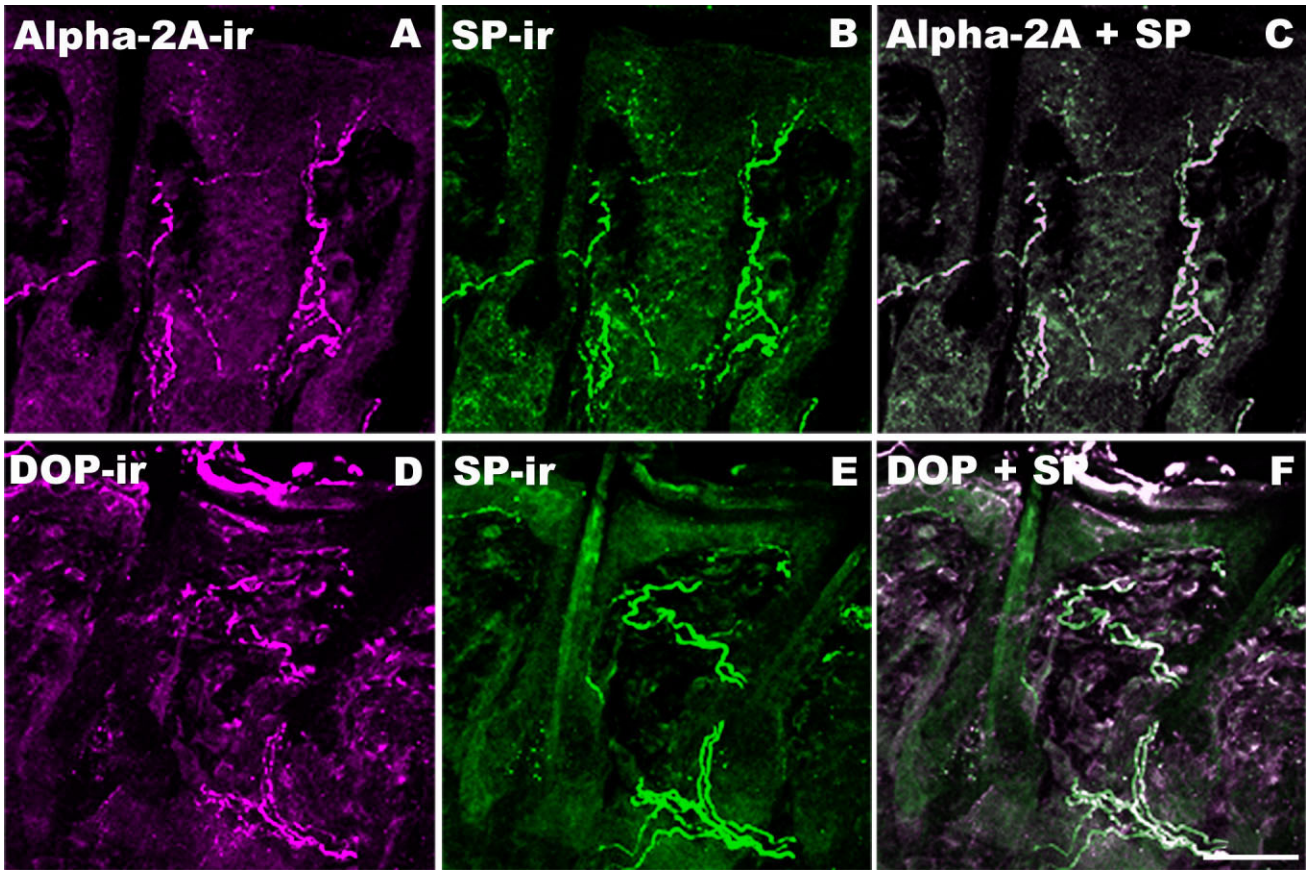

Figure 5.
Colocalization of α_{2A}AR and DOP with SP in rat skin. **A–C:** Representative images of rat lower lip skin double labeled with rabbit-derived α_{2A}AR (A, magenta) and rat-derived SP (B, green) antisera. When images A and B are digitally merged (C), instances of colocalization appears as white. **D–F:** Representative section of rat spinal cord double labeled with rabbit-derived DOP (D, magenta) and guinea pig-derived SP (E, green) antisera. When images D and E are digitally merged (F), instances of colocalization appears as white. The extensive colocalization observed between both α_{2A}AR and DOP with SP suggests that α_{2A}AR and DOP colocalize on SP-containing fibers in the periphery. Scale bar = 50 μm.

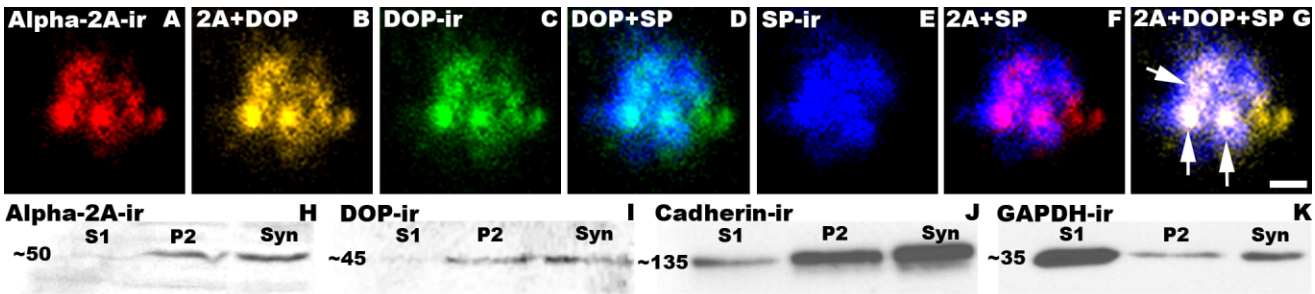

Figure 6.
Labeling of α_{2A}AR-ir, DOP-ir, and SP-ir in spinal cord synaptosomes. **A–G:** Nerve terminals were isolated from rat spinal cord and triple labeled with rabbit-derived α_{2A}AR (A, red), rat-derived DOP (C, green), and guinea pig-derived SP (E, blue) antisera. Each of the possible digital pairings of these images is shown, where B = α_{2A}AR-ir + DOP-ir (colocalization = yellow); D = DOP-ir + SP-ir (colocalization = turquoise); F = α_{2A}AR-ir + SP-ir (colocalization = fuchsia). G is the result of digital combination of A, C, and E in which triple-labeled elements appear white. Arrows in G indicate several structural elements within the synaptosome that are triple labeled. **H–K:** Enrichment of α_{2A}AR-ir and DOP-ir in isolated nerve terminals. Subcellular fractions S1 (total protein), P2 (membrane fraction), and Syn (synaptosomes) were analyzed by Western blot. Immunoreactive bands for anti-α_{2A}AR (~50 kDa), anti-DOP (~45 kDa), and the membrane marker pan-cadherin (~135 kDa) were all enriched in the purified membrane and synaptosome fractions. The cytosolic marker GAPDH was most abundant in the S1 fraction (~35 kDa). Scale bar in G (applies to A–G) = 2 μm.

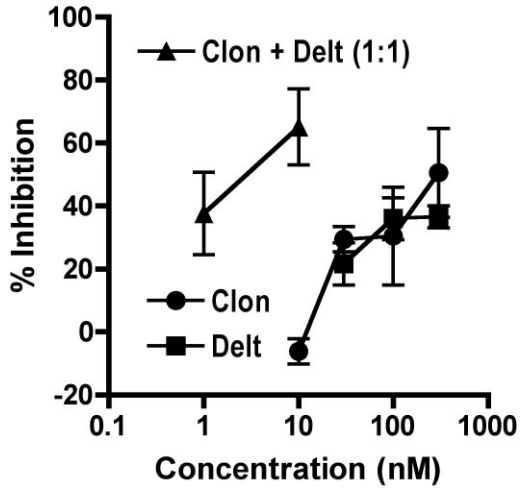

Figure 7.
Inhibition of neuropeptide release by α_2AR and DOR agonists in spinal cord synaptosomes. Synaptosomes were exposed to vehicle, the α_2AR agonist clonidine (circles), the DOP agonist deltorphin II (squares), or the combination of clonidine + deltorphin II (triangles) and stimulated with 60 mM K^+. Clonidine and deltorphin II inhibited calcitonin gene-related peptide (CGRP) release in a concentration-dependent manner. Coincubation with both agonists together resulted in enhanced effectiveness over either agonist alone. Error bars represent ± SEM for each concentration (n = 3 replicates/concentration).

colocalization, the synergy observed here in isolated synaptic terminals strongly argues for colocalization at the level of primary afferent terminals in a manner not dependent on the specificity of receptor-directed antisera; synergy is unlikely to have occurred if the receptors were localized in separate terminals.

DOP and α_{2A}AR colocalization in primary afferent nerve terminals

The extensive overlap between α_{2A}AR-ir and DOP-ir in SP-containing fibers and nerve terminals is consistent with previous reports localizing DOP-ir and α_{2A}AR-ir to peptidergic primary afferent fibers (Dado et al., 1993; Arvidsson et al., 1995a; Stone et al., 1998; Zhang et al., 1998). The presence of SP suggests that these are likely to be C- or A-delta fibers (Lawson et al., 1993). Spinal α_{2A}AR-ir and DOP-ir have both been shown to be decreased following dorsal rhizotomy, suggesting that a major source of these receptors in the spinal cord is the central terminals of primary afferent fibers (Dado et al., 1993; Stone et al., 1998). Similarly, autoradiographic labeling showed that most DOP receptor binding is lost after unilateral dorsal rhizotomy (Besse et al., 1990). The observation in the current study that both DOP-ir and α_{2A}AR-ir colocalize with SP-ir in peripheral nerve terminals in skin strongly suggests that SP-expressing, dorsal root ganglion neurons express DOP and α_{2A}AR and traffic both receptors to both central and peripheral nerve terminals. The examples of colocalization obtained using double- or triple-labeled immunofluorescence histochemistry presented here most likely represents colocalization rather than superposition, because the estimated thickness of the high-magnification optical sections (<1.0 μm) minimizes the possibility of superposition of terminals with dimensions of 1–2 μm. However, light microscopy lacks the resolution required to 1) confirm colocalization within the same neuronal structures and 2) identify the nature of DOP-ir and α_{2A}AR-ir structures (e.g., axons vs. nerve terminals). Further studies examining the anatomical relationship between DOP-ir and α_{2A}AR-ir at the ultrastructural level within spinal cord are necessary to confirm and extend the present data.

The immunohistochemical demonstration of colocalization of both receptors and SP-ir in isolated nerve terminals (Fig. 6) is augmented by the enrichment of both receptor immunoreactivities shown in the synaptosomal fraction by Western blot and by the supraadditive interaction observed between agonists targeting the two receptors. Although the synaptosomes in this study were isolated from whole spinal cord, the colocalization of α_{2A}AR-ir and DOP-ir with SP-ir in both superficial dorsal horn and in the synaptosome preparation indicates that a subset of the isolated nerve terminals is derived from SP-ir terminals. In addition, the inhibition of CGRP-ir by α_2AR and DOP agonists in the synaptosome preparation suggests that their site of action is the terminals of primary afferent fibers, because dorsal root ganglia neurons are thought to be the only source of CGRP within the spinal cord (Chung et al., 1988).

The following observations support the hypothesis that DOP/α_{2A}AR colocalization is not due to cross-reactivity between anti-DOP and anti-α_{2A}AR antisera: 1) α_{2A}AR-ir and DOP-ir coexisted with SP-ir in the presence and absence of antisera to the other receptor. In the case of α_{2A}AR/SP, colocalization was observed with the rabbit-derived anti-α_{2A}AR antiserum and both rat- and guinea pig-derived SP antibodies. In the case of DOP/SP, two DOP antisera, each raised in a different species against a different region of the receptor, colocalized with two different SP antibodies (rabbit-DOP with rat and guinea pig SP, rat-DOP with rabbit and guinea pig SP). 2) Colocalization was abolished by the omission of either the DOP or the α_{2A}AR antisera. 3) Colocalization was abolished by preadsorption of either the DOP or the α_{2A}AR antisera with the respective cognate peptides.

Functional studies further support the localization patterns of α_{2A}AR and DOP observed in the current study. Activation of both α_2ARs and ORs has been shown to inhibit release of excitatory neurotransmitters (Jessell and Iversen, 1977; Kuraishi et al., 1985; Kamisaki et al., 1993; Takano et al., 1993; Zachariou and Goldstein, 1996; Li and Eisenach, 2001) and to reduce excitatory neurotransmission from primary afferent fibers onto neurons in the superficial dorsal horn (Glaum et al., 1994; Kohno et al., 1999; Kawasaki et al., 2003; Sonohata et al., 2004; Kondo et al., 2005). Spinal analgesic synergy between DOP and α_{2A}AR agonists has been previously documented (Stone et al., 1997). In the current study, we demonstrate inhibition of CGRP release from spinal cord synaptosomes by α_2AR and DOP agonists, consistent with prior reports, and found a greater-than-additive interaction between these agonists. This greater-than-additive interaction in synaptosomes, where no neuronal circuitry remains intact, further supports colocalization at the terminal level, because coactivation of receptors localized in separate CGRP-positive synaptosomes could result only in an additive interaction. These data also indicate that synergistic interactions observed in vivo between α_{2A}AR and DOP likely occur at

the level of colocalized receptor pairs within single nerve terminals.

Lack of colocalization of α_{2A}AR/MOP, α_{2C}AR/MOP, or α_{2C}AR/DOP in rat spinal cord

Synergy between MOP and α_2AR agonists has been widely reported (Sullivan et al., 1987, 1992; Wilcox et al., 1987; Ossipov et al., 1989, 1990a–c, 1997; Stone et al., 1997; Fairbanks et al., 2000a,b, 2002; Guo et al., 2003). The present study did not detect colocalization of MOP-ir with either α_{2A}AR-ir or α_{2C}AR-ir. One possible interpretation of this finding is that synergy between noncolocalized receptor pairs relies on multicellular mechanisms that have not yet been elucidated. An alternative possibility is that the antisera used in this study do not recognize their target receptors in all possible cellular environments or in all forms.

The lack of coexpression between MOP-ir and either α_{2A}AR-ir or DOP-ir (or SP; data not shown) is potentially surprising. First, functional studies have shown that incubation with morphine results in receptor-mediated inhibition of neuropeptide release in vitro in slices of spinal trigeminal nucleus (Jessell and Iversen, 1977) and in vivo following intrathecal administration (Yaksh et al., 1980). This inhibition is thought to result from activation of both MOP and DOP (Kondo et al., 2005). Second, anatomical studies clearly localize MOP to the cell bodies and/or central terminals of primary afferent neurons by mRNA (Mansour et al., 1995), autoradiography (Besse et al., 1990), and immunohistochemisty (Arvidsson et al., 1995b). However, careful examination of the relationship between MOP-ir and SP-ir in the spinal cord revealed that colocalization is only occasionally detected (Ding et al., 1995). In fact, the percentages of SP-ir terminals in trigeminal and cervical spinal cord that were also MOP-ir were only 12% and 6%, respectively (Aicher et al., 2000). In contrast, SP-ir terminals are often (>50%) contacted by MOP-ir dendrites (Aicher et al., 2000). The apparent contradiction inherent in the aforementioned studies may be explained by the existence of MOP splice variants. Specifically, in the superficial laminae of the rat spinal cord, immunoreactivity produced by antisera generated against the MOP-1C splice variant differed from that of MOP-1 despite being derived from the same gene (Abbadie et al., 2000); whereas MOP-1 rarely colocalized with SP-ir or CGRP-ir, MOP-1C-ir was often colocalized with CGRP. In the current study, we used an antibody directed against MOP-1 and not MOP-1C. It is therefore possible that DOP and α_{2A}AR will be found in future studies to coexist with MOP-1C, and this colocalization may provide another anatomical substrate for synergistic receptor interactions.

In addition to MOP, other antisera used in this study may not recognize their target receptors in all possible cellular environments or in all forms. The presence of mRNA encoding α_{2A}AR in spinal cord neurons stands in contrast to the absence of immunohistochemical staining (Shi et al., 1999), and different DOP antibodies differentially label somatodendritic vs. axonal compartments (Cahill et al., 2001a). The absence of colocalization between any of the other α_2AR/OP receptor subtype pairs (α_{2A}AR/MOP, α_{2C}AR/MOP, and α_{2C}AR/DOP) may therefore be attributable to technical limitations of the antisera used rather than an absence of colocalization. Furthermore, the use of fluorescence for the detection of immunoreactivity may result in under- or over-representation of fiber subtypes.

Regardless, the possibility that our antisera did not recognize all forms of the receptors under evaluation does not detract from the significance of the positive colocalization results; the triple labeling reported in this study is likely to represent expression of both DOP and α_{2A}AR within the same SP-expressing neuronal processes.

Implications of DOP and α_{2A}AR colocalization

The current results suggest an anatomical substrate for the formation of α_{2A}AR and DOP heterooligomers in vivo. Such associations between GPCRs have been shown to result in novel pharmacological properties distinct from either component receptor, including enhancement of ligand binding affinity, changes in functional coupling, and altered receptor trafficking (for reviews see George et al., 2002; Bulenger et al., 2005). Thus, the generation of novel properties upon α_{2A}AR and DOP heterooligomer formation may represent a molecular mechanism for the synergistic interactions previously observed between these receptors in vivo and that we report here in vitro. Physical associations suggestive of heterooligomer formation have been demonstrated between α_{2A}ARs and both DOP and MOP in transfected cells in vitro (Jordan et al., 2003; Rios et al., 2004; Zhang and Limbird, 2004; Vilardaga et al., 2008). The relevance of these in vitro studies to spinal α_{2A}AR-DOP synergy requires the expression of both receptors within the same subcellular structures in native tissues as well as the demonstration of a functional interaction that can be attributed to that cellular localization. The combination of the previous in vitro studies and the current findings provide a structural and functional framework for the existence of α_{2A}AR and DOP heterooligomers in vivo.

DOP-ir is associated with large, dense-core vesicles (LDCVs) in axon terminals, and ultrastructural evidence exists that these vesicles contain SP (Cheng et al., 1995; Zhang et al., 1998; Bao et al., 2003; Guan et al., 2005). It is thought that DOPs are trafficked to axon terminals in the membranes of these vesicles, where they may be inserted into the plasma membrane in a stimulus-dependent manner (Bao et al., 2003; Guan et al., 2005). DOP availability for binding and activation by extracellular ligands in the terminal is regulated, at least in part, by LDCV release. In addition to direct stimulation, DOP may be translocated to the plasma membrane in response to DOP agonists, chronic morphine exposure, peripheral inflammation, inflammatory mediators, and chronic nociceptive stimuli (Cahill et al., 2001b; Bao et al., 2003; Morinville et al., 2003, 2004a,b; Guan et al., 2005; Hack et al., 2005; Lucido et al., 2005; Patwardhan et al., 2005; Gendron et al., 2006, 2007). As a consequence, sensitivity to DOP agonists is increased. For example, Cahill and colleagues (2001b) demonstrated an increase in both intrathecal DOP agonist-induced analgesia and the number of plasma membrane-associated DOP-ir particles after chronic morphine treatment. This stimulus-triggered exocytosis and consequent surface insertion of DOP are reported to be dependent on the SP domain of preprotachykinin A present in DOP-containing LDCVs (Guan et al., 2005).

We report here that both DOP-ir and α_{2A}AR-ir are highly colocalized with SP-ir at the light microscope level in primary afferent fiber terminals in both skin and spinal cord. This three-way colocalization raises two possibilities: 1) the α_{2A}AR is trafficked and stored within the same vesicles that contain SP and DOP (Zhang et al., 1998), and 2) the availability of

α_{2A}AR on the plasma membrane is controlled by the same regulatory factors that control DOP availability. Evaluation of these possibilities will require further anatomical studies by electron microscopy. We hypothesize that DOP agonist-mediated translocation of DOP will also result in translocation and subsequent enhanced availability of α_{2A}AR. The presence of a small amount of the DOP agonist deltorphin-II would potentially result in a dramatic increase in α_{2A}AR agonist efficacy as a result of vesicle fusion and receptor translocation. This scenario would similarly apply if α_{2A}AR agonists cause vesicle fusion and receptor translocation in a manner similar to that already demonstrated for DOP agonists, resulting in mutual potentiation between DOP and α_{2A}AR. This proposed model for DOP-α_{2A}AR synergy is based entirely on cooperative receptor trafficking and would predict a greater-than-additive interaction between DOP-α_{2A}AR in isolated synaptosomes, as we currently demonstrate, and represents an alternative hypothesis regarding the mechanism(s) underlying synergy that is supported by the current findings.

CONCLUSIONS

This study provides definitive evidence of extensive colocalization between α_{2A}AR and DOP in SP-containing peripheral and central nerve terminals. α_{2A}AR/DOP colocalization can be observed in axonal terminals and isolated nerve terminals. Agonists acting at α_2AR and DOP inhibited K^+-induced neuropeptide release from synaptosomes and interacted in a greater-than-additive manner, indicating a synergistic interaction. This supraadditive interaction in isolated nerve terminals provides a functional implication to the immunohistochemically demonstrated receptor colocalization. Taken together, these data raise the possibility that DOP and α_{2A}AR heterooligomeric receptor complexes could exist in vivo and may represent a molecular substrate for the analgesic synergy commonly observed between agonists acting at these receptors.

ACKNOWLEDGMENTS

We thank Jeromy Dooyema, Cory Goracke-Postle, and H. Oanh Nguyen for technical support; Drs. Martin W. Wessendorf, Carolyn A. Fairbanks, and Lucy Vulchanova for valuable discussions; and Dr. Martin W. Wessendorf for use of the rat-derived anti-DOR antiserum.

LITERATURE CITED

Aantaa R, Marjamaki A, Scheinin M. 1995. Molecular pharmacology of alpha 2-adrenoceptor subtypes. Ann Med 27:439–449.

Abbadie C, Pan YX, Pasternak GW. 2000. Differential distribution in rat brain of mu opioid receptor carboxy terminal splice variants MOR-1C-like and MOR-1-like immunoreactivity: evidence for region-specific processing. J Comp Neurol 419:244–256.

Aicher SA, Sharma S, Cheng PY, Liu-Chen LY, Pickel VM. 2000. Dual ultrastructural localization of mu-opiate receptors and substance P in the dorsal horn. Synapse 36:12–20.

Alguacil LF, Morales L. 2004. Alpha-2 adrenoceptor ligands and opioid drugs: pharmacological interactions of therapeutic interest. Curr Neuropharmacol 2:343–352.

Arvidsson U, Dado RJ, Riedl M, Lee JH, Law PY, Loh HH, Elde R, Wessendorf MW. 1995a. Delta-opioid receptor immunoreactivity: distribution in brain stem and spinal cord and relationship to biogenic amines and enkephalin. J Neurosci 15:1215–1235.

Arvidsson U, Riedl M, Chakrabarti S, Lee JH, Nakano AH, Dado RJ, Loh HH, Law PY, Wessendorf MW, Elde R. 1995b. Distribution and targeting of a mu-opioid receptor (MOR1) in brain and spinal cord. J Neurosci 15:3328–3341.

Bao L, Jin SX, Zhang C, Wang LH, Xu ZZ, Zhang FX, Wang LC, Ning FS, Cai HJ, Guan JS, Xiao HS, Xu ZQ, He C, Hokfelt T, Zhou Z, Zhang X. 2003. Activation of delta opioid receptors induces receptor insertion and neuropeptide secretion. Neuron 37:121–133.

Besse D, Lombard MC, Zajac JM, Roques BP, Besson JM. 1990. Pre- and postsynaptic distribution of mu, delta and kappa opioid receptors in the superficial layers of the cervical dorsal horn of the rat spinal cord. Brain Research 521:15–22.

Bulenger S, Marullo S, Bouvier M. 2005. Emerging role of homo- and heterodimerization in G-protein-coupled receptor biosynthesis and maturation. Trends Pharmacol Sci 26:131–137.

Cahill CM, McClellan KA, Morinville A, Hoffert C, Hubatsch D, O'Donnell D, Beaudet A. 2001a. Immunohistochemical distribution of delta opioid receptors in the rat central nervous system: evidence for somatodendritic labeling and antigen-specific cellular compartmentalization. J Comp Neurol 440:65–84.

Cahill CM, Morinville A, Lee MC, Vincent JP, Collier B, Beaudet A. 2001b. Prolonged morphine treatment targets delta opioid receptors to neuronal plasma membranes and enhances delta-mediated antinociception. J Neurosci 21:7598–7607.

Cheng PY, Svingos AL, Wang H, Clarke CL, Jenab S, Beczkowska IW, Inturrisi CE, Pickel VM. 1995. Ultrastructural immunolabeling shows prominent presynaptic vesicular localization of delta-opioid receptor within both enkephalin- and nonenkephalin-containing axon terminals in the superficial layers of the rat cervical spinal cord. J Neurosci 15:5976–5988.

Chung K, Lee WT, Carlton SM. 1988. The effects of dorsal rhizotomy and spinal cord isolation on calcitonin gene-related peptide-labeled terminals in the rat lumbar dorsal horn. Neurosci Lett 90:27–32.

Cuello AC, Galfre G, Milstein C. 1979. Detection of substance P in the central nervous system by a monoclonal antibody. Proc Natl Acad Sci U S A 76:3532–3536.

Dado RJ, Law PY, Loh HH, Elde R. 1993. Immunofluorescent identification of a delta (delta)-opioid receptor on primary afferent nerve terminals. Neuroreport 5:341–344.

Ding YQ, Nomura S, Kaneko T, Mizuno N. 1995. Colocalization of mu-opioid receptor-like and substance P-like immunoreactivities in axon terminals within the superficial layers of the medullary and spinal dorsal horns of the rat. Neurosci Lett 198:45–48.

Fairbanks CA, Nguyen HO, Grocholski BM, Wilcox GL. 2000a. Moxonidine, a selective imidazoline-alpha2-adrenergic receptor agonist, produces spinal synergistic antihyperalgesia with morphine in nerve-injured mice. Anesthesiology 93:765–773.

Fairbanks CA, Posthumus IJ, Kitto KF, Stone LS, Wilcox GL. 2000b. Moxonidine, a selective imidazoline/alpha(2) adrenergic receptor agonist, synergizes with morphine and deltorphin II to inhibit substance P-induced behavior in mice. Pain 84:13–20.

Fairbanks CA, Stone LS, Kitto KF, Nguyen HO, Posthumus IJ, Wilcox GL. 2002. Alpha(2C)-adrenergic receptors mediate spinal analgesia and adrenergic-opioid synergy. J Pharmacol Exp Ther 300:282–290.

Fried G, Franck J, Brodin E, Born W, Fischer JA, Hiort W, Hokfelt T. 1989. Evidence for differential storage of calcitonin gene-related peptide, substance P and serotonin in synaptosomal vesicles of rat spinal cord. Brain Res 499:315–324.

Gendron L, Lucido AL, Mennicken F, O'Donnell D, Vincent JP, Stroh T, Beaudet A. 2006. Morphine and pain-related stimuli enhance cell surface availability of somatic delta-opioid receptors in rat dorsal root ganglia. J Neurosci 26:953–962.

Gendron L, Esdaile MJ, Mennicken F, Pan H, O'Donnell D, Vincent JP, Devi LA, Cahill CM, Stroh T, Beaudet A. 2007. Morphine priming in rats with chronic inflammation reveals a dichotomy between antihyperalgesic and antinociceptive properties of deltorphin. Neuroscience 144:263–274.

George SR, O'Dowd BF, Lee SP. 2002. G-protein-coupled receptor oligomerization and its potential for drug discovery. Nat Rev Drug Discov 1:808–820.

Glaum SR, Miller RJ, Hammond DL. 1994. Inhibitory actions of delta 1-, delta 2-, and mu-opioid receptor agonists on excitatory transmission in lamina II neurons of adult rat spinal cord. J Neurosci 14:4965–4971.

Goracke-Postle CJ, Nguyen HO, Stone LS, Fairbanks CA. 2006. Release of tritiated agmatine from spinal synaptosomes. Neuroreport 17:13–17.

Goracke-Postle CJ, Overland AC, Riedl MS, Stone LS, Fairbanks CA.

2007. Potassium- and capsaicin-induced release of agmatine from spinal nerve terminals. J Neurochem 102:1738–1748.

Gray EG, Whittaker VP. 1962. The isolation of nerve endings from brain: an electron-microscopic study of cell fragments derived by homogenization and centrifugation. J Anat 96:79–88.

Guan JS, Xu ZZ, Gao H, He SQ, Ma GQ, Sun T, Wang LH, Zhang ZN, Lena I, Kitchen I, Elde R, Zimmer A, He C, Pei G, Bao L, Zhang X. 2005. Interaction with vesicle luminal protachykinin regulates surface expression of delta-opioid receptors and opioid analgesia. Cell 122:619–631.

Guo XH, Fairbanks CA, Stone LS, Loh HH. 2003. DPDPE-UK14,304 synergy is retained in mu opioid receptor knockout mice. Pain 104:209–217.

Hack SP, Bagley EE, Chieng BC, Christie MJ. 2005. Induction of delta-opioid receptor function in the midbrain after chronic morphine treatment. J Neurosci 25:3192–3198.

Ho RH, DePalatis LR. 1980. Substance P immunoreactivity in the median eminence of the North American opossum and domestic fowl. Brain Res 189:565–569.

Hylden JL, Wilcox GL. 1983. Pharmacological characterization of substance P-induced nociception in mice: modulation by opioid and noradrenergic agonists at the spinal level. J Pharmacol Exp Ther 226:398–404.

Jessell TM, Iversen LL. 1977. Opiate analgesics inhibit substance P release from rat trigeminal nucleus. Nature 286:549–551.

Jordan BA, Gomes I, Rios C, Filipovska J, Devi LA. 2003. Functional interactions between mu opioid and alpha 2A-adrenergic receptors. Mol Pharmacol 64:1317–1324.

Kamisaki Y, Hamada T, Maeda K, Ishimura M, Itoh T. 1993. Presynaptic alpha 2 adrenoceptors inhibit glutamate release from rat spinal cord synaptosomes. J Neurochem 60:522–526.

Kawasaki Y, Kumamoto E, Furue H, Yoshimura M. 2003. Alpha 2 adrenoceptor-mediated presynaptic inhibition of primary afferent glutamatergic transmission in rat substantia gelatinosa neurons. Anesthesiology 98:682–689.

Kieffer BL. 1999. Opioids: first lessons from knockout mice [review]. Trends Pharmacol Sci 20:19–26.

Kohno T, Kumamoto E, Higashi H, Shimoji K, Yoshimura M. 1999. Actions of opioids on excitatory and inhibitory transmission in substantia gelatinosa of adult rat spinal cord. J Physiol 518:803–813.

Kondo I, Marvizon JC, Song B, Salgado F, Codeluppi S, Hua XY, Yaksh TL. 2005. Inhibition by spinal mu- and delta-opioid agonists of afferent-evoked substance P release. J Neurosci 25:3651–3660.

Kuraishi Y, Hirota N, Sato Y, Kaneko S, Satoh M, Takagi H. 1985. Noradrenergic inhibition of the release of substance P from the primary afferents in the rabbit spinal dorsal horn. Brain Res 359:177–182.

Lai J, Riedl M, Stone LS, Arvidsson U, Bilsky EJ, Wilcox GL, Elde R, Porreca F. 1996. Immunofluorescence analysis of antisense oligodeoxynucleotide-mediated "knock-down" of the mouse delta opioid receptor in vitro and in vivo. Neurosci Lett 213:205–208.

Law PY, Loh HH. 1999. Regulation of opioid receptor activities [review]. J Pharmacol Exp Ther 289:607–624.

Lawson SN, Perry MJ, Prabhakar E, McCarthy PW. 1993. Primary sensory neurones: neurofilament, neuropeptides, and conduction velocity. Brain Res Bull 30:239–243.

Li X, Eisenach JC. 2001. Alpha2A-adrenoceptor stimulation reduces capsaicin-induced glutamate release from spinal cord synaptosomes. J Pharmacol Exp Ther 299:939–944.

Lucido AL, Morinville A, Gendron L, Stroh T, Beaudet A. 2005. Prolonged morphine treatment selectively increases membrane recruitment of delta-opioid receptors in mouse basal ganglia. J Mol Neurosci 25:207–214.

MacDonald E, Kobilka BK, Scheinin M. 1997. Gene targeting—homing in on alpha 2-adrenoceptor-subtype function. Trends Pharmacol Sci 18: 211–219.

Mansour A, Fox CA, Akil H, Watson SJ. 1995. Opioid-receptor mRNA expression in the rat CNS: anatomical and functional implications. Trends Neurosci 18:22–29.

Monasky MS, Zinsmeister AR, Stevens CW, Yaksh TL. 1990. Interaction of intrathecal morphine and ST-91 on antinociception in the rat: dose-response analysis, antagonism and clearance. J Pharmacol Exp Ther 254:383–392.

Morinville A, Cahill CM, Esdaile MJ, Aibak H, Collier B, Kieffer BL, Beaudet A. 2003. Regulation of delta-opioid receptor trafficking via mu-opioid receptor stimulation: evidence from mu-opioid receptor knock-out mice. J Neurosci 23:4888–4898.

Morinville A, Cahill CM, Aibak H, Rymar VV, Pradhan A, Hoffert C, Mennicken F, Stroh T, Sadikot AF, O'Donnell D, Clarke PB, Collier B, Henry JL, Vincent JP, Beaudet A. 2004a. Morphine-induced changes in delta opioid receptor trafficking are linked to somatosensory processing in the rat spinal cord. J Neurosci 24:5549–5559.

Morinville A, Cahill CM, Kieffer B, Collier B, Beaudet A. 2004b. Mu-opioid receptor knockout prevents changes in delta-opioid receptor trafficking induced by chronic inflammatory pain. Pain 109:266–273.

Omote K, Kitahata L, Collins J, Nakatani K, Nakagawa I. 1990. The antinociceptive role of μ and delta-opiate receptors and their interactions in the spinal dorsal horns of cats. Anesth Analg 71:23–28.

Ossipov MH, Suarez LJ, Spaulding TC. 1989. Antinociceptive interactions between alpha 2-adrenergic and opiate agonists at the spinal level in rodents. Anesth Analg 68:194–200.

Ossipov MH, Harris S, Lloyd P, Messineo E. 1990a. An isobolographic analysis of the antinociceptive effect of systemically and intrathecally administered combinations of clonidine and opiates. J Pharmacol Exp Ther 255:1107–1116.

Ossipov MH, Harris S, Lloyd P, Messineo E, Lin BS, Bagley J. 1990b. Antinociceptive interaction between opioids and medetomidine: systemic additivity and spinal synergy. Anesthesiology 73:1227–1235.

Ossipov MH, Lozito R, Messineo E, Green J, Harris S, Lloyd P. 1990c. Spinal antinociceptive synergy between clonidine and morphine, U69593, and DPDPE: isobolographic analysis. Life Sci 47:PL71–PL76.

Ossipov MH, Lopez Y, Bian D, Nichols ML, Porreca F. 1997. Synergistic antinociceptive interactions of morphine and clonidine in rats with nerve-ligation injury. Anesthesiology 86:1–9.

Patwardhan AM, Berg KA, Akopain AN, Jeske NA, Gamper N, Clarke WP, Hargreaves KM. 2005. Bradykinin-induced functional competence and trafficking of the delta-opioid receptor in trigeminal nociceptors. J Neurosci 25:8825–8832.

Philipp M, Brede M, Hein L. 2002. Physiological significance of alpha(2)-adrenergic receptor subtype diversity: one receptor is not enough. Am J Physiol Regul Integr Comp Physiol 283:R287–R295.

Rios C, Gomes I, Devi LA. 2004. Interactions between delta opioid receptors and alpha-adrenoceptors. Clin Exp Pharmacol Physiol 31:833–836.

Roerig SC, Lei S, Kitto K, Hylden JK, Wilcox GL. 1992. Spinal interactions between opioid and noradrenergic agonists in mice: multiplicativity involves delta and alpha-2 receptors. J Pharmacol Exp Ther 262:365–374.

Shi TJS, Winzer-Serhan U, Leslie F, Hokfelt T. 1999. Distribution of alpha(2)-adrenoceptor mRNAs in the rat lumbar spinal cord in normal and axotomized rats. Neuroreport 10:2835–2839.

Sonohata M, Furue H, Katafuchi T, Yasaka T, Doi A, Kumamoto E, Yoshimura M. 2004. Actions of noradrenaline on substantia gelatinosa neurones in the rat spinal cord revealed by in vivo patch recording. J Physiol 555:515–526.

Stevens CW, Monasky MS, Yaksh TL. 1988. Spinal infusion of opiate and alpha-2 agonists in rats: tolerance and cross-tolerance studies. J Pharmacol Exp Ther 244:63–70.

Stone LS, MacMillan LB, Kitto KF, Limbird LE, Wilcox GL. 1997. The alpha2a adrenergic receptor subtype mediates spinal analgesia evoked by alpha2 agonists and is necessary for spinal adrenergic-opioid synergy. J Neurosci 17:7157–7165.

Stone LS, Broberger C, Vulchanova L, Wilcox GL, Hokfelt T, Riedl MS, Elde R. 1998. Differential distribution of alpha2A and alpha2C adrenergic receptor immunoreactivity in the rat spinal cord. J Neurosci 18:5928–5937.

Sullivan AF, Dashwood MR, Dickenson AH. 1987. Alpha 2-adrenoceptor modulation of nociception in rat spinal cord: location, effects and interactions with morphine. Eur J Pharmacol 138:169–177.

Sullivan AF, Kalso EA, McQuay HJ, Dickenson AH. 1992. Evidence for the involvement of the mu but not delta opioid receptor subtype in the synergistic interaction between opioid and alpha 2 adrenergic antinociception in the rat spinal cord. Neurosci Lett 139:65–68.

Takano M, Takano Y, Yaksh TL. 1993. Release of calcitonin gene-related peptide (CGRP), substance P (SP), and vasoactive intestinal polypeptide (VIP) from rat spinal cord: modulation by alpha 2 agonists. Peptides 14:371–378.

Vilardaga JP, Nikolaev VO, Lorenz K, Ferrandon S, Zhuang Z, Lohse MJ. 2008. Conformational cross-talk between alpha2A-adrenergic and mu-opioid receptors controls cell signaling. Nat Chem Biol 4:126–131.

Walker SM, Goudas LC, Cousins MJ, Carr DB. 2002. Combination spinal

analgesic chemotherapy: a systematic review. Anesth Analg 95:674–715.

Wessendorf MW, Elde RP. 1985. Characterization of an immunofluorescence technique for the demonstration of coexisting neurotransmitters within nerve fibers and terminals. J Histochem Cytochem 33:984–994.

Wilcox GL, Carlsson KH, Jochim A, Jurna I. 1987. Mutual potentiation of antinociceptive effects of morphine and clonidine on motor and sensory responses in rat spinal cord. Brain Res 405:84–93.

Yaksh TL, Jessell TM, Gamse R, Mudge AW, Leeman SE. 1980. Intrathecal morphine inhibits substance P release from mammalian spinal cord in vivo. Nature 286:155–157.

Zachariou V, Goldstein BD. 1996. Delta-opioid receptor modulation of the release of substance P-like immunoreactivity in the dorsal horn of the rat following mechanical or thermal noxious stimulation. Brain Res 736:305–314.

Zhang X, Bao L, Arvidsson U, Elde R, Hokfelt T. 1998. Localization and regulation of the delta-opioid receptor in dorsal root ganglia and spinal cord of the rat and monkey: evidence for association with the membrane of large dense-core vesicles. Neuroscience 82:1225–1242.

Zhang YQ, Limbird LE. 2004. Hetero-oligomers of alpha2A-adrenergic and mu-opioid receptors do not lead to transactivation of G-proteins or altered endocytosis profiles. Biochem Soc Trans 32:856–860.

Zhu Y, King MA, Schuller AG, Nitsche JF, Reidl M, Elde RP, Unterwald E, Pasternak GW, Pintar JE. 1999. Retention of supraspinal delta-like analgesia and loss of morphine tolerance in delta opioid receptor knockout mice. Neuron 24:243–252.

Cellular/Molecular

Protein Kinase C Mediates the Synergistic Interaction Between Agonists Acting at α_2-Adrenergic and Delta-Opioid Receptors in Spinal Cord

Aaron C. Overland,[1,3] Kelley F. Kitto,[2,3,4] Anne-Julie Chabot-Doré,[9] Patrick E. Rothwell,[1,3] Carolyn A. Fairbanks,[1,2,3,4] Laura S. Stone,[6,7,8] and George L. Wilcox[1,3,4,5]

[1]Graduate Program in Neuroscience, [2]Department of Pharmaceutics, College of Pharmacy, and Departments of [3]Neuroscience, [4]Pharmacology, and [5]Dermatology, Medical School, University of Minnesota, Minneapolis, Minnesota 55455, and [6]Faculty of Dentistry, Alan Edwards Centre for Research on Pain, Departments of [7]Pharmacology and Toxicology and [8]Anesthesia, Faculty of Medicine, and [9]Alan Edwards Centre for Research on Pain, McGill University, Montreal, Quebec H3A 1A4, Canada

Coactivation of spinal α_2-adrenergic receptors (ARs) and opioid receptors produces antinociceptive synergy. Antinociceptive synergy between intrathecally administered α_2AR and opioid agonists is well documented, but the mechanism underlying this synergy remains unclear. The delta-opioid receptor (DOP) and the α_{2A}ARs are coexpressed on the terminals of primary afferent fibers in the spinal cord where they may mediate this phenomenon. We evaluated the ability of the DOP-selective agonist deltorphin II (DELT), the α_2AR agonist clonidine (CLON) or their combination to inhibit calcitonin gene-related peptide (CGRP) release from spinal cord slices. We then examined the possible underlying signaling mechanisms involved through coadministration of inhibitors of phospholipase C (PLC), protein kinase C (PKC) or protein kinase A (PKA). Potassium-evoked depolarization of spinal cord slices caused concentration-dependent release of CGRP. Coadministration of DELT and CLON inhibited the release of CGRP in a synergistic manner as confirmed statistically by isobolograpic analysis. Synergy was dependent on the activation of PLC and PKC, but not PKA, whereas the effect of agonist administration alone was only dependent on PLC. The importance of these findings was confirmed *in vivo*, using a thermal nociceptive test, demonstrating the PKC dependence of CLON-DELT antinociceptive synergy in mice. That inhibition of CGRP release by the combination was maintained in the presence of tetrodotoxin in spinal cord slices suggests that synergy does not rely on interneuronal signaling and may occur within single subcellular compartments. The present study reveals a novel signaling pathway underlying the synergistic analgesic interaction between DOP and α_2AR agonists in the spinal cord.

Introduction

Opioid analgesics remain the mainstay for treatment of moderate to severe pain states (American Pain Society, 2008). However, development of adverse side effects such as tolerance, dependence, constipation, addiction liability and opioid-induced hyperalgesia limit their utility (Angst and Clark, 2006). Many approaches have been investigated to bypass these untoward side effects, but use of multimodal analgesic techniques offers distinct advantages as combination therapies may produce analgesia at lower total drug doses. Extensive behavioral (Hylden and Wilcox, 1983; Stevens et al., 1988; Monasky et al., 1990; Ossipov et al., 1990a,b,c; Roerig et al., 1992) and electrophysiological (Sullivan et al., 1987; Wilcox et al., 1987; Omote et al., 1990) studies document that that coactivation of α_2-adrenergic receptors (α_2ARs) and opioid receptors (ORs) produces synergistic interactions in spinal cord, although characterization of the mechanisms underlying this phenomenon have yet to be elucidated. Therefore, understanding the molecular mechanisms involved in the synergistic interactions of these receptors is of both clinical and theoretical importance in development of more efficacious therapies for pain management, as synergy-enabled decreases in dose may mitigate unwanted side effects.

Both α_2ARs and ORs belong to the seven transmembrane-spanning domain G-protein-coupled receptor superfamily and share common signal transduction systems mediated primarily through inhibitory G-proteins, the activation of which inhibits pain transmission. It has been proposed that two receptor populations, acting through common signaling systems, can only synergize if they are anatomically localized to different locations within the pathway (e.g., presynaptic vs postsynaptic) (Honoré et al., 1996). In contrast, previous literature suggests that two analgesic receptor subtypes, α_{2A}ARs (Stone et al., 1998) and delta-opioid receptors (DOP) (Dado et al., 1993; Arvidsson et al., 1995; Cheng et al., 1997; Zhang et al., 1998), are extensively colocalized in terminals of capsaicin-sensitive, substance P (SP)-

Received April 21, 2009; revised Sept. 8, 2009; accepted Sept. 14, 2009.

This work was supported by National Institutes of Health (NIH) Grant R01DA015438 to G.L.W., and Canadian Institutes of Health Research Grant MOP-86691 and Fonds de la Recherche en Santé du Québec Chercheur Boursier #14312 to L.S.S; NIH Training Grant T32DA07234 supported A.C.O. We thank Dr. Walter Bowles for providing perfusion equipment and Cicely Schramm for thoughtful reading of this manuscript.

Correspondence should be addressed to George L. Wilcox, University of Minnesota, Department of Neuroscience, 6-145 Jackson Hall, Minneapolis, MN 55455. E-mail: george@umn.edu.

DOI:10.1523/JNEUROSCI.1907-09.2009

 0270-6474/09/2913264-10$15.00/0

expressing primary afferent fibers in rat (Riedl et al., 2009) and that agonists acting at these receptors are able to produce analgesic synergy *in vivo* in both mouse (Stone et al., 1997) and rat (Ossipov et al., 1990c).

Given that the mechanisms underlying supra-additive receptor interactions remain unknown, we sought to determine which intracellular signaling pathways are necessary for synergy to occur between α_2ARs and DOPs. Because of the striking correspondence of the actions and interactions between α_2ARs and DOPs in mouse and rat, we used immunohistochemical and *in vivo* behavioral studies in mice combined with a more reduced *in vitro* spinal cord slice preparation in rats to determine whether the observed synergy between agonists acting at α_2ARs/DOPs results from something other than multicellular interactions mediated by neuronal circuitry. We then used inhibitors of specific signaling pathways affected by the aforementioned receptor pair to elucidate the mechanisms involved in the synergistic outcome of receptor coactivation. Here, we report that coactivation of α_2ARs and DOPs produces a synergistic interaction both *in vivo* and *in vitro*, and that this interaction takes place within the terminals of primary afferent neurons in spinal cord. Whereas the analgesic efficacy of both receptors required PLC activation, the synergistic interaction uniquely required PKC activation. These studies are the first to identify a signaling pathway underlying synergy between agonists acting at α_2ARs and DOPs and may lead to improved understanding and increased clinical utilization of polyanalgesic therapy.

Materials and Methods

Animals. Male CD-1 ICR mice (20 ± 5 g; Harlan), male C57BL/6 mice (20 ± 5 g; Charles River) and adult male Sprague Dawley rats (300 ± 25 g; Harlan) were maintained on a 12 h light/dark cycle and food and water were available *ad libitum* to all animals. All experiments were approved by the Institutional Animal Care and Use Committee of the University of Minnesota or the McGill University Animal Care and Ethics Committees.

Immunohistochemistry. Immunohistochemistry was performed as previously described (Wessendorf and Elde, 1985; Fairbanks et al., 2002; Riedl et al., 2009). In brief, male C57BL/6 mice were anesthetized with a ketamine/xylazine/acepromazine mixture and perfused transcardially with 4% paraformaldehyde and 0.2% picric acid in 0.1 M PBS, pH 6.9. Spinal cords were dissected and stored overnight in 10% sucrose at 4°C. Tissue sections were prepared using a cryostat at a thickness of 10–14 μm, thaw-mounted onto gelatin-coated slides and stored at −20°C. Sections were incubated for 1 h at room temperature in diluent containing 1% normal donkey serum, 0.3% Triton X-100, 0.01% sodium azide and 1% bovine serum albumin in PBS. Sections were then incubated overnight at 4°C in a humid chamber with primary antisera, rinsed 3 × 10 min with PBS, incubated with fluorescently tagged species-specific secondary antisera (Jackson Immunoresearch) for 1 h at room temperature, rinsed 3 × 10 min with PBS and coverslipped using a mixture of glycerol and PBS containing 0.1% *p*-phenylenediamine. The α_{2A}AR antiserum (1:1000) was prepared in rabbit against a synthetic peptide corresponding to $\alpha_{2A}AR_{436\text{-}450}$ (AFKKILCRGDRKRIV) of the rat sequence and has been previously characterized (Stone et al., 1998; Riedl et al., 2009). The rabbit DOP antiserum (1:1000) was prepared against a synthetic peptide corresponding to anti-$DOP_{3\text{-}17}$ (1:1000; LVPSARAELQSSPLV) and has been previously characterized (Dado et al., 1993; Riedl et al., 2009). SP antibodies raised in two different species and obtained from two different sources were used in these studies and produced similar results: rat anti-SP (1:1000; Accurate Chemical) and guinea pig anti-SP (1:500; Neuromics Antibodies) and have been previously characterized (Cuello et al., 1979; Riedl et al., 2009). Images were collected using a Bio-Rad MRC 1000 confocal microscope (Bio-Rad Microscience Division) or an Olympus BX-51 equipped with a DP-71 camera and assembled in photoshop.

Drug preparation and administration. Drugs used were clonidine (CLON), chelerythrine, U73122 [1-[6-[((17β)-3-methoxyestra-1,3,5[10]-trien-17-yl)amino]hexyl]-1*H*-pyrrole-2,5-dione], idazoxan, H89 [*N*-[2-(4-bromocinnamylamino)ethyl]-5-isoquinoline], tetrodotoxin (TTX) (all from Sigma), deltorphin II (DELT) (Tocris Bioscience), and naltrindole (gift from Dr. Philip Portoghese, University of Minnesota, Minneapolis, MN). All drugs for behavioral experiments were dissolved in 0.9% saline and administered intrathecally (i.t.) in a volume of 5 μl according to the method of Hylden and Wilcox (1980) as modified by Wigdor and Wilcox (1987) in conscious mice. For spinal cord neuropeptide release experiments, U73122 was dissolved in ethanol and diluted in HEPES buffer. All other drugs were dissolved in dH_2O and diluted in HEPES buffer. Control experiments with HEPES (shown) and HEPES with ethanol (data not shown) demonstrated that diluted ethanol had no effect on either basal or K^+-stimulated CGRP release.

Antinociception. Thermal nociceptive responsiveness was assessed using the warm water (52.5°C) tail-immersion assay, as described previously (Janssen et al., 1963). Briefly, mice were gently wrapped in a soft cloth such that their tails were exposed, and three-quarters of the length of the tail was dipped into the warm water. Tail-flick latencies were obtained before drug application to establish a baseline response. Opioid and adrenergic receptor agonists were injected i.t. as 5 and 10 min pretreatments, respectively. The opioid receptor antagonist was injected concomitant with agonist injection and the adrenergic receptor antagonist was injected i.t. as a 10 min pretreatment before adrenergic receptor agonist injection. PLC and PKC antagonists were injected i.t. as 1 h pretreatments before latency determination, whereas PKA antagonist was injected i.t. as a 30 min pretreatment. A maximum cutoff of 12 s was set to avoid tissue damage. The results were then expressed as a percentage of the maximum possible effect (%MPE) according to the equation: % MPE = Postdrug latency − Predrug latency × 100/Cutoff − Predrug latency.

Neuropeptide release from spinal cord slices. For determination of calcitonin gene-related peptide (CGRP) release from spinal cord slices, adult male Sprague Dawley rats (275–325 g) were used. Animals were anesthetized with isoflurane and quickly decapitated. Spinal cords were removed by hydraulic extrusion and placed in ice-cold, oxygenated HEPES buffer containing (in mM): 120 NaCl, 5.4 KCl, 0.8 $MgCl_2$, 1.8 $CaCl_2$, 20 HEPES, 0.01 glycine, 15 glucose, and commercial protease inhibitor cocktail (Roche). Two centimeter segments of the lumbar enlargement were removed, divided midsagittally, and chopped into 0.3 × 0.3 mm pieces (McIllwain tissue chopper), and the halves were placed into separate 1 ml perfusion chambers. The tissue was perfused at a flow rate of 0.35–0.4 ml/min in HEPES buffer maintained at 37°C, aerated with 95% O_2-5% CO_2 and pH adjusted to 7.4. The tissue was allowed a perfusion equilibration period of 30 min to stabilize peptide release and then collected for 6 min periods in 12 × 75 mm glass test tubes. Basal release was assessed by perfusing the tissue with HEPES buffer for 6 min. After this period, peptide release was evoked by perfusing the tissue for an additional 6 min with HEPES buffer containing 60 mM K^+. In release inhibition experiments, tissue was perfused for 6 min with HEPES buffer containing DELT, CLON, or the combination in a 1:1 concentration ratio before the K^+ stimulation. When PLC inhibitor, PKC inhibitor, PKA inhibitor, or TTX were used, these compounds were present in the superfusate throughout the entire experiment. Immunoreactive CGRP in the collected samples was assayed by enzyme-linked immunosorbent assay (ELISA) (SPI Bio, Catalog No. 589001). No difference in either basal or K^+-evoked CGRP release was observed from slices made from either whole cord or cord separated to exclude the ventral horn (data not shown).

Electrophysiological recording. Adult male Sprague Dawley rats (275–325 g) were anesthetized with isoflurane and quickly decapitated. Spinal cords were removed by hydraulic extrusion and placed in ice-cold, oxygenated artificial CSF (aCSF) with the following composition (in mM): 119 NaCl, 2.5 KCl, 1.0 NaH_2PO_4, 1.3 $MgSO_4$, 2.5 $CaCl_2$, 26.2 $NaHCO_3$ and 11 glucose. The lumbar enlargement was cut into 1 cm sections, from which dorsal horizontal slices with a thickness of ~500 μm were taken using a vibratome while the spinal cord was immersed in aCSF. The slicing solution also contained 10 mM kynurenic acid to maintain viability. After recovery, slices were superfused with normal aCSF (22−23°C) containing 100 μM picrotoxin. Field EPSPs (fEPSPs) were evoked every

10 s using a suction electrode placed on the dorsal root entry zone, and recorded using a glass electrode filled with aCSF and placed in the ipsilateral superficial dorsal horn 2–5 mm rostral or caudal of the stimulating electrode. Data were digitized at 5 kHz using a Multiclamp 700A amplifier (Molecular Devices), and analyzed using custom software (Igor Pro, Wavemetrics). fEPSP amplitude following application of TTX (0.1 or 1 μM) is expressed as the percentage of baseline amplitude recorded for 5 min before TTX application.

Data analysis. The ED_{50} (nanomoles, *in vivo*) or EC_{50} (nanomolar, *in vitro*) values and 95% confidence intervals (CIs) of both CLON and DELT were calculated using the graded dose–response curve method of Tallarida and Murray (Tallarida, 1992). A minimum of three doses or concentrations were used for each drug or drug combination. In some instances (e.g., multiple doses or concentrations with efficacies approaching 0 or 100%), only the linear portion of the dose/concentration–response curve was included in the ED_{50}/EC_{50} value calculation. To determine differences in agonist potency between groups, nonoverlapping 95% CIs were considered to represent statistically significant differences. In the experiments testing for synergistic interactions, dose/concentration–response curves, ED_{50}/EC_{50} values, and 95% CIs were first generated for CLON and DELT administered alone as described above. CLON and DELT were then coadministered at a constant dose/concentration ratio based on the potency ratio of the two drugs given separately. For example, if CLON had an ED_{50} or EC_{50} value of 1 nmol or nM (*in vivo* and *in vitro*, respectively) and DELT had an ED_{50} or EC_{50} value of 1 nmol or nM, the agents were coadministered in a 1:1 ratio and a third dose/concentration–response curve was generated for the combination treatment.

Isobolographic analysis. Isobolographic analysis is the accepted standard for quantitative evaluation of drug interactions (Tallarida, 1992). Dose/concentration–response curves were first constructed for CLON and DELT administered separately and the ED_{50}/EC_{50} values were calculated and then used to determine an equieffective dose/concentration ratio between the two as described above. The interaction between the two drugs was tested by comparing the theoretical additive ED_{50}/EC_{50} value for the combination based on the dose/concentration–response curves of each drug administered separately and the observed experimental ED_{50}/EC_{50} value of the combination using a *t* test. These values are based on the total dose of both drugs. An interaction is considered synergistic if the experimental ED_{50}/EC_{50} value is significantly less ($p < 0.05$) than the calculated theoretical additive ED_{50}/EC_{50} values.

Isobolographic analysis allows for graphical representation of drug interactions (see Figs. 2*B*,*D*, 4*B*). This representation depicts the ED_{50}/EC_{50} value of each agent as the *x*- or *y*-intercept. For example, Figure 2*B* represents the ED_{50} value of CLON as the *y*-intercept and the ED_{50} of DELT as the *x*-intercept. The line connecting these two points is the theoretical additive line and depicts the dose combinations expected to yield 50% efficacy if the drug interaction is strictly additive. The theoretical additive ED_{50} value and its confidence interval are determined mathematically and plotted spanning this line. The observed ED_{50} value for the combination is plotted at the corresponding *x*,*y* coordinates along with its 95% confidence interval for comparison to the theoretical additive ED_{50} value. The same comparisons are made for EC_{50} values.

The magnitude of drug synergism can also be expressed in terms of an Interaction Index (γ) (Tallarida, 2002). The index is defined by the equation: $a/A + b/B = \gamma$, where *A* and *B* are the doses/concentrations of drugs A and B administered separately that give a specified level of effect and (*a*,*b*) is the combination dose/concentration that produces this same level of effect (the ED_{50}/EC_{50} values are commonly used for this calculation). In the absence of a drug interaction, $\gamma = 1$. If the interaction is synergistic, $\gamma < 1$. The interaction index is used here as a quantitative measure to characterize the magnitude of synergism by the CLON-DELT combination between treatment groups.

All dose–response and concentration–response and isobolographic analyses were performed with the FlashCalc 4.5.3 pharmacological statistics software package generously supplied by Dr. Michael Ossipov (Department of Pharmacology, University of Arizona College of Medicine, Tucson, AZ).

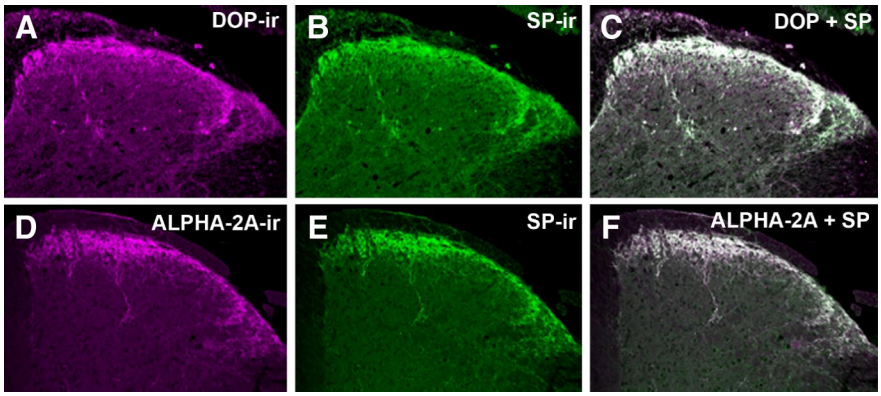

Figure 1. Colocalization of α_{2A}AR and DOP with SP in mouse spinal cord. ***A–C***, Representative images of the dorsal horn of mouse spinal cord double-labeled with DOP (***A***, magenta) and SP (***B***, green) antisera. When images ***A*** and ***B*** are digitally merged (***C***), instances of colocalization appear as white. ***D–F***, Representative images of mouse spinal cord double-labeled with α_{2A}AR (***D***, magenta) and SP (***E***, Green) antisera. When images ***D*** and ***E*** are digitally merged (***F***), instances of colocalization appear white. The extensive colocalization observed between both α_{2A}AR and DOP with SP suggests that α_{2A}AR and DOP colocalize on SP-containing fibers in the mouse spinal cord. This extensive colocalization, already well characterized in rats (Riedl et al., 2009), appears to generalize to mice.

Results

Colocalization of α_2AR, DOP, and SP immunoreactivity in the dorsal horn of mouse spinal cord

Previous reports have demonstrated that both α_{2A}AR and DOP are expressed in the peptidergic population of primary afferent sensory neurons in rat (Dado et al., 1993; Arvidsson et al., 1995; Stone et al., 1998; Zhang et al., 1998; Riedl et al., 2009). However, anatomical characterization of α_{2A}AR and DOP has not been fully investigated in mice. Therefore, we double-labeled mouse spinal cord sections with antibodies directed against α_{2A}AR, DOP, and the neuropeptide SP (Fig. 1). On merging of the digital images of sections, double-labeled elements appear white (Fig. 1*C*,*F*). Colocalization of α_{2A}AR immunoreactivity (α_{2A}AR-IR) and SP-IR was observed with the rabbit-derived α_{2A}AR and both rat- and guinea pig-derived SP antibodies obtained from independent sources (Fig. 1*D–F*; data not shown). Similarly, rabbit-derived anti-DOP labeling colocalized with both the rat- and the guinea pig-derived SP antibodies (Fig. 1*A–C*; data not shown). The independent colocalization of α_{2A}AR-IR and DOP-IR with multiple SP antibodies is entirely consistent with anatomical localization in rat and strongly suggests that the colocalization observed is not artifactual. The extensive colocalization observed between both α_{2A}AR and DOP with SP suggests that α_{2A}AR and DOP colocalize in SP-containing fibers in the mouse spinal cord and may be positioned to mediate the antinociceptive effects of spinally delivered agonists for these receptors.

Intrathecal CLON-DELT: Behavioral antinociceptive synergy

Intrathecal administration of either CLON or DELT produced dose-dependent antinociception at 10 and 5 min postinjection, respectively (Fig. 2*A*); these pretreatment times were chosen to match the time of peak effect of each agent given alone (data not shown). Comparison of the respective ED_{50} values revealed a potency ratio between CLON and DELT of ~1:1. Coadministra-

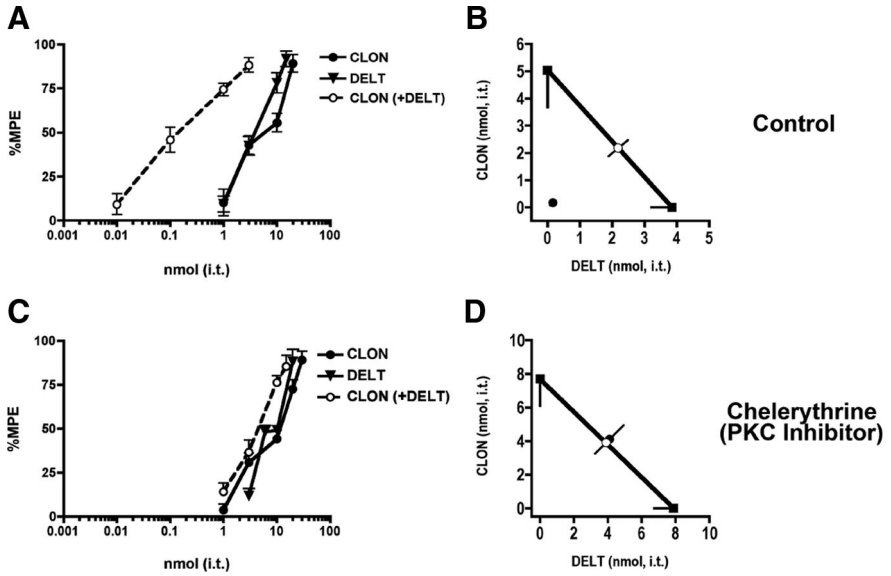

Figure 2. Coadministration of DELT and CLON is synergistic in the tail flick test. ***A***, Nociceptive thermal responses were challenged by intrathecal administration of DELT, CLON, and their combination. DELT (filled triangles) and CLON (filled circles) inhibited the behavior in a dose-dependent manner with similar potency and efficacy. When both DELT and CLON were coadministered at a constant dose ratio of 1:1 (open circles), the resulting potency was ~30-fold higher than either drug given alone, suggesting that the interaction was synergistic. Error bars represent mean ± SEM for each dose point ($n = 6$ animals/dose). ***B***, Isobolographic analysis of the data in Figure 1*A*. The *y*-intercept represents the CLON ED_{50} (5 nmol; 95% CI = 3.6–6.4), and the *x*-intercept represents the DELT ED_{50} (3.9 nmol; 95% CI = 3.2–4.5) when each was administered alone. The heavy line connecting the intercepts is the theoretical additive line and the open circle represents the theoretical additive combined ED_{50}. Coordinates for drug combinations falling below this line and outside the confidence limits indicate a synergistic interaction. When the two compounds were coadministered at a 1:1 dose ratio, the resultant ED_{50} (closed circle) (0.17 nmol; 95% CI = 0.11–0.23) of DELT in the presence of CLON fell well below the additive line, indicating that the interaction was synergistic. Error bars parallel to each axis represent the lower 95% CI for each compound given alone. The error bars on the combined dose points represent the upper and lower 95% CIs. ***C***, Coadministration of DELT and CLON show additivity in the presence of the PKC inhibitor chelerythrine. Nociceptive thermal responses were challenged by intrathecal administration of DELT, CLON, and their combination in the presence of an inhibitor of PKC. DELT (filled triangles) and CLON (filled circles) inhibited the responses in a dose-dependent manner with similar potency and efficacy. Coadministration of DELT and CLON at a 1:1 dose ratio (open circles) was ~1.9-fold more potent than either drug given alone, compared with ~30-fold potency shift in the absence of chelerythrine (see Fig. 1*A*). Error bars represent mean ± SEM for each dose point ($n = 6$ animals/dose). ***D***, Isobolographic analysis was applied to the data in Figure 1*C*. The *y*-intercept represents the ED_{50} (7.7 nmol; 95% CI = 6.1–9.3) for CLON, and the *x*-intercept represents the ED_{50} (7.9 nmol; 95% CI = 6.8–9.0) for DELT when each was administered alone. Coadministration at a 1:1 dose ratio resulted in an ED_{50} (closed circle) (4.1 nmol; 95% CI = 3.2–5.0) for DELT in the presence of CLON that fell on the theoretical additive line, indicating a strictly additive interaction in the presence of the PKC inhibitor.

tion of the drugs (CLON at 10 min and DELT at 5 min) at a constant dose ratio equal to the potency ratio (1:1) yielded a third antinociceptive dose–response curve shown in Figure 2*A*. This combination dose–response curve is expressed in terms of the doses of CLON (0.01, 0.1, 1, 3) given in the presence of the same doses of DELT (0.01, 0.1, 1, 3) as opposed to total drug (e.g., 0.02, 0.2, 2, 6) to facilitate visual appreciation of the potency shifts of each drug in the presence of the other. The potency of each drug was increased ~30-fold in the presence of the other, suggesting that the interaction was synergistic. The dose–response data from Figure 2*A* are represented graphically as an isobologram in Figure 2*B*, which shows that the ED_{50} value of the combination (closed circle) is significantly lower than the theoretical additive ED_{50} value (open circle). This interaction was confirmed as synergistic by statistical comparison (*t* test) between the observed combined ED_{50} value and the theoretical additive ED_{50} value. The interaction index, γ, was 0.04; this small γ value indicates that the synergistic interaction between CLON and DELT is of a high magnitude.

Inhibition of PKC completely and selectively reverses CLON-DELT synergistic inhibition of nociceptive responses in the tail flick test

To assess the signaling mechanisms mediating the observed behavioral antinociceptive synergy between α_2AR and DOP agonists, we evaluated the effect of intrathecally coadministered CLON and DELT in the tail flick assay when mice were pretreated with selective inhibitors of PLC, PKC and PKA (U73122, 3 nmol, i.t.; chelerythrine, 1 nmol, i.t.; and H89, 6 nmol, i.t., respectively). PKC inhibition was selected because of its activation downstream of diacylglycerol produced and Ca^{2+} mobilized by PLC, previous behavioral work (Roerig, 1998) and recent evidence in trigeminal nociceptors showing that application of the inflammatory mediator bradykinin (BK) rapidly induces functional DOP competence through a PKC-dependent signaling mechanism (Patwardhan et al., 2005). PKA inhibition was chosen as a negative control to show specificity of the PKC effect.

After administration of the PKC inhibitor, CLON (50 min) and DELT (55 min) were administered separately or coadministered at a constant dose ratio equal to the potency ratio (1:1), and three antinociceptive dose–response curves were generated (Fig. 2*C*). The dose–response data from Figure 2*C* and the resulting isobologram (Fig. 2*D*) show that the ED_{50} value of the combination did not differ significantly from the theoretical additive ED_{50}. This interaction was confirmed as additive by statistical comparison (*t* test) between the observed combined ED_{50} value and the theoretical additive ED_{50} value. The interaction index, γ, was 1.05, indicating an absence of a supra-additive drug interaction in the presence of the PKC inhibitor. Although pretreatment with PKC inhibitor completely abolished the synergy between CLON and DELT, it did not significantly change the relative potency of the agonists given separately.

In contrast to the PKC inhibitor, pretreatment with U73122 (a PLC inhibitor) (Fig. 3*A*, dark bars) reversed or reduced the inhibitory effects of high-efficacy doses of both CLON and DELT as well as a synergistic combination dose. This result permits speculation that PLC-mediated vesicle translocation to the plasma membrane contributes to both the inhibitory effects of single agonist administration and their synergistic interaction, whereas PKC is unique to the synergistic interaction. Inhibition of PKA with H89 (Fig. 3*B*, vertical striped bars) had no effect on CLON administered alone or the synergistic CLON-DELT combination, indicating that PKA, unlike PKC, is not required for CLON-DELT synergy. Pretreatment with H89 consistently reduced the inhibitory effect of DELT administered alone (Fig. 3*B*).

It is known that there is a low basal level of adrenergic tone in the form of norepinepherine release from descending noradrenergic neurons that terminate in the dorsal horn of the spinal cord (Pertovaara, 2006). Therefore, we hypothesized that the observed inhibitory effect of DELT in the tail flick assay was partially mediated through α_2-adrenergic receptor activation by endogenous NE. PKA has been implicated in modulation of neurotransmitter

release dynamics from nerve terminals (Trudeau et al., 1996); thus, inhibiting PKA with H89 could be interfering with the aforementioned descending noradrenergic tone, thus reducing the inhibitory effect of DELT administration.

To test this hypothesis, the effects of CLON, DELT, and the CLON-DELT combination were challenged with i.t. pretreatment of the α_2AR antagonist, idazoxan (10 nmol, i.t.) (Fig. 3*C*, downward diagonal stripes). As expected, i.t. pretreatment with idazoxan completely reversed the inhibitory effect of CLON administered alone. Pretreatment with idazoxan also reduced the inhibitory effect of the CLON-DELT combination. In support of the hypothesized ongoing noradrenergic tone, i.t. pretreatment with idazoxan also reduced the inhibitory effect of DELT, supporting a role for endogenous α_2AR activation in the effect of DELT administration alone. Activation of α_2ARs by endogenous NE has previously been reported to be involved in opioid receptor-mediated antinociception, as mice lacking functional α_{2A}ARs or wild-type mice treated with idazoxan showed decreased morphine potency in inhibiting nocifensive responses to i.t. administration of SP (Stone et al., 1997). We also challenged both agonists administered separately and in combination with the DOP antagonist, naltrindole (8.8 nmol, i.t.) (Fig. 3*D*, upward diagonal stripes). The inhibitory effects of both DELT alone and the CLON-DELT combination were reduced with DOP antagonist pretreatment. However, i.t. pretreatment with the DOP antagonist had no effect on CLON administered alone. These data suggest that, although the effect of CLON administered alone *in vivo* is mediated solely through α_2ARs, the effect of i.t. DELT administration is primarily mediated through DOP but partially mediated through α_2AR activation by endogenous NE.

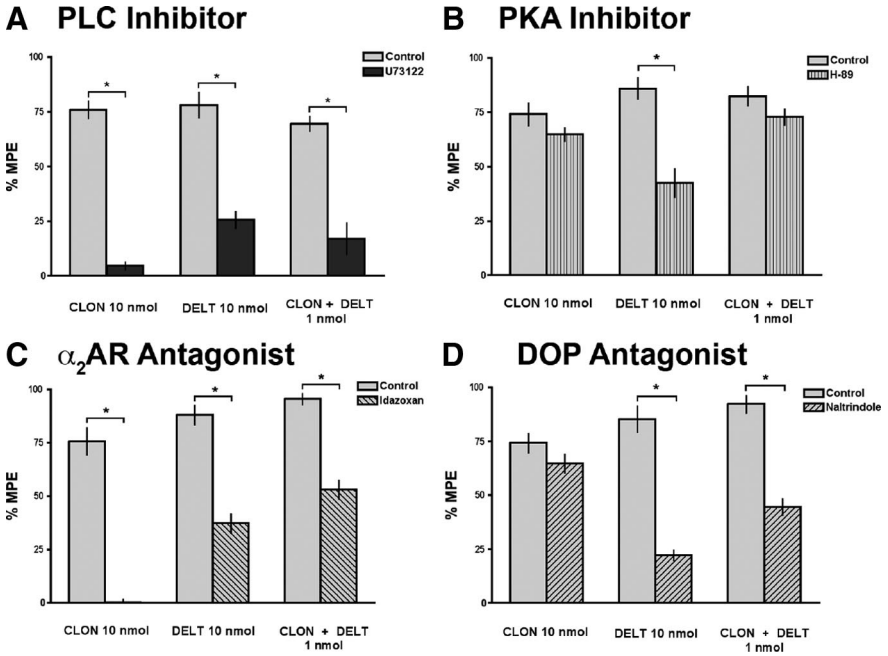

Figure 3. Effect of the PLC inhibitor U73122, the PKA inhibitor H89, the α_2AR antagonist idazoxan, and the DOP antagonist naltrindole on the ability of CLON, DELT, and the CLON-DELT combination to inhibit nociceptive thermal responses in the tail flick test. High-efficacy doses of CLON and DELT as well as the low-dose CLON-DELT combination were tested under control conditions (light bars) and in the presence of U73122 (3 nmol i.t., dark bars), H89 (6 nmol i.t., vertical striped bars), idazoxan (10 nmol i.t., downward diagonal stripes), and naltrindole (8.8 nmol i.t., upward diagonal stripes). ***A***, The upstream inhibitor of PLC, U73122, abolished the inhibitory effects of the agonists administered alone (76.0 ± 3.9% vs 4.6 ± 1.6% inhibition for CLON and 78.1 ± 5.7% vs 25.7 ± 3.7% inhibition for DELT in the presence of U73122) as well as the synergistic effect of their low-dose combination (69.6 ± 3.3% vs 17.0 ± 7.1% inhibition in the presence of U73122). ***B***, Pretreatment with the PKA inhibitor, H89, had no effect on either CLON administered alone (74.1 ± 5.1% vs 64.9 ± 3.0% inhibition in the presence of H89) or the low-dose combination (82.5 ± 4.5% vs 72.9 ± 3.8% inhibition for in the presence of H89). Pretreatment with H89 reduced the effect of DELT administered alone (88.4 ± 4.2% vs 40.8 ± 6.2% inhibition for DELT in the presence of H89). ***C***, Pretreatment with the α_2AR antagonist, idazoxan, completely reversed the effect of CLON administered alone (75.7 ± 6.3% vs 0.2 ± 1.5% inhibition in the presence of idazoxan), and reduced the effects of both DELT alone (87.9 ± 4.4% vs 37.3 ± 4.5% inhibition in the presence of idazoxan) and the CLON-DELT combination (95.4 ± 2.6% vs 53.0 ± 4.4% inhibition in the presence of idazoxan). ***D***, Pretreatment with the DOP antagonist, naltrindole, had no effect on CLON administered alone (74.2 ± 4.5% vs 64.7 ± 4.4% inhibition in the presence of naltrindole), but reduced the inhibitory effect of DELT administered alone (85.3 ± 5.9% vs 22.1 ± 2.4% inhibition in the presence of naltrindole). Pretreatment with naltrindole also reduced the effect of the CLON-DELT combination (92.3 ± 4.0% vs 44.6 ± 3.7% inhibition in the presence of naltrindole). Error bars represent mean ± SEM ($n = 6$ animals/dose). *$p < 0.05$; Student's *t* test.

CLON-DELT: Synergistic inhibition of K^+-stimulated CGRP release from spinal cord slices

To determine whether the antinociceptive interaction observed *in vivo* was attributable to activation of receptors at the level of primary afferent terminals, we determined the ability of α_2AR and DOP agonists to inhibit K^+-stimulated release of the neuropeptide CGRP *in vitro* using the spinal cord slice preparation. Measurement of CGRP release was chosen because, although K^+ stimulation causes depolarization of all cells in the slice preparation, CGRP in the spinal cord is exclusively released by primary afferent terminals (Franco-Cereceda et al., 1987; Plenderleith et al., 1990). Stimulation of spinal cord slices with 60 mM K^+ significantly increased the concentration of immunoreactive CGRP (iCGRP) in the superfusate from 44.7 ± 5.2 pg/ml (basal level) to 221 ± 44.4 pg/ml (data not shown). This increase was inhibited in a concentration-dependent manner by pretreatment with either the α_2AR agonist CLON (closed circles) or the DOP agonist DELT (closed squares) (Fig. 4*A*). To determine whether a synergistic interaction exists between these receptors in this preparation, slices were superfused with both drugs in combination. The resultant concentration–response curve (Fig. 4*A*, open squares and open triangles) shows the effect of fixed-ratio combinations of the two agents administered simultaneously. The potency of each drug was increased ~30-fold in the presence of the other, similar to results obtained *in vivo*, suggesting that the interaction is synergistic. The concentration–response data from Figure 4*A* are represented graphically as an isobologram in Figure 4*B*, which shows that the EC_{50} of the combination (closed circle) is significantly lower than the theoretical additive EC_{50} (open circle). Statistical comparison (*t* test) between the observed combined EC_{50} value and the theoretical additive EC_{50} value demonstrates that this interaction is synergistic. The interaction index, γ, for the combination was 0.06, indicating a substantial synergistic interaction between α_2AR and DOP agonists at the level of primary afferent terminals. Pretreatment of spinal cord slices with the nonselective OR antagonist naloxone (1 μM) or the α_2AR antagonist idazoxan (1 μM) abolished the inhibitory action of DELT and CLON, respectively, confirming that the observed effects were OR- and α_2AR-mediated (data not shown).

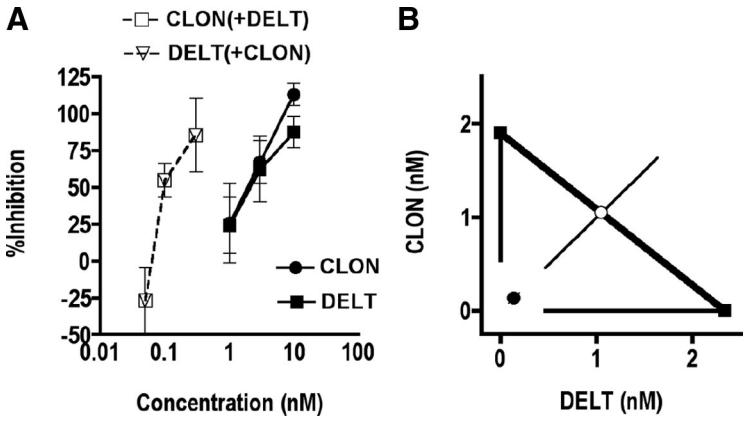

Figure 4. Coadministration of DELT and CLON inhibits K^+-evoked release of CGRP from spinal cord slices in a synergistic manner. ***A***, K^+-evoked release of CGRP was challenged by administration of DELT, CLON and their combination. DELT (filled squares) and CLON (filled circles) inhibited the release of CGRP in a concentration-dependent manner with similar potency and efficacy. Coadministration of DELT and CLON at constant concentration ratio of 1:1 (open squares and open triangles) was ~30-fold more potent than either drug given alone, suggesting that the interaction was synergistic. Error bars represent mean ± SEM for each concentration point ($n = 3$–9 samples/concentration). ***B***, Isobolographic analysis of the data in Figure 3*A*. The *y*-intercept represents the CLON EC_{50} (1.9 nM; 95% CI = 0.5–3.3), and the *x*-intercept represents the DELT EC_{50} (2.3 nM; 95% CI = 0.5–4.2) when each was administered alone. The heavy line connecting the intercepts is the theoretical additive line and the open circle represents the theoretical additive combined EC_{50}. Coordinates for drug combinations falling below this line and outside the confidence limits indicate a synergistic interaction. Coadministration of CLON and DELT at a 1:1 concentration ratio resulted in an EC_{50} (0.06; 95% CI = 0.01–0.1) of DELT in the presence of CLON that fell well below the additive line, indicating that the interaction was synergistic. Error bars parallel to each axis represent the lower 95% CI for each compound given alone. The error bars on the combined concentration points represent the upper and lower 95% CIs.

Inhibition of PKC completely and selectively reverses CLON-DELT synergistic inhibition of CGRP release from spinal cord slices

To determine whether the reduction of antinociceptive synergy with PKC inhibition observed *in vivo* generalized to the level of primary afferent terminals, we tested whether the PKC inhibitor could similarly affect the synergistic interaction between CLON and DELT in reducing inhibition of K^+-stimulated release of the neuropeptide CGRP *in vitro* using the spinal cord slice preparation. To determine whether there are differential signaling mechanisms mediating the effects of these agonists administered alone and in the synergistic combination, we challenged the ability of CLON, DELT and the combination to inhibit K^+-stimulated CGRP release from rat spinal cord slices with selective inhibitors of PLC, PKC and PKA (Fig. 5). High-efficacy concentrations of CLON and DELT were tested under control conditions (light bars) and in the presence of the PKA inhibitor H89 (1 μM), the PLC inhibitor U73122 (10 μM), or the PKC inhibitor chelerythrine (2.5 μM) (vertical striped bars, dark bars, and horizontal striped bars, respectively). Only the PLC inhibitor significantly reversed the inhibitory effects of CLON and DELT when administered alone, consistent with behavioral results. Furthermore, neither inhibition of PKC nor inhibition of PKA with H89 administration reversed the effect of either CLON or DELT administered alone *in vitro*.

When the effect of inhibitors of PLC, PKC and PKA on DELT-CLON synergy were evaluated, inhibition of both PLC and PKC, but not PKA, blocked the synergistic interaction. These data suggest that, although the effect of both agonists administered separately and together requires activation of the PLC pathway, only the synergistic effect of both agonists coadministered relies on activation of PKC. PKC, but not PKA dependence in the spinal cord slice preparation is consistent with the *in vivo* data in Figures 2 and 3.

CLON-DELT synergy is maintained in the presence of tetrodotoxin

The similar results reported in (Riedl et al., 2009) for greater-than-additive inhibition of CGRP release from spinal cord synaptosomes suggests that this interaction takes place in subcellular compartments co-containing the receptors. To determine whether the synergistic interaction between the two agonists requires colocalization within subcellular compartments rather than through interneuronal circuitry, we evaluated whether CLON-DELT synergy in the spinal cord slice preparation is maintained in the presence of the sodium channel blocker, TTX, which inhibits neural transmission. We chose a concentration of 1 μM TTX based on (1) a literature survey of rat (Murase and Randic, 1983; Ryu et al., 1988; Yoshimura and Jessell, 1989; Yoshimura and Jessell, 1990) and mouse (Han et al., 2007) studies, and (2) a positive control experiment showing that 1 μM TTX, but not 0.1 μM, completely blocked fEPSPs in rat spinal cord slices (4.9 ± 5.9% response in the presence of TTX vs baseline) (Fig. 6*A*). The presence of TTX (1 μM) in the superfusate throughout the experiment did not affect the synergistic inhibition of the CLON-DELT combination (0.1 nM, 1:1 concentration ratio) of K^+-evoked CGRP release from spinal cord slices (72.7 ± 10.4% vs 60.9 ± 8.9% inhibition in the presence of TTX) (Fig. 6*B*). Together, these results support and extend recent findings in spinal cord synaptosomes (Riedl et al., 2009) that the observed synergy between agonists acting at these two receptors occurs within single subcellular compartments (i.e., the terminals of primary afferent nociceptive fibers in the dorsal horn of the spinal cord).

CLON-DELT combination causes significant CGRP release in the absence of K^+ stimulation

Since DOP agonist-induced CGRP release from cultured DRG neurons has been shown to correlate with functional DOP insertion into the plasma membrane (Bao et al., 2003), we sought to determine whether the low-concentration CLON-DELT combination could also cause CGRP release in the absence of K^+ stimulation (Fig. 7). Spinal cord slices were superfused with CLON, DELT, and the CLON-DELT combination (10 nM, 10 nM and 0.1 nM, respectively) to test for CGRP release in the absence of K^+ depolarization. Stimulation of spinal cord slices with CLON (10 nM) failed to cause significant release of CGRP. In agreement with (Bao et al., 2003), however, stimulation of spinal cord slices with DELT (10 nM) caused significant release of CGRP. Stimulation of spinal cord slices with a 100-fold lower concentration of the CLON-DELT combination also caused significant release of CGRP in the absence of K^+ stimulation. These data suggest that the CLON-DELT combination may act synergistically at DOP and α_2AR to externalize large dense-core vesicles containing CGRP, and thus may act to insert functional receptors into the membrane in the same manner as DOP agonist alone.

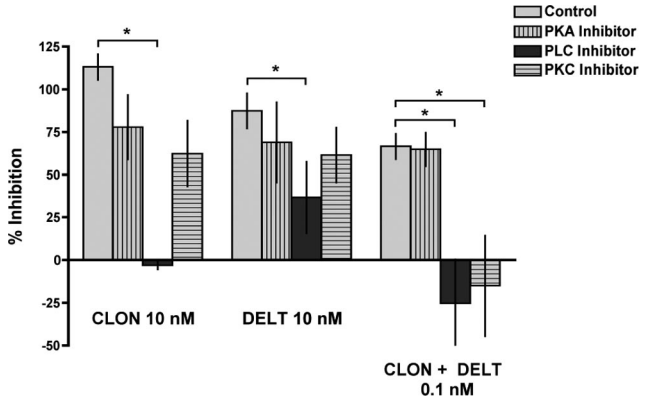

Figure 5. Effect of the PKC inhibitor chelerythrine, the PLC inhibitor U73122 and the PKA inhibitor H89 on the ability of CLON, DELT, and the CLON-DELT combination to inhibit CGRP release from spinal cord slices. (Note: ordinate represents percentage inhibition of release; values near 0 indicate blockade of release inhibition.) High-efficacy concentrations of CLON and DELT, as well as the low-concentration CLON-DELT combination were tested under control conditions (light bars) and in the presence of H89 (1 μM, vertical striped bar), U73122 (10 μM, dark bars), or chelerythrine (2.5 μM, horizontal striped bars). Chelerythrine did not significantly affect the ability of the individual agonists to inhibit CGRP release (113 $\pm$ 7.6% vs 62.3 $\pm$ 19.3% inhibition for CLON in the presence of chelerythrine and 87.4 $\pm$ 10.4% vs 61.5 $\pm$ 16.2% inhibition for DELT in the presence chelerythrine); however, chelerythrine abolished the synergistic effect of the low-concentration combination (61.5 $\pm$ 8.2% vs $-$15.0 $\pm$ 29.5% inhibition in the presence of chelerythrine). In contrast, U73122 blocked the inhibition of release by either agent alone (113 $\pm$ 7.6% vs $-$3.1 $\pm$ 2.5% inhibition for CLON in the presence of U73122 and 87.4 $\pm$ 10.4% vs 36.7 $\pm$ 21.0% inhibition for DELT in the presence U73122) as well as the synergistic inhibition of release (66.6 $\pm$ 7.5% vs $-$25.3 $\pm$ 25.8% inhibition in the presence of U73122), indicating that PLC activation is required for inhibition of release. H89 did not significantly affect the ability of the individual agonists to inhibit CGRP release (113 $\pm$ 7.6% vs 77.9 $\pm$ 18.9% inhibition for CLON in the presence of H89 and 87.4 $\pm$ 10.4% vs 68.9 $\pm$ 23.6% inhibition for DELT in the presence H89). Treatment with H89 also had no effect on CLON-DELT synergism (66.6 $\pm$ 7.5% vs 64.8 $\pm$ 10.0% inhibition in the presence of H89), supporting the specific requirement of PKC activation for synergy. Error bars represent mean $\pm$ SEM ($n = 3$–8 samples/group). *$p < 0.05$; Student's t test.

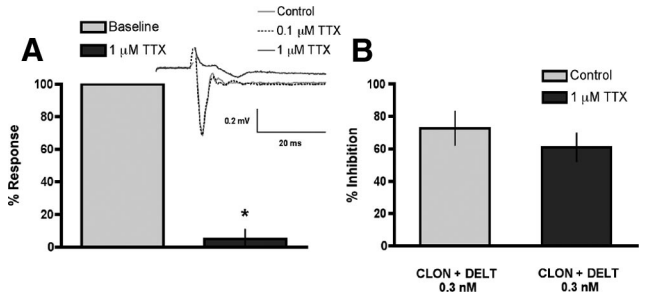

Figure 6. CLON-DELT combination synergy in the spinal cord slice preparation is maintained in the presence of the sodium channel blocker, TTX. ***A***, Positive control for the efficacy of 1 μM TTX to eliminate interneuronal signaling: TTX completely blocked evoked fEPSPs in rat spinal cord slice preparations [4.9 $\pm$ 5.9% response in the presence of TTX (dark bar) vs baseline (light bar)]. ***A*** (Inset), Representative traces of evoked fEPSPs in the presence or absence of TTX (0.1 or 1 μM). ***B***, The inhibitory action of a synergistic CLON-DELT combination was challenged by the addition of TTX (1 μM) to the superfusate. TTX did not alter the synergistic inhibition of K^+-evoked (60 mM) CGRP release invoked by the CLON-DELT combination (0.1 nM, 1:1 concentration ratio) (72.7 $\pm$ 10.4% vs 60.9 $\pm$ 8.9% inhibition in the presence of TTX), supporting that synergy between α_2ARs and DOPs does not rely on multicellular circuitry. Error bars represent mean $\pm$ SEM ($n = 3$–4 slices or samples/group). *$p < 0.05$ compared with baseline; Student's t test.

Discussion

The results from this study indicate that the synergistic interaction between agonists acting at α_2ARs and DOPs can occur at the level of primary afferent terminals to inhibit release of nociceptive neuropeptides from spinal cord slices and that this inhibition translates to synergistic antinociception *in vivo*. Whereas PLC activation is required for both antinociception and inhibition of neuropeptide release by α_2AR and DOP agonists given singly or together, PKC activation is specifically required for the synergistic interaction between coadministered agonists. In contrast, PKA is not involved in the effects of α_2AR and DOP agonists administered separately or in combination, reinforcing the unique ability of PKC to mediate α_2AR/DOP synergy. That the synergistic interaction observed *in vitro* is maintained in the presence of TTX indicates that α_2AR/DOP synergy can take place in single subcellular compartments in the absence of multicellular circuitry. These *in vivo* and *in vitro* results confirm and extend a recent report showing that these receptors inhibit neuropeptide release in a greater-than-additive manner from spinal cord synaptosomes (Riedl et al., 2009).

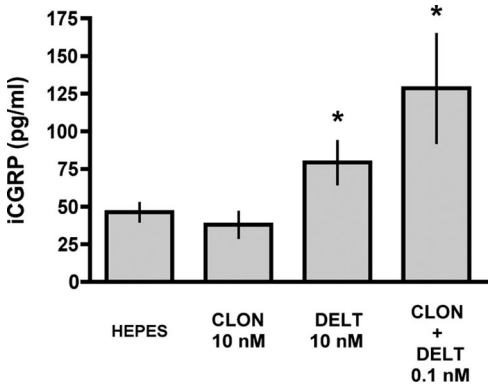

Figure 7. Low-concentration CLON-DELT combination causes significant CGRP release in the spinal cord slice preparation in the absence of K^+ stimulation. The ability of CLON, DELT, and the CLON-DELT combination to cause release of CGRP in spinal cord slices was investigated in the absence of K^+ depolarization. CLON did not significantly increase CGRP levels above baseline levels [46.3 $\pm$ 5.9 pg/ml (basal level) vs 37.9 $\pm$ 8.5 pg/ml (CLON, 10 nM)]. In contrast, both DELT [46.3 $\pm$ 5.9 pg/ml (basal level) vs 79.2 $\pm$ 14.3 pg/ml (DELT, 10 nM)] and a 100-fold lower concentration of the CLON-DELT combination [46.3 $\pm$ 5.9 pg/ml (basal level) vs 128.5 $\pm$ 35.9 pg/ml (CLON-DELT, 0.1 nM)] were able to stimulate significant CGRP release without K^+ stimulation, suggesting that the CLON-DELT combination may act synergistically at DOPs and α_2ARs to externalize large dense-core vesicles. Error bars represent mean $\pm$ SEM ($n = 3$–11 samples/group). *$p < 0.05$ compared with HEPES; Student's t test.

Behavioral and *in vitro* synergy between agonists acting at α_2AR and DOP

Synergistic interactions between classes of analgesic agonists have been frequently reported in the literature, although the mechanisms underlying this phenomenon remain to be fully defined. It has been suggested, for example, that synergy will be observed between agonists acting at the following receptor pairs: δ-opioid/α_{2A}-adrenergic (Stone et al., 1997), δ-opioid/α_{2C}-adrenergic (Fairbanks et al., 2002), μ-opioid/α_{2A}-adrenergic (Stone et al., 1997) and μ-opioid/α_{2C}-adrenergic (Fairbanks et al., 2000). We and others have previously demonstrated that both α_{2A}ARs and DOPs are localized on the terminals of capsaicin-sensitive, SP-expressing primary afferent neurons in the dorsal horn of the spinal cord in rat (Dado et al., 1993; Arvidsson et al., 1995; Stone et al., 1998; Zhang et al., 1998) where they are highly colocalized (Riedl et al., 2009). The present study demonstrates that these two receptors colocalize identically in mouse, underscoring the congruence between species. The localization of the α_{2A}AR subtype together with previous studies showing that the effect of CLON is eliminated in mice lacking functional α_{2A}ARs (Stone et al., 1997) suggests that the CLON effect seen in the CLON-DELT

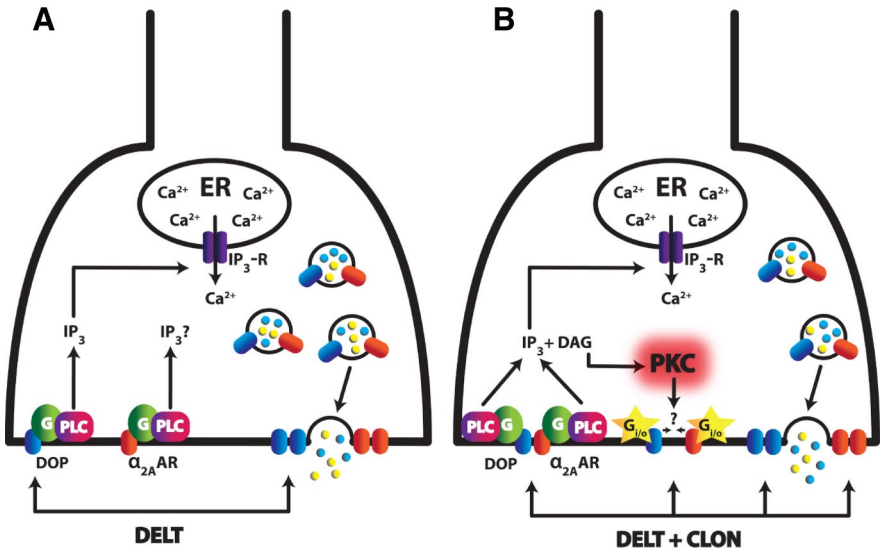

Figure 8. Proposed mechanism of CLON-DELT analgesic synergy localized to primary afferent terminals in the dorsal horn of the spinal cord. ***A***, Model of DOP agonist-induced DOP insertion coinciding with neuropeptide release (adapted from Bao et al., 2003). Activation of DOPs through administration of DELT causes activation of PLC (presumably through G_q), thereby increasing intracellular Ca^{2+} concentrations via IP_3 receptors. This spike in Ca^{2+} mediates exocytosis of LDCVs, thus releasing neuropeptides and inserting intracellular "reserve" DOPs to the plasma membrane. ***B***, Proposed model of CLON-DELT synergy mediated by PKC through coactivation of α_2ARs and DOPs. Coactivation of α_2ARs and DOPs causes neuropeptide release at a 100-fold lower concentration than DELT administration alone via the same mechanism as ***A***. In contrast to DOP agonist-induced DOP insertion, however, coactivation of α_2ARs and DOPs causes activation of PKC through increased levels of DAG. Activation of PKC, in turn, mediates the synergistic interaction of α_2ARs and DOPs. One of several hypotheses for this mechanism is that the phosphorylation target(s) of PKC allow enhanced $G_{i/o}$ coupling of both the α_{2A}AR and DOP (yellow stars). An alternative hypothesis is that activation of PKC favors the formation of α_2AR/DOP heterodimers with an enhanced inhibitory mode of action.

synergistic interaction is mediated through this particular α_2AR subtype. Because α_{2A}ARs and DOPs colocalize in the terminals of primary afferent neurons (Riedl et al., 2009), we sought to use selective agonists for the α_2AR and DOP in both a behavioral model and a more reduced spinal cord slice preparation to determine whether the synergistic interaction between these agonists to colocalized receptors could take place within a single subcellular compartment. This study shows that the selective α_2AR and DOP agonists CLON and DELT are each able to dose-dependently inhibit nociceptive responses when administered i.t. in the tail flick assay and to synergize in producing this antinociceptive effect. These results confirm previous findings using a different α_2AR agonist (brimonidine, also known as UK-14,304) (Stone et al., 1997). Furthermore, this interaction appears to take place within the terminals of primary afferent neurons: CLON and DELT inhibit K^+-evoked release of CGRP in a greater-than-additive manner from both spinal cord synaptosomes (Riedl et al., 2009) and superfused spinal cord slices (this study). That this synergy is maintained in the presence of the sodium channel blocker, TTX, further indicates that this interaction does not rely on multineuronal circuitry.

Signaling mechanisms mediating α_2AR and DOP synergy in the spinal cord

Because we observed that the analgesic synergy between agonists acting at α_2ARs and DOPs in spinal cord occurs within the terminals of primary afferent neurons, we sought to address the signaling mechanisms involved in this interaction. In small dorsal root ganglion (DRG) neurons, DOPs are known to predominantly localize to the cytoplasm and have been shown through immunofluorescence (Dado et al., 1993; Arvidsson et al., 1995), electron microscopy (Cheng et al., 1995; Zhang et al., 1998) and biochemical evidence (Wang et al., 2008) to often associate with the membrane of large dense-core vesicles that contain neuropeptides (e.g., CGRP, SP), with only a limited number of DOPs distributed in the plasma membrane. Because, under basal conditions, DOPs are mainly localized to the cytoplasm, it has been suggested that the majority are "reserve" receptors that are then targeted to and inserted in the plasma membrane in response to physiological changes (Zhang et al., 1998; Cahill et al., 2001a,b; Bao et al., 2003; Cahill et al., 2003; Gendron et al., 2006). Activation of DOPs through agonist binding has been shown to trigger a slow but long-lasting exocytosis of large dense core vesicles (Wang et al., 2008), leading to an increase in cell surface area, insertion of functional DOPs, and CGRP release in a PLC- and Ca^{2+}-dependent manner, presumably through activation of G_q (Bao et al., 2003). It is also known that activation of either the DOP (Yoon et al., 1999) or α_{2A}AR (Dorn et al., 1997) can mobilize IP_3-sensitive Ca^{2+} stores through a signal transduction pathway that involves activation of PLC by $G_{\beta\gamma}$subunits released from agonist-induced dissociation of the G_i heterotrimer. That DOPs and α_2ARs share common signaling pathways through similar G-proteins and can both mobilize intracellular Ca^{2+} through activation of PLC suggests that trafficking mechanisms for α_2ARs in primary afferent terminals are similar to those of DOPs.

Whereas GPCR-mediated activation of PLC and subsequent release of Ca^{2+} from internal stores is often associated with receptors coupling to stimulatory G-proteins (e.g., G_s and G_q), α_2ARs and DOPs preferentially couple through inhibitory G-proteins. However, evidence exists in the literature suggesting that ORs can couple not only to G_i/G_o, but to a variety of G-proteins. For instance, opioids can produce analgesia through activation of PLA_2 and have been shown to act through various G-proteins to activate phospholipase C (PLC), thereby mobilizing Ca^{2+}, activating PKC and enhancing presynaptic voltage-gated, ATP-gated and Ca^{2+}-gated K^+-channel activity (for review, see Aantaa et al., 1995; Connor and Christie, 1999; Millan, 1999, 2002; Law et al., 2000).

In support of the mechanism of DOP agonist-induced receptor externalization via PLC (Bao et al., 2003), the results from this study show that the effect of α_2AR and DOP agonists administered separately or in combination is blocked by an inhibitor of PLC both behaviorally and *in vitro*. This outcome suggests that agonist-driven externalization via PLC is involved in the analgesic effects of CLON, DELT, and the CLON-DELT combination. Therefore, the possibility exists that each agonist also promotes the externalization of the other receptor, presenting an opportunity for mutual enhancement of receptor number. This mechanism is further supported by the present results showing that administration of the CLON-DELT combination results in significant release of CGRP (thus enabling/signaling externalization of "reserve" receptors) from spinal cord slices in the absence of K^+ stimulation at a 100-fold lower concentration than is needed to produce release with agonist alone.

In contrast to PLC, however, downstream activation of PKC seems to be uniquely involved in the synergistic interaction between CLON and DELT. We have shown that inhibition of PKC completely blocked the synergistic combination, but did not significantly blunt the action of either agonist alone in either the tail flick test or inhibition of K^+-evoked CGRP release from spinal cord slices. This involvement of PKC in the synergistic interaction is consistent with the role of PKC in enhancing DOP "competence" (Patwardhan et al., 2005). Furthermore, the failure of PKA inhibition to block the synergistic effect underscores the specificity of PKC's involvement. These data are also consistent with previous antinociception results indicating that PKC, but not PKA, activity regulates the synergistic interaction between morphine and CLON in inhibiting nocifensive responses to i.t. administration of SP (Wei and Roerig, 1998), suggesting that PKC may mediate multiple opioid and α_2AR subtype interactions in the spinal cord.

In the proposed model (Fig. 8), we postulate that agonist-induced receptor insertion via PLC is necessary for the spinal analgesic effects of CLON and DELT by allowing "reserve" receptors to be trafficked to the plasma membrane. We further speculate that, when α_2ARs and DOPs are coactivated in the primary afferent terminal, PKC is activated, presumably through increased levels of diacylglycerol (DAG) downstream of PLC, is translocated to the plasma membrane and functions to mediate/facilitate the synergistic interaction.

One of several possible explanations for the differential signaling following receptor coactivation is the formation of heterodimeric complexes between α_{2A}ARs and DOPs. The emergence of novel pharmacological properties from heterodimer activation distinct from either component receptor alone has been previously investigated for dopamine receptors (Rashid et al., 2007). In the case of ORs, *in vitro* evidence indicates synergistic binding and coupling potentiation of coactivated κ-ORs and DOPs (Jordan and Devi, 1999) and conformational changes via crosstalk that modulate receptor function between α_2ARs and μ-ORs (Vilardaga et al., 2008). Furthermore, α_2AR-DOP synergy is lost in mice lacking functional α_{2A}ARs (Stone et al., 1997), whereas it is retained in μ-OR KO mice (Guo et al., 2003), supporting the specific involvement of DOPs in the synergistic interaction. Together these data demonstrate that α_2AR-DOP synergy is dependent on the presence of both receptors, but, to this point, α_2AR-DOP heterodimer formation *in vivo* is purely theoretical. An alternative hypothesis is that the phosphorylation target(s) of PKC allow enhanced $G_{i/o}$ coupling of both the α_{2A}AR and DOP. Evidence for a specific role for PKC is a first step in elucidating the pathways involved in α_2AR/DOP synergy, but further work is needed to determine the contribution of downstream targets of PKC.

Conclusion

Synergy is important in clinical pain management as much lower doses of each drug can be administered to produce analgesia, thus reducing unwanted side effects and improving treatment outcomes. These results provide strong evidence that synergy between analgesic agonists acting at anatomically colocalized receptor populations in spinal cord can occur, and that this interaction is not dependent on multineuronal circuitry. In the case of α_2AR and DOP agonist combinations, the synergistic interaction appears to be mediated through the activation of PKC. The phosphorylation target(s) of PKC mediating the enhanced potency remain unknown, as does the mechanism of enhancement. Identifying the molecular basis of spinal analgesic synergy may contribute to improved therapeutic strategies to control chronic pain and understand mechanisms of chronic pain induction.

References

Aantaa R, Marjamäki A, Scheinin M (1995) Molecular pharmacology of alpha 2-adrenoceptor subtypes. Ann Med 27:439–449.

American Pain Society (2008) Principles of analgesic use in the treatment of acute pain and cancer pain, Ed 6. Glenview, IL: American Pain Society.

Angst MS, Clark JD (2006) Opioid-induced hyperalgesia: a qualitative systematic review. Anesthesiology 104:570–587.

Arvidsson U, Dado RJ, Riedl M, Lee JH, Law PY, Loh HH, Elde R, Wessendorf MW (1995) delta-Opioid receptor immunoreactivity: distribution in brainstem and spinal cord, and relationship to biogenic amines and enkephalin. J Neurosci 15:1215–1235.

Bao L, Jin SX, Zhang C, Wang LH, Xu ZZ, Zhang FX, Wang LC, Ning FS, Cai HJ, Guan JS, Xiao HS, Xu ZQ, He C, Hökfelt T, Zhou Z, Zhang X (2003) Activation of delta opioid receptors induces receptor insertion and neuropeptide secretion. Neuron 37:121–133.

Cahill CM, Morinville A, Lee MC, Vincent JP, Collier B, Beaudet A (2001a) Prolonged morphine treatment targets delta opioid receptors to neuronal plasma membranes and enhances delta-mediated antinociception. J Neurosci 21:7598–7607.

Cahill CM, McClellan KA, Morinville A, Hoffert C, Hubatsch D, O'Donnell D, Beaudet A (2001b) Immunohistochemical distribution of delta opioid receptors in the rat CNS: evidence for somatodendritic labeling and antigen-specific cellular compartmentalization. J Comp Neurol 440:65–84.

Cahill CM, Morinville A, Hoffert C, O'Donnell D, Beaudet A (2003) Up-regulation and trafficking of delta opioid receptor in a model of chronic inflammation: implications for pain control. Pain 101:199–208.

Cheng PY, Svingos AL, Wang H, Clarke CL, Jenab S, Beczkowska IW, Inturrisi CE, Pickel VM (1995) Ultrastructural immunolabeling shows prominent presynaptic vesicular localization of delta-opioid receptor within both enkephalin- and nonenkephalin-containing axon terminals in the superficial layers of the rat cervical spinal cord. J Neurosci 15:5976–5988.

Cheng PY, Liu-Chen LY, Pickel VM (1997) Dual ultrastructural immunocytochemical labeling of mu and delta opioid receptors in the superficial layers of the rat cervical spinal cord. Brain Res 778:367–380.

Connor M, Christie MD (1999) Opioid receptor signalling mechanisms. Clin Exp Pharmacol Physiol 26:493–499.

Cuello AC, Galfre G, Milstein C (1979) Detection of substance P in the central nervous system by a monoclonal antibody. Proc Natl Acad Sci U S A 76:3532–3536.

Dado RJ, Law PY, Loh HH, Elde R (1993) Immunofluorescent identification of a delta (delta)-opioid receptor on primary afferent nerve terminals. Neuroreport 5:341–344.

Dorn GW 2nd, Oswald KJ, McCluskey TS, Kuhel DG, Liggett SB (1997) Alpha 2A-adrenergic receptor stimulated calcium release is transduced by Gi-associated G(beta gamma)-mediated activation of phospholipase C. Biochemistry 36:6415–6423.

Fairbanks CA, Posthumus IJ, Kitto KF, Stone LS, Wilcox GL (2000) Moxonidine, a selective imidazoline/alpha(2) adrenergic receptor agonist, synergizes with morphine and deltorphin II to inhibit substance P-induced behavior in mice. Pain 84:13–20.

Fairbanks CA, Stone LS, Kitto KF, Nguyen HO, Posthumus IJ, Wilcox GL (2002) Alpha(2C)-Adrenergic receptors mediate spinal analgesia and adrenergic-opioid synergy. J Pharmacol Exp Ther 300:282–290.

Franco-Cereceda A, Henke H, Lundberg JM, Petermann JB, Hökfelt T, Fischer JA (1987) Calcitonin gene-related peptide (CGRP) in capsaicin-sensitive substance P-immunoreactive sensory neurons in animals and man: distribution and release by capsaicin. Peptides 8:399–410.

Gendron L, Lucido AL, Mennicken F, O'Donnell D, Vincent JP, Stroh T, Beaudet A (2006) Morphine and pain-related stimuli enhance cell surface availability of somatic delta-opioid receptors in rat dorsal root ganglia. J Neurosci 26:953–962.

Guo XH, Fairbanks CA, Stone LS, Loh HH (2003) DPDPE-UK14,304 synergy is retained in mu opioid receptor knockout mice. Pain 104:209–217.

Han SK, Park JR, Park SA, Chun SW, Lee JC, Lee SY, Ryu PD, Park SJ (2007) Noradrenaline inhibits substantia gelatinosa neurons in mice trigeminal subnucleus caudalis via alpha(2) and beta adrenoceptors. Neurosci Lett 411:92–97.

Honoré P, Chapman V, Buritova J, Besson JM (1996) To what extent do spinal interactions between an alpha-2 adrenoceptor agonist and a mu

opioid agonist influence noxiously evoked c-Fos expression in the rat? A pharmacological study. J Pharmacol Exp Ther 278:393–403.
Hylden JL, Wilcox GL (1980) Intrathecal morphine in mice: a new technique. Eur J Pharmacol 67:313–316.
Hylden JLK, Wilcox GL (1983) Pharmacological characterization of Substance P-induced nociception in mice: modulation by opioid and noradrenergic agonists at the spinal level. J Pharmacol Exp Ther 226:398–404.
Janssen PA, Niemegeers CJ, Dony JG (1963) The inhibitory effect of fentanyl and other morphine-like analgesics on the warm water induced tail withdrawl reflex in rats. Arzneimittelforschung 13:502–507.
Jordan BA, Devi LA (1999) G-protein-coupled receptor heterodimerization modulates receptor function. Nature 399:697–700.
Law PY, Wong YH, Loh HH (2000) Molecular mechanisms and regulation of opioid receptor signaling. Annu Rev Pharmacol Toxicol 40:389–430.
Millan MJ (1999) The induction of pain: an integrative review. Prog Neurobiol 57:1–164.
Millan MJ (2002) Descending control of pain. Prog Neurobiol 66:355–474.
Monasky MS, Zinsmeister AR, Stevens CW, Yaksh TL (1990) Interaction of intrathecal morphine and ST-91 on antinociception in the rat: dose-response analysis, antagonism and clearance. J Pharmacol Exp Ther 254:383–392.
Murase K, Randiæ M (1983) Electrophysiological properties of rat spinal dorsal horn neurones in vitro: calcium-dependent action potentials. J Physiol 334:141–153.
Omote K, Kitahata LM, Collins JG, Nakatani K, Nakagawa I (1990) The antinociceptive role of mu- and delta-opiate receptors and their interactions in the spinal dorsal horn of cats. Anesth Analg 71:23–28.
Ossipov MH, Harris S, Lloyd P, Messineo E (1990a) An isobolographic analysis of the antinociceptive effect of systemically and intrathecally administered combinations of clonidine and opiates. J Pharmacol Exp Ther 255:1107–1116.
Ossipov MH, Harris S, Lloyd P, Messineo E, Lin BS, Bagley J (1990b) Antinociceptive interaction between opioids and medetomidine: systemic additivity and spinal synergy. Anesthesiology 73:1227–1235.
Ossipov MH, Lozito R, Messineo E, Green J, Harris S, Lloyd P (1990c) Spinal antinociceptive synergy between clonidine and morphine, U69593, and DPDPE: isobolographic analysis. Life Sci 47:PL71–PL76.
Patwardhan AM, Berg KA, Akopain AN, Jeske NA, Gamper N, Clarke WP, Hargreaves KM (2005) Bradykinin-induced functional competence and trafficking of the delta-opioid receptor in trigeminal nociceptors. J Neurosci 25:8825–8832.
Pertovaara A (2006) Noradrenergic pain modulation. Prog Neurobiol 80:53–83.
Plenderleith MB, Haller CJ, Snow PJ (1990) Peptide coexistence in axon terminals within the superficial dorsal horn of the rat spinal cord. Synapse 6:344–350.
Rashid AJ, So CH, Kong MM, Furtak T, El-Ghundi M, Cheng R, O'Dowd BF, George SR (2007) D1–D2 dopamine receptor heterooligomers with unique pharmacology are coupled to rapid activation of Gq/11 in the striatum. Proc Natl Acad Sci U S A 104:654–659.
Riedl MS, Schnell SA, Overland AC, Chabot-Doré AJ, Taylor AM, Ribeiro-da-Silva A, Elde RP, Wilcox GL, Stone LS (2009) Coexpression of alpha(2A)-adrenergic and delta-opioid receptors in substance P-containing terminals in rat dorsal horn. J Comp Neurol 513:385–398.
Roerig SC, Lei S, Kitto K, Hylden JK, Wilcox GL (1992) Spinal interactions between opioid and noradrenergic agonists in mice: multiplicativity involves delta and alpha-2 receptors. J Pharmacol Exp Ther 262:365–374.
Ryu PD, Gerber G, Murase K, Randic M (1988) Actions of calcitonin gene-related peptide on rat spinal dorsal horn neurons. Brain Res 441:357–361.
Stevens CW, Monasky MS, Yaksh TL (1988) Spinal infusion of opiate and alpha-2 agonists in rats: tolerance and cross-tolerance studies. J Pharmacol Exp Ther 244:63–70.
Stone LS, MacMillan LB, Kitto KF, Limbird LE, Wilcox GL (1997) The alpha2a adrenergic receptor subtype mediates spinal analgesia evoked by alpha2 agonists and is necessary for spinal adrenergic-opioid synergy. J Neurosci 17:7157–7165.
Stone LS, Broberger C, Vulchanova L, Wilcox GL, Hökfelt T, Riedl MS, Elde R (1998) Differential distribution of alpha2A and alpha2C adrenergic receptor immunoreactivity in the rat spinal cord. J Neurosci 18:5928–5937.
Sullivan AF, Dashwood MR, Dickenson AH (1987) Alpha 2-adrenoceptor modulation of nociception in rat spinal cord: location, effects and interactions with morphine. Eur J Pharmacol 138:169–177.
Tallarida RJ (1992) Statistical analysis of drug combinations for synergism. Pain 49:93–97.
Tallarida RJ (2002) The interaction index: a measure of drug synergism. Pain 98:163–168.
Trudeau LE, Emery DG, Haydon PG (1996) Direct modulation of the secretory machinery underlies PKA-dependent synaptic facilitation in hippocampal neurons. Neuron 17:789–797.
Vilardaga JP, Nikolaev VO, Lorenz K, Ferrandon S, Zhuang Z, Lohse MJ (2008) Conformational cross-talk between alpha2A-adrenergic and mu-opioid receptors controls cell signaling. Nat Chem Biol 4:126–131.
Wang HB, Guan JS, Bao L, Zhang X (2008) Distinct subcellular distribution of delta-opioid receptor fused with various tags in PC12 cells. Neurochem Res 33:2028–2034.
Wei ZY, Roerig SC (1998) Spinal morphine/clonidine antinociceptive synergism is regulated by protein kinase C, but not protein kinase A activity. J Pharmacol Exp Ther 287:937–943.
Wessendorf MW, Elde RP (1985) Characterization of an immunofluorescence technique for the demonstration of coexisting neurotransmitters within nerve fibers and terminals. J Histochem Cytochem 33:984–994.
Wigdor S, Wilcox GL (1987) Central and systemic morphine antinociception in the mouse: contribution of descending noradrenergic and serotonergic pathways. J Pharmacol Exp Ther 242:90–95.
Wilcox GL, Carlsson KH, Jochim A, Jurna I (1987) Mutual potentiation of antinociceptive effects of morphine and clonidine on motor and sensory responses in rat spinal cord. Brain Res 405:84–93.
Yoon SH, Lo TM, Loh HH, Thayer SA (1999) Delta-opioid-induced liberation of Gbetagamma mobilizes Ca2+ stores in NG108-15 cells. Mol Pharmacol 56:902–908.
Yoshimura M, Jessell TM (1989) Primary afferent-evoked synaptic responses and slow potential generation in rat substantia gelatinosa neurons in vitro. J Neurophysiol 62:96–108.
Yoshimura M, Jessell T (1990) Amino acid-mediated EPSPs at primary afferent synapses with substantia gelatinosa neurones in the rat spinal cord. J Physiol 430:315–335.
Zhang X, Bao L, Arvidsson U, Elde R, Hökfelt T (1998) Localization and regulation of the delta-opioid receptor in dorsal root ganglia and spinal cord of the rat and monkey: evidence for association with the membrane of large dense-core vesicles. Neuroscience 82:1225–1242.